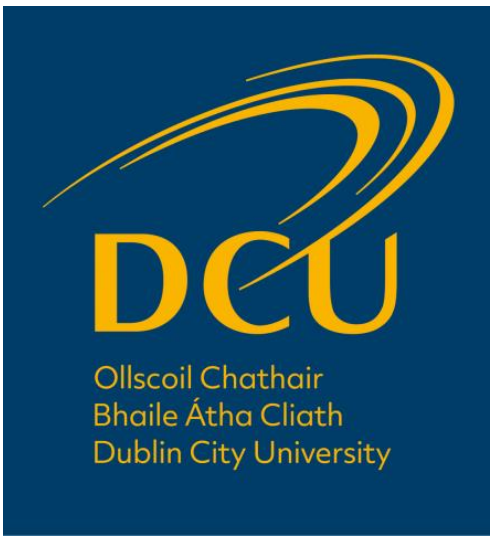

The Monitoring, Modelling and Chemical Interactions of Pollen

by

Emma Markey, BSc.

PhD Thesis

Dublin City University

School of Chemical Sciences

Supervisor: Dr. David O'Connor

Submitted: January 2024

Declaration

I hereby certify that this material, which I now submit for assessment on the programme of study leading to the award of Doctor of Philosophy is entirely my own work, and that I have exercised reasonable care to ensure that the work is original and does not to the best of my knowledge breach any law of copyright and has not been taken from the work of others save and to the extent that such work has been cited and acknowledged within the text of my work.

Signed: 

ID No.: 21270549

Date: 10/10/2023

When the Man waked up he said, 'What is Wild Dog doing here?' And the Woman said, 'His name is not Wild Dog any more, but the First Friend, because he will be our friend for always and always and always.'

- Rudyard Kipling (The Jungle Book)

In Memory of Sox, the best dog (and friend) a girl could ever have!

Acknowledgements

There are so many people who have helped support and guide me through the last 4 years. My thanks translated into typed word will never be able to fully explain the gratitude I feel but here it goes. Firstly, I would like to thank my parents Janet and Paddy (AKA Jan-Jan and Paddington). Thank you for encouraging me to follow my interests, nurturing and loving me throughout my entire life! Everything I do is because of you and I hope I have made you proud. Thank you to my twin Gary for always providing healthy competition and teaching me how to use ImageJ! I wish you all the best as you finish your own PhD, I am very proud of you and remember this is just the first step in Markey et. al taking over the scientific world!

Of course, I couldn't have made it this far without the help of my research team (Moisés, Becca, Gemma and Alex)! Especially Dr David O'Connor. Thank you for the years of advice, freedom, ranting sessions and pep talks! I pinkie promise to help work on some papers (and corral Jerry) even when I finish!

Now to Jerry, my best friend bonded by post-grad trauma. You have been my biggest fan and biggest bully over the past 4 years and I wouldn't have had it any other way. Your consistency in distracting me (although a hindrance at times!) really helped me enjoy the PhD experience. I have learned so much about random historical events and cinema! I'm sure we will continue to frequent the cinema to distract ourselves from our big-girl jobs. I am also extremely proud of you; you have earned you PhD and can finally start your podcast. I look forward to seeing where your star quality takes you!

There are several others I need to thank. Shannon, Jerry told me I need to write a nice acknowledgement to you so here we go. Thanks for being my bestie for the last 15 years, that is an amazing triumph in itself! You are an unproblematic queen, amazing human and my number one hype man. As a former DCU postgrad hun yourself, I thank you for sarcastically encouraging me to finish my PhD just to undoubtedly make fake doctor jokes for the rest of my life! Even though we aren't mushy people I want you to know I appreciate you (even if your dog tries to eat me on a regular basis).

Last but certainly not least, to Michaela (AKA Kale). Thank you for your love, support, encouragement and Chinese food over the last 4 years. You have successfully learned how to defuse my ever stress-filled head! And for that I am forever grateful. Thank you for all the amazing trips (past and future) and for letting me embrace being a passenger princess, I am really good at it (and should probably pay you an admin fee). You really are the best human I know (but please stop winding the dog up) and I can't wait for our future adventures!

Publications, Presentations and Professional Achievements

During the course of the project period, a number of publications were completed. Including several journal articles, EPA Ireland reports as well as dissemination efforts such as multiple media articles and radio/television appearances. Several academic presentations and posters were also completed, and awards earned. A detailed list of these contributions is summarised below.

Academic Journal Articles and Published EPA Reports

Upcoming publication (submitted to journal – awaiting review)

- Journal: Journal of the American Society for Mass Spectrometry
  Title: "Predicting Chronological Age via the Skin Volatile Profile"
  Authors: Finnegan, M.; Fitzgerald, S.; Duroux, R.; Attia, J.; **Markey, E.**; O'Connor, D.; Morrin, A.

Academic presentations and Conferences attended

- Attended and presented at the European Aerosol Conference in Malaga (04/09/2023 - 08/09/2023)
  Poster presented: Ambient measurement of bioaerosols at a semi-urban site: detection, sources and interferents
- Attended Advanced course on aerobiology in Riga, Latvia (22/08/2022 – 27/08/2022)
- NCSR Research Day, DCU: 16/06/2022
  Presented poster: Modified fluorescent sensor for bioaerosol detection
- 15th EAS basic course on aerobiology. Brussels, Belgium: 06/09/2021 – 10/09/2021
- Eli Lilly - Dublin Chemistry Talks, UCD (Online, 22/06/2021)
  Presentation: Monitoring, Modelling and Chemical Interactions of Pollen via Novel Methodologies
- Annual Graduate Research Symposium, TU Dublin (Online): 09/12/2020
  Online Poster Presented: Preliminary findings of Irish pollen network

Awards

- Awarded EAS grant for attending the 15th EAS Basic Course on Aerobiology 2021.
- Awarded Dr. Noel Russel Postgraduate Award 2021 (€500).
- EPA Researchers Award 2022 – Photography.
- DCU 2023 School of Chemical Sciences Travel bursary (€500).

Online media articles

"Why hay fever is going to get worse because of climate change", 2021. https://www.rte.ie/brainstorm/2021/0401/1207481-pollen-hayfever-allergies/

- "Are you allergic to your Christmas tree?", 2021. https://www.rte.ie/brainstorm/2021/1208/1265580-christmas-tree-syndrome-wreaths-garlands/
- "Thunder fever: the thunderstorms causing hay fever and asthma attacks", 2022. https://www.rte.ie/brainstorm/2022/0712/1309765-thunder-fever-pollen-hay-fever-thunderstorms/

Table of Contents

Abbreviations

30T – pollen threshold of 30 grains/m^3

AF - Asymmetry Factor

ANN -Artificial Neural Networks

APIn – Annual Pollen Integral

APS - Airborne Particulate Sensor

ADB - Ash Dieback

ATR - Attenuated Total Reflection

Betula.1 – Daily Betula concentration of previous day

Betula.7 – Average daily Betula concentration of the previous 7 day

Betula.10 - Average daily Betula concentration of the previous 10 day

BOR - Boruta

CCN- Cloud Condensation Nuclei

Cld_Amt – Cloud Amount

Day_L – Daily sun duration

DMT - Droplet Measurement Technologies

Evap - Evaporation

FAPs -Fluorescent Aerosol Particles

FL – Fluorescent particles

GDD – Growing Degree Days

Gmin – Grass minimum temperature

G_rad – Global radiation

HULIS - Humic-Like Substances

IN – Ice Nuclei

INP - Increase in Node Purity

IR - Fourier Transform Infrared Spectroscopy

LIF - Light Induced Fluorescence

MAE – Mean Absolute Error

MSE – Mean Square Error

MDG - Mean Decrease in Gini

MLR – Multiple Linear Regression

MPS – Main Pollen Season

NF – Non-fluorescent particles

NWR - Non-parametric Wind Regression

PAH – Polyaromatic Hydrocarbons

PBAP - Primary Biological Aerosol Particles

PC – Principal Component

PCA – Principal Component Analysis

PCGs - Pollen Cytoplasmic Granules

Pe – Potential Evapotranspiration

PM – Particulate Matter

PMT – Photomultiplier Tube

Poaceae.1 – Daily Poaceae concentration of previous day

Poaceae.7 – Average daily Poaceae concentration of the previous 7 day

Poaceae.10 - Average daily Poaceae concentration of the previous 10 day

POMMEL - Pollen Monitoring and Modelling

PRP – Pre-peak Period

PSP – Post-peak Period

r – Correlation coefficient (Spearman or Pearson)

r^2 – Coefficient of determination

Rain – Daily rainfall amount

Rain_1 - Rainfall of previous day

Rain_10 – Mean daily rainfall over previous 10 days

Rain_7 - Average Rainfall of previous 7 days

RBF - Radial Basis Function

RF – Random Forest

Rh – Relative Humidity

RMSE – Root Mean Square Error

ROS – Reactive Oxygen Species

SMAPE - Symmetric Mean Absolute Percentage Error

SOA – Secondary Organic Aerosols

SPP – Sub Pollen Particles

SVM – Support Vector Machines

Tmax – Maximum daily temperature

Tmed – Mean daily temperature

Tmed_7 - Average Mean Temperature of previous 7 days

Tmed_10 – Mean daily temperature of previous 10 days

Tmin – Minimum daily temperature

TOL - Tolerance

UKT – Pollen thresholds used by the UK met office

VIF - Variance Inflation Factor

WIBS - Wideband Integrated Bioaerosol Sensor

List of Figures

- *Figure D13: FTIR spectra obtained from the ATR analysis of wood ash*
- *Figure D14: FTIR spectra obtained from the ATR analysis of coal ash*
- *Figure D15: FTIR spectra obtained from the ATR analysis of Saharan dust*

List of Equations and Tables

The monitoring, modelling and chemical interactions of pollen

Emma Markey

Ireland had one of the highest incident rates of asthma worldwide, with 80% of Irish asthmatics also possessing pollen allergies. These figures are expected to further increase due to climate change and urbanisation. Despite concerns pollen monitoring has largely gone undocumented in Ireland for many years, while much of Europe continued to advance monitoring/modelling approaches. Therefore, the aim of the thesis is to bridge this gap and establish a functioning pollen network in Ireland. Chapters 1-2 introduce the theory and instrumentation used in the project. Chapter 3 focuses on the traditional monitoring of airborne pollen, primarily in Dublin city. Prevalent pollen types and seasonal trends were noted – highlighting a bimodal season, dominated by the allergenic *Betula* and Poaceae pollen. The first pollen calendar for Dublin was created, indicating potentially high exposure periods for allergy sufferers. Prediction efforts were further explored in Chapter 4 which explored the use of regression and classification models for forecasting *Betula* and Poaceae pollen. Due to the lack of extensive monitoring data, classification models were found to be more reliable, with accuracies ranging from 61-67%. Chapter 5 investigates the potential of utilising real-time devices for pollen monitoring (WIBS), promising results were found for total/Urticaceae pollen ($r=0.73$). However, influencing interferences were noted. The synergy between pollen and pollutants has been linked to increasing pollen allergenicity. In Chapter 6 IR spectroscopy was used to examine compositional changes to pollen samples during exposure to hydration, particulate, and gaseous pollutants (O_3 and exhaust fumes). Differences were observed in protein, lipid and carbohydrate composition. Confocal microscopy was used to determine if these changes could lead to difficulties in identification when using real-time fluorescence sensors. Changes in fluorescence intensity were observed for hydration and particulate matter exposure but not gaseous exposure. Additional work is required to determine any changes in emission maxima.

Overall, this thesis addresses the need for pollen monitoring in Ireland, presenting valuable insights into pollen types, seasonality, forecasting, real-time monitoring, and the potential impact of pollution on composition and fluorescence detection.

Chapter 1: Introduction

The objective of this chapter is to offer a comprehensive introduction to the concepts/methodologies employed in this project, with the intention of establishing a foundation for the subsequent chapters. An adaption of this review has previously been published in the EPA POMMEL report (O'Connor et al., 2022).

1.1 Pollen structure and composition

Pollen is the male gametophyte generated by flowering plants and trees (Dahl et al., 2013) as part of their sexual reproduction. The pollen grain itself acts as a vessel that protects gametes from the time it is released from the anther until it reaches the stigma of a corresponding plant. Pollen is dispersed through various mechanisms; however, the aerobiological nature of this thesis will focus on anemophilous pollen which is transported via wind. It is this fraction of pollen that is responsible for the onslaught of seasonal allergies experienced by many.

Pollen grains are produced by both angiosperms and gymnosperms. In angiosperms pollen develops within the anthers of the plant whereas in gymnosperms it develops in microsporangia (Breygina et al., 2021; Dahl et al., 2013). While the pollen is developing and maturing within the anther (angiosperms) or cone (gymnosperms) it is continuously nourished by the tapetum. This is a secretory tissue that provides the grains with nutrients through the locular fluid (Pacini, 2010). This layer disintegrates shortly before anthesis (release of pollen from anther), however before doing so it can excrete viscous components on to the surface of the maturing pollen grain wall such as tryphine and pollenkitt. These coatings can have various protective and practical functions eg. to protect pollen grains from water loss and UV damage during pollination and aid in adhesion to the receiving stigma (Dickinson and Lewis, 1973; Pacini and Hesse, 2005). The adhesive properties of these pollen components are therefore popular among entomophilous mediated pollen but are also found on anemophilous pollen.

Following adequate maturation and dehydration, pollen grains are then released from the anther/cone. The final pollen grain structure is generally composed of an external wall called the exine and an internal wall called the intine as shown in Figure 1.1. However, a great degree of variation can exist between pollen grains on a family, genus and even species level. This is so apparent that for decade the identification of pollen in aerobiological studies has largely been based on the visual differences in intricate surface features such as pores, furrows, striations, textures, and general pollen grain size. This indicates that during development different species of pollen grains evolve morphological, cytological and physiological differences (Pacini and Franchi, 2020).

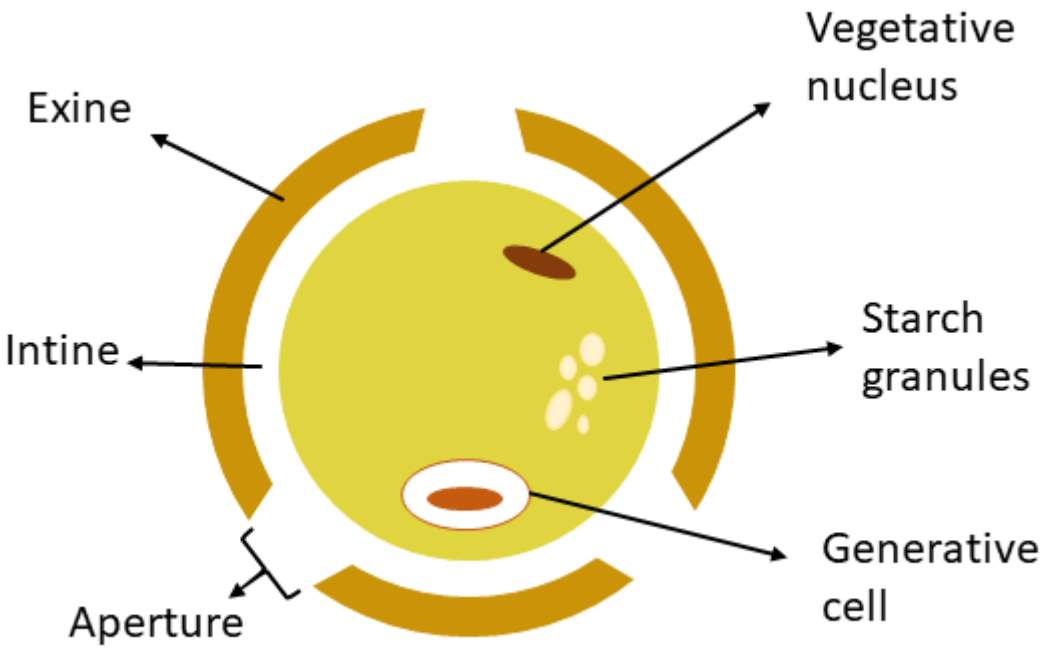

Figure 1.1: General structure of pollen grain (inspired by (Burkart et al., 2021; Katifori et al., 2010)*)*

The external layer of a pollen grain (exine) is developed first and is largely composed of a biopolymer known as sporopollenin which is made of various lipids and polyphonic compounds (Scott, 1994). The exine is composed of an outer portion that is sculptured and ornate called the sexine and a simple inner portion known as the nexine (Scott, 1994). Varying types and number of apertures can be seen on the exine of a pollen grain. These apertures, be they furrows (colpi), pores or a combination of the two (colpori), function as the sites of origin of pollen tube growth during germination. Depending on the species, these can vary is shape, size and number. The type of aperture present can be linked to the degree of pollen hydration of the released grains as well as changes in hydration expected during pollen release and transport, allowing for changes in pollen grain shape (Pacini and Franchi, 2020). These apertures are generally covered by the nexine or intine (Scott, 1994). In the case of gymnosperms, pollen exine can further extend to encompass large air-sac structures used to promote the transport of these larger pollen grains (Pacini and Franchi, 2020).

The composition of the exine, although largely composed of similar building blocks, is not uniform across different species which can be seen as variations in chemical resistance, autofluorescence, staining efficiency etc. (Driessen et al., 1989; Wiermann and Gubatz, 1992). The exine can also contain various components originally introduced by the tapetum/pollenkitt which can be reabsorbed or left as a coating (Pacini and Hesse, 2005). The composition of such layers/coatings has also been found to vary depending on species but generally is composed of lipids as well as phenolic compounds such as carotenoids and flavonoids with the additional presence of carbohydrate

and proteinaceous components (Hesse, 1993; Lunau, 1995; Pacini and Hesse, 2005; Wang and Dobritsa, 2018).

The intine resides below the exine and is mainly composed of polysaccharides such as cellulose and pectin and surrounds the protoplast of the male gametophyte (Nakamura and Suzuki, 1981; Wiermann and Gubatz, 1992). The protoplast of the pollen grain contains various structures such as the vegetive nucleus, generative nucleus and vesicle. Internal carbohydrate reserves are also known to be present within the pollen grain – derived from starch which is stored within the vegetative cell during pollen development (Franchi et al., 1996). Polysaccharides such as starch can be found either in amyloplasts or in cytoplasmic vesicles. Polysaccharides can also undergo hydrolysation, depending on the metabolism and water content of the cell, to disaccharides like sucrose and monosaccharides such as glucose and fructose (Pacini, 1996; Pacini et al., 2006; Speranza et al., 1997).

1.2 Pollen in the atmosphere

Bioaerosols are a type of aerosols derived from biological sources including bacteria, viruses, fungal spores, and pollen grains. Pollen grains can exist in sizes ranging from 10-100 µm, thus representing the coarser fraction of the bioaerosol class (Dahl et al., 2013). Initially, atmospheric pollen concentrations were considered unimportant compared to other bioaerosols (Penner et al., 2011). However, researchers have argued that measurements and contributions of pollen within the atmosphere have been underestimated (Cariñanos et al., 2021; Núñez et al., 2016). Bioaerosols account for approximately 16.5% and 16.3% of PM2.5 and PM10 atmospheric concentrations, respectively (Hyde and Mahalov, 2019), with slightly lower contributions observed for the indoor environment (Marcovecchio and Perrino, 2021). Pollen derived particles (and fungal spores) account for ~7.5% of the biological fraction of these particulate matter (PM) measurements. This might be surprising due to the coarse nature of pollen grains, however, under the correct conditions pollen grains can swell and burst – releasing particles within the range of 0.03 – 5 µm (Knox and Suphioglu, 1996; Mampage et al., 2022; Miguel et al., 2006; Taylor et al., 2004). In conclusion, pollen contributions to varying fractions of atmospheric bioaerosols warrant additional exploration and consideration in air quality assessments.

1.2.1 Pollen dispersion and transport

By design, dispersal and transport are integral parts of the anemophilous pollen life cycle. Atmospheric transport of varying distances is required for plant/tree pollen to arrive at the stigma of receptor plants. Although the dispersion of pollen through atmospheric pathways is essential for pollination and increasing genetic diversity, it can also lead to the spread of invasive plant species

and pathogens as well as exposing humans to increased allergen concentrations (discussed further in section 1.2.2.

The degree of dispersion and transport of individual pollen taxa depends on a variety of factors (morphological features, meteorological conditions etc.) (Després et al., 2012; Myszkowska et al., 2021; Sofiev et al., 2013, 2006) leading to varying scales of transport being possible. These include microscale processes which take places within several metres from the point of pollen release, local-scale processes which extend slightly further to encompass several kilometres from the source, regional (or meso) scale processes that include distances of up to 100 kilometres from the source, and long-range transport that encompass pollen transport at much higher distances (1,000-5000 km or higher) (Sofiev et al., 2013). The extent of pollen transport is also dependent on the atmospheric lifetime of the particle. This is reliant on the deposition intensity of the particle, for coarse particles like pollen, the most important means of deposition in gravitational settling (Skjøth et al., 2013; Wörl et al., 2022). Therefore, the deciding factor of a pollen grain's atmospheric lifetime is its sedimentation velocity. Several studies have calculated the sedimentation velocity of different pollen taxa such as for birch pollen (1.2 cm sec-1) (Sofiev et al., 2006) and grass pollen (Skjøth et al., 2013). Wet deposition by rain can also result in the further removal of pollen grains from the atmosphere (Sofiev et al., 2006), however, following deposition pollen can experience resuspension and can be involved in further airborne transport (Williams, 2008).

Despite the influence of deposition processes, released pollen can be transported by prevailing winds as a result of turbulent vertical mixing (D'Amato et al., 2007) and can be found within the atmospheric boundary layer (Gregory, 1973; Raynor et al., 1974). It is this turbulent vertical mixing process that determines the fraction of the released pollen that will undergo larger-scale dispersion (Gregory, 1973). Following this, pollen can remain suspended from anywhere from several hours to several days, depending on the meteorological conditions, particles size etc.(Sofiev et al., 2013). Removal of the pollen from the atmosphere can take several days if purely reliant on gravitational settling, this means that some pollen can be transported long distances in this time (Skjøth et al., 2007). Other factors such the height at which pollen is released from the source as well as the paticles's aerodynamic properties are also important factors that influences the degree of dispersion/transport experienced (Skjøth et al., 2013). An increased release height is typically associated with a resulting decrease in near-source concentration and increased dispersion area, these trends have been documented for various air pollutants and bioaerosols (Zhang and Wang, 2022). Therefore, smaller pollen grains released above ground level such as *Betula* pollen generally experience longer suspension time than larger pollen grains emitted closer to the ground such as Poaceae pollen, the dispersal of which has been shown to be limited to several hundred metres (Skjøth et al., 2013).

Although the majority of pollen released is dispersed locally without travelling considerable distances, regional and long-range transport of pollen has been documented since the 1930's

(Edwards and Östensson, 2023; Erdtman, 1937). The transport of pollen to aerobiological sampling sites from varying distances has been well documented throughout literature (Sofiev et al., 2013). These studies have largely focused on the detection of allergenic pollen concentration and are often first noticed when ambient concentrations peak devoid of comparable local sources or phenological changes, indicating pollen transport from elsewhere (Ranta et al., 2006). Many studies have investigated the transport of *Betula* (Alarcón et al., 2022; Mahura et al., 2007; J.M. Maya-Manzano et al., 2021; Myszkowska et al., 2021; Šauliene and Veriankaite, 2006; Skjøth et al., 2007; Wörl et al., 2022), *Ambrosia* (Šikoparija et al., 2013; Smith et al., 2008; Stępalska et al., 2020; de Weger et al., 2016) and even Poaceae (Frisk et al., 2022; Skjøth et al., 2013) pollen using various transport modelling approaches and back trajectory analyses. These studies have identified pollen transport ranging from nearby regions (Skjøth et al., 2009) to regions over 1,400-1,700 km apart (Myszkowska et al., 2021; Stępalska et al., 2020), once again illustrating that smaller pollen grains favour increasing long-range transport compared to larger pollen grains (Skjøth et al., 2013; Williams, 2008).

1.2.2 Health effects

Pollen is notorious for triggering health issues like hay-fever and exacerbating conditions such as COPD, eczema, and asthma (Brzezińska-Pawłowska et al., 2016; Cirera et al., 2012; Davies et al., 2018; Fölster-Holst et al., 2015; Jantunen et al., 2012). More worryingly, pollen allergies have increased considerably in recent years (Asam et al., 2015; Biedermann et al., 2019; D'Amato et al., 2007; Davies et al., 1998; Lee et al., 2021) with 30-40% of the current European population being affected and figures predicted to double by 2060 (Lake et al., 2017). This is largely related to the synergistic impacts of pollution and climate change on the allergenic and phenological trends of pollen (Beggs et al., 2017; D'Amato et al., 2010; Lake et al., 2017; Subiza et al., 2021). Changes induced through increasing urbanisation and greenhouse gas emissions have been shown to promote pollen production and allergen potency while also extending the length of pollen seasons (D'Amato et al., 2015; El Kelish et al., 2014; Oh, 2018; Paudel et al., 2021). This is also likely to increase the financial burden associated with treating such conditions. Currently, the effects of seasonal allergies puts substantial strain on the European health system, with direct and indirect health costs equating to an estimated €50 billion/year and €50–150 billion/year, respectively (Clot et al., 2020; Zuberbier et al., 2014). Direct and indirect costs for an individual (within the EU) are estimated to be in the range of €2,400 per year (Zuberbier et al., 2014). The medical and financial implications of seasonal allergies are likely even more severe for Ireland due to the remarkably high asthma prevalence. Asthma rates within Ireland are currently ranked fourth globally (Asthma Society of Ireland, 2022a), impacting approximately 890,000 individuals (over the course of their lifetimes), resulting in an annual healthcare cost estimated at €472 million (Asthma Society of Ireland, 2022b).

Exposure to ambient pollen has also been shown to enhance the susceptibility of respiratory viral infections such as rhinovirus (Gilles et al., 2020), even in those who do not possess pollen

allergies. Exposure to pollen can suppress the body's innate antiviral immunity. During the midst of the COVID-19 pandemic, pollen exposure was linked to increased SARS-CoV-2 infection rates (Damialis et al., 2021). The study concluded that infection rates increased after higher pollen concentrations, suggesting that high-risk population groups should avoid extensive outdoor activities when periods of high pollen and respiratory virus exposure coincide. In addition to its impact on human health, pollen has also been shown to impact the health of animals by triggering allergic reactions. These allergies generally take the form of atopic dermatitis or other inflammatory skin symptoms, however, some animals can also experience allergic rhinitis, conjunctivitis and asthma like their human counterparts (Jensen-Jarolim et al., 2015). Furthermore, pollen release and transport can impact plant health through the spread of plant pathogens (Card et al., 2007). A review by Card et al., (2007) outlined a prospective 39 viruses that are pollen-transmitted, including pathogens derived from bacterial and fungal sources.

Pollen monitoring and forecasting networks thus offer a range of health and agricultural benefits to the people of Ireland; providing suitable warnings to allergy sufferers and valuable information on plant pathology, plant distributions and presence of invasive species (Bastl et al., 2016).

1.2.3 Climate effects

Historical records of fossilised pollen can provide a great deal of information regarding past climates and biodiversity (Von Post, 1946). However, current ambient concentrations of pollen and other primary biological aerosol particles (PBAP) can impact the climate by influencing cloud formation and radiative forcing through the absorption and scattering of light (Conen et al., 2017). Given enough relative humidity, clouds can form when water condenses on the surfaces of soluble particles. These particles are called Cloud condensation nuclei (CCN). Clouds also occur in cooler air at temperatures between 0 and -36°C due to particles acting as Ice Nuclei (IN), resulting in the freezing of droplets (Phillips et al., 2009). PBAP may include soluble coatings that enable them to function as CCN while also containing insoluble components that contribute to IN potential (Möhler et al., 2007; Phillips et al., 2009). The increased interest in cloud forming PBAP in recent times, has stemmed from non-biological IN (mineral dust and combustion aerosols) losing their IN ability at temperatures warmer than -15°C and -20°C. As such, these aerosols cannot account for cloud formation above this temperature, which has been witnessed (DeMott and Prenni, 2010).

The only particles found that are capable of serving as IN in these warmer conditions have been biological in nature and were found to catalyse the freezing of cloud droplets at temperatures between −1 and −15 ◦C (Després et al., 2012; Murray et al., 2012). The first biological IN (*Pseudomonas syringae* bacteria) were discovered in the early 1970's (Maki et al., 1974; Schnell and Vali, 1972). Since then, many biological components have been identified as potentially important

CCN and IN (Bauer et al., 2002; Christner et al., 2008; Pratt et al., 2009; Prenni et al., 2009), including pollen (von Blohn et al., 2005; Diehl et al., 2002, 2001; Mikhailov et al., 2019; Möhler et al., 2007; Pope, 2010; Pummer et al., 2012; Steiner et al., 2015). To date, a number of laboratory studies have illustrated the CNN and IN capabilities of pollen grains. Pope, (2010) investigated the CNN abilities of four different pollen taxa and concluded that whilst pollen is only moderately hygroscopic; it will still act as effective CCN under very low supersaturations and that during pollen seasons when concentrations exceed $\sim 10^{-3}$ cm^{-3} this extra source of giant CCN is likely important for cloud processes (Levin and Cotton, 2009; Pope, 2010).

Several laboratory studies have also investigated the IN ability of pollen (Casans et al., 2023). Ice nucleation occurs according to one of four main mechanisms/modes: deposition nucleation, condensation freezing, immersion freezing and contact freezing (Paramonov et al., 2020). The temperature dependent IN behaviour of pollen in these four modes has been examined in several studies (von Blohn et al., 2005; Diehl et al., 2002, 2001). Although, no significant deposition nucleation was recorded for the investigated pollen types, at temperatures as low as −32.5◦C and ice supersaturation of up to 35% (Diehl et al., 2001), different pollen types were shown to possess increasing ice activity in the condensation and immersion modes for temperatures between −8 and −18◦C (Diehl et al., 2001). Contact nucleation occurred at even warmer temperatures of up to −5◦C (Diehl et al., 2002). In a follow-up study immersion and contact freezing modes were investigated for additional pollen types and similar trends were observed with increasing ice activity in the immersion mode at temperatures typically below −10 to −16◦C (von Blohn et al., 2005).

In the past, pollen was dismissed as important atmospheric IN (or CCN), due to low atmospheric concentrations compared to bacteria or mineral dust and their inability to reach higher altitudes. However, a study by Pummer et al., (2012) illustrated that full pollen grains are not required to act as IN (Pummer et al., 2012). Some macromolecules within the pollen grain can be separated during rupturing. These submicron particles released from pollen grains are often termed sub-pollen particles (SPP) and can act as IN (Dreischmeier et al., 2017; Gute and Abbatt, 2020; Pummer et al., 2012) and CNN (Casans et al., 2023; Mikhailov et al., 2019; Steiner et al., 2015; Steiner and Solmon, 2018). SPPs are present at higher concentrations and higher altitudes than whole pollen grains. A recent study has suggested that chemical processing, especially UV exposure, can alters SPPs such that ice nucleation is no longer effectively promoted. These findings imply that the role SPPs play in cloud formation may be reduced the longer they are exposed to atmospheric processing (Gute et al., 2020).

Although many of these investigations have highlighted the potential importance of pollen as effective IN/CNN on a regional and seasonal scale, a significant contrast is observed when compared to larger/global studies. Several studies have highlighted the contributions of SPPs and other PBAP to the total number concentrations of particles activated in clouds is only minor (Hader et al., 2014; Haga et al., 2014; Hummel et al., 2018; Sesartic et al., 2013; Spracklen and Heald, 2014).

In two distinct research investigations (C Hoose et al., 2010; C. Hoose et al., 2010), it was determined that the simulated impact of PBAP on cloud formation was insignificant compared to the influence of mineral dust and soot, which accounted for 93% of the IN composition. Even with abnormally heightened freezing efficiency, the global contribution of PBAP to IN was not greater than 1% (C. Hoose et al., 2010). However, this does not negate the influence of pollen and other PBAP as IN/CNN on a regional/seasonal basis, especially at lower altitudes where warmer temperatures inhibit the nucleation of other particles (Prenni et al., 2009; Spracklen and Heald, 2014). These contrasting results indicate that the true IN/CNN activity of pollen/PBAP remains somewhat uncertain.

1.3 Airborne Pollen monitoring methods

1.3.1 Traditional volumetric methods

Given the increased interest in pollen monitoring over the last few decades, it is somewhat surprising that the vast majority (80%) of all documented sampling sites still use the traditional volumetric methods developed in the 1950s (Buters et al., 2018; Sodeau and O'Connor, 2016). These methods have endured the test of time for several reasons: affordability, operational simplicity, and resilience to outdoor conditions (Beggs et al., 2017) and is a standardised method (EN 16868) (CEN, 2019). The Hirst volumetric trap (Hirst, 1952) is the most widely used sampler for pollen monitoring, recommended by the EAN and EAS (Oteros et al., 2015a). It operates continuously, using a pump to impact aerosols onto a rotating drum with a silica substrate coated onto plastic tape. Following the microscopic identification of pollen, daily results are generated.

This off-line technique is notoriously time-consuming and suffers from low time resolution (usually daily averages), extrapolation to hourly or bi-hourly resolution is possible but is affected by larger uncertainties (Clot et al., 2020). A highly skilled operator is also required to optically identify pollen types correctly. The precision of results therefore heavily relies on the skills of the operator. Overall, this method is incredibly impractical, labour intensive and can take up to a week to circulate results. Due to this slow process, only a portion of the mounted slides are analysed with the overall count determined by extrapolation (Jose María Maya-Manzano et al., 2021). Therefore, the biggest problem that pollen monitoring networks face is the time delay from sample analysis to result dissemination. Therefore, novel pollen monitoring technologies are currently the focus of aerobiological research.

1.3.2 Real-time methods

Real-time methods provide a practical alternative to traditional Hirst-type approaches. They were initially developed to address public health and national defence concerns related to aeroallergens and bioterrorism (Huffman et al., 2020). Commercially available real-time pollen monitoring

devices, which examine the physical/chemical properties of bioaerosols, have emerged in recent years and have since been extensively reviewed (Fennelly et al., 2017; Huffman et al., 2020; Martinez-Bracero et al., 2022; Jose María Maya-Manzano et al., 2021). The majority of these instruments utilise either image recognition and/or air-flow cytometry (Clot et al., 2020; Huffman et al., 2020). A range of instruments employed for real-time pollen monitoring can be classified as using air-flow cytometry, although the overall operating principles of each instrument can differ, including light-induced fluorescence (LIF), light scatter and holographic imaging. These instruments include the KH-3000-01, the Wideband Integrated Bioaerosol Sensor (WIBS), the Plair Rapid-E and the Swisens Poleno.

The KH-3000-01 Japanese pollen sensor by Yamatronics uses light scattering to collect and process air samples, providing immediate real-time results (Kawashima et al., 2007). It has been deployed in Japan for the monitoring of Japanese Cedar pollen since 2002 (Kawashima et al., 2017). While it is effective for distinguishing the large and distinct allergenic Japanese Cedar species, several studies have also tested a range of different pollen types like Urticaceae, Poaceae, *Ambrosia*, *Cupressaceae, Fraxinus*, *Betula*, and *Quercus* by comparing scattered light intensity and degree of polarization (Kawashima et al., 2007; Huffman et al., 2020). However, its capability for analysing a complex mixture of pollen types remains uncertain.

Fluorescence spectroscopy, particularly LIF is one of the most documented and freely available real-time techniques for the detection of pollen/PBAP (Huffman et al., 2020). The operating principle behind LIF focuses on exploiting the presence of naturally occurring fluorophores found in many biological particles. The prominent fluorescent components of PBAP have been well documented in literature and include a vast array of compounds such as amino acids and structural carbohydrates (Fennelly et al., 2017; Manninen et al., 2014). Therefore, fluorescence spectroscopy can be used to discern aerosols of biological origin from other non-fluorescent aerosols. The WIBS is one such instrument which utilises a 635 nm laser, 2 excitation wavelengths (280 nm and 370 nm) and 2 detection bands (310–400 nm and 420–650 nm) to determine the size, shape and fluorescent characteristics of atmospheric particles. The emission wavebands are specifically selected for the detection of two common bio-fluorophores: tryptophan and NAD(P)H. Sampled particles can then be categorised according to their fluorescent properties.

The WIBS has been deployed at a myriad of different sites to monitor ambient bioaerosol variations, including in rainforests (Gabey et al., 2010; Whitehead et al., 2010), urban (Gabey et al., 2011; Markey et al., 2022b), biowaste (Feeney et al., 2018), green-waste (O'Connor et al., 2015), coastal (Daly et al., 2019) and indoor environments (Li et al., 2020), including several Irish campaigns (Healy et al. 2012a, b, 2014; O'Connor et al. 2013, 2014) and lab studies (Healy et al., 2012b, 2012a; O'Connor et al., 2013; Robinson et al., 2017; Toprak and Schnaiter, 2013). Field studies have highlighted the proficiency of the WIBS to identify ambient bioaerosols compared to volumetric sampling (R^2 >0.9) (O'Connor et al., 2014). However, only a select few have specifically

attempted to use the WIBS as a means to monitor and differentiate between pollen types (Healy et al., 2012a; Markey et al., 2022b; O'Connor et al., 2014). Laboratory studies using the WIBS-4 (now surpassed by the WIBS-NEO) also illustrated the potential for the WIBS to discriminate pollen grains from other bioaerosols and aerosols of non-biological origin (Healy et al., 2012a).

The Plair Rapid-E (formerly the PA-300) instrument utilises both fluorescence and optical scatter to differentiate between aerosols (Kiselev et al., 2013, 2011). The sampled particle passes through a 405 nm laser - providing time-resolved data of the scattered light. The scattered light provides information on the size, shape and surface characteristics of the particle (Crouzy et al., 2016). The particle is then exposed to a laser of 337 nm, inducing fluorescence which is recorded using 32 photodetectors covering a range from 350-800 nm (Tummon et al., 2021). Fluorescence lifetime is also recorded for four bands at nanosecond resolution (Tummon et al., 2021). The resulting signals produce a spectrum for each particle. Field tests have shown the potential of the Rapid-E and the PA-300 for pollen monitoring (Crouzy et al., 2016; Šauliene et al., 2019). Studies have also highlighted the use of mathematical algorithms for pollen identification using data obtained from the Rapid-E (Crouzy et al., 2016; Šauliene et al., 2019; Tešendić et al., 2020). Using a combination of algorithms Šauliene et al., (2019) attempted to differentiate between a range of different pollen taxa, exceeding 80% accuracy for 5 out of 11 species.

The Swisens Poleno also utilises LIF for particle detection, it differs from previous examples by the addition of holographic imaging. Laser scattering provides information on the particle shape, size, velocity, and alignment. Two images are then taken at 90° from each other using digital holography (Sauvageat et al., 2020). UV-induced fluorescence provides additional information regarding particle composition. Fluorescence lifetime and spectra are measured using excitation wavelengths at 280, 365 and 405 nm at detection windows between 320-720 nm (Sauvageat et al., 2020). However, the majority of studies have focussed on analysing pollen based on holographic imaging, the true potential of the LIF functioning is yet to be fully realised, although early studies suggest the promising influence on pollen differentiation/identification (Erb et al., 2023).

Other methods of detection have also seen promising results in recent times. One such method, with the suitability for taxon-level identification of ambient pollen, is image recognition-based approaches. The BAA 500 by Hund-Wetzlar is one such instrument (Oteros et al., 2015; Plaza et al., 2022). This method mimics the microscopic identification process carried out in traditional monitoring methods and is restricted to pollen and some spores >10 μm (Huffman et al., 2020). The pollen sample enters the instrument and is examined under a microscope system that measures images of the pollen at 8 different focal positions. While the images are being analysed the next sample is loaded etc. Identification is dependent on training the device with known samples. An initial study by Oteros et al., 2015a, in which over 480,000 particles were analysed, showed that the BAA500 was capable of differentiating between different pollen taxa, yielding a total accuracy of over 93%. Another sensor utilising an image recognition system is the PollenSense Airborne

Particulate Sensor (APS) (Lucas et al., 2016). The PollenSense examines particles present in ambient air by acquiring microscopic images. The images are then processed to determine particle identification within a time frame of several hours (Huffman et al., 2020) but this has yet to be fully discussed in literature.

Although the incorporation of real-time instruments into bioaerosol monitoring networks offers the potential for rapid retrieval and subsequent dissemination of data, only 2 real-time monitoring networks are currently in operation in Europe. This includes networks in Bavaria, Germany currently using the BAA500 instrument utilising the principle of image recognition (Oteros et al., 2015) and in Switzerland, which employs the Poleno air-flow cytometry system which uses optical discrimination, based on fluorescence and holography (Crouzy et al., 2016; Sauvageat et al., 2020). In addition, the Plair Rapid-E has been used in a preliminary network study between Serbia and Croatia, under the RealforAll project (Clot et al., 2020; Tešendić et al., 2020). In total, only 4 European countries (France, Germany, Luxemburg and Switzerland) utilise real-time monitoring instruments regularly but not at all sampling locations (Buters et al., 2018). Outside of Europe, there are an additional two sampling sites in the US and 120 in Japan that also regularly employ real-time instruments (Kawashima et al., 2007).

Real-time monitoring also has the potential to be integrated directly into forecasting models, further improving the accuracy of regional forecasts (Adamov and Pauling, 2023; Clot et al., 2020). At this crucial moment in monitoring development, it is important that any networks developed are standardised and validated accordingly. This rationale has led to the development of Europe-wide projects such as the EUMETNET AutoPollen programme, which aimed to develop a prototype automatic pollen monitoring network across Europe (Clot et al., 2020). One aspect involved the intercomparison of real-time instrumentation to the Hirst (Maya-Manzano et al., 2023; Tummon et al., 2021). This was done to compare how different instruments function under different ambient conditions and to better understand their limits of detection, accuracy levels and establish necessary minimum acceptance criteria (Clot et al., 2020).

1.3.3 Pollen monitoring in Ireland

Many European countries have been routinely monitoring pollen for decades, leading to the establishment of the European Aeroallergen Network (EAN) in 1986 (Nilsson, 1988). Although Ireland was one of the original countries to initially join the EAN, the monitoring efforts were prematurely adjourned in the early 1980's. A recent study documented and mapped all the active pollen and fungal spore monitoring sites around the globe, thus excluding the original Irish monitoring site (Buters et al., 2018; Nilsson, 1988). By the end of 2016 over 525 sampling sites existed across Europe with an additional 182 and 151 sampling sites in Asia and the US (Buters et

al., 2018). However, since the 1980's Ireland has largely refrained from carrying out any extensive monitoring campaigns.

Excluding the work carried out during this PhD project, there exists only two other traditional (Hirst based) aerobiological monitoring studies conducted in Ireland (McDonald, 1980; McDonald and O'Driscoll, 1980). These studies, although decades old, provide some insight into the aerobiology surrounding a former site in Galway. The studies covered two summer periods (May-September) in 1977 and 1978. The first study aimed at assessing general pollen and fungal spore trends over these summer months and equating changes in ambient concentration to meteorological conditions. It was found that this period was mainly dominated by Poaceae pollen with mention of several other herbaceous pollen taxa such as *Chenopodium, Rumex* and *Urtica*. Changes in pollen concentrations were shown to positively correlate with wind speed and negatively correlate with rainfall, mirroring similar trends established throughout literature. Any notable disparities between the sampling years was also attributed to changes in wind direction, with low concentrations equating to prevailing winds coming from the ocean (McDonald and O'Driscoll, 1980).The second of these studies reiterated many of the same findings and correlations to meteorological factors, instead focussing specifically on grass pollen (McDonald, 1980). Although these studies offer a promising start to Irish aerobiological work and provide key fundamental findings (especially for the selected summer months), they provide little information on the full pollen season and spectrum encountered at this site with no indication of what arboreal pollens were present. It was not until 2021 that any other traditional pollen monitoring study using Irish data was published again (Markey et al., 2022a; J.M. Maya-Manzano et al., 2021), illustrating a clear disparity in long-term monitoring efforts since these original studies.

Other recent Irish aerobiological research has instead focused on assessing the suitability of real-time methods such as the WIBS in monitoring PBAP such as fungal spores and pollen (Healy et al. 2012a, b, 2014; O'Connor et al. 2013, 2014). Several field monitoring campaigns were conducted around Ireland using the WIBS but the durations of the campaigns were relatively short, offering little information on the seasonal concentrations and trends of PBAP. Likewise, the inability of the WIBS to discriminate between a large range of pollen types provided little detail on the prevalent pollen types. Overall, the understanding of allergenic bioaerosols within the historical Irish context has been severely limited with little known about the species and seasonality of different pollen types throughout the year.

1.4 Pollen modelling and forecasting methods

There are three general categories of models commonly used to forecast ambient pollen concentrations/trends. These categories encompass observational models, process-based models, and

source-oriented models. Detailed and extensive reviews of which have received much attention in recent years (Jose María Maya-Manzano et al., 2021; Vélez-Pereira et al., 2022, 2021).

1.4.1 Observational based models

Observational models use mathematical and statistical algorithms to predict dependent variables like pollen concentrations, using independent variables like meteorological and phenological parameters. However, these predictions are limited to a specific location, making them difficult to apply elsewhere. Techniques like traditional regression, time-series methods, and modern machine learning are used to forecast daily airborne pollen variations.

Regression models are currently the most documented modelling techniques used for pollen forecasting. However, more recently, these simple techniques have been overtaken in popularity by more sophisticated machine learning methods (Vélez-Pereira et al., 2021). This does not negate the vast array of literature available detailing the use of these models. One of the simplest iterations is linear regression, where a straight line is used to establish a relationship between two variables (one dependent and one independent), which has been widely used in pollen forecasting (Frenguelli et al., 2016; García-Mozo et al., 2014; Piotrowska-Weryszko, 2013a). However, many factors affect pollen release and as such multiple and polynomial regression analyses are also used (Jarlan et al., 2014; Novara et al., 2016; Sabariego et al., 2012; Tseng et al., 2018). These include methods like backward elimination, stepwise multiple regression (Howard and Levetin, 2014; Janati et al., 2017; Sicard et al., 2012), logistic regression (Katz and Batterman, 2019; Myszkowska, 2014a; Myszkowska and Majewska, 2014), and partial least squares (Brighetti et al., 2014; Lara et al., 2019).

Regression models have been used to predict daily pollen concentrations (Janati et al., 2017; Smith and Emberlin, 2005), season start/peak (García-Mozo et al., 2009; Myszkowska, 2014a, 2014b; Zhang et al., 2015), season duration (Zhang et al., 2015), and season intensity (Bonini et al., 2015). Regression models have primarily targeted pollen taxa of known allergenic or invasive importance, including *Alnus* (Myszkowska, 2014a; Novara et al., 2016), *Betula* (Robichaud and Comtois, 2017; Zhang et al., 2015), *Corylus* (Myszkowska, 2014a; Novara et al., 2016), Poaceae (Janati et al., 2017; Piotrowska, 2012; de Weger et al., 2014), *Quercus* (Myszkowska et al., 2011; Picornell et al., 2019), Cupressaceae (Picornell et al., 2019; Sabariego et al., 2012), *Artemisia* (Piotrowska-Weryszko, 2013b; Zhang et al., 2015) and *Ambrosia* (Howard and Levetin, 2014; Zhang et al., 2015).

Despite their ease of use, regression models frequently rely on linear/normal assumptions, failing to capture the seasonality in aerobiological data, resulting in poor predictability (Astray et al., 2010; Damialis and Gioulekas, 2006). This limitation can be addressed through time-series analysis, which forecasts future values based on past data, considering components like general and seasonal trends, unknown cycles, and random variations (Maya-Manzano et al., 2021). Time-series methods

aim to separate various patterns and disturbances in the dataset caused by ordinary seasonal behaviours like weather conditions. These methods, such as ARIMA (García-Mozo et al., 2014; Muzalyova et al., 2021) and LOESS based models (Rojo et al., 2017) have been used to predict many different pollen types, including *Alnus* (Nowosad, 2016; Siniscalco et al., 2015), *Ambrosia* (Puc and Wolski, 2013), *Betula, Corylus* (Nowosad et al., 2016), Poaceae (Fernández-Rodríguez et al., 2018; Rojo et al., 2017; Tassan-Mazzocco et al., 2015), *Quercus* (Fernández-Rodríguez et al., 2016), and Urticaceae (Tassan-Mazzocco et al., 2015; Valencia et al., 2019).

While traditional models are still widely used, they frequently struggle to capture the intricate relationship between pollen concentrations and explanatory variables. Consequently, advanced machine learning methods have gained popularity in atmospheric and aerobiological research including Artificial Neural Networks (ANN) (Astray et al., 2016; Burki et al., 2019; Liu et al., 2017; Puc, 2012), Support Vector Machines (SVM) (Bogawski et al., 2019; Du et al., 2017; Liu et al., 2017) and ensemble techniques like Random Forests (RF) (Navares and Aznarte, 2019; Zewdie et al., 2019b, 2019a). However, these algorithms require a lot of training data to develop suitably accurate and robust models. Machine learning models frequently aim to replicate the functionality of biological information processing systems (Recknagel, 2001) to simulate the intricate relationships between variables. ANNs are one such method – designed to mimic the thought process of the human brain and have gained popularity in aerobiology due to their ability to easily analyse non-linear and discontinuous data (Jedryczka et al., 2015). ANNs have recently been applied to predict *Ambrosia* (Csépe et al., 2019, 2014), *Betula* (Puc, 2012), *Quercus* (González-Naharro et al., 2019), *Olea* (Iglesias-Otero et al., 2015) and Poaceae (Lops et al., 2020; Muzalyova et al., 2021; Sánchez-Mesa et al., 2002; Sánchez Mesa et al., 2005) pollen concentrations. RF is another popular model type used for forecasting pollen, this method involves constructing multiple decision trees and combining their results to make more accurate predictions. RF models have been developed for a range of different pollen types, such as *Alnus, Betula, Corylus* (Novo-Lourés et al., 2023; Nowosad, 2016), *Quercus*, Cupressaceae, *Ambrosia* (Lo et al., 2021) and Poaceae (Navares and Aznarte, 2019). SVMs have also been used to forecast daily concentrations and flowering periods (Bogawski et al., 2019; Zewdie et al., 2019c; Zhao et al., 2018) but are often outperformed by ANN and RF. While these advanced methods have not received as much attention in the literature as traditional deterministic models, their high accuracy and robustness hold promise.

1.4.2 Phenological models

Phenological data has proven to be valuable in enhancing aerobiological research and constructing effective models for forecasting crucial stages in plant growth, particularly flowering periods for pollen forecasting (Grundström et al., 2019; Tormo et al., 2011). These models establish the timing of phenological phases based on environmental conditions and are commonly integrated into atmospheric transport models (Jose María Maya-Manzano et al., 2021). Phenological models have

been developed for a range of pollen including *Alnus* (Pauling et al., 2014; Siniscalco et al., 2015), *Betula* (Pauling et al., 2014), *Corylus* (Novara et al., 2016; Pauling et al., 2014), *Olea* (Achmakh et al., 2015) and Poaceae (Pauling et al., 2014).

1.4.3 Source – orientated models

Pollen levels can be predicted spatially and temporally using source-oriented and transport models (Verstraeten et al., 2019). Transport models can address the data-intensive limitations of observational models but do require knowledge of specific aerosol features such as diffusion as well as pollen emission sources. These models are based on chemical transport models that were later modified to account for pollen dispersal. SILAM, COSMO-ART (Adamov and Pauling, 2023; Zink et al., 2017, 2012), ENVIRO-HIRLAM (Mahura et al., 2009), CMAQ-pollen (Efstathiou et al., 2011), and the WRF-CHEM model (Skjøth et al., 2015) are among several transport models capable of modelling pollen dispersion. Recent studies have investigated the dispersion of several different pollen types, including *Alnus* (Prank et al., 2016), *Ambrosia* (Prank et al., 2013; Zink et al., 2012), *Artemisia* (Prank et al., 2016), *Betula* (Sofiev et al., 2015; Verstraeten et al., 2019; Werner et al., 2021; Zhang et al., 2014), Poaceae (Sofiev et al., 2017) and *Quercus* (Zhang et al., 2014).

1.4.4 Pollen calendar

Despite the advantages of previously discussed modelling techniques, they require a great deal of site-specific data. This is not always available, especially in areas that do not have a long history of pollen monitoring, such as Ireland. Pollen calendars may offer a suitable alternative. Pollen calendars are the most rudimentary form of pollen forecasting tool and consists of a graphical representation of the average annual/seasonal trends of selected pollen types (Pecero-Casimiro et al., 2020). Pollen calendars have been used for decades and help to understand the distribution and concentration of varying pollen taxa at different locations (Elvira-Rendueles et al., 2019; Emberlin et al., 1990; Katotomichelakis et al., 2015; Lo et al., 2019; Markey et al., 2022a; Martínez-Bracero et al., 2015; O'Rourke, 1990; Pecero-Casimiro et al., 2020; Šikoparija et al., 2018; Werchan et al., 2018). It is recommended that a minimum of 5 years of data is used in construction, to fully capture reoccurring trends and account for annual fluctuations (Galán et al., 2017). Several different methods have been suggested for developing pollen calendars over the years (D'amato and Spieksma, 1992; Lo et al., 2019; O'Rourke, 1990; Rojo et al., 2019; Werchan et al., 2018). Most studies tend to use methods based on Spieksma's model, originally developed in 1992 (Rojo et al., 2019). The temporal resolution of these models tends to be in the order of several days which makes these models limited with regards to daily predictions (Šikoparija et al., 2018).

1.5 Chemical interactions of pollen grains

Numerous studies have showcased the growing trend in allergic diseases in recent decades (D'Amato et al., 2015), particularly in urbanised areas (D'Amato et al., 2010; Nicolaou et al., 2005). The exact cause of this upward trend is still a subject of debate among immunologists, however, the effect of air pollution is among one of the leading hypotheses (Berger et al., 2020). A number of studies have already highlighted the direct effect pollution can have on human health alone (Bernstein et al., 2004; Haahtela et al., 2013). Pollutants can also exacerbate symptoms associated with allergen exposure. This is due to the direct effect pollutants have on epithelial cells, provoking oxidative stress that disrupts the protective barrier (Bernstein et al., 2004; Reinmuth-Selzle et al., 2017). This allows allergens to access immune cells more easily, leading to more acute allergic symptoms (Sénéchal et al., 2015). This has led to increased interest in the interactions between air pollutants and aeroallergens (mainly pollen) in urban environments, including several detailed reviews (Sedghy et al., 2018; Sénéchal et al., 2015; Visez et al., 2020). Exposure to anthropogenic pollution can induce numerous changes in pollen. To date, various studies have identified several physiochemical alterations, including modifications to pollen grain surfaces, elemental composition, allergen, and protein composition/content, as well as effects on the reproductive functions of pollen and plants (Sénéchal et al., 2015).

1.5.1 Changes to pollen surface

Pollution can damage the external surface of pollen grains, making them more fragile and causing breaks and ruptures to the cell wall (Ouyang et al., 2016; Rezanejad, 2009). This can increase allergen release and absorption by mucus membranes, allowing these allergen-containing components and SPPs to penetrate deeper into the respiratory tract than intact pollen grains. Studies have compared the outer surface of pollen (known as the exine) collected from polluted and unpolluted sites (Azzazy, 2016; Ouyang et al., 2016; Rezanejad, 2009; Shahali et al., 2009a, 2009b), with several focussing on Cupressaceae pollen, which has a thinner exine. Pollen exposed to chemical pollution has been shown to increase the release of pollen cytoplasmic granules (PCGs), which can penetrate deep into the airways. Pollen, such as *Phleum pratense*, can spontaneously release allergen-containing PCGs, which can penetrate deep into the airways following exposure to NO_x and O_3 (Motta et al., 2006).

Exposure to PM pollution can also result in the adhesion and accumulation of particles to the exine surface resulting in changes to its shape and appearance (Azzazy, 2016; Choël et al., 2022a, 2022b, 2020; Guedes et al., 2009; Lu et al., 2014; Ribeiro et al., 2015; Visez et al., 2020). Guedes et al., (2009) compared *Chenopodium alba* L. pollen samples collected from rural and urban sites in Portugal and found that the urban pollen was covered with a fine layer of diesel exhaust particles. These results were further corroborated by Amjad and Shafighi, (2012) who noted similar particle coverage on *Chenopodium album* pollen exposed to traffic-related pollution. To further investigate the origin of such adsorbed particles, Ribeiro et al., (2015) examined particle matter adhered to the

surface of pollen using a field emission probe microanalyzer. The size of adhered particles on the pollen surface ranged from 0.1-2.8 um and were identified as Si, organic, SO, metal, oxides, and Cl rich particles.

Laboratory studies have shown that pollen grains artificially exposed to gaseous (Cerceau-Larrival et al., 1991; Cuinica et al., 2013; Pereira et al., 2021; Ribeiro et al., 2017) and particulate pollution (Chehregani and Kouhkan, 2008; Choël et al., 2020; Lu et al., 2014) undergo changes to their exine surface. Another study found that pollen types like *Platanus x acerifolia* (Aiton) Willd., *Betula pendula* Roth, *Corylus avellana* L., *Acer negundo* L., and *Quercus robur* L. (Pereira et al., 2021) showed different degrees of modification, indicating that while exposure to pollutants increases exine fragility, the magnitude of modification can vary depending on pollutant type and pollen species. Exine coverage was observed for *Lilium* (Chehregani and Kouhkan, 2008) and *Platanus* (Lu et al., 2014) pollen after exposure to PM, but co-current exposure to gaseous pollutants resulted in swelling of the pollen grain.

1.5.2 Changes in elemental/chemical composition

Pollutant exposure can affect the external surface of pollen grains and alter the elemental/chemical composition of the pollen. The compositional changes induced in pollen grains by exposure to pollutant has been investigated in literature for decades. In the early 1980's Williams et al., (1983) conducted a laboratory study in which they exposed *Ulmus pumila* L., *Quercus rubra* L., *Pinus taeda* L., and *Festuca elatior* L. pollen to gaseous pollutants (NO_2, SO_2, and CO). Analysis of pollen extracts following exposure indicated changes in the composition of structural proteins. Since then a range of other studies have also investigated the compositional analysis of pollen extracts following exposure to different pollutants (Farah et al., 2020a; Kalbande et al., 2008; Okuyama et al., 2007; Rezanejad, 2009; Roshchina and Karnaukhov, 1999; Roshchina and Mel'nikova, 2001; Temizer et al., 2018; Wang et al., 2009; Zhu et al., 2018).

Pollen's ability to bioaccumulate certain metals following heavy metal exposure has also been a topic of interest for years (Kalbande et al., 2008; Oleksyn et al., 1999; Temizer et al., 2018; Yousefi et al., 2011). Although current studies focus on pollinators and their products, an early study by Oleksyn et al., (1999) examined the changes in the elemental composition of pine pollen and needles collected near a phosphate fertilizer factory compared to pine pollen collected from a site devoid of acute air pollution. The study found that pollen from the polluted site had significantly higher concentrations of S, Mn, Al, Na, Cu, Ni, and Cd, and lower Zn. However, concentrations of P, K, Ca, Fe, Mg, and B remained relatively unchanged between the two sites. A more recent laboratory study exposed pollen to metal pollution to test their ability to bioaccumulate several trace metals (Kalbande et al., 2008). Pollen samples exposed to pollution had higher concentrations of Ca, Al, and Fe compared to the unexposed pollen. It was also possible to rank the pollen types based on

their ability to accumulate metal pollution. The different results from these two studies may indicate that certain pollen types might be more prone to accumulating certain metal pollutants.

Exposure to chemical pollution has also been shown to increase the presence of ionic components originating from both particulate (NO_3^-, SO_4^{2-}, and NH_4^+) and gaseous pollutants (NO_2, SO_2, and NH_3) (Okuyama et al., 2007; Wang et al., 2009). It has been found that pollen grains from urban areas have higher concentrations of such compounds and anthropogenic PM, while those from unpolluted areas have lower concentrations (Okuyama et al., 2007; Wang et al., 2009). Acid gases can also acidify the surface of pollen grains and dissolve into the inner portion of the pollen grain. Exposure experiments to nitric acid gas suggest that the concentration of the gas adsorbed by pollen outweighs the adsorption capabilities of other natural particles like humic acid or sand (Okuyama et al., 2007).

Exposure to air pollution can alter the composition of certain pollen components and induce a defence mechanism in pollinating plants through increased production of secondary metabolites. Flavonoid compounds, which are phenolic compounds found in plants, play a crucial role in various processes such as plant growth, fertility, pollen germination, cell cycle regulation, and protection against UV radiation. These compounds also indicate how plants respond to environmental stress, such as lack of nutrients, UV radiation, and air pollution. Several studies have highlighted the increased production of flavonoid compounds in plants and pollen exposed to pollution in urban areas, mainly SO_2, NO_2, CO and PM (Dixon and Paiva, 1995; Giertych and Karolewski, 1993; Nandi et al., 1990; Rezanejad, 2012, 2009). In two studies by Rezanejad (2012, 2009), pollen from polluted areas was found to accumulate significantly higher concentrations of flavonoids than their unpolluted counterparts. This increase in flavonoid production could be due to the importance of flavonoid content for successful pollination, specifically for pollen germination and pollen tube growth, which are inhibited by air pollution exposure (Rezanejad, 2007; Rezanejad et al., 2003). To limit potential pollen abnormalities introduced by air pollutants, plants and pollen exposed to reactive oxygen species (ROS) can produce higher amounts of flavonoids, which have been shown to scavenge ROS (Bors et al., 1994).

Research on the allergenic potential of different pollen taxa has historically focused on protein and allergens. However, in the last few years, research has expanded to include adjuvant mediators including lipids (Dahl, 2018; Farah et al., 2020a, 2020b; Gilles et al., 2009; Naas et al., 2016; Roldán et al., 2019; Smith et al., 1992; Traidl-Hoffmann et al., 2002; Zhu et al., 2018). Studies have shown that exposure to anthropogenic pollution can alter these lipids. Naas et al., (2016) investigated the changes in the coating of *Pinus halepensis* Mill. pollen when exposed to ozone, revealing an increase in dicarboxylic acids, short-chain fatty acids, and aldehydes after extraction in organic solvent. Similarly, *Betula pendula* (Zhu et al., 2018) and *Phleum pratense* L. (Farah et al., 2020b) pollen exposed to ozone showed notable changes in their lipid fractions, including the consumption of alkenes and formation of aldehydes, nonanoic acid, and octadecanoic acid (Zhu et

al., 2018). These findings highlight the chemical changes induced in the lipid fraction of different pollen upon exposure to ozone pollution, even for very short durations. Further study is needed to determine whether these modified lipid fractions also undergo changes in their ability to act as inflammatory/allergenic stimulants.

Previous studies have also used techniques to analyse the "intact" pollen grain. Techniques such as SEM-EDX (Chehregani and Kouhkan, 2008; Heredia Rivera and Gerardo Rodriguez, 2016; Okuyama et al., 2007; Ribeiro et al., 2015), electron probe microanalyzer (Duque et al., 2013; Guimarães et al., 2012; Ribeiro et al., 2015), and vibrational spectroscopic methods such as Raman and Infrared spectroscopy (Depciuch et al., 2017; Guedes et al., 2009; Kanter et al., 2013; Pereira et al., 2021; Zhao et al., 2016) have been used to examine compositional changes. Almost all methods were able to note changes induced by differences in pollen type, environment and/or anthropogenic exposure. In the case of *Corylus* pollen from unpolluted and urbanised locations a notable increase/changes were observed in protein content from the urban site (Depciuch et al., 2017), using vibrational spectroscopy. These changes can lead to more potent allergenic proteins and worsen allergic responses.

1.5.3 Allergen modification

The main concern with exposing pollen to pollution is whether it can enhance the allergenicity of the pollen. However, the results remain inconsistent. Some studies have found that exposure to pollutants increases the allergenicity of pollen through different mechanisms (Aina et al., 2010; Armentia et al., 2002; Chehregani and Kouhkan, 2008; Cortegano et al., 2004; Cuinica et al., 2015, 2014; Ferreira et al., 2016; Ghiani et al., 2012; Lu et al., 2014; Motta et al., 2006; Sedghy et al., 2017). Many investigations have demonstrated increased expression of particular pollen-specific allergens such as in *Lolium perenne* L. (Lol p 5) (Armentia et al., 2002), *Cupressus arizonica* Greene (Cup a 3) (Cortegano et al., 2004), *Betula pendula, Ostrya carpinifolia* Scop. and *Carpinus betulus* L. (Bet v 1) (Cuinica et al., 2015, 2014) pollen. Conversely, some studies have also concluded the opposite findings (Helander et al., 1997; Pasqualini et al., 2011; Rezanejad, 2009; Ribeiro et al., 2014; Rogerieux et al., 2007; Shahali et al., 2009b), highlighting the potentially complex relationship between pollen and pollutants. For example, a study by Helander et al., (1997) found that distance from the pollution source did not affect the levels of allergens within the pollen. A similar decrease in allergen expression and IgE recognition for grass pollen allergens was also observed in a laboratory study examining modifications of allergens following O_3, NO_2, and SO_2 exposure (Rogerieux et al., 2007).

Interestingly, an investigation by Ribeiro et al., (2014) noted increased IgE reactivity for O_3 exposed *Acer negundo* and *Quercus robur* protein but the opposite was observed for *Platanus x acerifolia*. Such conflicting studies suggest that the modifications seen in pollen allergenicity may

be species dependent. Overall, while these findings suggest that exposure to pollutants can enhance the allergenic potential of pollen proteins, they also highlight the need for further research and understanding of the complex relationship between pollen and pollutants.

1.5.4 Changes in reproductive function

Pollen exposure to various forms of pollution can significantly impact plant and pollen functions, particularly reproductive functions. Pollen viability and germination can be altered by pollution, with various plant species experiencing these effects (Chehregani et al., 2011; Cuinica et al., 2014; Keller and Beda, 1984; Mohsenzadeh et al., 2011; Ouyang et al., 2016; Wolters and Martens, 1987; Yousefi et al., 2011). Studies have shown that pollen viability is typically inversely proportional to pollution exposure, with conflicting results seen for some pollen types (Iannotti et al., 2000; Kaur et al., 2016). For instance, in a study by Iannotti et al., (2000), *Parietaria diffusa* Mert. & W.D.J.Koch pollen showed higher viability when collected from polluted areas, while *Quercus ilex* L. pollen showed no difference in viability between sites. Another study by Kaur et al., (2016) again found that pollen viability was inversely proportional to the degree of traffic pollution. This suggests that the viability implications following pollen exposure could be plant dependent. Overall, studies on pollen exposed to pollution have shown that atmospheric pollution affects the physical, chemical, and biological properties of pollen (Sénéchal et al., 2015). Although the degree of modification varies depending on pollution and pollen type, exposure has been shown to induce several harmful effects on pollen.

1.6 Aims and Objectives

The aims of this project are threefold:

(i) To determine the concentration and species of ambient pollen at several Irish locations via novel real-time and traditional instrumentation.

(ii) Development of pollen models for Ireland using collected data, with a particular focus on potentially allergenic pollen types.

(iii) Investigate the impact that anthropogenic/environmental conditions have on pollen characteristics and composition.

The research objectives are as follows:

- Maintain the pollen monitoring network in Ireland (Hirst) for the duration of the project, primarily at the Dublin site. Thus, seasonal ambient concentrations of pollen will be determined, and a pollen calendar developed (seasonality of pollen).

- Enhance the traditional network via the use of novel spectroscopic instrumentation such as the WIBS-NEO.
- Create several preliminary pollen forecast models for Dublin – focusing on Poaceae and *Betula* pollen.
- Determine the effect anthropogenic pollution/environmental conditions have on the surface/chemical composition of pollen using various spectroscopic methods.

References

Achmakh, L., Bouziane, H., Aboulaich, N., Trigo, M.M., Janati, A., Kadiri, M., 2015. Aerobiologia (Bologna). 31, 191–199.

Adamov, S., Pauling, A., 2023. Aerobiologia (Bologna). 39, 327–344.

Aina, R., Asero, R., Ghiani, A., Marconi, G., Albertini, E., Citterio, S., 2010. Allergy Eur. J. Allergy Clin. Immunol. 65, 1313–1321.

Alarcón, M., Periago, C., Pino, D., Mazón, J., Casas-Castillo, M. del C., Ho-Zhang, J.J., De Linares, C., Rodríguez-Solà, R., Belmonte, J., 2022. Sci. Total Environ. 818.

Amjad, L., Shafighi, M., 2012. J. Agric. Sci. Technol. A 2, 143–148.

Armentia, A., Lombardero, M., Callejo, A., Barber, D., Martín Gil, F.J., Martín-Santos, J.M., Vega, J.M., Arranz, M.L., 2002. Allergol. Immunopathol. (Madr). 30, 218–224.

Asam, C., Hofer, H., Wolf, M., Aglas, L., Wallner, M., 2015. Allergy Eur. J. Allergy Clin. Immunol. 70, 1201–1211.

Asthma Society of Ireland, 2022a. Our History [WWW Document]. URL https://www.asthma.ie/about-us/who-we-are/our-direction/our-history (accessed 5.16.22).

Asthma Society of Ireland, 2022b. Asthma Facts & Figures [WWW Document]. URL https://www.asthma.ie/get-help/resources/facts-figures-asthma (accessed 1.13.22).

Astray, G., Fernández-González, M., Rodríguez-Rajo, F.J., López, D., Mejuto, J.C., 2016. Sci. Total Environ. 548–549, 110–121.

Astray, G., Rodríguez-Rajo, F.J., Ferreiro-Lage, J.A., Fernández-González, M., Jato, V., Mejuto, J.C., 2010. J. Environ. Monit. 12, 2145–2152.

Azzazy, M., 2016. J. Appl. Biol. Biotechnol.

Bastl, K., Berger, M., Maximilian, K.B., Uwe, K., 2016.

Bauer, H., Kasper-Giebl, A., Löflund, M., Giebl, H., Hitzenberger, R., Zibuschka, F., Puxbaum, H.,

2002. Atmos. Res. 64, 109–119.

Beggs, P.J., Šikoparija, B., Smith, M., 2017. Aerobiology in the International Journal of Biometeorology, 1957–2017. Int. J. Biometeorol.

Berger, M., Bastl, K., Bastl, M., Dirr, L., Hutter, H.P., Moshammer, H., Gstöttner, W., 2020. Environ. Pollut. 263, 1–9.

Bernstein, J.A., Alexis, N., Barnes, C., Bernstein, I.L., Bernstein, J.A., Nel, A., Peden, D., Diaz-Sanchez, D., Tarlo, S.M., Williams, P.B., 2004. J. Allergy Clin. Immunol. 114, 1116–1123.

Biedermann, T., Winther, L., Till, S.J., Panzner, P., Knulst, A., Valovirta, E., 2019. Allergy Eur. J. Allergy Clin. Immunol. 74, 1237–1248.

von Blohn, N., Mitra, S.K., Diehl, K., Borrmann, S., 2005. Atmos. Res. 78, 182–189.

Bogawski, P., Grewling, Ł., Jackowiak, B., 2019. Sci. Total Environ. 658, 1485–1499.

Bonini, M., Šikoparija, B., Prentović, M., Cislaghi, G., Colombo, P., Testoni, C., Grewling, L., Lommen, S.T.E., Müller-Schärer, H., Smith, M., 2015. Aerobiologia (Bologna). 31, 499–513.

Bors, W., Michel, C., Saran, M., 1994. Methods Enzymol. 234, 420–429.

Breygina, M., Klimenko, E., Schekaleva, O., 2021. Plants 10.

Brighetti, M.A., Costa, C., Menesatti, P., Antonucci, F., Tripodi, S., Travaglini, A., 2014. Aerobiologia (Bologna). 30, 25–33.

Brzezińska-Pawłowska, O.E., Rydzewska, A.D., Łuczyńska, M., Majkowska-Wojciechowska, B., Kowalski, M.L., Makowska, J.S., 2016. J. Asthma 53, 139–145.

Burkart, J., Gratzl, J., Seifried, T., Bieber, P., Grothe, H., 2021. Biogeosciences Discuss. 1–15.

Burki, C., Šikoparija, B., Thibaudon, M., Oliver, G., Magyar, D., Udvardy, O., Leelőssy, Á., Charpilloz, C., Pauling, A., 2019. Atmos. Environ. 218, 116969.

Buters, J.T.M., Antunes, C., Galveias, A., Bergmann, K.C., Thibaudon, M., Galán, C., Schmidt-Weber, C., Oteros, J., 2018. Clin. Transl. Allergy 8, 1–5.

Card, S.D., Pearson, M.N., Clover, G.R.G., 2007. Australas. Plant Pathol. 36, 455–461.

Cariñanos, P., Foyo-Moreno, I., Alados, I., Guerrero-Rascado, J.L., Ruiz-Peñuela, S., Titos, G., Cazorla, A., Alados-Arboledas, L., Díaz de la Guardia, C., 2021. J. Environ. Manage. 282.

Casans, A., Rejano, F., Maldonado-Valderrama, J., Casquero-Vera, J.A., Ruiz-Peñuela, S., van Drooge, B.L., Lyamani, H., Cazorla, A., Andrews, E., Lin, J.J., Mirza-Montoro, F., Pérez-Ramírez, D., Olmo, F.J., Alados-Arboledas, L., Cariñanos, P., Titos, G., 2023. Atmos. Environ. 310.

CEN, 2019. EN 16868:2019 Ambient air - Sampling and analysis of airborne pollen grains and fungal spores for networks related to allergy - Volumetric Hirst method.

Cerceau-Larrival, M.T., Nilsson, S., Cauneau-Pigot, A., Berggren, B., Derouet, L., Verhille, A.M., Carbonnier-Jarreau, M.C., 1991. Grana 30, 532–546.

Chehregani, A., Kouhkan, F., 2008. Ecotoxicol. Environ. Saf. 69, 568–573.

Chehregani, A., Mohsenzadeh, F., Hosseini, S., 2011. Toxicol. Environ. Chem. 93, 526–536.

Choël, M., Ivanovsky, A., Roose, A., Hamzé, M., Blanchenet, A.M., Deboudt, K., Visez, N., 2020. Aerobiologia (Bologna). 36, 657–668.

Choël, M., Ivanovsky, A., Roose, A., Hamzé, M., Blanchenet, A.M., Visez, N., 2022a. J. Aerosol Sci. 161.

Choël, M., Visez, N., Secordel, X., Deboudt, K., 2022b. Aerobiologia (Bologna). 38, 151–162.

Christner, B.C., Morris, C.E., Foreman, C.M., Cai, R., Sands, D.C., 2008. Science (80-.). 319, 1214.

Cirera, L., García-Marcos, L., Giménez, J., Moreno-Grau, S., Tobías, A., Pérez-Fernández, V., Elvira-Rendeles, B., Guillén, J.J., Navarro, C., 2012. Allergol. Immunopathol. (Madr). 40, 231–237.

Clot, B., Gilge, S., Hajkova, L., Magyar, D., Scheifinger, H., Sofiev, M., Bütler, F., Tummon, F., 2020. Aerobiologia (Bologna). 4.

Conen, F., Eckhardt, S., Gundersen, H., Stohl, A., Yttri, K.E., 2017. Atmos. Chem. Phys. Discuss. 1–13.

Cortegano, I., Civantos, E., Aceituno, E., Del Moral, A., López, E., Lombardero, M., Del Pozo, V., Lahoz, C., 2004. Allergy Eur. J. Allergy Clin. Immunol. 59, 485–490.

Crouzy, B., Stella, M., Konzelmann, T., Calpini, B., Clot, B., 2016. Atmos. Environ. 140, 202–212.

Csépe, Z., Leelőssy, Mányoki, G., Kajtor-Apatini, D., Udvardy, O., Péter, B., Páldy, A., Gelybó, G., Szigeti, T., Pándics, T., Kofol-Seliger, A., Simčič, A., Leru, P.M., Eftimie, A.M., Šikoparija, B., Radišić, P., Stjepanović, B., Hrga, I., Večenaj, A., Vucić, A., Peroš-Pucar, D., Škorić, T., Ščevková, J., Bastl, M., Berger, U., Magyar, D., 2019. Aerobiologia (Bologna). 0123456789.

Csépe, Z., Makra, L., Voukantsis, D., Matyasovszky, I., Tusnády, G., Karatzas, K., Thibaudon, M., 2014. Sci. Total Environ. 476–477, 542–552.

Cuinica, L.G., Abreu, I., Esteves Da Silva, J., 2014. Environ. Pollut. 186, 50–55.

Cuinica, L.G., Abreu, I., Gomes, C.R., Esteves da Silva, J.C.G., 2013. Grana 52, 299–304.

Cuinica, L.G., Cruz, A., Abreu, I., Da Silva, J.C.G.E., 2015. Int. J. Environ. Health Res. 25, 312–

321.

D'Amato, G., Cecchi, L., Bonini, S., Nunes, C., Annesi-Maesano, I., Behrendt, H., Liccardi, G., Popov, T., Van Cauwenberge, P., 2007. Allergy Eur. J. Allergy Clin. Immunol. 62, 976–990.

D'Amato, G., Cecchi, L., D'Amato, M., Liccardi, G., 2010. J. Investig. Allergol. Clin. Immunol. 20, 95–102.

D'Amato, G., Holgate, S.T., Pawankar, R., Ledford, D.K., Cecchi, L., Al-Ahmad, M., Al-Enezi, F., Al-Muhsen, S., Ansotegui, I., Baena-Cagnani, C.E., Baker, D.J., Bayram, H., Bergmann, K.C., Boulet, L.P., Buters, J.T.M., D'Amato, M., Dorsano, S., Douwes, J., Finlay, S.E., Garrasi, D., Gómez, M., Haahtela, T., Halwani, R., Hassani, Y., Mahboub, B., Marks, G., Michelozzi, P., Montagni, M., Nunes, C., Oh, J.J.W., Popov, T.A., Portnoy, J., Ridolo, E., Rosário, N., Rottem, M., Sánchez-Borges, M., Sibanda, E., Sienra-Monge, J.J., Vitale, C., Annesi-Maesano, I., 2015. World Allergy Organ. J. 8, 25.

D'amato, G., Spieksma, F.T.M., 1992. Aerobiologia (Bologna). 8, 447–450.

Dahl, Å., 2018. Front. Immunol. 9, 2816.

Dahl, Å., Galán, C., Hajkova, L., Pauling, A., Sikoparija, B., Smith, M., Vokou, D., 2013. The Onset, Course and Intensity of the Pollen Season, in: Allergenic Pollen. Springer Netherlands, Dordrecht, pp. 29–70.

Daly, S.M., O'Connor, D.J., Healy, D.A., Hellebust, S., Arndt, J., McGillicuddy, E., Feeney, P., Quirke, M., Wenger, J., Sodeau, J., 2019. Atmos. Chem. Phys. 19, 5737–5751.

Damialis, A., Gilles, S., Sofiev, M., Sofieva, V., Kolek, F., Bayr, D., Plaza, M.P., Leier-Wirtz, V., Kaschuba, S., Ziska, L.H., Bielory, L., Makra, L., del Mar Trigo, M., Traidl-Hoffmann, C., 2021. Proc. Natl. Acad. Sci. U. S. A. 118, 1–10.

Damialis, A., Gioulekas, D., 2006. Grana 45, 122–129.

Davies, J.M., Thien, F., Hew, M., 2018. BMJ 360, 4–5.

Davies, R.J., Rusznak, C., Devalia, J.L., 1998. Clin. Exp. Allergy, Suppl. 28, 8–14.

DeMott, P.J., Prenni, A.J., 2010. Atmos. Environ. 44, 1944–1945.

Depciuch, J., Kasprzyk, I., Sadik, O., Parlińska-Wojtan, M., 2017. Aerobiologia (Bologna). 33, 1–12.

Després, V.R., Alex Huffman, J., Burrows, S.M., Hoose, C., Safatov, A.S., Buryak, G., Fröhlich-Nowoisky, J., Elbert, W., Andreae, M.O., Pöschl, U., Jaenicke, R., 2012. Tellus, Ser. B Chem. Phys. Meteorol. 64.

Dickinson, H.G., Lewis, D., 1973. Proc. R. Soc. London - Biol. Sci. 184, 149–165.

Diehl, K., Matthias-Maser, S., Jaenicke, R., Mitra, S.K., 2002. Atmos. Res. 61, 125–133.

Diehl, K., Quick, C., Matthias-Maser, S., Mitra, S.K., Jaenicke, R., 2001. Atmos. Res. 58, 75–87.

Dixon, R.A., Paiva, N.L., 1995. Plant Cell 7, 1085–1097.

Dreischmeier, K., Budke, C., Wiehemeier, L., Kottke, T., Koop, T., 2017. Sci. Rep. 7, 1–13.

Driessen, M.N.B.M., Willemse, M.T.M., Van Luijn, J.A.G., 1989. Grana 28, 115–122.

Du, J., Liu, Y., Yu, Y., Yan, W., 2017. Algorithms 10.

Duque, L., Guimarães, F., Ribeiro, H., Sousa, R., Abreu, I., 2013. Atmos. Environ. 75, 296–302.

Edwards, K.J., Östensson, P., 2023. Palynology 0.

Efstathiou, C., Isukapalli, S., Georgopoulos, P., 2011. Atmos. Environ. 45, 2260–2276.

Elvira-Rendueles, B., Moreno, J.M., Costa, I., Bañón, D., Martínez-García, M.J., Moreno-Grau, S., 2019. Aerobiologia (Bologna). 35, 477–496.

Emberlin, J., Norris-Hill, J., Bryant, R.H., 1990. Grana 29, 301–309.

Erb, S., Graf, E., Zeder, Y., Lionetti, S., Berne, A., Clot, B., Lieberherr, G., Tummon, F., Wullschleger, P., Crouzy, B., 2023. EGU Sph. Prepr. Repos. 1–20.

Erdtman, G., 1937. Medd. Från Göteborgs Bot. Trädgård 12, 185–196.

Farah, J., Choël, M., de Nadaï, P., Balsamelli, J., Gosselin, S., Visez, N., 2020a. Aerobiologia (Bologna). 36, 683–695.

Farah, J., Choël, M., de Nadaï, P., Gosselin, S., Petitprez, D., Baroudi, M., Visez, N., 2020b. Aerobiologia (Bologna). 36, 171–182.

Feeney, P., Rodríguez, S.F., Molina, R., McGillicuddy, E., Hellebust, S., Quirke, M., Daly, S., O'Connor, D., Sodeau, J., 2018. Waste Manag. 76, 323–338.

Fennelly, M., Sewell, G., Prentice, M., O'Connor, D., Sodeau, J., 2017. Atmosphere (Basel). 9, 1.

Fernández-Rodríguez, S., Durán-Barroso, P., Silva-Palacios, I., Tormo-Molina, R., Maya-Manzano, J.M., Gonzalo-Garijo, Á., 2016. Process Saf. Environ. Prot. 101, 152–159.

Fernández-Rodríguez, S., Durán-Barroso, P., Silva-Palacios, I., Tormo-Molina, R., Maya-Manzano, J.M., Gonzalo-Garijo, Á., Monroy-Colin, A., 2018. J. Clean. Prod. 176, 1304–1315.

Ferreira, B., Ribeiro, H., Pereira, M.S., Cruz, A., Abreu, I., 2016. Aerobiologia (Bologna). 32, 421–430.

Fölster-Holst, R., Galecka, J., Weißmantel, S., Dickschat, U., Rippke, F., Bohnsack, K., Werfel, T., Wichmann, K., Buchner, M., Schwarz, T., Vogt, A., Lademann, J., Meinke, M.C., 2015. Clin.

Cosmet. Investig. Dermatol. 8, 539–548.

Franchi, G.G., Bellani, L., Nepi, M., Pacini, E., 1996. Flora 191, 143–159.

Frenguelli, G., Ghitarrini, S., Tedeschini, E., 2016. Ann. Agric. Environ. Med. 23, 92–96.

Frisk, C.A., Apangu, G.P., Petch, G.M., Adams-Groom, B., Skjøth, C.A., 2022. Sci. Total Environ. 814.

Gabey, A.M., Gallagher, M.W., Whitehead, J., Dorsey, J.R., Kaye, P.H., Stanley, W.R., 2010. Atmos. Chem. Phys. 10, 4453–4466.

Gabey, A.M., Stanley, W.R., Gallagher, M.W., Kaye, P.H., 2011. Atmos. Chem. Phys. 11, 5491–5504.

Galán, C., Ariatti, A., Bonini, M., Clot, B., Crouzy, B., Dahl, A., Fernandez-González, D., Frenguelli, G., Gehrig, R., Isard, S., Levetin, E., Li, D.W., Mandrioli, P., Rogers, C.A., Thibaudon, M., Sauliene, I., Skjoth, C., Smith, M., Sofiev, M., 2017. Aerobiologia (Bologna). 33, 293–295.

García-Mozo, H., Galán, C., Belmonte, J., Bermejo, D., Candau, P., Díaz de la Guardia, C., Elvira, B., Gutiérrez, M., Jato, V., Silva, I., Trigo, M.M., Valencia, R., Chuine, I., 2009. Agric. For. Meteorol. 149, 256–262.

García-Mozo, H., Yaezel, L., Oteros, J., Galán, C., 2014. Sci. Total Environ. 473–474, 103–109.

Ghiani, A., Aina, R., Asero, R., Bellotto, E., Citterio, S., 2012. Allergy Eur. J. Allergy Clin. Immunol. 67, 887–894.

Giertych, M.J., Karolewski, P., 1993. Arbor Kórnickie 38, 43–52.

Gilles, S., Blume, C., Wimmer, M., Damialis, A., Meulenbroek, L., Gökkaya, M., Bergougnan, C., Eisenbart, S., Sundell, N., Lindh, M., Andersson, L.M., Dahl, Å., Chaker, A., Kolek, F., Wagner, S., Neumann, A.U., Akdis, C.A., Garssen, J., Westin, J., van't Land, B., Davies, D.E., Traidl-Hoffmann, C., 2020. Allergy Eur. J. Allergy Clin. Immunol. 75, 576–587.

Gilles, S., Mariani, V., Bryce, M., Mueller, M.J., Ring, J., Behrendt, H., Jakob, T., Traidl-Hoffmann, C., 2009. Allergy, Asthma Clin. Immunol. 5.

González-Naharro, R., Quirós, E., Fernández-Rodríguez, S., Silva-Palacios, I., Maya-Manzano, J.M., Tormo-Molina, R., Pecero-Casimiro, R., Monroy-Colin, A., Gonzalo-Garijo, Á., 2019. Sci. Total Environ. 676, 407–419.

Gregory, P.H., 1973. The microbiology of the atmosphere. L. Hill.

Guedes, A., Ribeiro, N., Ribeiro, H., Oliveira, M., Noronha, F., Abreu, I., 2009. J. Aerosol Sci. 40, 81–86.

Guimarães, F., Duque, L., Ribeiro, H., Sousa, R., Abreu, I., 2012. IOP Conf. Ser. Mater. Sci. Eng. 32.

Gute, E., Abbatt, J.P.D., 2020. Atmos. Environ. 231, 117488.

Gute, E., David, R.O., Kanji, Z.A., Abbatt, J.P.D., 2020. ACS Earth Sp. Chem. 4, 2312–2319.

Haahtela, T., Holgate, S., Pawankar, R., Akdis, C.A., Benjaponpitak, S., Caraballo, L., Demain, J., Portnoy, J., Von Hertzen, L., 2013. World Allergy Organ. J. 6, 1–18.

Hader, J.D., Wright, T.P., Petters, M.D., 2014. Atmos. Chem. Phys. 14, 5433–5449.

Haga, D.I., Burrows, S.M., Iannone, R., Wheeler, M.J., Mason, R.H., Chen, J., Polishchuk, E.A., Pöschl, U., Bertram, A.K., 2014. Atmos. Chem. Phys. 14, 8611–8630.

Healy, D.A., Huffman, J.A., O'Connor, D.J., Pöhlker, C., Pöschl, U., Sodeau, J.R., 2014. Atmos. Chem. Phys. 14, 8055–8069.

Healy, D.A., O'Connor, D.J., Burke, A.M., Sodeau, J.R., 2012a. Atmos. Environ. 60, 534–543.

Healy, D.A., O'Connor, D.J., Sodeau, J.R., 2012b. J. Aerosol Sci. 47, 94–99.

Helander, M.L., Savolainen, J., Ahlholm, J., 1997. Allergy Eur. J. Allergy Clin. Immunol. 52, 1207–1214.

Heredia Rivera, B., Gerardo Rodriguez, M., 2016. Int. J. Environ. Res. Public Health 13.

Hesse, M., 1993. Pollenkitt development and composition in Tilia platyphyllos (Tiliaceae) analysed by conventional and energy filtering TEM. pp. 39–52.

Hirst, J.M., 1952. Ann. Appl. Biol. 39, 257–265.

Hoose, C., Kristjánsson, J.E., Burrows, S.M., 2010. Environ. Res. Lett. 5.

Hoose, C, Kristjánsson, J.E., Chen, J.P., Hazra, A., 2010. J. Atmos. Sci. 67, 2483–2503.

Howard, L.E., Levetin, E., 2014. Ann. Allergy, Asthma Immunol. 113, 641–646.

Huffman, J.A., Perring, A.E., Savage, N.J., Clot, B., Crouzy, B., Tummon, F., Shoshanim, O., Damit, B., Schneider, J., Sivaprakasam, V., Zawadowicz, M.A., Crawford, I., Gallagher, M., Topping, D., Doughty, D.C., Hill, S.C., Pan, Y., 2020. Aerosol Sci. Technol. 54, 465–495.

Hummel, M., Hoose, C., Pummer, B., Schaupp, C., Fröhlich-Nowoisky, J., Möhler, O., 2018. Atmos. Chem. Phys. 18, 15437–15450.

Hyde, P., Mahalov, A., 2019. J. Air Waste Manag. Assoc. 0, 1–7.

Iannotti, O., Mincigrucci, G., Bricchi, E., Frenguelli, G., 2000. Aerobiologia (Bologna). 16, 361–365.

Iglesias-Otero, M.A., Astray, G., Vara, A., Galvez, J.F., Mejuto, J.C., Rodriguez-Rajo, F.J., 2015. Fresenius Environ. Bull. 24, 4574–4580.

Janati, A., Bouziane, H., del Mar Trigo, M., Kadiri, M., Kazzaz, M., 2017. Aerobiologia (Bologna). 33, 517–528.

Jantunen, J., Saarinen, K., Rantio-Lehtimäki, A., 2012. Aerobiologia (Bologna). 28, 169–176.

Jarlan, L., Abaoui, J., Duchemin, B., Ouldbba, A., Tourre, Y.M., Khabba, S., Le Page, M., Balaghi, R., Mokssit, A., Chehbouni, G., 2014. Int. J. Biometeorol. 58, 1489–1502.

Jedryczka, M., Strzelczak, A., Grinn-Gofron, A., Nowak, M., Wolski, T., Siwulski, M., Sobieralski, K., Kaczmarek, J., 2015. Agric. For. Meteorol. 201, 209–217.

Jensen-Jarolim, E., Einhorn, L., Herrmann, I., Thalhammer, J.G., Panakova, L., 2015. Clin. Transl. Allergy 5, 1–9.

Kalbande, D.M., Dhadse, S.N., Chaudhari, P.R., Wate, S.R., 2008. Environ. Monit. Assess. 138, 233–238.

Kanter, U., Heller, W., Durner, J., Winkler, J.B., Engel, M., Behrendt, H., Holzinger, A., Braun, P., Hauser, M., Ferreira, F., Mayer, K., Pfeifer, M., Ernst, D., 2013. PLoS One 8.

Katifori, E., Alben, S., Cerda, E., Nelson, D.R., Dumais, J., 2010. Proc. Natl. Acad. Sci. U. S. A. 107, 7635–7639.

Katotomichelakis, M., Nikolaidis, C., Makris, M., Zhang, N., Aggelides, X., Constantinidis, T.C., Bachert, C., Danielides, V., 2015. Int. Forum Allergy Rhinol. 5, 1156–1163.

Katz, D.S.W., Batterman, S.A., 2019. Landsc. Urban Plan. 190, 103615.

Kaur, M., Sharma, A., Kaur, R., Katnoria, J.K., Nagpal, A.K., 2016. Aerobiologia (Bologna). 32, 245–254.

Kawashima, S., Clot, B., Fujita, T., Takahashi, Y., Nakamura, K., 2007. Atmos. Environ. 41, 7987–7993.

El Kelish, A., Zhao, F., Heller, W., Durner, J., Winkler, J.B., Behrendt, H., Traidl-Hoffmann, C., Horres, R., Pfeifer, M., Frank, U., Ernst, D., 2014. BMC Plant Biol. 14, 1–16.

Keller, T., Beda, H., 1984. Environ. Pollution. Ser. A, Ecol. Biol. 33, 237–243.

Kiselev, D., Bonacina, L., Wolf, J.-P., 2011. Opt. Express 19, 24516.

Kiselev, D., Bonacina, L., Wolf, J.P., 2013. Rev. Sci. Instrum. 84.

Knox, B., Suphioglu, C., 1996. Trends Plant Sci. 1, 156–164.

Lake, I.R., Jones, N.R., Agnew, M., Goodess, C.M., Giorgi, F., Hamaoui-Laguel, L., Semenov, M.A., Solomon, F., Storkey, J., Vautard, R., Epstein, M.M., 2017. Environ. Health Perspect. 125, 385–391.

Lara, B., Rojo, J., Fernández-gonzález, F., Pérez-badia, R., 2019. Landsc. Urban Plan. 189, 285–295.

Lee, K.S., Kim, K., Choi, Y.J., Yang, S., Kim, C.R., Moon, J.H., Kim, K.R., Lee, Y.S., Oh, J.W., 2021. Pediatr. Allergy Immunol. 32, 872–879.

Levin, Z., Cotton, W.R., 2009. Aerosol pollution impact on precipitation: A scientific review, Aerosol Pollution Impact on Precipitation: A Scientific Review.

Li, J., Wan, M.P., Schiavon, S., Tham, K.W., Zuraimi, S., Xiong, J., Fang, M., Gall, E., 2020. Indoor Air 30, 942–954.

Liu, X., Wu, D., Zewdie, G.K., Wijerante, L., Timms, C.I., Riley, A., Levetin, E., Lary, D.J., 2017. Environ. Health Insights 11, 117863021769939.

Lo, F., Bitz, C.M., Battisti, D.S., Hess, J.J., 2019. Aerobiologia (Bologna). 35, 613–633.

Lo, F., Bitz, C.M., Hess, J.J., 2021. Sci. Total Environ. 773, 145590.

Lops, Y., Choi, Y., Eslami, E., Sayeed, A., 2020. Neural Comput. Appl. 32, 11827–11836.

Lu, S., Ren, J., Hao, X., Liu, D., Zhang, R., Wu, M., Yi, F., Lin, J., Shinich, Y., Wang, Q., 2014. Aerobiologia (Bologna). 30, 281–291.

Lucas, R.W., Bunderson, L.D., Allan, N., 2016.

Lunau, K., 1995. Plant Syst. Evol. 198, 235–252.

Mahura, A., Baklanov, A., Korsholm, U., 2009. Aerobiologia (Bologna). 25, 203–208.

Mahura, A.G., Korsholm, U.S., Baklanov, A.A., Rasmussen, A., 2007. Aerobiologia (Bologna). 23, 171–179.

Maki, L.R., Galyan, E.L., Chang-Chien, M.M., Caldwell, D.R., 1974. Appl. Microbiol. 28, 456–459.

Mampage, C.B.A., Hughes, D.D., Jones, L.M., Metwali, N., Thorne, P.S., Stone, E.A., 2022. Atmos. Environ. X 15, 1–23.

Manninen, H.E., Sihto-Nissilä, S.L., Hiltunen, V., Aalto, P.P., Kulmala, M., Petäjä, T., Manninen, H.E., Bäck, J., Hari, P., Huffman, J.A., Huffman, J.A., Saarto, A., Pessi, A.M., Hidalgo, P.J., 2014. Boreal Environ. Res. 19, 383–405.

Marcovecchio, F., Perrino, C., 2021. Sustainability 13, 1149.

Markey, E., Clancy, J.H., Martínez-Bracero, M., Maya-Manzano, J.M., Smith, M., Skjøth, C.,

Dowding, P., Sarda-Estève, R., Baisnée, D., Donnelly, A., McGillicuddy, E., Sewell, G., O'Connor, D.J., 2022a. Aerobiologia (Bologna). 38, 343–366.

Markey, E., Hourihane Clancy, J., Martínez-Bracero, M., Neeson, F., Sarda-Estève, R., Baisnée, D., McGillicuddy, E.J., Sewell, G., O'Connor, D.J., 2022b. Sensors 22, 8747.

Martínez-Bracero, M., Alcázar, P., Díaz de la Guardia, C., González-Minero, F.J., Ruiz, L., Trigo Pérez, M.M., Galán, C., 2015. Aerobiologia (Bologna). 31, 549–557.

Martinez-Bracero, M., Markey, E., Clancy, J.H., McGillicuddy, E.J., Sewell, G., O'Connor, D.J., 2022. Atmosphere (Basel). 13, 308.

Maya-Manzano, J.M., Skjøth, C.A., Smith, M., Dowding, P., Sarda-Estève, R., Baisnée, D., McGillicuddy, E., Sewell, G., O'Connor, D.J., 2021. Agric. For. Meteorol. 298–299, 108298.

Maya-Manzano, Jose María, Smith, M., Markey, E., Hourihane Clancy, J., Sodeau, J., O´Connor, D.J., 2021. Grana 60, 1–19.

Maya-Manzano, J.M., Tummon, F., Abt, R., Allan, N., Bunderson, L., Clot, B., Crouzy, B., Daunys, G., Erb, S., Gonzalez-Alonso, M., Graf, E., Grewling, Ł., Haus, J., Kadantsev, E., Kawashima, S., Martinez-Bracero, M., Matavulj, P., Mills, S., Niederberger, E., Lieberherr, G., Lucas, R.W., O'Connor, D.J., Oteros, J., Palamarchuk, J., Pope, F.D., Rojo, J., Šaulienė, I., Schäfer, S., Schmidt-Weber, C.B., Schnitzler, M., Šikoparija, B., Skjøth, C.A., Sofiev, M., Stemmler, T., Triviño, M., Zeder, Y., Buters, J., 2023. Sci. Total Environ. 866.

McDonald, M.S., 1980. Grana 19, 53–56.

McDonald, M.S., O'Driscoll, B.J., 1980. Clin. Exp. Allergy 10, 211–215.

Miguel, A.G., Taylor, P.E., House, J., Glovsky, M.M., Flagan, R.C., 2006. Aerosol Sci. Technol. 40, 690–696.

Mikhailov, E.F., Ivanova, O.A., Nebosko, E.Y., Vlasenko, S.S., Ryshkevich, T.I., 2019. Izv. - Atmos. Ocean Phys. 55, 357–364.

Möhler, O., DeMott, P.J., Vali, G., Levin, Z., 2007. Biogeosciences Discuss. 4, 2559–2591.

Mohsenzadeh, F., Chehregani, A., Yousefi, N., 2011. Biol. Trace Elem. Res. 143, 1777–1788.

Motta, A.C., Marliere, M., Peltre, G., Sterenberg, P.A., Lacroix, G., 2006. Int. Arch. Allergy Immunol. 139, 294–298.

Murray, B.J., O'sullivan, D., Atkinson, J.D., Webb, M.E., 2012. Chem. Soc. Rev. 41, 6519–6554.

Muzalyova, A., Brunner, J.O., Traidl-Hoffmann, C., Damialis, A., 2021. Aerobiologia (Bologna). 37, 425–446.

Myszkowska, D., 2014a. Aerobiologia (Bologna). 30, 307–321.

Myszkowska, D., 2014b. Int. J. Biometeorol. 58, 975–986.

Myszkowska, D., Jenner, B., Stępalska, D., Czarnobilska, E., 2011. Aerobiologia (Bologna). 27, 229–238.

Myszkowska, D., Majewska, R., 2014. Ann. Agric. Environ. Med. 21, 681–688.

Myszkowska, D., Piotrowicz, K., Ziemianin, M., Bastl, M., Berger, U., Dahl, Å., Dąbrowska-Zapart, K., Górecki, A., Lafférsová, J., Majkowska-Wojciechowska, B., Malkiewicz, M., Nowak, M., Puc, M., Rybnicek, O., Saarto, A., Šaulienė, I., Ščevková, J., Kofol Seliger, A., Šikoparija, B., Piotrowska-Weryszko, K., Czarnobilska, E., 2021. Aerobiologia (Bologna). 37, 543–559.

Naas, O., Mendez, M., Quijada, M., Gosselin, S., Farah, J., Choukri, A., Visez, N., 2016. Environ. Pollut. 214, 816–821.

Nakamura, N., Suzuki, H., 1981. Phytochemistry 20, 981–984.

Nandi, P.K., Agrawal, M., Agrawal, S.B., Rao, D.N., 1990. Ecotoxicol. Environ. Saf. 19, 64–71.

Navares, R., Aznarte, J.L., 2019. Theor. Appl. Climatol.

Nicolaou, N., Siddique, N., Custovic, A., 2005. Allergy Eur. J. Allergy Clin. Immunol. 60, 1357–1360.

Nilsson, S., 1988. Aerobiologia (Bologna). 4, 4–7.

Novara, C., Falzoi, S., La Morgia, V., Spanna, F., Siniscalco, C., 2016. Aerobiologia (Bologna). 32, 555–569.

Novo-Lourés, M., Fernández-González, M., Pavón, R., Espinosa, K.C.S., Laza, R., Guada, G., Méndez, J.R., Fdez-Riverola, F., Rodríguez-Rajo, F.J., 2023. Forests 14.

Nowosad, J., 2016. Int. J. Biometeorol. 60, 843–855.

Nowosad, J., Stach, A., Kasprzyk, I., Weryszko-Chmielewska, E., Piotrowska-Weryszko, K., Puc, M., Grewling, Ł., Pędziszewska, A., Uruska, A., Myszkowska, D., Chłopek, K., Majkowska-Wojciechowska, B., 2016. Aerobiologia (Bologna). 32, 453–468.

Núñez, A., Amo de Paz, G., Rastrojo, A., García, A.M., Alcamí, A., Gutiérrez-Bustillo, A.M., Moreno, D.A., 2016. Int. Microbiol. 19, 1–13.

O'Connor, D., Markey, E., Maya-manzano, J.M., Dowding, P., Donnelly, A., Sodeau, J., 2022. Pollen Monitoring and Modelling (POMMEL).

O'Connor, D.J., Daly, S.M., Sodeau, J.R., 2015. Waste Manag. 42, 23–30.

O’Connor, D.J., Healy, D.A., Hellebust, S., Buters, J.T.M., Sodeau, J.R., 2014. Aerosol Sci. Technol. 48, 341–349.

O’Connor, D.J., Healy, D.A., Sodeau, J.R., 2013. Atmos. Environ. 80, 415–425.

O’Rourke, M.K., 1990. Aerobiologia (Bologna). 6, 136–140.

Oh, J.-W., 2018. Pollen Allergy a Chang. World.

Okuyama, Y., Matsumoto, K., Okochi, H., Igawa, M., 2007. Atmos. Environ. 41, 253–260.

Oleksyn, J., Reich, P.B., Karolewski, P., Tjoelker, M.G., Chalupka, W., 1999. n Water Air Soil Pollut. 110, 195–212.

Oteros, J., Pusch, G., Weichenmeier, I., Heimann, U., Möller, R., Röseler, S., Traidl-Hoffmann, C., Schmidt-Weber, C., Buters, J.T.M., 2015. Int. Arch. Allergy Immunol. 167, 158–66.

Ouyang, Y., Xu, Z., Fan, E., Li, Y., Zhang, L., 2016. Int. Forum Allergy Rhinol. 6, 95–100.

Pacini, E., 1996. Sex. Plant Reprod. 9, 362–366.

Pacini, E., 2010. Int. J. Plant Sci. 171, 1–11.

Pacini, E., Franchi, G.G., 2020. Bot. J. Linn. Soc. 193, 141–164.

Pacini, E., Guarnieri, M., Nepi, M., 2006. Protoplasma 228, 73–77.

Pacini, E., Hesse, M., 2005. Flora Morphol. Distrib. Funct. Ecol. Plants 200, 399–415.

Paramonov, M., Paramonov, M., Van Dusseldorp, S.D., Gute, E., Abbatt, J.P.D., Heikkilä, P., Keskinen, J., Chen, X., Chen, X., Luoma, K., Heikkinen, L., Hao, L., Petäjä, T., Kanji, Z.A., 2020. Atmos. Chem. Phys. 20, 6687–6706.

Pasqualini, S., Tedeschini, E., Frenguelli, G., Wopfner, N., Ferreira, F., D’Amato, G., Ederli, L., 2011. Environ. Pollut. 159, 2823–2830.

Paudel, B., Chu, T., Chen, M., Sampath, V., Prunicki, M., Nadeau, K.C., 2021. Sci. Rep. 11, 1–12.

Pauling, A., Gehrig, R., Clot, B., 2014. Aerobiologia (Bologna). 30, 45–57.

Pecero-Casimiro, R., Maya-Manzano, J.M., Fernández-Rodríguez, S., Tormo-Molina, R., Silva-Palacios, I., Monroy-Colín, A., Gonzalo-Garijo, Á., 2020. Aerobiologia (Bologna). 36, 731–748.

Penner, J.E., Xu, L., Wang, M., 2011. Proc. Natl. Acad. Sci. U. S. A. 108, 13404–13408.

Pereira, S., Fernández-González, M., Guedes, A., Abreu, I., Ribeiro, H., 2021. Forests 12, 88.

Phillips, V.T.J., Andronache, C., Christner, B., Morris, C.E., Sands, D.C., Bansemer, A., Lauer, A., McNaughton, C., Seman, C., 2009. Biogeosciences 6, 987–1014.

Picornell, A., Oteros, J., Trigo, M.M., Gharbi, D., Docampo Fernández, S., Melgar Caballero, M., Toro, F.J., García-Sánchez, J., Ruiz-Mata, R., Cabezudo, B., Recio, M., 2019. Chemosphere 234, 668–681.

Piotrowska-Weryszko, K., 2013a. Grana 52, 221–228.

Piotrowska-Weryszko, K., 2013b. Acta Sci. Pol. Hortorum Cultus 12, 155–168.

Piotrowska, K., 2012. Grana 51, 263–269.

Plaza, M.P., Kolek, F., Leier-Wirtz, V., Brunner, J.O., Traidl-Hoffmann, C., Damialis, A., 2022. Int. J. Environ. Res. Public Health 19.

Pope, F.D., 2010. Environ. Res. Lett. 5.

Von Post, L., 1946. New Phytol. Trust 45, 193–217.

Prank, M., Chapman, D.S., Bullock, J.M., Belmonte, J., Berger, U., Dahl, A., Jäger, S., Kovtunenko, I., Magyar, D., Niemelä, S., Rantio-Lehtimäki, A., Rodinkova, V., Sauliene, I., Severova, E., Sikoparija, B., Sofiev, M., 2013. Agric. For. Meteorol. 182–183, 43–53.

Prank, M., Sofiev, M., Siljamo, P., Kauhaniemi, M., 2016. Increasing the number of allergenic pollen species in SILAM forecasts., in: Estimating the Impact of Air Pollution Controls on Ambient Concentrations. pp. 313–317.

Pratt, K.A., Demott, P.J., French, J.R., Wang, Z., Westphal, D.L., Heymsfield, A.J., Twohy, C.H., Prenni, A.J., Prather, K.A., 2009. Nat. Geosci. 2, 398–401.

Prenni, A.J., Petters, M.D., Kreidenweis, S.M., Heald, C.L., Martin, S.T., Artaxo, P., Garland, R.M., Wollny, A.G., Pöschl, U., 2009. Nat. Geosci. 2, 402–405.

Puc, M., 2012. Int. J. Biometeorol. 56, 395–401.

Puc, M., Wolski, T., 2013. Ann. Agric. Environ. Med. 20, 36–47.

Pummer, B.G., Bauer, H., Bernardi, J., Bleicher, S., Grothe, H., 2012. Atmos. Chem. Phys. 12, 2541–2550.

Ranta, H., Kubin, E., Siljamo, P., Sofiev, M., Linkosalo, T., Oksanen, A., Bondestam, K., 2006. Grana 45, 297–304.

Raynor, G.S., Hayes, J. V., Ogden, E.C., 1974. J. Appl. Meteorol. 13, 87–95.

Recknagel, F., 2001. Ecol. Modell. 146, 303–310.

Reinmuth-Selzle, K., Kampf, C.J., Lucas, K., Lang-Yona, N., Fröhlich-Nowoisky, J., Shiraiwa, M., Lakey, P.S.J., Lai, S., Liu, F., Kunert, A.T., Ziegler, K., Shen, F., Sgarbanti, R., Weber, B., Bellinghausen, I., Saloga, J., Weller, M.G., Duschl, A., Schuppan, D., Pöschl, U., 2017.

Environ. Sci. Technol. 51, 4119–4141.

Rezanejad, F., 2007. Turk. J. Botany 31, 183–191.

Rezanejad, F., 2009. Grana 48, 205–213.

Rezanejad, F., 2012. Turk. J. Botany 36, 49–54.

Rezanejad, F., Majd, A., Shariatzadeh, S.M.A., Moein, M., Aminzadeh, M., Mirzaeian, M., 2003. Acta Biol. Cracoviensia Ser. Bot. 45, 129–132.

Ribeiro, H., Costa, C., Abreu, I., Esteves da Silva, J.C.G., 2017. Sci. Total Environ. 599–600, 291–297.

Ribeiro, H., Duque, L., Sousa, R., Cruz, A., Gomes, C., Esteves Da Silva, J., Abreu, I., 2014. Int. J. Environ. Health Res. 24, 515–527.

Ribeiro, H., Guimarães, F., Duque, L., Noronha, F., Abreu, I., 2015. Environ. Pollut. 206, 7–16.

Robichaud, A., Comtois, P., 2017. Aerobiologia (Bologna). 33, 529–554.

Robinson, E.S., Gao, R.S., Schwarz, J.P., Fahey, D.W., Perring, A.E., 2017. Atmos. Meas. Tech. 10, 1755–1768.

Rogerieux, F., Godfrin, D., Sénéchal, H., Motta, A.C., Marlière, M., Peltre, G., Lacroix, G., 2007. Int. Arch. Allergy Immunol. 143, 127–134.

Rojo, J., Picornell, A., Oteros, J., 2019. Methods Ecol. Evol. 10, 1371–1376.

Rojo, J., Rivero, R., Romero-Morte, J., Fernández-González, F., Pérez-Badia, R., 2017. Int. J. Biometeorol. 61, 335–348.

Roldán, N.G., Engel, R., Düpow, S., Jakob, K., Koops, F., Orinska, Z., Vigor, C., Oger, C., Galano, J.M., Durand, T., Jappe, U., Duda, K.A., 2019. Front. Immunol. 10, 1–11.

Roshchina, V. V., Karnaukhov, V.N., 1999. Biol. Plant. 42, 273–278.

Roshchina, V. V., Mel'nikova, E. V., 2001. Russ. J. Plant Physiol. 48, 74–83.

Sabariego, S., Cuesta, P., Fernández-González, F., Pérez-Badia, R., 2012. Int. J. Biometeorol. 56, 253–258.

Sánchez-Mesa, J.A., Galan, C., Martínez-Heras, J.A., Hervás-Martínez, C., 2002. Clin. Exp. Allergy 32, 1606–1612.

Sánchez Mesa, J.A., Galán, C., Hervás, C., 2005. Int. J. Biometeorol. 49, 355–362.

Šauliene, I., Šukiene, L., Daunys, G., Valiulis, G., Vaitkevičius, L., Matavulj, P., Brdar, S., Panic, M., Sikoparija, B., Clot, B., Crouzy, B., Sofiev, M., 2019. Atmos. Meas. Tech. 12, 3435–3452.

Šauliene, I., Veriankaite, L., 2006. J. Environ. Eng. Landsc. Manag. 14, 113–120.

Sauvageat, E., Zeder, Y., Auderset, K., Calpini, B., Clot, B., Crouzy, B., Konzelmann, T., Lieberherr, G., Tummon, F., Vasilatou, K., 2020. Atmos. Meas. Tech. 13, 1539–1550.

Schnell, R.C., Vali, G., 1972. Nature 236, 163–165.

Scott, R.J., 1994. Pollen exine – the sporopollenin enigma and the physics of pattern, in: Molecular and Cellular Aspects of Plant Reproduction. Cambridge University Press, pp. 49–82.

Sedghy, F., Sankian, M., Moghadam, M., Ghasemi, Z., Mahmoudi, M., Varasteh, A.R., 2017. Int. J. Biometeorol. 61, 1–9.

Sedghy, F., Varasteh, A.R., Sankian, M., Moghadam, M., 2018. Interaction between air pollutants and pollen grains: The role on the rising trend in allergy. Reports Biochem. Mol. Biol.

Sénéchal, H., Visez, N., Charpin, D., Shahali, Y., Peltre, G., Biolley, J.-P., Lhuissier, F., Couderc, R., Yamada, O., Malrat-Domenge, A., Pham-Thi, N., Poncet, P., Sutra, J.-P., 2015. Sci. World J. 2015, 1–29.

Sesartic, A., Lohmann, U., Storelvmo, T., 2013. Environ. Res. Lett. 8.

Shahali, Y., Pourpak, Z., Moin, M., Mari, A., Majd, A., 2009a. Allergy 64, 1773–9.

Shahali, Y., Pourpak, Z., Moin, M., Zare, A., Majd, A., 2009b. J. Phys. Conf. Ser. 151, 012027.

Sicard, P., Thibaudon, M., Besancenot, J.P., Mangin, A., 2012. Grana 51, 52–62.

Šikoparija, B., Marko, O., Panić, M., Jakovetić, D., Radišić, P., 2018. Aerobiologia (Bologna). 34, 203–217.

Šikoparija, B., Skjøth, C.A., Alm Kübler, K., Dahl, A., Sommer, J., Grewling, L., Radišić, P., Smith, M., 2013. Agric. For. Meteorol. 180, 112–117.

Siniscalco, C., Caramiello, R., Migliavacca, M., Busetto, L., Mercalli, L., Colombo, R., Richardson, A.D., 2015. Int. J. Biometeorol. 59, 837–848.

Skjøth, C.A., Ørby, P. V., Becker, T., Geels, C., Schlünssen, V., Sigsgaard, T., Bønløkke, J.H., Sommer, J., Søgaard, P., Hertel, O., 2013. Biogeosciences 10, 541–554.

Skjøth, C.A., Smith, M., Brandt, J., Emberlin, J., 2009. Int. J. Biometeorol. 53, 75–86.

Skjøth, C.A., Sommer, J., Stach, A., Smith, M., Brandt, J., 2007. Clin. Exp. Allergy 37, 1204–1212.

Skjøth, C.A., Werner, M., Kryza, M., Adams-Groom, B., Wakeham, A., Lewis, M., Kennedy, R., 2015. Adv. Meteorol. 2015.

Smith, H.R., Larsen, G.L., Cherniack, R.M., Wenzel, S.E., Voelkel, N.F., Westcott, J.Y., Bethel,

R.A., 1992. J. Allergy Clin. Immunol. 89, 1076–1084.

Smith, M., Emberlin, J., 2005. Clin. Exp. Allergy 35, 1400–1406.

Smith, M., Skjøth, C.A., Myszkowska, D., Uruska, A., Puc, M., Stach, A., Balwierz, Z., Chlopek, K., Piotrowska, K., Kasprzyk, I., Brandt, J., 2008. Agric. For. Meteorol. 148, 1402–1411.

Sodeau, J.R., O'Connor, D.J., 2016. Bioaerosol Monitoring of the Atmosphere for Occupational and Environmental Purposes, in: Comprehensive Analytical Chemistry. Elsevier Ltd, pp. 391–420.

Sofiev, M., Belmonte, J., Gehrig, R., Izquierdo, R., Smith, M., Dahl, Å., Siljamo, P., 2013. Airborne Pollen Transport, in: Allergenic Pollen. Springer Netherlands, Dordrecht, pp. 127–159.

Sofiev, M., Berger, U., Prank, M., Vira, J., Arteta, J., Belmonte, J., Bergmann, K.C., Chéroux, F., Elbern, H., Friese, E., Galan, C., Gehrig, R., Khvorostyanov, D., Kranenburg, R., Kumar, U., Marécal, V., Meleux, F., Menut, L., Pessi, A.M., Robertson, L., Ritenberga, O., Rodinkova, V., Saarto, A., Segers, A., Severova, E., Sauliene, I., Siljamo, P., Steensen, B.M., Teinemaa, E., Thibaudon, M., Peuch, V.H., 2015. Atmos. Chem. Phys. 15, 8115–8130.

Sofiev, M., Ritenberga, O., Albertini, R., Arteta, J., Belmonte, J., Bernstein, C.G., Bonini, M., Celenk, S., Damialis, A., Douros, J., Elbern, H., Friese, E., Galan, C., Oliver, G., Hrga, I., Kouznetsov, R., Krajsek, K., Magyar, D., Parmentier, J., Plu, M., Prank, M., Robertson, L., Marie Steensen, B., Thibaudon, M., Segers, A., Stepanovich, B., Valdebenito, A.M., Vira, J., Vokou, D., 2017. Atmos. Chem. Phys. 17, 12341–12360.

Sofiev, M., Siljamo, P., Ranta, H., Rantio-Lehtimäki, A., 2006. Int. J. Biometeorol. 50, 392–402.

Speranza, A., Calzoni, G.L., Pacini, E., 1997. Sex. Plant Reprod. 10, 110–115.

Spracklen, D. V., Heald, C.L., 2014. Atmos. Chem. Phys. 14, 9051–9059.

Steiner, A.L., Brooks, S.D., Deng, C., Thornton, D.C.O., Pendleton, M.W., Bryant, V., 2015. Geophys. Res. Lett. 42, 3596–3602.

Steiner, A.L., Solmon, F., 2018. Geophys. Res. Lett. 45, 7156–7164.

Stępalska, D., Myszkowska, D., Piotrowicz, K., Kluska, K., Chłopek, K., Grewling, Ł., Lafférsová, J., Majkowska-Wojciechowska, B., Malkiewicz, M., Piotrowska-Weryszko, K., Puc, M., Rodinkova, V., Rybníček, O., Ščevková, J., Voloshchuk, K., 2020. Sci. Total Environ. 736.

Subiza, J., Cabrera, M., Cárdenas-Rebollo, J.M., Craciunescu, J.C., Narganes, M.J., 2021. Clin. Exp. Allergy 1–4.

Tassan-Mazzocco, F., Felluga, A., Verardo, P., 2015. Aerobiologia (Bologna). 31, 559–574.

Taylor, P.E., Flagan, R.C., Miguel, A.G., Valenta, R., Glovsky, M.M., 2004. Clin. Exp. Allergy 34, 1591–1596.

Temizer, İ.K., Güder, A., Temel, F.A., Avci, E., 2018. Environ. Monit. Assess. 190.

Tešendić, D., Boberić Krstićev, D., Matavulj, P., Brdar, S., Panić, M., Minić, V., Šikoparija, B., 2020. Enterp. Inf. Syst. 00, 1–17.

Toprak, E., Schnaiter, M., 2013. Atmos. Chem. Phys. 13, 225–243.

Traidl-Hoffmann, C., Kasche, A., Jakob, T., Huger, M., Plötz, S., Feussner, I., Ring, J., Behrendt, H., 2002. J. Allergy Clin. Immunol. 109, 831–838.

Tseng, Y.T., Kawashima, S., Kobayashi, S., Takeuchi, S., Nakamura, K., 2018. Agric. For. Meteorol. 249, 35–43.

Tummon, F., Adamov, S., Clot, B., Crouzy, B., Gysel-Beer, M., Kawashima, S., Lieberherr, G., Manzano, J., Markey, E., Moallemi, A., O'Connor, D., 2021. Aerobiologia (Bologna). 0.

Valencia, J.A., Astray, G., Fernández-González, M., Aira, M.J., Rodríguez-Rajo, F.J., 2019. Int. J. Biometeorol. 63, 735–745.

Vélez-Pereira, A.M., De Linares, C., Belmonte, J., 2021. Sci. Total Environ. 795.

Vélez-Pereira, A.M., De Linares, C., Belmonte, J., 2022. Sci. Total Environ. 845.

Verstraeten, W.W., Dujardin, S., Hoebeke, L., Bruffaerts, N., Kouznetsov, R., Dendoncker, N., Hamdi, R., Linard, C., Hendrickx, M., Sofiev, M., Delcloo, A.W., 2019. Aerobiologia (Bologna). 35, 703–717.

Visez, N., Ivanovsky, A., Roose, A., Gosselin, S., Sénéchal, H., Poncet, P., Choël, M., 2020. Aerobiologia (Bologna). 36, 49–62.

Wang, Q., Gong, X., Nakamura, S., Kurihara, K., Suzuki, M., Sakamoto, K., Miwa, M., Lu, S., 2009. Air pollutant deposition effect and morphological change of Cryptomeria japonica pollen during its transport in urban and mountainous areas of Japan, in: WIT Transactions on Biomedicine and Health. pp. 77–89.

Wang, R., Dobritsa, A.A., 2018. Exine and aperture patterns on the pollen surface: Their formation and roles in plant reproduction, Annual Plant Reviews Online.

de Weger, L.A., Beerthuizen, T., Hiemstra, P.S., Sont, J.K., 2014. Int. J. Biometeorol. 58, 1047–55.

de Weger, L.A., Pashley, C.H., Šikoparija, B., Skjøth, C.A., Kasprzyk, I., Grewling, Ł., Thibaudon, M., Magyar, D., Smith, M., 2016. Int. J. Biometeorol. 60, 1829–1839.

Werchan, M., Werchan, B., Bergmann, K.C., 2018. Allergo J. Int. 27, 69–71.

Werner, M., Guzikowski, J., Kryza, M., Malkiewicz, M., Bilińska, D., Skjøth, C.A., Rapiejko, P., Chłopek, K., Dąbrowska-Zapart, K., Lipiec, A., Jurkiewicz, D., Kalinowska, E., Majkowska-

Wojciechowska, B., Myszkowska, D., Piotrowska-Weryszko, K., Puc, M., Rapiejko, A., Siergiejko, G., Weryszko-Chmielewska, E., Wieczorkiewicz, A., Ziemianin, M., 2021. Int. J. Biometeorol. 65, 513–526.

Whitehead, J.D., Gallagher, M.W., Dorsey, J.R., Robinson, N., Gabey, A.M., Coe, H., McFiggans, G., Flynn, M.J., Ryder, J., Nemitz, E., Davies, F., 2010. Atmos. Chem. Phys. 10, 9369–9382.

Wiermann, R., Gubatz, S., 1992. Int. Rev. Cytol. 140, 35–72.

Williams, C.G., 2008. Can. J. For. Res. 38, 2177–2188.

Williams, D., Banerjee, U., Pinnix, K., Ruffin, J., 1983. Grana 22, 171–175.

Wolters, A.J.H.B., Martens, M.J.M., 1987. 53, 372–414.

Wörl, V., Jetschni, J., Jochner-Oette, S., 2022. Atmosphere (Basel). 13.

Yousefi, N., Chehregani, A., Malayeri, B., Lorestani, B., Cheraghi, M., 2011. Biol. Trace Elem. Res. 140, 368–376.

Zewdie, G.K., Lary, D.J., Levetin, E., Garuma, G.F., 2019a. Int. J. Environ. Res. Public Health 16.

Zewdie, G.K., Lary, D.J., Liu, X., Wu, D., Levetin, E., 2019b. Environ. Monit. Assess. 191.

Zewdie, G.K., Liu, X., Wu, D., Lary, D.J., Levetin, E., 2019c. Environ. Monit. Assess. 191.

Zhang, R., Duhl, T., Salam, M.T., House, J.M., Flagan, R.C., Avol, E.L., Gilliland, F.D., Guenther, A., Chung, S.H., Lamb, B.K., VanReken, T.M., 2014. Biogeosciences 11, 1461–1478.

Zhang, X., Wang, J., 2022. J. Saf. Sci. Resil. 3, 372–397.

Zhang, Y., Bielory, L., Cai, T., Mi, Z., Georgopoulos, P., 2015. Atmos. Environ. 103, 297–306.

Zhao, F., Elkelish, A., Durner, J., Lindermayr, C., Winkler, J.B., Ruioff, F., Behrendt, H., Traidl-Hoffmann, C., Holzinger, A., Kofler, W., Braun, P., Von Toerne, C., Hauck, S.M., Ernst, D., Frank, U., 2016. Plant Cell Environ. 39, 147–164.

Zhao, W., Wang, J., Zhang, G., 2018. Int. J. Performability Eng. 14, 2808–2819.

Zhu, C., Farah, J., Choël, M., Gosselin, S., Baroudi, M., Petitprez, D., Visez, N., 2018. Environ. Pollut. 242, 880–886.

Zink, K., Kaufmann, P., Petitpierre, B., Broennimann, O., Guisan, A., Gentilini, E., Rotach, M.W., 2017. Int. J. Biometeorol. 61, 23–33.

Zink, K., Vogel, H., Vogel, B., Magyar, D., Kottmeier, C., 2012. Int. J. Biometeorol. 56, 669–680.

Zuberbier, T., Lötvall, J., Simoens, S., Subramanian, S. V., Church, M.K., 2014. Allergy Eur. J. Allergy Clin. Immunol. 69, 1275–1279.

Chapter 2: Methods & Instrumentation

This chapter is composed of a series of general introductions regarding the specific instrumentation used throughout this project, as well as a summary of operating procedures and theoretical principles. The traditional volumetric Hirst method was used to monitor ambient pollen concentrations as well to act as a standard method to compare real-time devices to. The WIBS-NEO device was deployed to evaluate the possibility of its use for the real-time detection of pollen. Infrared spectroscopy and fluorescent confocal microscopy were employed to study the chemical composition of pollen grain surfaces of differing pollen taxa as well as changes induced as a result of varying exposure scenarios.

2.1 Traditional volumetric method – pollen sampling

2.1.1 Irish pollen network - sampling sites

The majority of work presented in this thesis is largely dedicated to sampling conducted at the Dublin sampling site(s) however, as of 2023 there are currently 3 active pollen sampling sites located across Ireland. These sites are located in Dublin, Cork and Sligo and are illustrated graphically in Figure 2.1 below. Sampling was conducted at a site in Carlow from 2018-2021 (also shown) but was then discontinued due to operational issues. These sampling sites were originally established as part of the EPA-funded POMMEL and FONTANA projects (O'Connor et al., 2022b, 2022a). Sampling is carried out in accordance with requirements/standards previously established by the EAN (Galán et al., 2014, 2007). Monitoring efforts at sites in Dublin have been operating continuously since 2017. Originally, the Dublin site was located at the former Kevin Street campus of TU Dublin. However, following campus closure and relocation, the sampling position was moved to the Met Éireann facilities in 2022. The sampling station at Cork (University College Cork) also commenced operation in 2018, however, this site has experienced several periods of interruption to sampling. In addition to these existing sampling sites, a new site was established in Sligo in March 2021. All established sampling stations in Ireland currently use the volumetric suction sampler, initially designed by Hirst, (1952).

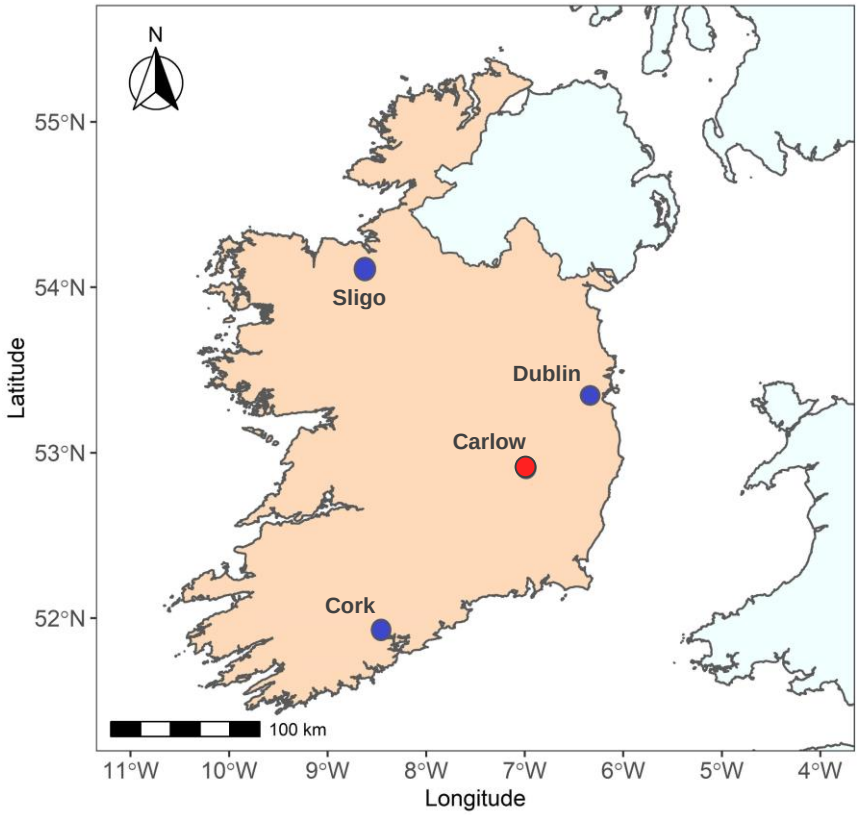

Figure 2.1: Irish pollen monitoring network (blue=current sites, red=retired sites)

2.1.2 Hirst operation

There are two Hirst-type samplers commercially available, these include the Lanzoni and Burkard 7-day samplers. An example of the Hirst-Lanzoni instrument used at the Dublin site is displayed below (Figure 2.2).

Figure 2.2: Hirst sampler deployed at Dublin sampling site

The Hirst sampler operates on the basis of volumetric impaction and is composed of three main instrumental components: an impact unit, a wind vane and a vacuum pump (Galán et al., 2007). The different components can be seen in Figure 2.3.

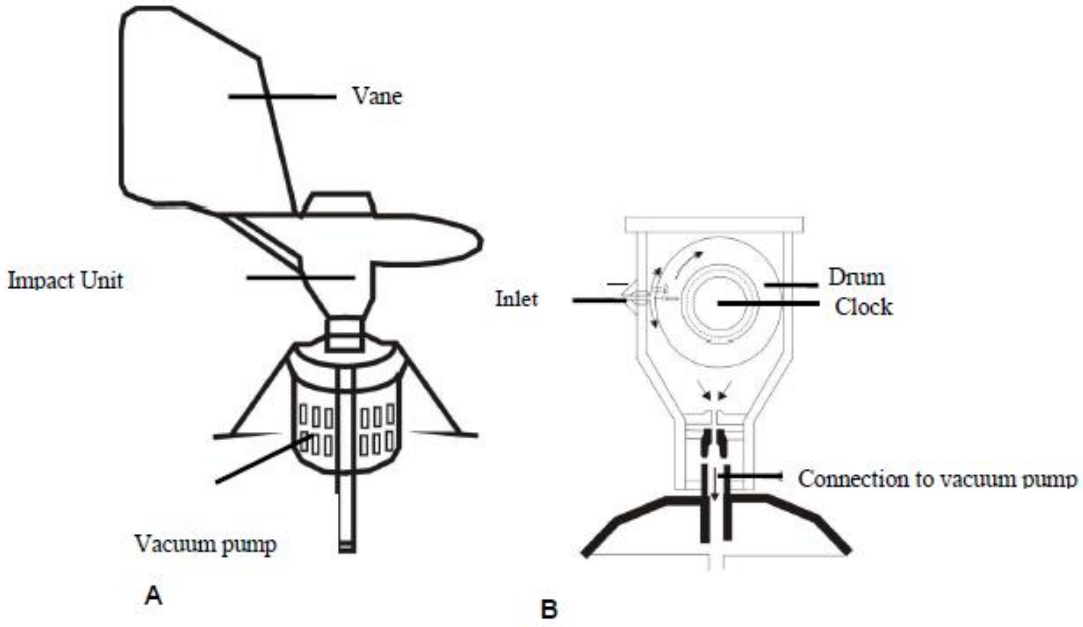

Figure 2.3: Schematic of (A) Hirst-Volumetric sampler and (B) Impact Unit, adapted from (Galán et al., 2007)

The impact unit is comprised of the sample inlet (14 x 2 mm) and sample drum. The drum operates using a clockwork mechanism which rotates at a rate of 2 mm per hour allowing for the determination of both hourly/bi-hourly and daily data. Particles entering the sampler are impacted onto a suitable substrate such as a silicone-coated tape (obtained from Lanzoni). The tape is attached to the outer circumference of the drum, which can later be removed and prepared accordingly for microscopic analysis. The second component of the Hirst system is the wind vane. The addition of a wind vane to the outer metal casing of the Hirst ensures that the sample inlet is always facing the prevailing wind direction to efficiently capture airborne particles (Galán et al., 2007). The final component of the Hirst instrument is the vacuum pump which is used to regulate the air flow entering the sampler. The flow rate of the Hirst is set to 10 L/min which mimics the rate of the human respiratory system.

2.1.3 Establishing suitable site - requirements

When choosing sampling sites and installing the samplers for monitoring there are several requirements that need to be met (Galán et al., 2007):

1. The sampler should be positioned on a flat, easily accessible surface.

2. The sampler should be positioned at a suitable location such that adjacent buildings etc. do not hinder air flow. In Dublin and Cork, this meant positioning the Hirst samplers at appropriate sampling points on roof, whereas in Carlow and Sligo, samplers were positioned atop constructed platforms due to the lack of surrounding infrastructure.
3. The sampler itself should be elevated accordingly using a small tripod which is used to reduce the impact of air turbulence.
4. Avoid placing the sampler in the direct vicinity of known sources of biological and non-biological particulate matter. In the case of known sources of pollen, this could result in the over-representation of some pollen types.
5. The sampling location must have access to electrical sockets as the vacuum pump requires a constant supply of electricity to function
6. Once a suitable location is selected, the sampler should be anchored securely in place

2.1.4 Preparing sampling drum

Apparatus Required:

- Hirst sample drum
- Drum case
- Lanzoni silicone tape
- Tweezers
- Double sided tape
- Flowmeter
- Turning key for Hirst clock mechanism

The initial step in preparing the Hirst samplers is to prepare the internal drum containing the silicone tape substrate, on which the ambient pollen/fungal spores will be impacted upon. The internal drum is removable and can function continuously for one week. The drums are marked with several lines indicating the start/end of the sampling period and how to position the drum inside the Hirst's inner cavity, illustrated below.

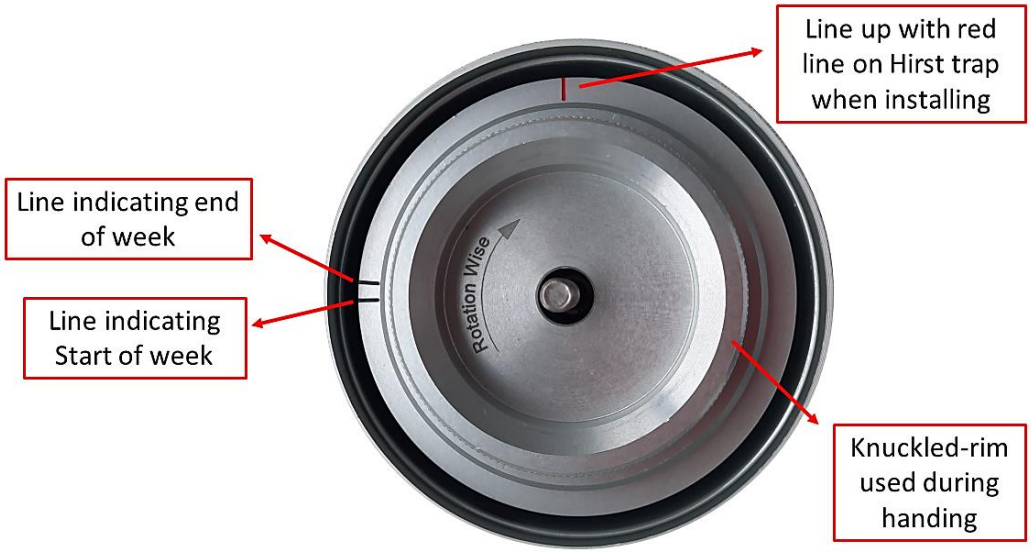

Figure 2.4: Hirst drum

The Lanzoni silicone tape is secured to the outside of the drum with a small piece of double-sided sticky tape placed between the black lines (Figure 2.5). Tweezers are used to avoid contaminating the tape or damaging the silicone coating. The two ends of the tape should meet at the middle black line without any gaps as shown below.

Figure 2.5: Hirst Drum: Tape Positioning

Once the drum has been prepared it is important to place it into a drum case, to avoid any possible contamination when transporting the drum to the Hirst device. When changing/installing the Hirst drum, there is a latch on the outer casing of the Hirst that prevents the wind vane from moving/rotating during set up. Once the sampler is secured, the locking arm of the sampler can be rotated 180° and the head of the Hirst can then be removed from inside the impact unit. This contains the clock mechanism and drum (from the previous week). If there is a drum already attached to the clock mechanism it is removed and placed in a drum case. It is important that prepared/collected drums are only handled by the outer knuckled rim, as shown in Figure 2.4, to avoid any contamination, sample removal or dislodging the secured tape.

The new (unexposed) drum can then be connected to the clockwork mechanism shown in Figure 2.6. When positioning the drum on the clock within the head of the Hirst, it is important that the red line on the drum is lined up with the red line or metal arrow of the Hirst since this marks the sequence of sample collection over the whole sampling period. The clock is then wound manually in an anti-clockwise direction using a turning key until it cannot be turned any further (without applying too much force). Once wound appropriately, the clock will be heard ticking and should last the full 7-day duration until the next drum changing.

Figure 2.6: Correct positioning of the drum, and clockwork mechanism.

The head containing the new drum and wound clock is then placed inside the internal Hirst casing. A wooden guide is attached to the inside of the Hirst to ensure correct positioning. Once

placed correctly inside the hirst the locking arm can be repositioned to lock the head in place. While the wind vane is still locked in place, the sampling orifice is examined and cleaned (if needed) and the flow rate is checked using a flowmeter and adjusted if required (to 10 L/min) using the bolt positioned on the outside of the Hirst in Lanzoni model.

The wind vane can then be released. This method is repeated weekly, ideally at the same hour (±20 mins). The used drum (collected) containing the sampling tape, can then be prepared for microscopic analysis.

2.1.5 Slide preparation

Apparatus Required:

- Perspex mounting ruler
- Scalpel
- Tweezers
- Microscope slides
- Coverslips
- Labels
- Fine tip permanent marker/pen
- Pasteur pipette
- Wash bottle

Reagents Required:

- Prepared slide media (see the following section for preparation instructions)
- Distilled water
- Ethanol
- Clear nail varnish

Label each microscope slide to be prepared with the corresponding date and time using a permanent marker. The drum containing exposed tape is first removed from the drum case. Using tweezers and/or dissecting needle the end of the tape attached to the double-sided tape is lifted, making sure to only handle the edge with tweezers. The tape is carefully removed from the drum and transferred to the Perspex cutting ruler. A holder can be used to hold the drum when doing this. A few drops of

water are placed on the Perspex ruler prior to using a Pasteur pipette or wash bottle; this allows for suction between the tape and ruler when cut, making the process easier.

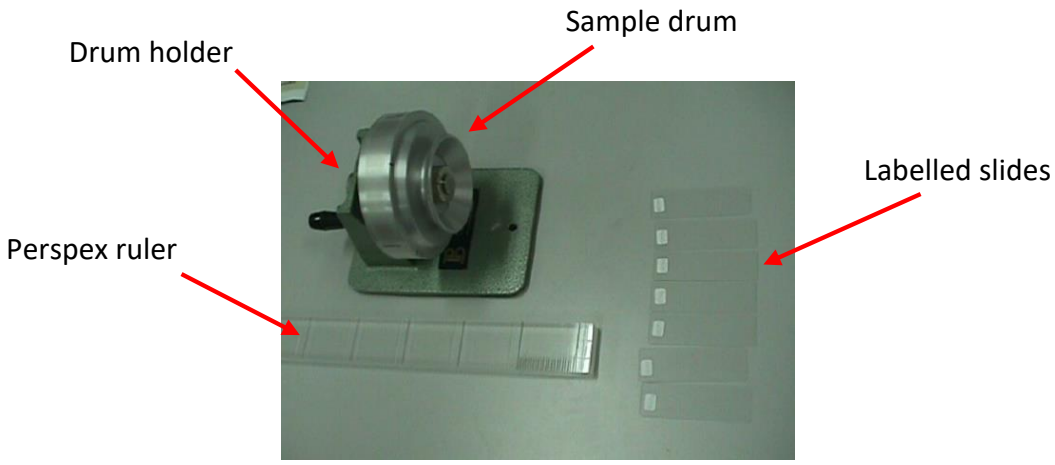

Figure 2.7: Experimental set-up for preparing slides

The Perspex ruler, shown in Figure 2.8, makes it possible to cut the tape into daily sections. The start of sampling it lined up with the first notch. A sharp scalpel is then used to cut the tape at each of the segments (48 mm apart) – signifying a 24-hour period. Each segment is transferred to the corresponding labelled slide using tweezers.

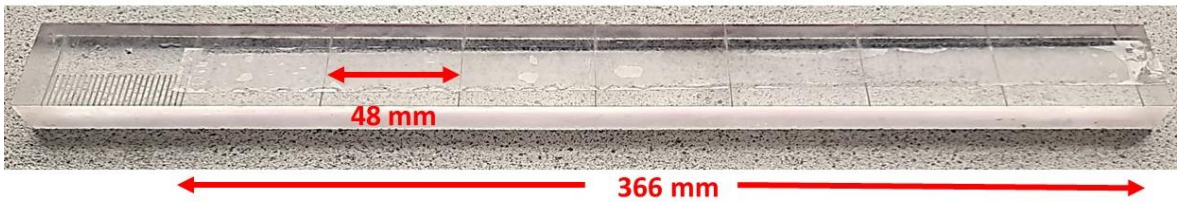

Figure 2.8: Schematic of tape over Perspex ruler showing daily segments

The slides are then mounted using a glycerine jelly media containing fuchsin stain, the preparation of which is described in the following section. The media is heated on a heating mantle until the consistency is sufficiently thin (glycerine gelatine is solid at room temperature). A Pasteur pipette is then used to apply thin beads of the colourant directly onto the tape (Figure 2.9A). A coverslip is then quickly applied, taking care to spread the media evenly by applying gentle pressure to the coverslip. Any air bubbles should be removed using gentle pressure to the coverslip. The slides are then placed upside-down to dry on some tissue paper. This is done to absorb any excess gelatine.

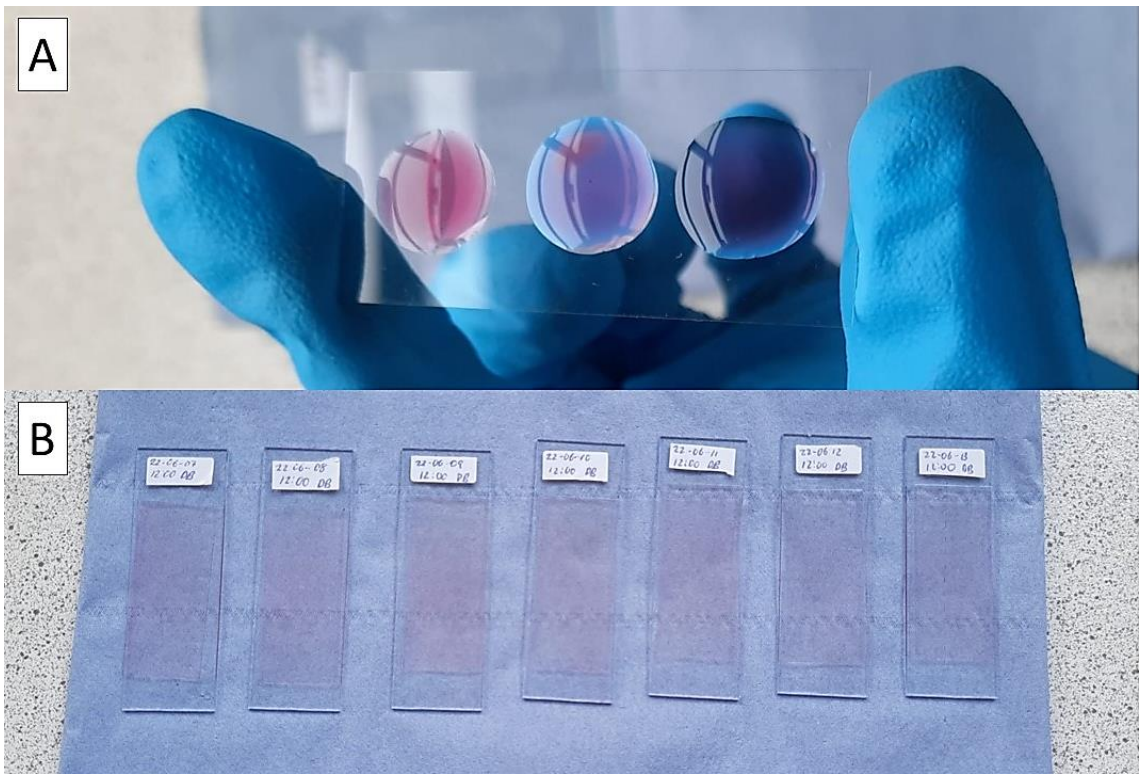

Figure 2.9: (A) Colorant media addition to coverslip, and (B) Final prepared slides

Once dry, any excess gelatine that has not been removed is done using a scalpel and the slides are cleaned using an ethanol solution. Cleaning the slides with ethanol will also remove labels made with a permanent marker so new sticker labels containing details of the sample date, time and location are added to the slides (Figure 2.9B). Transparent nail varnish is then used to seal along the edges of the coverslip. Once dry the prepared slides can be stored in a slide box until counted.

2.1.6 Colourant preparation

Apparatus Required:

- 250 ml beaker
- Stirring rod
- Spatula

Reagents Required:

- 50 ml Glycerine
- 7 g Gelatine
- Fuchsin

- 42 ml Distilled water

Generally, the mounting media is made from a fuchsin containing glycerine gelatine. Powdered reagents (Gelatine) are weighed accurately using an electronic balance and liquid reagents (Glycerine and water) are measured to appropriate volumes using graduated cylinders. Suggested masses/volumes are provided in the reagents section above.

Gelatine is first dissolved in warm water in a beaker using a stirring rod. Glycerine is then added and incorporated into the solution by stirring. A small amount of fuchsin is added and mixed to colour the media. The media should be a distinct pink colour but not too dark. Adding too much fuchsin can make the media too dark and make pollen identification more challenging. Fuchsin is added as it acts as a selective stain for plant material and aids in pollen observation and identification by staining pollen grains a notable pink colour. The mounting media is then stored in a sealed vessel or beaker, that can be heated for subsequent use of media. The media is solid when cooled and should be heated until a liquefied state is reached using a heating mantle before slide preparation. After use the media can be allowed to cool before storing.

2.1.7 Sample analysis

Prepared slides are analysed via light microscopy at a magnification of 400X (X40 objective lens). According to the EAN guidelines, at least 10% of the total slide surface (Galán et al., 2014) is required to be counted, since counting the entire slide surface would be too time-consuming. As such the utilised counting method is based on the procedure used by the Spanish Aerobiology Network and consists of counting 4 horizontal transects. This provides a subsample of approximately 12-13% of the total surface area. Each transect is marked with a permanent marker as shown in Figure 2.10.

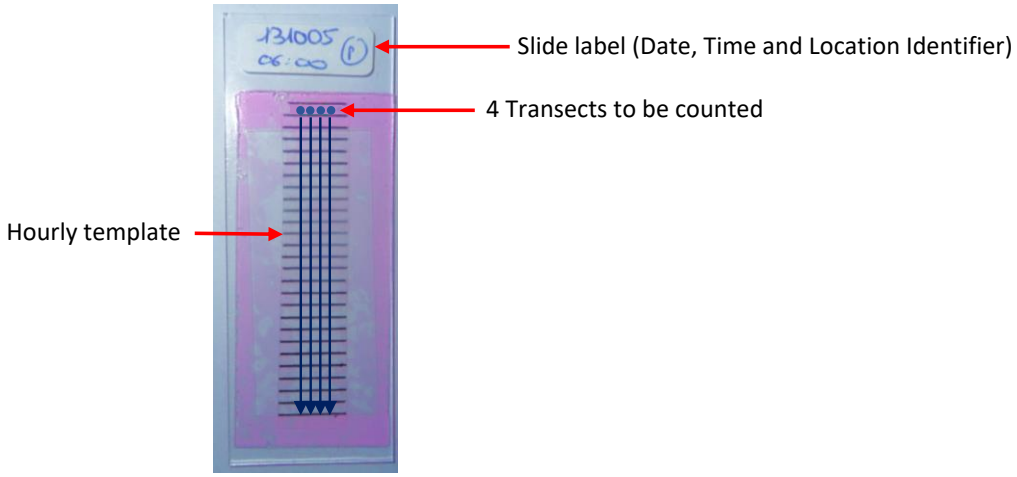

Figure 2.10: Sample Slide

During the examination of each transect, the number and specific identity of each pollen is recorded. Pollen can be identified to various taxonomic levels based on their physical features such as size, shape, type of pores, number of pores, surface features/texture, time of year etc. To record hourly pollen values, a custom clear plastic template is used which is divided into 24 X 2 mm sections. The template is attached to the back of the slide using sticky tape. The pollen per hour can now be recorded. Hourly results are recorded using an electronic form (Figure 2.11) which can be used co-currently during microscopic analysis and identification.

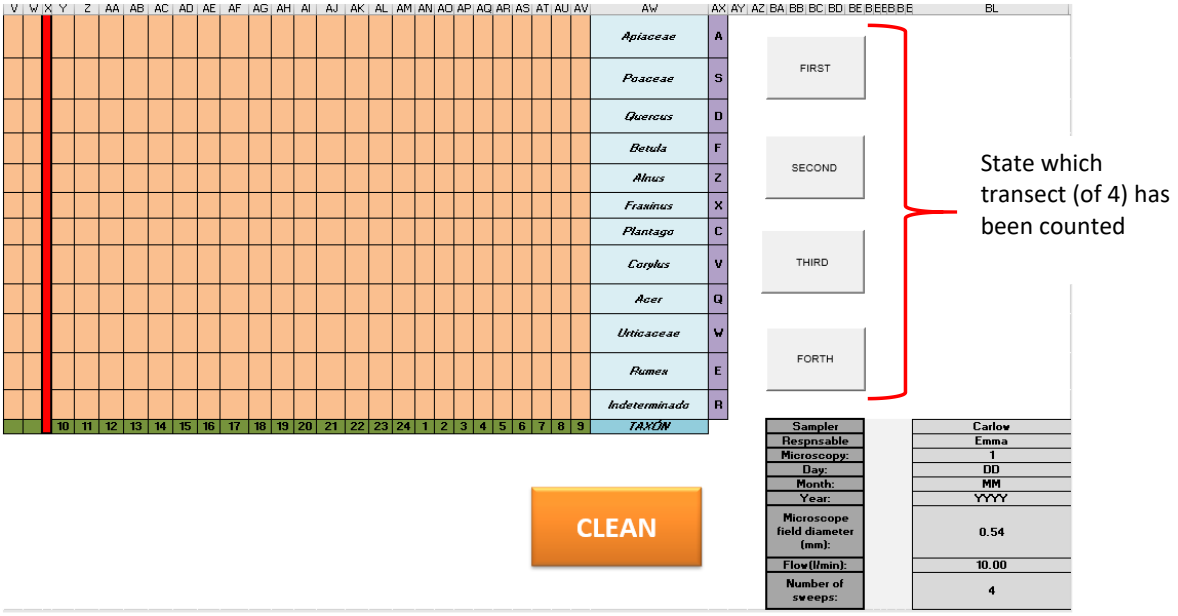

Figure 2.11: Pollen Counting Template

Once all data for a single transect has been recorded it can be logged as the FIRST, SECOND, THIRD or FORTH sweep (Figure 2.11) data is converted into a combined template for all 4 transects. Data can then be exported using the export function within the macro file. Hourly results can be summed to get daily pollen counts for each pollen type identified. Daily pollen counts are expressed per cubic metre of air sampled. To convert between counts daily observed counts and daily counts per cubic meter, the observed counts are multiplied by a calculated correction factor that considers both the volume sampled and the size of the field of vision observed through the microscope. The correction factor will vary depending on the objective lens and microscope used, an example calculation is provided below. The correction factor is applied automatically to data using a generated R script – the same script is used to determine hourly and daily datasets.

An example calculation is provided below for a field diameter of 0.55 mm:

Air sampling rate: 10 L/min = 600 L/hour = 14400 L/day = 14.4 m^3

The mean diameter of the microscope field of vision: 0.55 mm

Area of one horizontal sweep = 48 mm x 0.55 mm = 26.4 mm^2

Surface analysed = 26.4 x 4 sweeps = 105.6 mm^2

Total surface sampled = 48 mm length x 14 mm width = 672 mm^2

Particle content per cubic metre of air = (672 mm^2/105.6 mm^2) x (1/14.4 m^3) x N

N = number of pollen grains in four sweeps

Particle content per cubic metre of air = N x 0.442

2.2 Real-time WIBS method – bioaerosol sampling

The WIBS is a single aerosol particle fluorescence monitor that uses LIF to detect fluorescent aerosol particles (FAPs). The original instrument was invented by Professor Paul Kaye and co-workers at the University of Hertfordshire. It is now commercially available from Droplet Measurement Technologies (DMT) and is one of the most widely used instruments for monitoring PBAP in real time. It offers detailed information on the size and asymmetry (shape) of individual fluorescent and non-fluorescent particles allowing for the potential characterisation of bioaerosols. Several publications have extensively discussed the internal works of the WIBS instrument while thoroughly discussing the underpinning principles of its operation and potential application (Healy et al., 2012b, 2012a; Perring et al., 2015; Savage et al., 2017), a summary of which is provided below. The work presented in this thesis was acquired using the WIBS-NEO model (Figure 2.12).

Figure 2.12: WIBS-NEO (DMT, 2021)

2.2.1 WIBS operation

The WIBS utilises a central optical chamber to characterise aerosols entering the instrument. The central optical chamber (shown in Figure 2.13) can be subdivided into 4 separate components (DMT, 2020):

1. A 635 nm laser used for particle sizing and shape detection

2. A quadrant photomultiplier tube used to detect forward light scatter for shape determination

3. Two pulsed Xenon lamps set to emit UV light at 280 nm and 370 nm and

4. Two detector channels:

   - FL1 channel which detects particle fluorescence in the range of 310-400 nm
   - FL2 channel which detects particle fluorescence in the range of 420-650 nm, particle count and particle size

   .

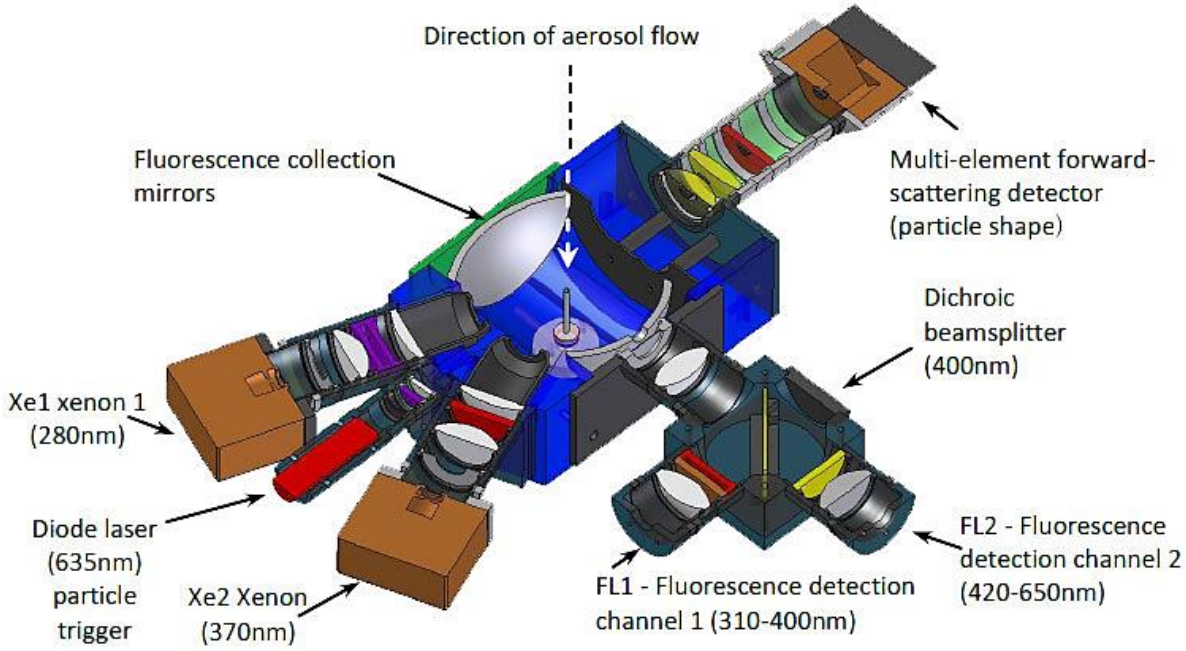

Figure 2.13: Central Optical Chamber of WIBS Instrument (DMT, 2021)

When an aerosol particle is drawn into the central optical chamber it first passes through the 635 nm continuous diode laser. When the particle is irradiated by the laser, elastic light scatter is produced (forward and side scatter). This side scatter is detected and used to count and size the incoming particle. The process of determining particle size employs a calibration methodology that relies on a curve, assuming the particles possess a spherical shape and exhibit a particular refractive index as per Mie theory (Healy et al., 2012b). Two high numerical-aperture mirrors are used to collect the size scattered light, as the light passes through the aperture it is focussed onto a dichroic beam-splitter before detection using a Photomultiplier tube (PMT) at 90° from the laser beam (FL2 channel) (DMT, 2020). The detected light is converted into an electrical signal which is used to size and count the particles. Size is determined by the magnitude of the electrical pulse detected (Savage et al., 2017). Forward-scattered laser light is used to provide information on particle shape. Forward scatter is detected by a quadrant PMT which is used to calculate the asymmetry factor (AF) of each particle (Perring et al., 2015; Savage et al., 2017). The equation used to calculate AF is shown below (equation 2.1) (Gabey et al., 2010; Savage et al., 2017).

$$AF = \frac{k(\sum_{i=l}^{n}(E - E_i)^2)^{1/2}}{E}$$

Equation 2.1: AF Calculation

Where:

k= instrument defined constant

E= mean intensity measured over the entire PMT

E_i= E_i is the intensity measured at the i^{th} quadrant (Gabey et al., 2010; Savage et al., 2017)

A particle that exhibits an AF value of 0 would be considered a perfect sphere, whereas a particle with a larger AF value (greater than 0 and less than 100) would be rod-like in shape (Gabey et al., 2010; Kaye et al., 2007; Savage et al., 2017)

This scatter signal then sequentially triggers the two xenon flashlamps filtered to emit light at 280 nm and 370 nm, respectively. Fluorescence emitted by the incident particle following each excitation wavelength is detected co-currently using two PMT detectors. The first detector (FL1) is filtered to detect fluorescence in the range of 310-400 nm whereas the second detector (FL2) is filtered to detect fluorescence in the range of 420-650 nm. In total, three pieces of fluorescent information can be inferred for each particle:

- Fluorescence detected by FL1 PMT following excitation at 280 nm and/or
- Fluorescence detected by FL2 PMT following excitation at 280 nm and/or
- Fluorescence detected by FL2 PMT following excitation at 370 nm

The excitation of the 370 nm lamp saturates the FL1 PMT, hence no fluorescence can be detected in FL1 at excitation at 370 nm. Therefore, the WIBS provides details on the size, shape and fluorescent properties of particles allowing for differentiation and determination of different bioaerosol classes.

2.2.2 Data analysis

All data analysis steps were carried out using scripts written and run in R studio. Particles are considered to be fluorescent if the emission intensity exceeds the determined baseline threshold in any one of the 3 fluorescent channels (FL1, FL2 or FL3). The fluorescent baseline is determined by measuring the observed fluorescence in each channel when the WIBS is fired when the central optical chamber is devoid of any particles. This is known as “forced trigger” since the xenon lamps are not

triggered by the presence of and resulting light scatter of a particle. During the chosen Dublin campaign covered within this thesis (07/08/2019 – 16/09/2019), force trigger values were recorded daily to ensure no extreme deviations were experienced. The baseline in each channel is calculated as the average fluorescence during force trigger mode plus 3 standard deviations (3σ). However, this can occasionally be raised to 6σ (mean + 6 standard deviations) and 9σ (mean + 9 standard deviations). Upon determination of the fluorescent fraction, the particles can be further categorised utilising the Perring nomenclature (Perring et al., 2015). This annotation system was developed whereby particle fluorescence is categorised into one of seven types, depending on the three forms of fluorescence signals detected by the WIBS, shown in Figure 2.14 (Perring et al., 2015).

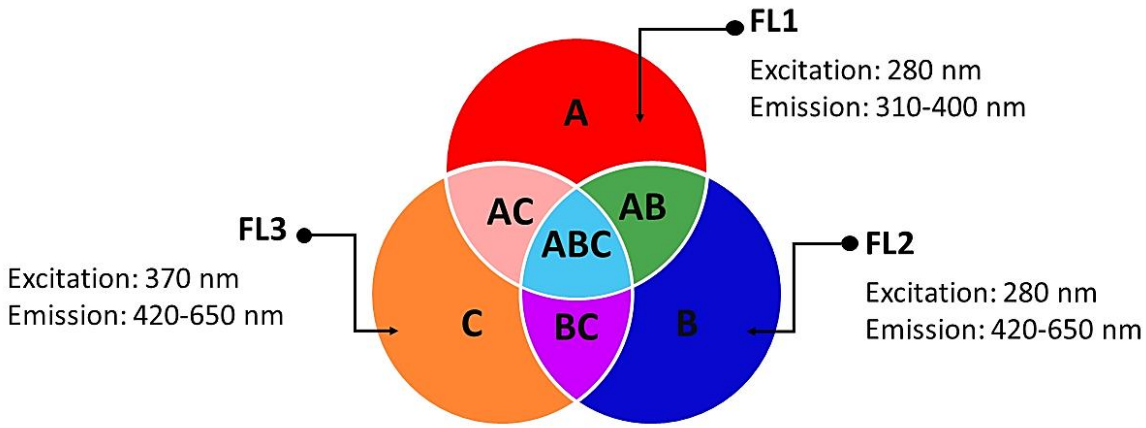

Figure 2.14: WIBS Particle Classification (inspired by Savage et al., 2017)

These categories consider each channel individually (FL1, FL2 and FL3) but also include all the possible combinations as shown in Table 2.1. Such cataloguing nomenclature allows for a more individual classification of each particle and a more detailed understanding of ambient particles' fluorescent characteristics.

Table 2.1: WIBS channel annotation classifications

Channel	Excitation (nm)	Emission (nm)
A	280	310-400
B	280	420-650
C	370	420-650
AB	280	310-400
		420-650
AC	280	310-400
	370	420-650
BC	280	420-650
	370	
ABC	280	310-400
		420-650
	370	420-650

This system denotes particles that fluoresce in only one channel (classified as A, B or C), any of two channels (classified as AB, AC or BC) or all channels (classified as ABC) (Perring et al., 2015). Using this method of classification, it is hoped that more complex environments can be better characterised by reference to the many different types of FAPs which are observed.

Details regarding any additional specific data analytics used during the included WIBS campaign are further covered in the designated chapter methodology section (Chapter 5).

2.3 Pollen sample collection

Reagents/Apparatus Required:

- Paper collection bag
- Scissors
- Sample tray
- Sieves

- Sample vials

To carry out several of the chemical analyses during this project, both purchased and collected pollen samples were required. Pollen samples sourced from around Dublin were initially collected into paper bags before catkins (for tree pollen) were dried slightly and then sieved to remove pollen. Samples were then stored in clean sample tubes. In the case of *Urtica dioica* L. and Poaceae pollen, samples were collected and transported to the lab where they were supplied with water and enclosed in individual storage chambers/boxes. Once pollen was released from the anthers, samples were collected and transferred to sample vials. All pollen samples were refrigerated at 4°C prior to analysis. A more detailed step-by-step guide (for tree pollen) with photographs is summarised below.

1. Ripe catkins are sampled using scissors/cutting tools from the desired tree (Figure 2.15)

Figure 2.15: (A) Sampled Betula trees and (B) catkins

2. Store collected catkins in a paper bag
3. Once in the lab, remove the catkins from the sample bag and place them on a drying tray
4. Leave the collected catkins in a clean fume hood (at low flow otherwise the pollen will be disrupted) for several hours
5. Once dried, pollen can be seen deposited at the bottom of the tray (Figure 2.16). Steps 4 and 5 are only required if catkins do not easily release pollen.

Figure 2.16: Catkin having shed pollen after drying

6. The catkins and pollen can then be sieved (using increasingly smaller mesh size) to aid in separating the pollen from the catkin and other plant materials (Figure 2.17)

Figure 2.17: Sieved pollen sample

7. The sieved pollen can then be transferred to a clean & labelled sample vial and refrigerated until its use

2.4 IR analysis of pollen samples

Instrument:

- Nicolet summit FTIR spectrometer by Thermo Scientific

Reagents/Apparatus Required:

- Pollen samples
- Spatula
- Isopropyl alcohol

2.4.1 Acquisition of IR spectra for individual pollen samples

Fourier transform infrared spectroscopy (IR) has been used as a non-destructive method to successfully differentiate between different pollen samples (Dell'Anna et al., 2009; Gottardini et al., 2007; Mularczyk-Oliwa et al., 2012; Pappas et al., 2003; Zimmermann et al., 2015a, 2015b). IR analysis of intact pollen grains provides detailed information about the chemical structure of the pollen grain. IR analysis operates on the basis that different chemical functional groups undergo vibration (bending or stretching) when exposed to certain wavelengths of light. Different chemical bonds and functional groups within the molecules vibrate at distinct frequencies, resulting in unique absorption patterns which can be detected by measuring the absorption of IR radiation as it interacts with a sample. Attenuated Total Reflection (ATR) spectral acquisition was used in conjunction with IR spectroscopy. ATR is based on total internal reflection which means when the sample is in contact with the crystal surface, the IR light and sample interact at the point where the IR light is totally internally reflected as a result of the different refractive indices of the crystal and sample. However, because a portion of the IR light will be absorbed by the sample, the emerging reflected light will be slightly reduced or attenuated.

IR spectra were acquired using an ATR IR spectrometer (Figure 2.18). A total of 32 scans between the spectral ranges of 400–4000 cm^{-1} with a spectral resolution of 4 cm^{-1} were generated for each sample using a similar method to Ba‡cio›lu, Zimmermann and Kohler, 2015. Background spectra and contamination checks were acquired first, before sample measurements. A small amount (half a spatula tip) of each sample was then placed upon the ATR crystal and the pressure tip was engaged. Three replicate measurements were obtained for each sample. The crystal surface and pressure tip were cleaned after every sample using isopropyl alcohol until a clear background was obtained. These tests operated as a quality control check between samples to ensure no carryover or contamination from previous samples.

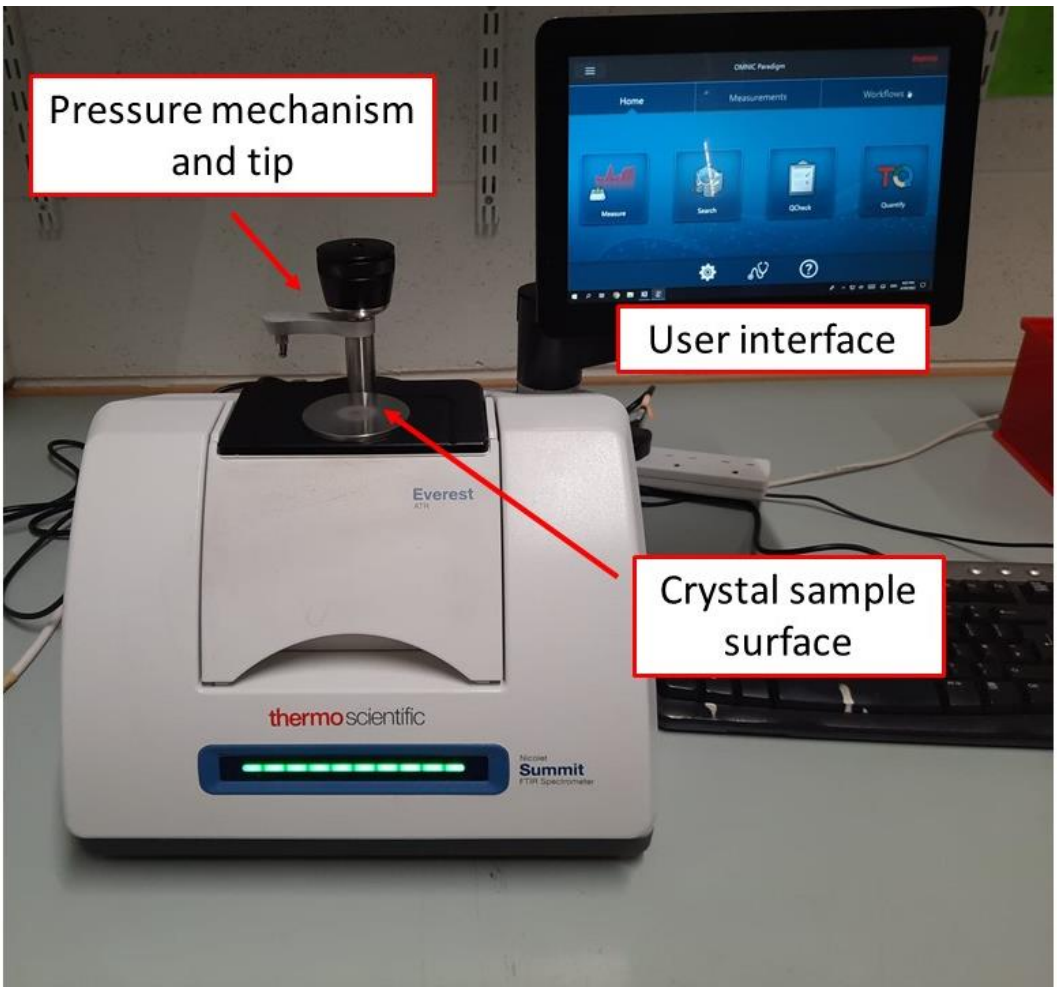

Figure 2.18: IR-ATR Instrument set-up

2.4.2 Spectral processing and data analysis

"Fingerprint" spectral regions were selected for data analysis (1900-800 cm^{-1}) of IR spectra. Prior to this, these spectra were pre-processed using two methods: Savitzky–Golay and extended multiplicative signal correction (EMSC). Both non-derivatised and second-derivative spectra were used. Initially, spectra were smoothed using the Savitzky–Golay algorithm (Zimmermann and Kohler, 2013) using a polynomial of degree two and a window size of 11 points for non-derivatised spectra (Kenđel and Zimmermann, 2020) and a window size of 15 for second derivative spectra (Zimmermann, 2018). The SG smoothing algorithm involves fitting a polynomial function to the data within a moving window. Therefore, the window size parameter refers to the number of neighbouring data points considered when doing this. Larger window sizes result in more extensive smoothing or filtering, while smaller window sizes preserve finer details but might not remove as much noise. Following this, the resulting spectra were normalised using EMSC (Guo et al., 2018). The Savitzky–Golay algorithm is initially used to enhance spectral features while EMSC is used to normalise spectra, enhance variations between spectra and apply a baseline correction (Zimmermann, 2018; Zimmermann and Kohler, 2013). An example of Savitzky–Golay algorithm EMSC analysis

and resulting spectra (using recorded spectral data obtained during this project) are highlighted in Figures 2.19 and 2.20. All processing and data analytic steps were carried out using a self-made R script and the EMSC package (Hovde, 2021)

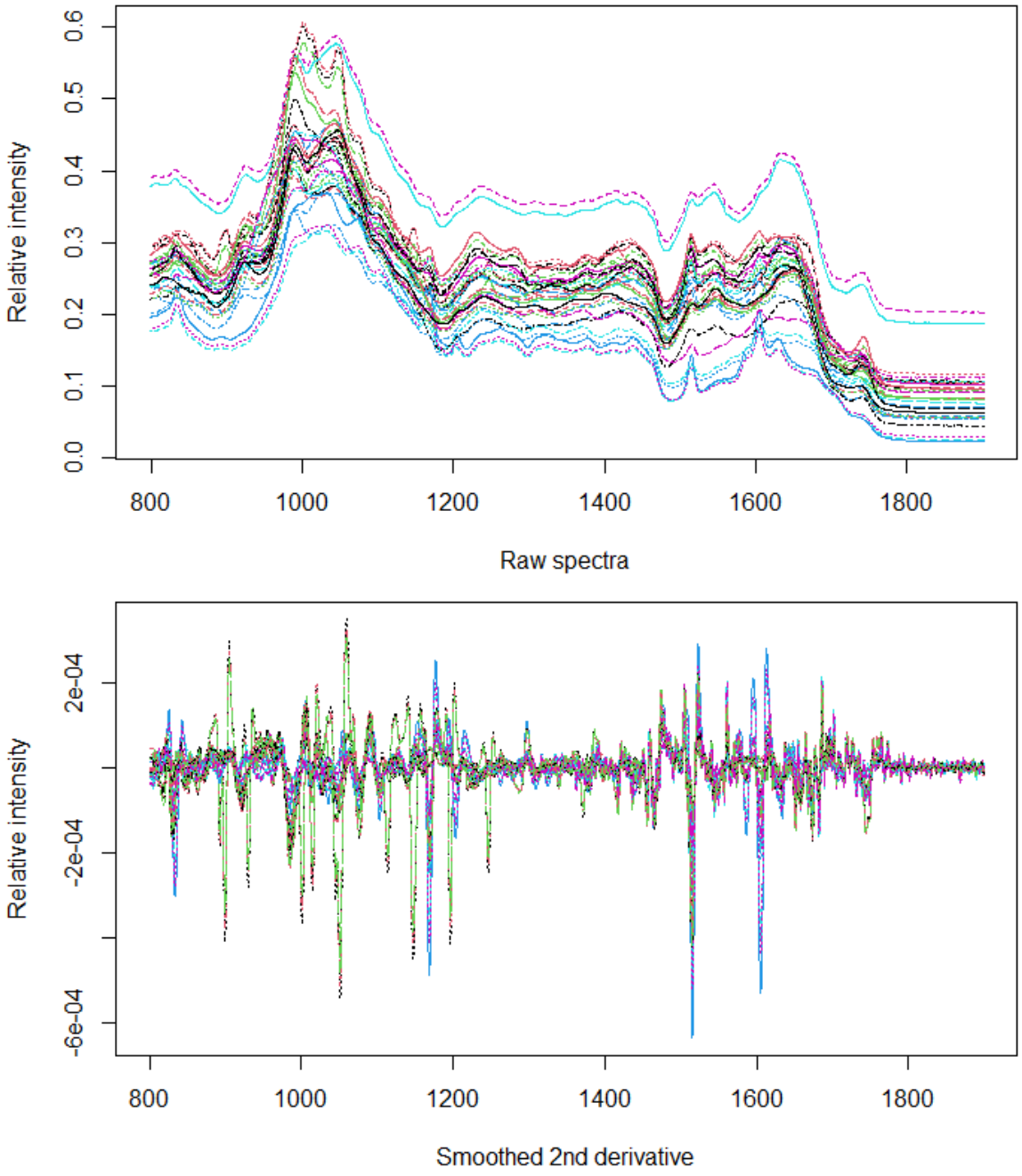

Figure 2.19: Example 2nd derivatization using Savitzky–Golay algorithm using multiple pollen samples collected from around Dublin and purchased from Bonapol

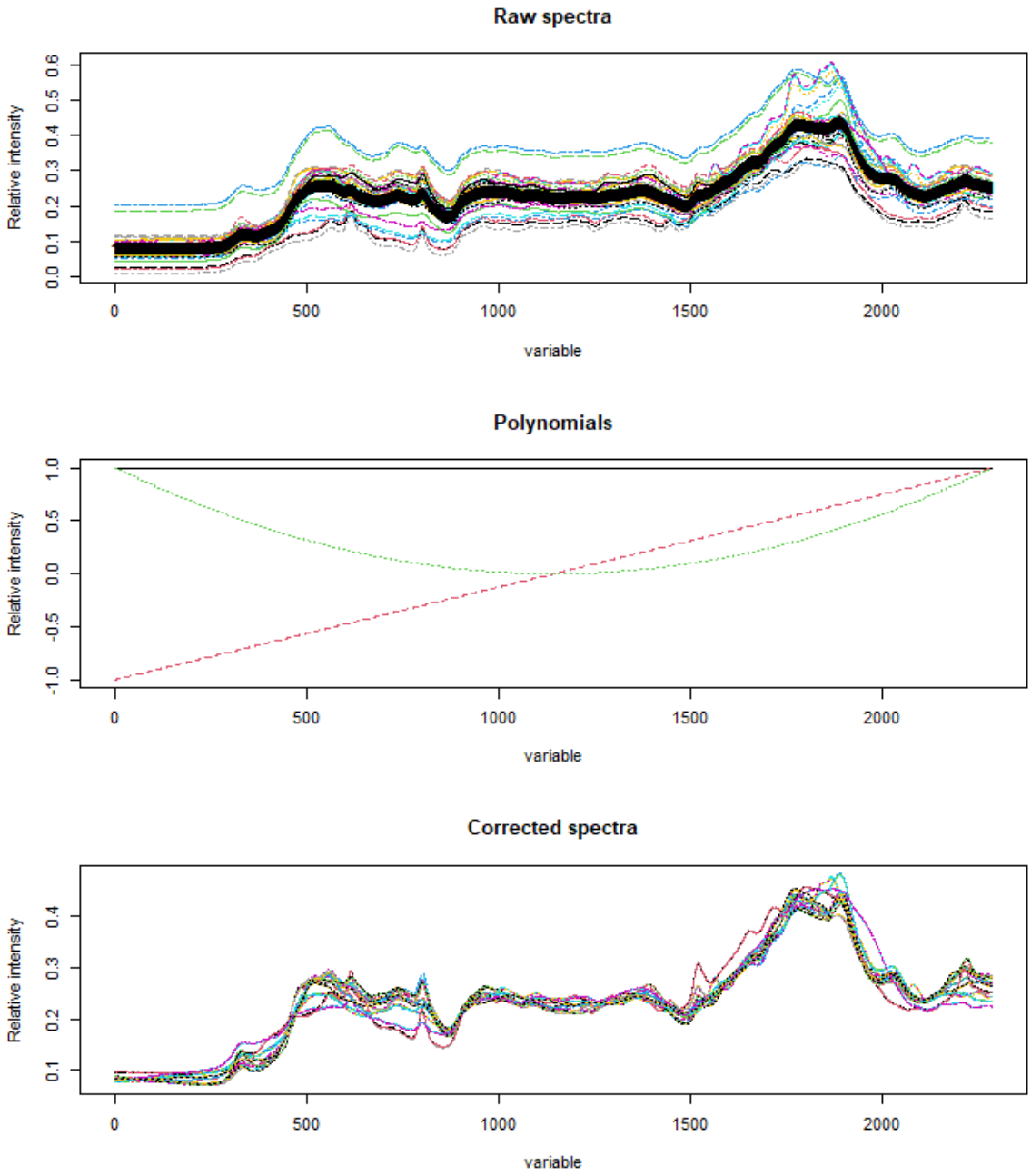

Figure 2.20: Example EMSC processing of spectra using multiple pollen samples collected from around Dublin and purchased from Bonapol

2.5 Confocal fluorescent microscopic analysis of pollen samples

Instrument:

Leica TCS SP8 SMD confocal microscope

Reagents/Apparatus Required:

- Pollen samples

- Spatula
- Ibidi 8-well sample holder
- Immersion oil

2.5.1 Sample analysis and image recognition

Confocal microscopy utilises the principle of fluorescence to record images where brightness and contrast are directly proportional to the fluorescence detected for that sample. This involves the utilisation of laser light sent through the objective lens of a conventional light microscope to excite a specimen within a restricted focal plane. The pinhole (confocal aperture) effectively filters out any light emissions originating from planes that are not in focus (Practices, 2020). Enhancing the image quality beyond the capabilities of conventional fluorescence microscopy. Emission photons are then recorded by the detector, which can include PMTs or hybrid detectors. In this case, second-generation hybrid detectors were used (often termed as HyD detectors). Hybrid detectors can be characterised as a combination of conventional PMTs with the addition of an avalanche photodiode, which is a semiconductor device known for its high sensitivity (Practices, 2020). This results in several advantages over traditional detectors, such as possessing a wide dynamic range, minimal noise levels, and high operational speeds (Practices, 2020). Confocal microscopy has been used several times to study and compare pollen grain fluorescence (Castro et al., 2010; Roshchina, 2003; Roshchina et al., 2015, 2009, 2022). Although spectral data can be achieved through confocal microscopy and has been shown previously for pollen analysis (Roshchina et al., 2015), this was not possible with the available setup and software.

Figure 2.21: Confocal Microscope set-up

Pollen samples were placed into a well within an Ibidi 8-well sample slide (Figure 2.22) using a clean spatula. Following this, immersion oil (refractive index of 1.518) was placed on the coverslip side of the sample holder. The sample slide was then positioned within the stage of the microscope and the X40 oil immersion objective was used. Samples are viewed and focused initially using a white-light source at the microscope section of the set-up. Pollen samples are then analysed using the fluorescence portion of the confocal microscope, operated remotely from the computer unit and Leica LASX software. Fluorescent image analysis was conducted using a 405nm excitation laser and detected between 410-750 nm using a HyD detector. Images were recorded using "counting" mode which refers to the direct measurement of the emitted photons that have undergone fluorescence and are expressed as pixel intensity. Any remaining acquisition features such as pinhole, objective magnification and laser intensity were kept constant between samples to enable comparisons of the recorded autofluorescence.

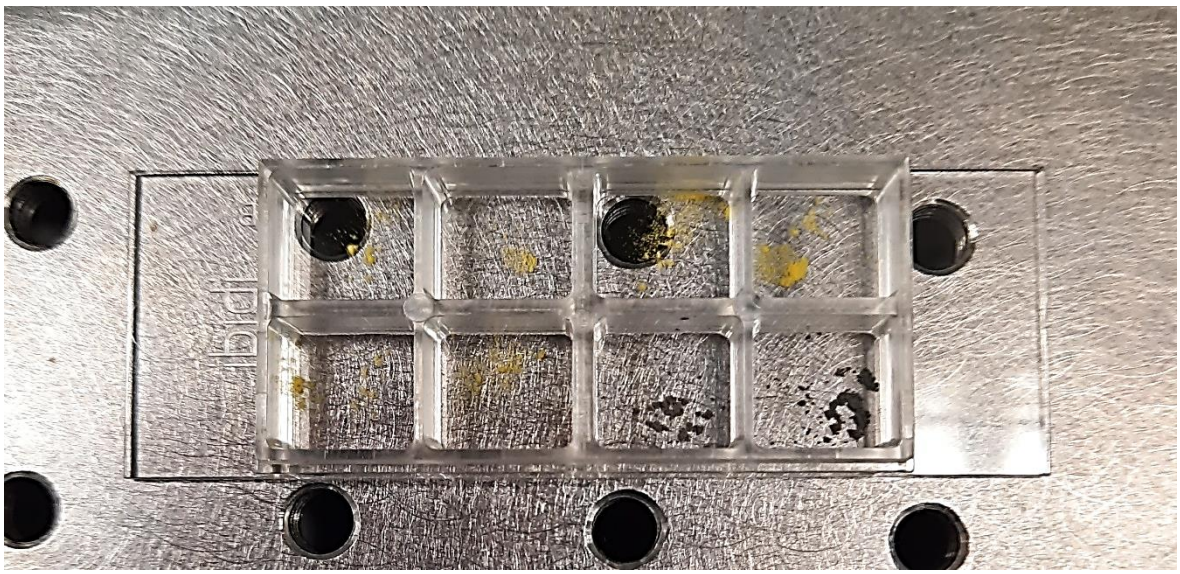

Figure 2.22: Ibidi 8-well sample slide (containing pollen and ash samples)

In each case, Z-stack images were captured for a sample and later transformed into maximum-intensity projections (single plane image). The z-stack image collection is a technique used to capture a series of two-dimensional images at different focal planes along the Z-axis (vertical axis) of a three-dimensional specimen or sample, in this case pollen. The number of stacks (2D images taken at different focal points) used was automatically determined by LASX software estimates, having manually specified the start and end points of the analysis. The result is a stack of images that represent the specimen at various depths or slices within the 3D space and allows for the reconstruction of 2D and 3D images. Image acquisition was performed using the LAS X software (Figure 2.23) and was saved in ".lif " format for analysis using ImageJ software.

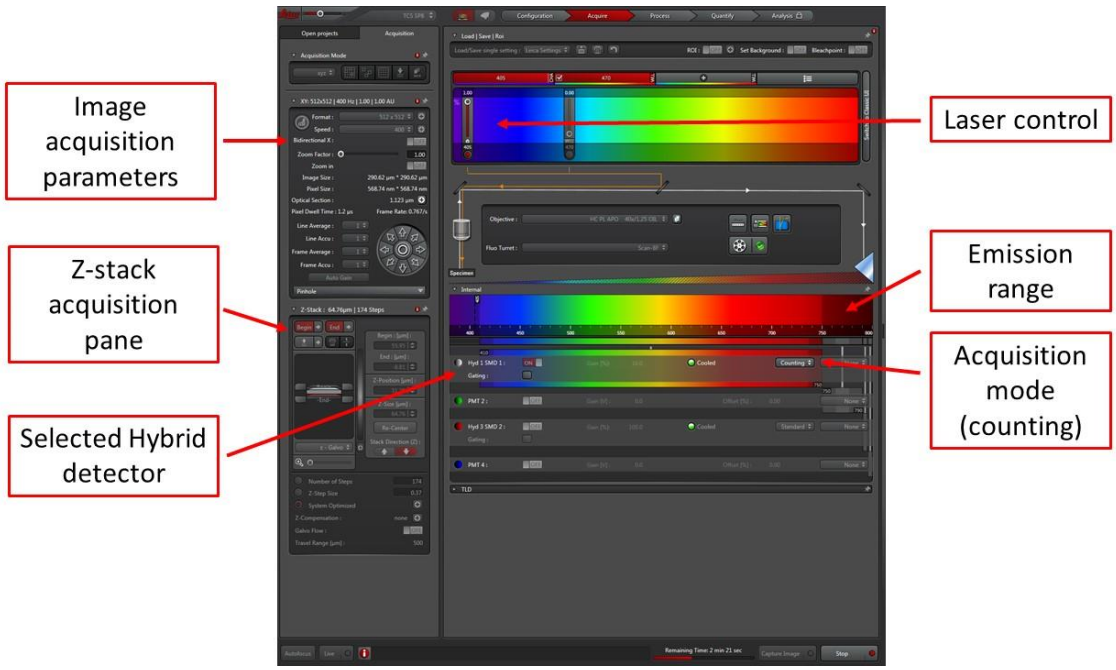

Figure 2.23: LASX image acquisition controls

2.5.2 Image processing using ImageJ

Once completed, sample files can be opened using the free image analysis software ImageJ. In this case, the Fiji adaption of ImageJ was used for image analysis (Schindelin et al., 2012). Firstly, the image series containing all individual slices of the Z-stack array needs to be rendered to produce one single 2D image – this was done by combining the individual stacks to generate the maximum intensity projection. Maximum Intensity projection (an example of which is provided in Figure 2.24) refers to selecting the highest intensity pixels from every slice throughout the Z-stack to construct a final 2D image. Since the counting method was used – this refers to the number of photons emitted by the sample (recorded as pixel intensity).

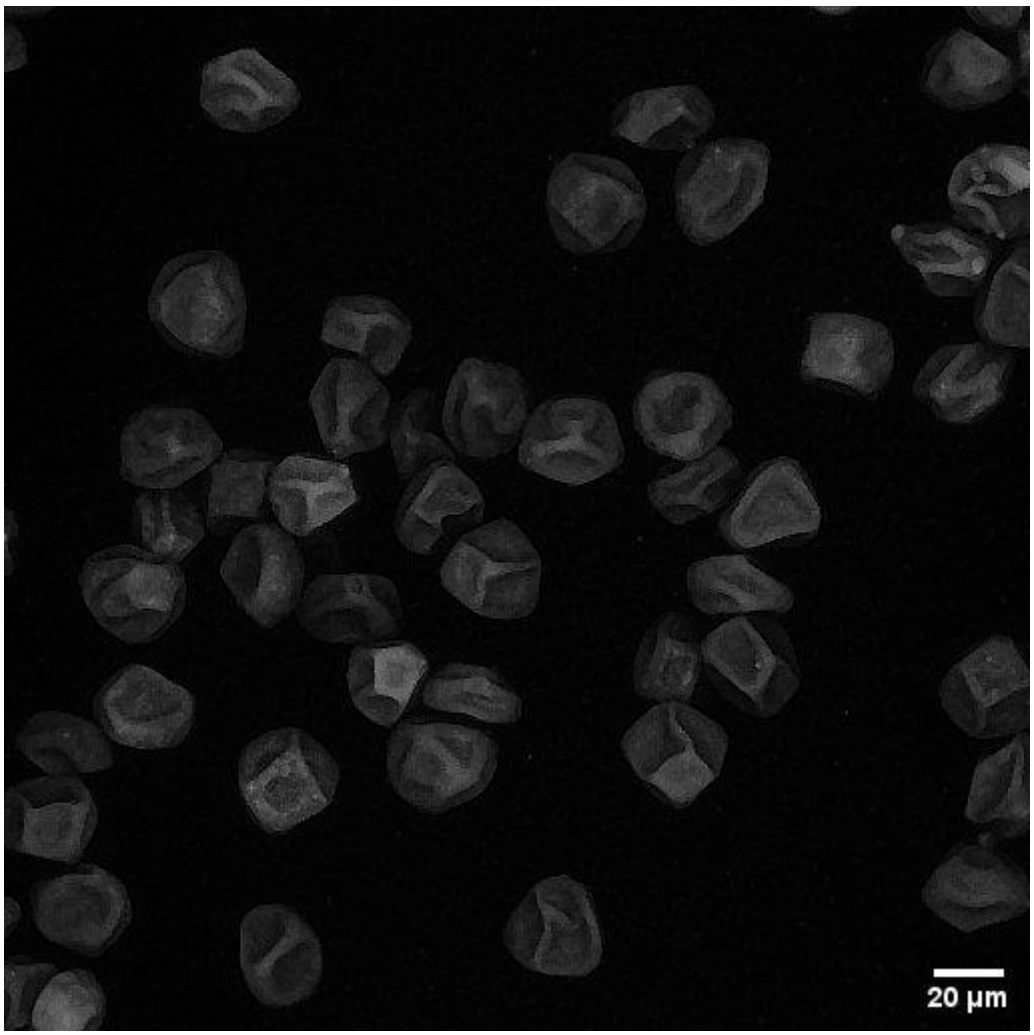

Figure 2.24: Example confocal image of maximum Z-stack projection obtained for the analysis of Betula pendula pollen

To get the average fluorescence intensity of each pollen grain examined, the total fluorescence intensity of the grain is divided by the area examined – having selected the pollen area and measuring function within ImageJ (Figure 2.25). This was repeated for 40 grains per sample to get a representative population, previous studies have used fewer repeats (n=20) (Castro et al., 2010) but efforts were made here to further reduce any uncertainties associated with a small sample size. Background readings were also taken (n=40) for each sample in order to ensure no dramatic increase/decrease was observed as well as to act as a baseline for fluorescence intensity. Further examination of fluorescence values was carried out in RStudio using created scripts for statistical and graphical analysis.

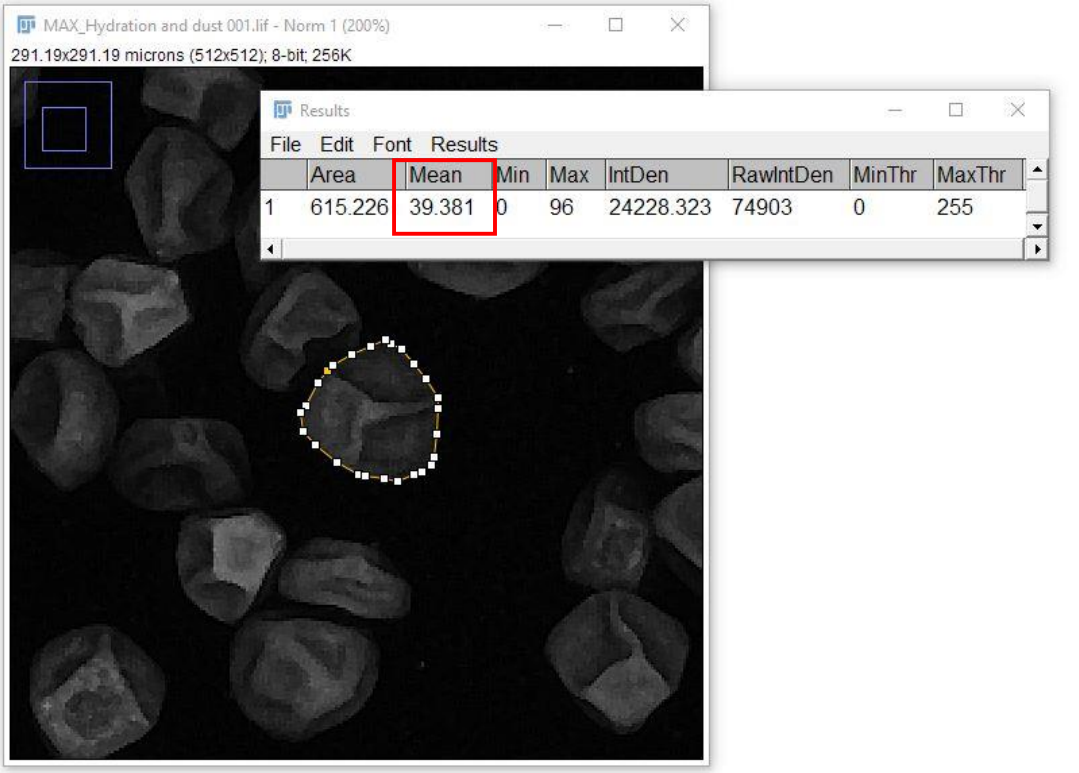

Figure 2.25: Fluorescent intensity analysis using ImageJ, average fluorescent intensity per unit area is shown in red box

References

Ba‡cio‡lu, M., Zimmermann, B., Kohler, A., 2015. PLoS One 10, 1–19.

Castro, A.J., Rejon, J.D., Fendri, M., Jimenez-Quesada, M.J., Zafra, A., Jimenez-Lopez, J.C., Rodriguez-Garcia, M.I., Alche, J.D., 2010. Microsc. Sci. Technol. Appl. Educ. 607–613.

Dell'Anna, R., Lazzeri, P., Frisanco, M., Monti, F., Malvezzi Campeggi, F., Gottardini, E., Bersani, M., 2009. Anal. Bioanal. Chem. 394, 1443–1452.

DMT, 2020. WIBS-NEO Wideband Integrated Bioaerosol Sensor New Electronics Option User Manual.

DMT, 2021. Wideband Integrated Bioaerosol Sensor - Technology [WWW Document]. URL https://www.dropletmeasurement.com/product/wideband-integrated-bioaerosol-sensor/ (accessed 8.4.21).

Gabey, A.M., Gallagher, M.W., Whitehead, J., Dorsey, J.R., Kaye, P.H., Stanley, W.R., 2010. Atmos. Chem. Phys. 10, 4453–4466.

Galán, C., Cariñanos, P., Alcázar, T., Domínguez-Vilches, E., 2007. Spanish Aerobiology Network (REA): management and quality manual, Servicio de publicaciones de la Universidad de Córdoba.

Galán, C., Smith, M., Thibaudon, M., Frenguelli, G., Oteros, J., Gehrig, R., Berger, U., Clot, B., Brandao, R., 2014. Aerobiologia (Bologna). 30, 385–395.

Gottardini, E., Rossi, S., Cristofolini, F., Benedetti, L., 2007. Aerobiologia (Bologna). 23, 211–219.

Guo, S., Kohler, A., Zimmermann, B., Heinke, R., Stöckel, S., Rösch, P., Popp, J., Bocklitz, T., 2018. Anal. Chem. 90, 9787–9795.

Healy, D.A., O'Connor, D.J., Burke, A.M., Sodeau, J.R., 2012a. Atmos. Environ. 60, 534–543.

Healy, D.A., O'Connor, D.J., Sodeau, J.R., 2012b. J. Aerosol Sci. 47, 94–99.

Hirst, J.M., 1952. Ann. Appl. Biol. 39, 257–265.

Hovde, K., 2021. Package 'EMSC', Extended Multiplicative Signal Correction.

Kaye, P.H., Aptowicz, K., Chang, R.K., Foot, V., Videen, G., 2007. ANGULARLY RESOLVED ELASTIC SCATTERING FROM AIRBORNE PARTICLES, in: Optics of Biological Particles. Springer Netherlands, Dordrecht, pp. 31–61.

Kenđel, A., Zimmermann, B., 2020. Front. Plant Sci. 11, 1–19.

Mularczyk-Oliwa, M., Bombalska, A., Kaliszewski, M., Włodarski, M., Kopczyński, K., Kwaśny, M., Szpakowska, M., Trafny, E.A., 2012. Spectrochim. Acta - Part A Mol. Biomol. Spectrosc. 97, 246–254.

O'Connor, D., Clancy, J.H., Martinez-bracero, M., McGillicuddy, E., Markey, E., 2022a. Fungal Monitoring Network and Algorithm.

O'Connor, D., Markey, E., Maya-manzano, J.M., Dowding, P., Donnelly, A., Sodeau, J., 2022b. Pollen Monitoring and Modelling (POMMEL).

Pappas, C.S., Tarantilis, P.A., Harizanis, P.C., Polissiou, M.G., 2003. Appl. Spectrosc. 57, 23–27.

Perring, A.E., Schwarz, J.P., Baumgardner, D., Hernandez, M.T., Spracklen, D. V., Heald, C.L., Gao, R.S., Kok, G., McMeeking, G.R., McQuaid, J.B., Fahey, D.W., 2015. J. Geophys. Res. Atmos. 120, 1153–1170.

Practices, M., 2020. Curr. Protoc. Cytom. 92, 1–18.

Roshchina, V. V., 2003. J. Fluoresc. 13, 403–420.

Roshchina, V. V., Yashin, V.A., Kuchin, A. V., 2015. J. Fluoresc. 25, 595–601.

Roshchina, V. V., Yashina, A. V., Yashin, V.A., Prizova, N.K., 2009. Allelopath. J. 23, 3–24.

Roshchina, V. V, Kuchin, A. V, Kunyev, A.R., Soltani, G.A., Khaibulaeva, L.M., Prizova, N.K., 2022. Biochem. (Moscow), Suppl. Ser. A Membr. Cell Biol. 16, 167–174.

Savage, N.J., Krentz, C.E., Könemann, T., Han, T.T., Mainelis, G., Pöhlker, C., Alex Huffman, J., 2017. Atmos. Meas. Tech. 10, 4279–4302.

Schindelin, J., Arganda-Carreras, I., Frise, E., Kaynig, V., Longair, M., Pietzsch, T., Preibisch, S., Rueden, C., Saalfeld, S., Schmid, B., Tinevez, J.Y., White, D.J., Hartenstein, V., Eliceiri, K., Tomancak, P., Cardona, A., 2012. Nat. Methods 9, 676–682.

Zimmermann, B., 2018. Planta 247, 171–180.

Zimmermann, B., Bağcıoğlu, M., Sandt, C., Kohler, A., 2015a. Planta 242, 1237–1250.

Zimmermann, B., Kohler, A., 2013. Appl. Spectrosc. 67, 892–902.

Zimmermann, B., Tkalčec, Z., Mešić, A., Kohler, A., 2015b. PLoS One 10, 1–22.

Chapter 3: Traditional Pollen Monitoring in Ireland

3.1 Introduction

This chapter describes the findings from a traditional pollen monitoring campaign conducted in Dublin from 2017 to 2020. While some of this work has been previously published (Markey et al., 2022a), this chapter expands upon those findings by incorporating subsequent data and additional analyses.

Despite significant health, agricultural and climate implications, bioaerosol monitoring has largely been overlooked in Ireland, often overshadowed by the monitoring of anthropogenic pollutants. The few pollen monitoring studies (traditional and real-time) that have been conducted in Ireland are decades old and/or provide little detail on the various pollen types and annual seasonal trends (reviewed in Chapter 1). In recent years, pollen monitoring efforts have recommenced at several sites in Ireland initiated by the EPA-funded POMMEL project (O'Connor et al., 2022). Since then several Irish aerobiological studies have been conducted, including a comprehensive assessment of long-term pollen data from multiple sites (Markey et al., 2022a), a study covering the spatiotemporal variations in the distribution of birch trees and *Betula* pollen (Maya-Manzano et al., 2021) and several other fungal spore studies (Martinez-Bracero et al., 2022; Martínez-Bracero et al., 2022). However, despite these pivotal first steps, there remains a clear disparity between the Irish network and that of the rest of Europe (Markey et al., 2022a).

3.2 Methods

3.2.1 Sampling locations

Pollen monitoring data was primarily carried out in the capital city of Dublin, located on the east coast of Ireland. Sampling was continuously carried out from May 2017 until October 2020 at the former TU Dublin Kevin Street campus (53°20'12.1"N, 6°16'04.0") – before the campus relocated in 2021. Comparisons were also drawn from a rural site established in Carlow (52°43'23.6"N, 6°39'36.0" W) for the 2018 and 2019 seasons. Both locations are depicted in Figure 3.1.

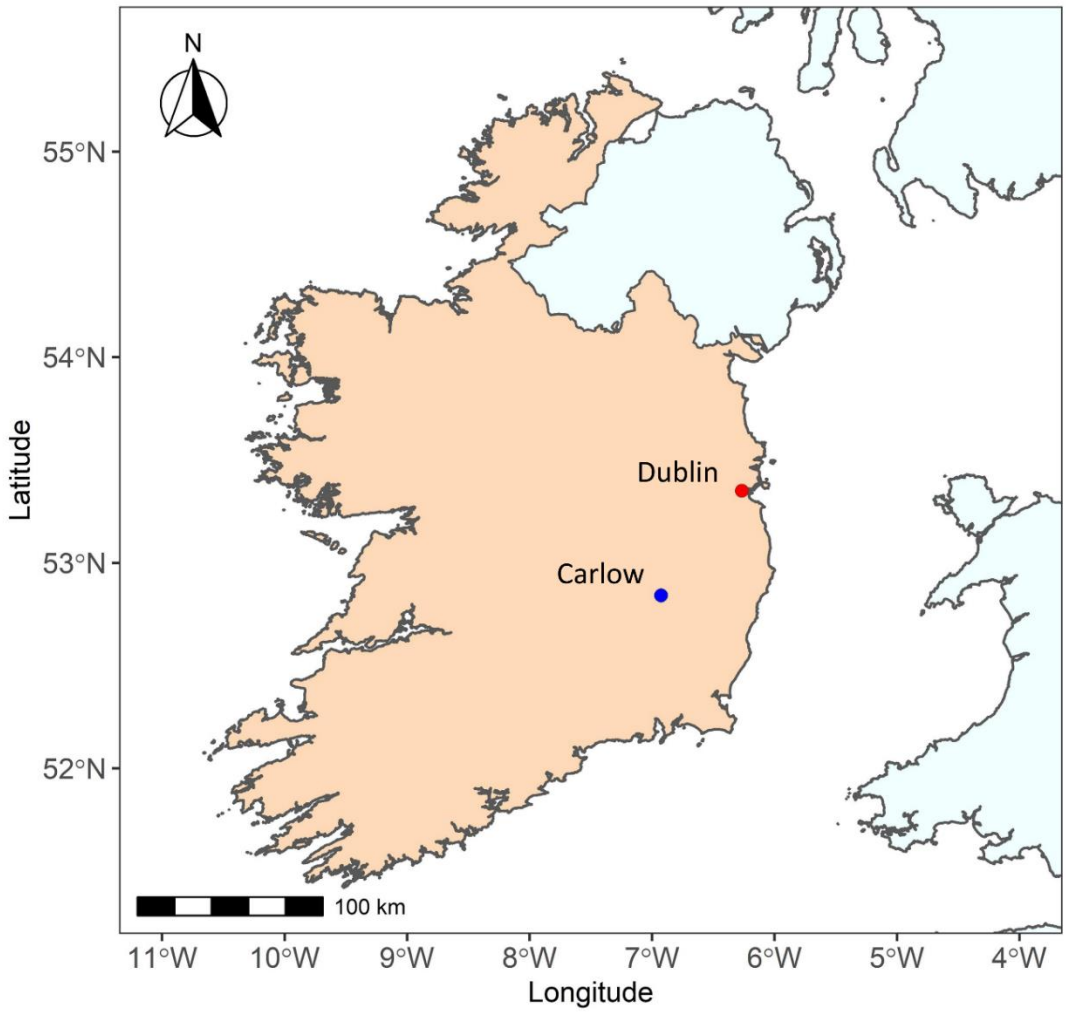

Figure 3.1: Map of sampling locations in Ireland (Dublin urban site - Red, Carlow rural site– Blue)

The Dublin site was located on the roof of the Technical University Dublin Kevin Street building (20 m high), located in the heart of Dublin city centre - covering approximately 318km^2 (CSO, 2012) with a population density of 4,811/km^2 (CSO, 2016). The rural site was located on a private rural farm in Carlow which has a population density of 63/km^2 (CSO, 2016). In this case, due to no nearby infrastructure, the Hirst pollen trap was positioned atop a 2-3m pedestal.

3.2.2 Pollen monitoring and analysis

Pollen monitoring was conducted from the 22nd of May 2017 continuously until the 1st of October 2020 in Dublin using a Hirst-Lanzoni 7-day pollen sampler (Hirst, 1952). Detail of this method is provided in Chapter 2. The annual pollen integral (APIn) was calculated for each pollen type by multiplying the average daily concentration of the annual sampling period by the season duration, using the recommended aerobiological method (Galán et al. 2017). The term "pollen type" refers to pollen grains sharing the same morphological characteristics observed under microscopic analysis. This includes pollen grains belonging to different taxonomical categories - either a specific genus or

family of plants, with all respective species included within (Markey et al., 2022a). In this case, the major pollen types were defined as the most prominent, re-occurring pollen types that represented approximately 87% of the total Dublin pollen concentrations recorded over the entire sampling campaign.

The Main Pollen Season (MPS) for each major pollen type was calculated as the start and end dates where the annual pollen concentration sum reached 5% and 95% of the total for the year (Cristofori et al., 2010; Nilsson and Persson, 1981). Several methods can be used to calculate the MPS (Jato et al., 2006). The 90% method of determining the MPS was selected due to its capability to suit plants/trees that pollinate early in the year (Kasprzyk, 2003; Nilsson and Persson, 1981), as well as allowing the MPS to be determined while excluding low concentrations that could be transported from other regions (Kasprzyk et al., 2004) such as the UK.

The relationship between pollen concentrations and meteorological factors tends to fluctuate throughout the MP. To further investigate this the MPS for each selected pollen type was further subdivided into two periods: the pre-peak and the post-peak. The pre-peak period (PRP) was defined as the time between the start of the pollen season and the peak day, while the post-peak period (PSP) was defined as the time between the peak day and the conclusion of the pollen season.

For comparison purposes, pollen monitoring in Carlow took place from the 18th of April until the 10th of December 2018 and recommenced from the 1st of February until the 30th of September 2019, using the same volumetric method specified above.

3.2.3 Meteorological data

Meteorological data was obtained from the Met Éireann website ("The Irish National Meteorological Service," 2023). The weather station in Dublin (Dublin Airport, 53°25'40.0"N 6°14'27.0"W, 11 km from the sampling site,74 masl), provided the following daily datasets of meteorological parameters (parameters represent daily means, unless otherwise stated): mean temperature [ºC] (Tmed), maximum temperature [ºC] (Tmax) and Minimum Temperature [ºC] (Tmin), average mean temperature [ºC] over the previous 10 days (Tmed_10), grass minimum temperature [ºC], 2 cm above the ground (Gmin), mean 10cm soil temperature [ºC] (Soil), precipitation amount [mm] (Rain), average precipitation amount [mm] over the previous 10 days (Rain_10), mean cbl pressure [hpa] (Pres), mean wind speed [kt] (Wind_s) and wind direction at max 10 min mean [deg] (Wind_d), global radiation [J/cm^2] (G_rad), Sunshine duration [hours] (Day_L), cloud amount [arbitrary unit between 1-10] (Cld_Amt), potential evapotranspiration [mm] (Pe), evaporation [mm] (Evap) and relative humidity [%] (Rh).

3.2.4 Land cover data

A land cover map was generated of the immediate 30 km radius encompassing the Dublin sampling site using CORINE Land cover data (Basu, 2021; Büttner et al., 2004) and was graphically constructed using GIS software. This 30km range is considered to be representative of the overall variety and distribution of pollen recorded when using a volumetric Hirst trap (Skjøth et al., 2010).

3.2.5 Statistical analysis

Shapiro-Wilk and Lilliefors tests (a version of the Kolmogorov-Smirnov test) were used to determine whether the recorded daily pollen/meteorological data had a normal distribution. Both of these tests are frequently employed in aerobiology (Galán et al., 2014; Grinn-Gofroń et al., 2015; Helfman-Hertzog et al., 2023; Maya-Manzano et al., 2021; O'Connor et al., 2014; Orlandi et al., 2014; Picornell et al., 2020). It was revealed that the daily data did not exhibit a normal distribution. Subsequently, a Spearman correlation test was used to determine the degree and significance of correlation existing between the selected meteorological and pollen parameters. The statistical analysis included only days within the MPS, PRP and PSP and was performed using the *nortest* (Gross and Ligges, 2015) and *corrplot* (Wei et al., 2021) packages available in R (R Development Core Team, 2020).

3.2.6 Geographical origins of major airborne pollen types

The geographical origin of ambient bioaerosols was examined using a source receptor approach available through the ZeFir-v3.7 package (Petit et al., 2017). Two-dimensional Non-parametric Wind Regression (NWR) was used to establish the potential geographical origin of selected pollen concentrations throughout the sampling campaign. This method has been previously used in similar Irish fungal spore (Martínez-Bracero et al., 2022) and air quality (Donnelly et al., 2015) studies. The NWR method, originally proposed by Henry et al., 2009 combines co-located measurements of wind speed and direction with ambient aerosol concentrations. The general idea is to give weight to concentration values associated with wind direction and speed with the weighing coefficients being determined through Gaussian-like functions (Petit et al., 2017).

3.2.7 Pollen calendar

Data from unpublished pollen monitoring campaigns from 1978-1980 (sampled at Trinity College Dublin), 2010-2011 (sampled at Baldonnel aerodrome) and from this monitoring campaign (2017-2020) were combined to construct an updated/simplified pollen calendar for Dublin, with the previous rendition published in (Markey et al., 2022a). The mean daily pollen levels (Pollen grains/m^3) were calculated for the 15 most common pollen types that were present for all sampling years. Early, late and main flowering periods were calculated using the method suggested by Werchan et al. (2018).

The main flowering period was defined as the 10-90% interval, beginning once the pollen interval reached 10% of the APIn and ending once 90% was reached. Early and late flowering periods, outside the main flowering period, were determined in a similar manner. The early flowering period is defined as the period within the interval where the pollen integral exceeds 0.5% of the APIn but is less than 10%. Similarly, the late flowering period corresponded to the period within the interval where the pollen integral exceeded 90% of the APIn but less than 99.5%. Finally, possible occurrence times were determined as any time outside of the 0.5-99.5 % range where pollen was observed. The earliest possible occurrence of a pollen type was limited to no more than 30 days before the earliest possible start of early flowering, and the latest possible occurrence to no more than 30 days after the latest flowering end, since theoretically individual pollens can occur all year round as a result of resuspension (Werchan et al., 2018). The pollen calendar was then constructed and coloured according to the level of allergenicity posed by each pollen type and shaded according to possible, early/late, and main flowering periods.

3.3 Results

3.3.1 Overview of major pollen types and seasonal features

Throughout the Dublin sampling campaign, a total of 65 pollen types were identified with varying degrees of prevalence and severity. Several dominant pollen types were identified based on their re-occurring annual prevalence, as shown in Figure 3.2, including Urticaceae (29%), Poaceae (28%), *Betula* (9%), Cupressaceae (9%), *Fraxinus* (4%), *Quercus* (4%), *Pinus* (2%) and *Alnus* (2%), which represent a combined 87% of the pollen recorded. In this case, the Cupressaceae classification refers to pollen grains from both the Cupressaceae and Taxaceae families that show similar optical features.

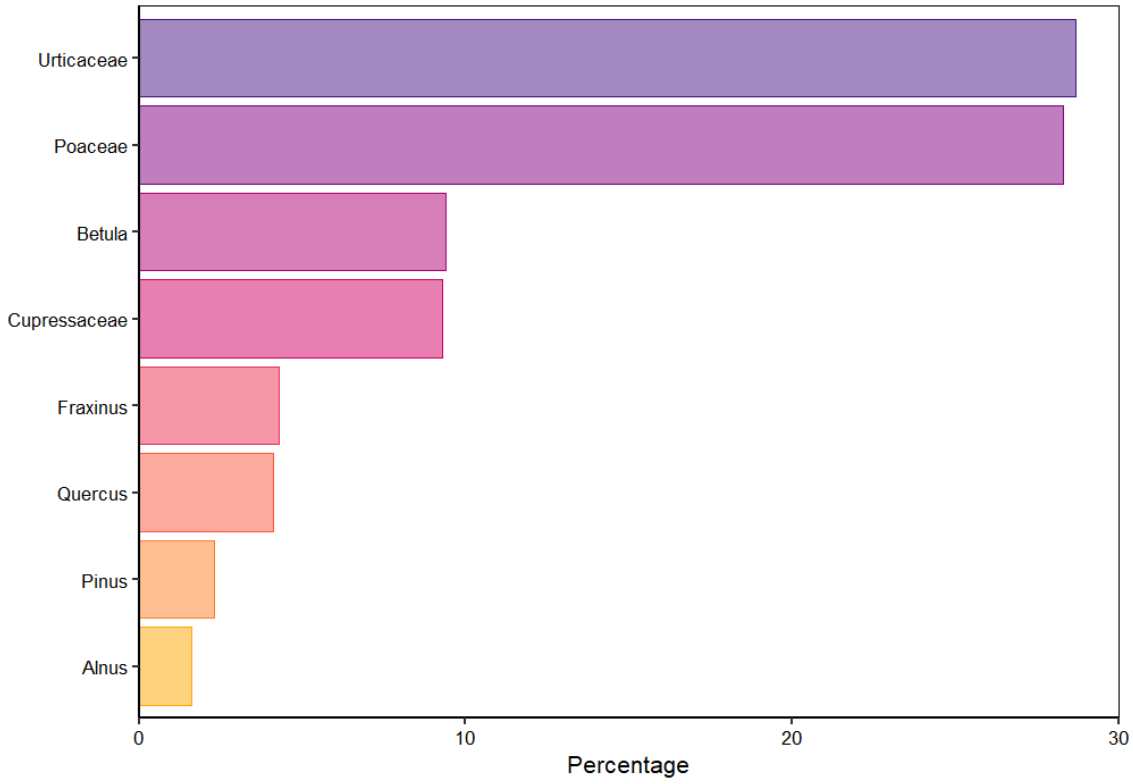

Figure 3.2: Percentage distribution of major pollen recorded in Dublin (2017-2020)

A time-series of the total annual pollen concentrations is depicted in Figure 3.3 highlighting the pollen season progression in Dublin as well as annual variations in intensity. Generally, the pollen season in Ireland commences in late January with the release of arboreal pollen, firstly with *Corylus*, followed by *Alnus*, Cupressaceae and *Fraxinus*. Other tree pollen types were also present during later spring months such as *Betula*, *Pinus*, *Salix*, *Platanus*, *Populus* and *Quercus*. The end of spring saw the commencement of the Poaceae pollen season, which is shortly accompanied by other herbaceous pollen types such as *Rumex, Plantago* and Urticaceae and several arboreal pollens such as *Tilia* and *Castanea*. The pollen season starts to decline in late summer until late September/October when it finally ceases until the return of early season *Corylus* pollen in December. Several pollen types were found to have a persistent presence throughout the year. This was particularly true for Cupressaceae, and *Pinus* with *Mercurialis* pollen exhibiting a heightened pervasiveness in 2020.

Overall, a bi-modal distribution is apparent with the first spring peak arising in March-April followed by a more intense summer peak from June to August. A more detailed monthly distribution of total pollen concentrations is given in Figure 3.4. The spring-time peak period during April is dominated by high concentrations of *Betula* (49%), *Fraxinus* (23%) and Cupressaceae (14%) pollen. Following a decrease in pollen concentrations during May, a sharp increase dominated by Poaceae (53%) and Urticaceae (33%) concentrations is then seen for June.

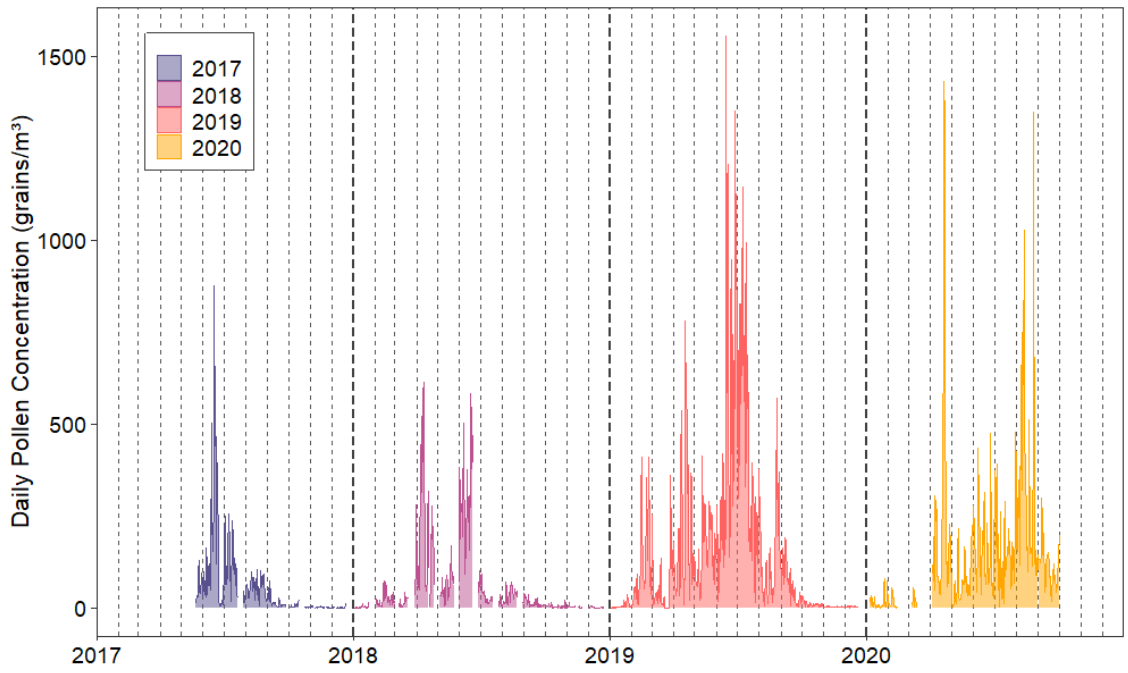

Figure 3.3: Time-series of total pollen concentrations from 2017 -2020 (Dublin)

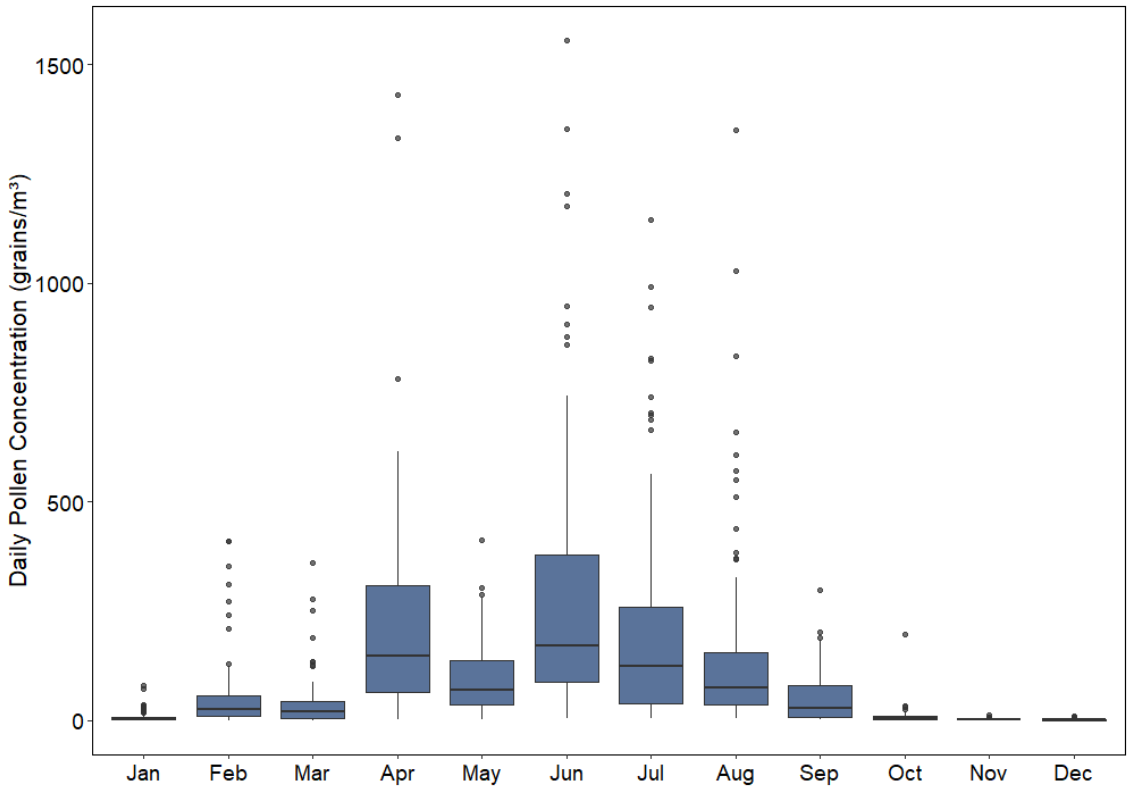

Figure 3.4: Monthly distribution of total pollen concentrations from 2017-2020 (Dublin)

Although these general seasonal trends were repeated annually, the analysis of total pollen concentrations between years reveals several notable deviations. 2018 had the lowest APIn for total pollen (16,233 Pollen * day/m^3), followed by 2020 concentrations which yielded an APIn of 34,010

Pollen * day/m^3, with 2019 possessing the highest APIn of 52,496 Pollen * day/m^3. The 2017 season was excluded from this comparison since sampling commenced in mid-May and thus, failed to record the spring peak period. Over the sampling campaign, eight major pollen types were identified, as shown in Figure 3.2. These pollen types are representative of the overall Dublin pollen season, further analysis of these pollen types was carried out with seasonal statistics depicted in Table 3.1, below. Due to the late sampling start of 2017, only Poaceae and Urticaceae pollen from this year will be examined.

Table 3.1 Major Pollen Types and Main Pollen Season Parameters for Dublin 2017-2020

2017							
Pollen type	**Start Date**	**End Date**	**Length (Days)**	**APIn (Pollen * day/m^3)**	**Peak value (grains/ m^3)**	**Peak date**	**% Total Pollen**
Poaceae	06/06/17	01/08/17	57	4438	547	17/06/17	43.3
Urticaceae	02/06/17	03/09/17	94	4584	285	17/06/17	44.7
2018							
Pollen type	**Start Date**	**End Date**	**Length (Days)**	**APIn (Pollen * day/m^3)**	**Peak value (grains/m^3)**	**Peak date**	**% Total Pollen**
Alnus	03/02/18	31/03/18	57	244	17	12/02/18	1.5
Betula	06/04/18	25/04/18	20	2623	346	11/04/18	16.1
Cupressaceae	14/02/18	09/07/18	146	3063	208	10/04/18	18.9
Fraxinus	31/03/18	23/04/18	24	1549	218	11/04/18	9.5
Pinus	06/04/18	08/06/18	64	304	43	20/05/18	1.9
Poaceae	20/05/18	05/07/18	47	3588	410	17/06/18	22.1
Quercus	22/04/18	29/07/18	99	331	18	10/05/18	2
Urticaceae	01/06/18	03/09/18	95	3535	257	19/06/18	21.7
2019							
Pollen type	**Start Date**	**End Date**	**Length (Days)**	**APIn (Pollen * day/m^3)**	**Peak value (grains/m^3)**	**Peak date**	**% Total Pollen**
Alnus	27/01/19	02/03/19	35	1501	168	15/02/19	2.9
Betula	28/03/19	11/05/19	45	4905	553	18/04/19	9.3
Cupressaceae	14/02/19	11/07/19	148	5164	243	25/02/19	9.8
Fraxinus	19/03/19	17/05/19	60	168	14	18/04/19	0.32
Pinus	05/05/19	29/06/19	56	1621	125	22/05/19	3.1
Poaceae	07/06/19	01/08/19	56	17401	1057	15/06/19	33.1
Quercus	22/04/19	05/07/19	75	2696	152	11/06/19	5.1
Urticaceae	10/06/19	08/09/19	91	14819	534	26/08/19	28.2

2020							
Pollen type	**Start Date**	**End Date**	**Length (Days)**	**APIn (Pollen * day/m^3)**	**Peak value (grains/m^3)**	**Peak date**	**% Total Pollen**
Alnus	09/01/20	12/04/20	95	90	8	30/01/20	0.3
Betula	05/04/20	29/04/20	25	3082	669	20/04/20	9.1
Cupressaceae	26/01/20	26/08/20	214	2105	206	25/08/20	6.2
Fraxinus	06/04/20	29/04/20	24	3149	704	21/04/20	9.3
Pinus	01/05/20	12/06/20	43	535	80	20/05/20	1.6
Poaceae	31/05/20	25/08/20	87	6546	325	07/06/20	19.2
Quercus	20/04/20	28/07/20	100	1496	94	10/05/20	4.4
Urticaceae	07/06/20	31/08/20	86	9439	761	12/08/20	27.8

Overall, the majority of pollen types experienced an increase in APIn from 2018-2019, followed by a decrease in 2020, with the exception of *Fraxinus*. Having said that, notable fluctuations and deviations were seen for many pollen types over the sampling period. This is particularly apparent for pollen taxa that exhibit starkly differing APIn concentrations, peak dates, season durations etc. between seasons. This is most clearly seen for *Alnus* pollen and *Fraxinus* pollen.

Alnus pollen experienced high peak value and APIn concentrations in 2019 with significantly lower concentrations recorded for the preceding season and even more so for the successive 2020 season. Although the 2019 season recorded peak *Alnus* concentrations, the season length was significantly shorter and commenced later than the 2020 season. The peak date also fluctuated, with the 2020 season exhibiting a notable deviation from *Alnus* peak dates recorded for the other years which only differed by 3 days.

Fraxinus pollen exhibited a unique behaviour over the sampling period. Unlike the other pollen types examined, *Fraxinus* pollen showed a significant decline in APIn in 2019, reaching peak daily concentrations of only 14 pollen grains/m^3. This is very different from the peak daily concentrations recorded in 2018 (218 grains/m^3), with an even further increase in peak concentrations seen in 2020 (704 grains/m^3). The pollen season for *Fraxinus* is more comparable for 2018 and 2020, having the same duration with an overall 6-day shift in start and end dates and a 10-day difference in peak days. The *Fraxinus* season began slightly earlier in 2018 than in 2020 and showed the earliest start date, longest duration in season length and overall muted concentrations

Both *Betula* and *Quercus* pollen exhibit similar trends from 2018 to 2020. Both pollen types exhibit similar seasonal statistics in terms of start and end date, and duration when comparing their 2018 to 2020 seasons. *Betula* pollen seasons differed slightly between 2018 and 2020 – ending

slightly later in 2020 with an additional 5-day length to the season. The peak day of *Betula* in 2018 occurred 1 week earlier than in 2019 and 9 days earlier than in 2020. In the case of *Quercus*, both the 2018 and 2020 seasons possessed the same peak day and a seasonal duration with a 1-day difference. In both cases, the 2018 season of *Betula*/*Quercus* had lower APIn concentration when compared to 2020. Both pollen types illustrated heightened APIn and peak day concentrations in 2019. Whereas the season length of *Betula* in 2019 increased from 20-25 days to 45, the *Quercus* season length decreased from 99-100 days to 75. *Quercus* pollen also exhibited a much later peak day, 1 month later than those seen in 2018 and 2020.

Pinus also exhibited several changes throughout the sampling seasons. Akin to the majority of the other major pollen types, *Pinus* APIn was considerably lower in 2018 than in the other seasons, with 2019 exhibiting the highest APIn. The duration of the *Pinus* pollen season appeared to gradually decrease in duration, while the start and end dates also fluctuated. In 2018 the *Pinus* season commenced almost a month earlier than in the following years and ended in the second week of June. A similar end date was seen for the 2020 season although the season started later at the start of May.

Although the 2018 and 2019 Cupressaceae pollen seasons exhibit similar start and end dates, both peak dates differ substantially. Cupressaceae pollen concentrations peaked in early April 2018 and in late February 2019. This is further contrasted with the 2020 peak date in late August. The 2020 season also commenced very early at the end of January and lasted until late August with a combined seasonal duration of 214 days, up substantially from the 2018 and 2019 seasons. The 2020 season was also accompanied by lower APIn concentrations, with comparable peak day concentrations to 2018. Once again, the highest APIn and peak day concentrations were recorded in 2019.

The 2017 season extended the data for both Poaceae and Urticaceae pollen types. The 2017 and 2019 Poaceae seasons had similar characteristics in terms of start date, end date, duration, and peak date. However, 2019 had higher concentrations than any other season. Peak day dates remained consistent from 2017-2019. However, the 2020 Poaceae peak date occurred 8-10 days earlier and the season lasted longer with a seasonal duration of 87 days. The Poaceae seasons of 2017 and 2019 lasted 57 and 56 days, respectively. The 2018 season commenced the earliest on the 20th of May and finished the earliest at the start of July. In comparison, both the 2017 and 2019 seasons started in early June and ended on the first of August. The 2020 season on the other hand started on the 31st of May and continued until the end of August.

Many parallels and comparisons can also be made between the different Urticaceae seasons. The 2017 and 2018 seasons held several similar characteristics, including start and end dates, season duration, peak date, and peak concentrations. Both seasons began within 1 day of each other and finished on the same day, with peak dates only differing by 2 days. The later 2019 and 2020 seasons are much more changeable in comparison. The 2019 season started the latest and had the highest

APIn and the latest peak date (end of August). The 2020 season began slightly earlier than that of 2019 and approximately a week later than the 2017-2018 seasons. Despite lower APIn, the peak day concentration in 2020 was the highest seen throughout the campaign at 761 pollen grains/m^3, over 200 grains/m^3 higher than the peak day concentration in 2019.

To find the bi-hourly peak distributions of pollen concentrations, bi-hourly resolution pollen data was also studied, as shown in Figure 3.5. In order to reduce the influence of days with high pollen concentrations each 24-hour period was standardised prior to analysis.

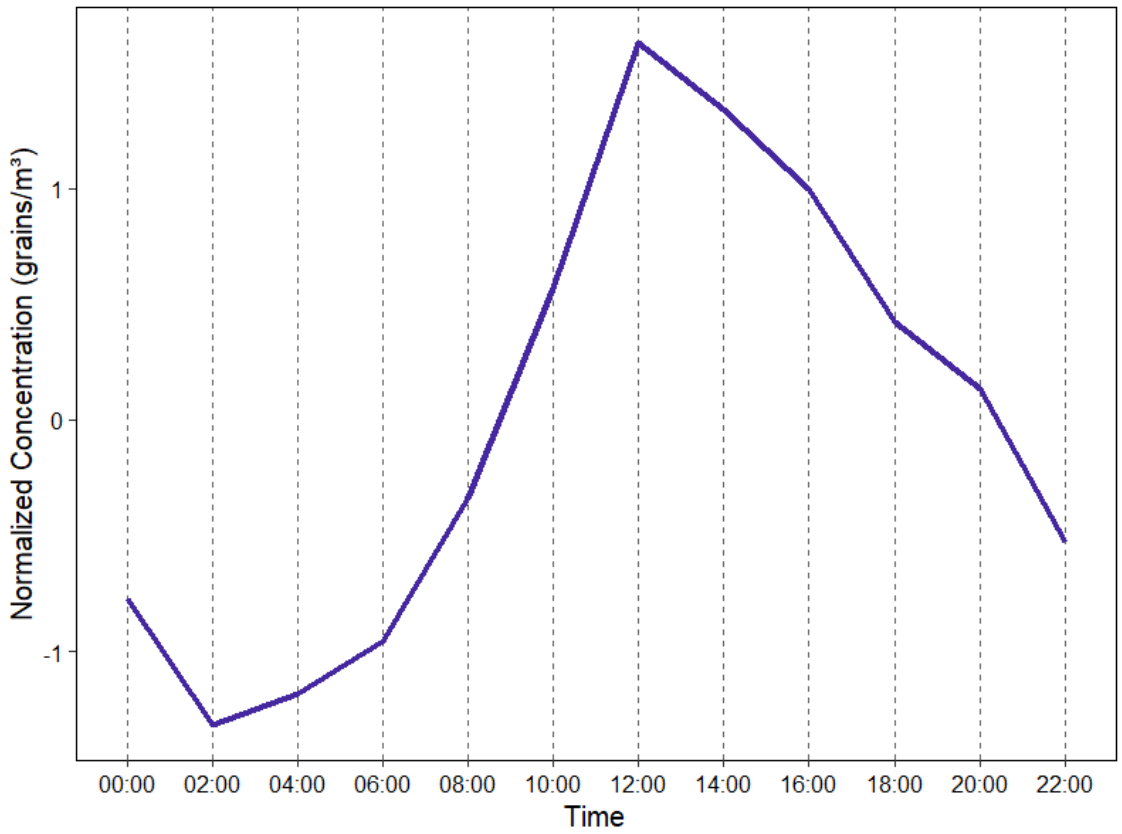

Figure 3.5: Average bi-hourly diurnal trend of total pollen concentrations (Dublin)

Overall, the total pollen concentrations in Dublin were shown to peak at midday with the beginning of the crest commencing at 06:00 and descending steadily throughout the afternoon-evening. The average daily distributions of the 8 prevailing pollen types were also investigated and illustrated in Figure 3.6. Many of the pollen types showcase a similar single peak in daily distributions such as Cupressaceae and *Pinus* which peaked at midday, and Poaceae and Urticaceae which peaked slightly later in the day at 16:00 and 14:00, respectively. Others showcased multi-peak distributions such as *Fraxinus* pollen, which experienced an early-day peak concentration at 08:00 and an evening peak at 18:00. *Alnus* pollen also experienced a multi-peak distribution with a slight early morning peak at 06:00 and two afternoon peaks at 12:00 and 15:00. Prolonged peak periods were also witnessed for *Betula* and *Quercus*. *Betula* pollen concentrations illustrated a weak forked distribution at 8:00 with concentration remaining high until another slight increase at 12:00, followed

by a successive decline. Similarly, *Fraxinus* pollen experiences an early peak at 08:00. However, this was followed by a slightly lower peak at 14:00 and a higher peak at 18:00.

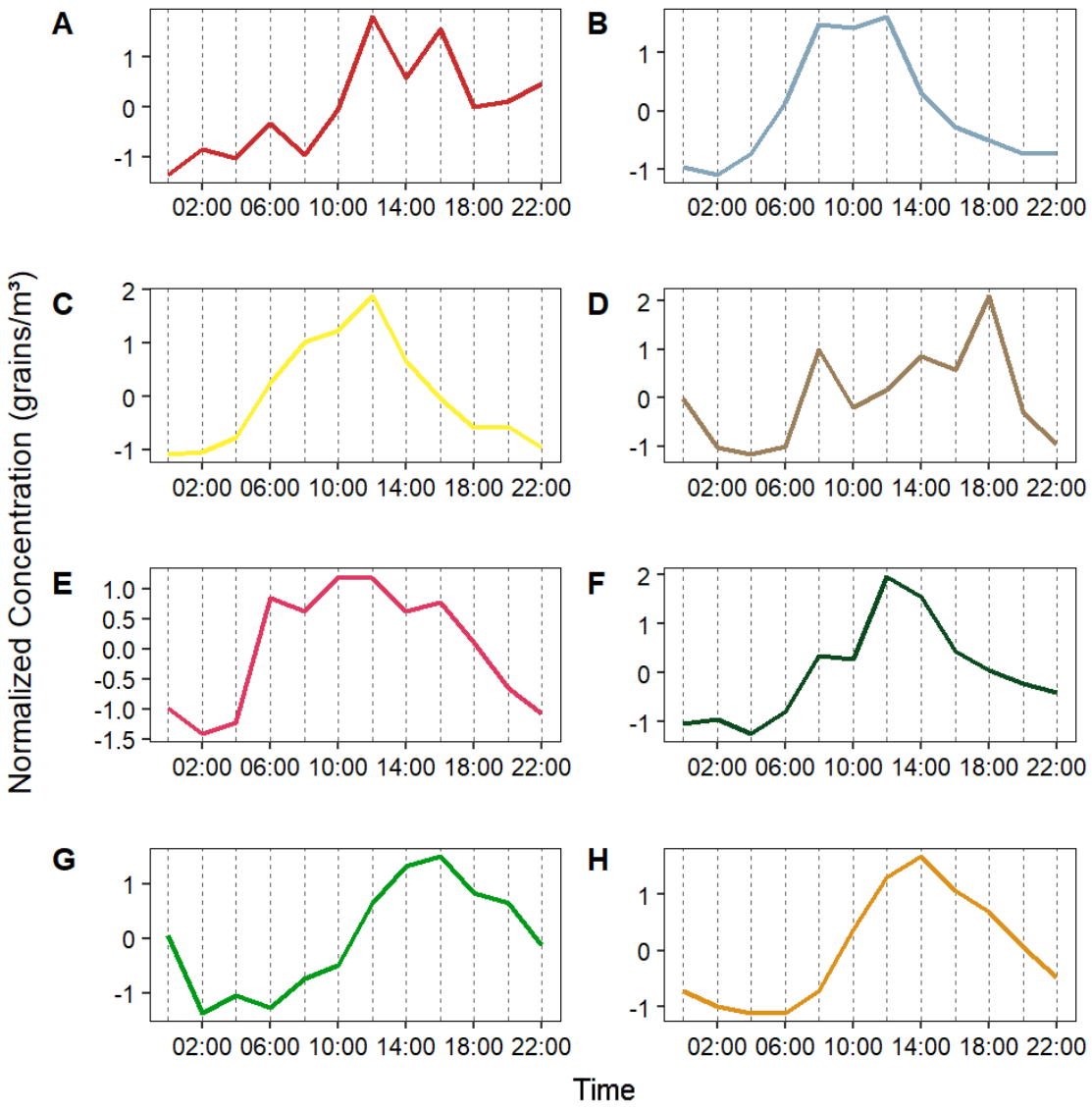

Figure 3.6: Average bi-hourly diurnal trends of (A) Alnus, (B) Betula, (C) Cupressaceae, (D) Fraxinus, (E) Quercus, (F) Pinus, (G) Poaceae and (H) Urticaceae pollen concentrations

3.3.2 Pollen calendar

A pollen calendar is a graphical representation of the average annual/seasonal trends of major pollen types, typically those of allergenic concern, for a particular location. Although an approximation of the seasonal trends in Ireland has been presented above, variations exist between each year. A start date for the MPS of one year could differ substantially from the next. Therefore, it is recommended that at least 5-7 years of data is incorporated into the construction of a pollen calendar (Galán et al. 2017). For this reason, the data obtained solely from this monitoring campaign is insufficient for the construction of a pollen calendar for Dublin (2017-2020). As a result, previously unpublished pollen

data from 1978-1980, and 2010-2011 were incorporated in creating an updated and simplified pollen calendar for Dublin (Figure 3.7). This is an adapted of the original first Dublin pollen calendar published by (Markey et al., 2022a).

The pollen calendar depicted in Figure 3.7, shows the average annual trends for the 15 most frequent and recurrent pollen taxa identified in the Dublin environment. In addition to being colour-coded according to the stages of the flowering period and their allergenic potential as described in the literature (Aerts et al., 2021; Bousquet et al., 2007; D'Amato et al., 2007; Gadermaier et al., 2014; Heinzerling et al., 2005; Pablos et al., 2016; Skjøth et al., 2013b; Solomon, 1969; Vallverdú et al., 1998; de Weger et al., 2013), the taxa were arranged in order of their appearance within the calendar year. As a factor of proportional exposure to the Irish population, general ambient concentrations observed during the sampling years were also considered.

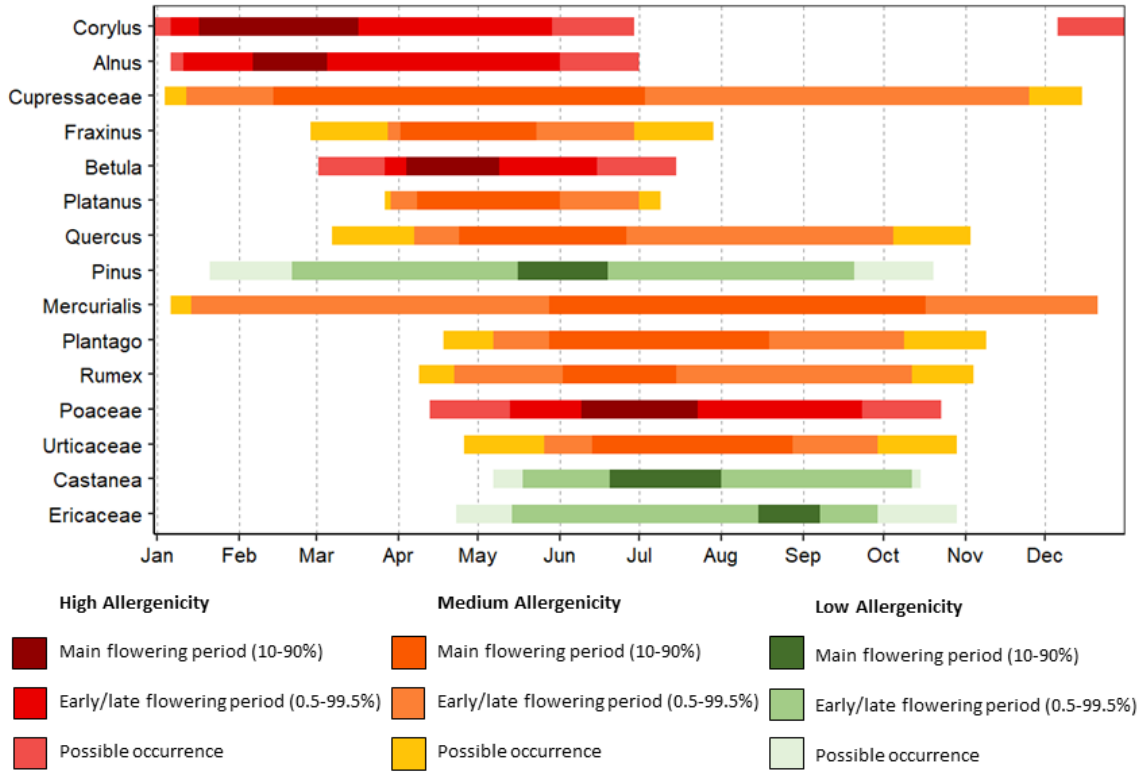

Figure 3.7: Dublin pollen calendar (periods of 1978-1980, 2010-2011 and 2017-2020).

3.3.3 Meteorological influence on pollen production and release

Association between seasonal pollen concentrations and individual meteorological factors were investigated for Dublin by calculating Spearman's rank coefficients between daily pollen concentrations and individual meteorological parameters (Table 3.2). Once again, due to the late sampling start of 2017, only Poaceae and Urticaceae pollen from this year was analysed for correlation with meteorological parameters.

It was observed that correlations between pollen types and meteorological parameters produced varying results depending on the year. Although a more detailed summary is provided, it was found generally that temperature and relative humidity were the most consistently influential meteorological parameters on pollen concentrations. Typically, increasing temperature led to increased concentrations of many of the analysed pollen taxa, whereas, increasing relative humidity led to the decline of ambient pollen concentrations. However, on occasion, there were periods for certain pollen taxa where the opposite was observed – indicating that the relationship is more complex and dependent on other environmental conditions.

During 2017, both Poaceae and Urticaceae pollen illustrated strong positive correlations with temperature, pressure, sun/global radiation, and evaporation variables, while strong negative correlations were seen for rain, relative humidity and cloud amount. In 2018, Poaceae concentrations illustrated differing relationships, now presenting a strong positive correlation with wind speed while correlations to sun duration and pressure were shown to have a negative impact. Urticaceae also showed a slightly positive significant correlation to wind speed and a strong negative correlation with the mean temperature over the previous 10 days. More changeable correlations were seen for the 2019 and 2020 seasons – with positive associations with pressure and global radiation seen, accompanied by negative associations with relative humidity and rain returning in 2019. Interestingly, in 2020, little significant correlation was seen for many of the pollen types – including Poaceae which now only showed a positive correlation with the mean temperature of the preceding 10 days. Urticaceae on the other hand once again shows positive correlations to temperature variables and negative associations with wind speed.

Similar unsettled behaviour was also witnessed for many of the arboreal pollen types. Many of the early season pollen types such as *Alnus, Betula* and Cupressaceae, showed very little significant correlation with meteorological parameters during 2018. *Alnus* exhibited a positive correlation with wind speed and *Betula* showed a positive correlation with average rainfall over the previous 10 days. In comparison, 2019 showed much stronger associations between these pollen types and weather. In the case of *Alnus* and *Betula* pollen, strong positive correlations were seen for many temperature, pressure and sun parameters and a negative correlation was seen for relative humidity. Conversely, Cupressaceae pollen showed notable negative correlations with temperature, sun and rain variables. Once again, the 2020 season showed very few significant correlations between these pollen taxa and weather.

The remaining tree pollen types (*Fraxinus, Quercus* and *Pinus*) appeared to be subject to more meteorological influence in 2018 than *Alnus, Betula* and Cupressaceae pollen. Both *Fraxinus* and *Quercus* pollen illustrated significant positive correlations with relative humidity and rain variables and negative correlations with temperature and global radiation. *Pinus* pollen showed significant positive correlations with pressure and soil temperature and a negative association with relative humidity. In comparison, *Fraxinus* showed significantly stronger positive correlations with

sun, global radiation and evaporation parameters in 2019, with little meteorological influence illustrated for *Quercus* pollen and a notable negative correlation seen for *Pinus* with the average temperature and rainfall over the previous 10 days. Once again, in 2020 different associations were witnessed, with *Fraxinus* showing no correlation with weather, *Quercus* showing a positive correlation with wind speed and negative correlations with sun and global radiation. *Pinus* on the other hand showed significant correlations with temperature variables, cloud amount and average rain concentrations over the previous 10 days.

Table 3.2: Spearman´s rank correlation coefficients between daily MPS 2017-2020 Dublin pollen data and meteorological parameters.

2017								
	Alnus	***Betula***	**Cupressaceae**	***Fraxinus***	***Quercus***	***Pinus***	**Poaceae**	**Urticaceae**
Tmax	-	-	-	-	-	-	**0.55****	**0.53****
Tmin	-	-	-	-	-	-	0.24	**0.22***
Tmin	-	-	-	-	-	-	**0.46****	**0.43****
Gmin	-	-	-	-	-	-	0.11	0.12
Rain	-	-	-	-	-	-	**-0.63***	**-0.55***
Pres	-	-	-	-	-	-	**0.62****	**0.43****
Wind_s	-	-	-	-	-	-	-0.20	**-0.12**
Wind_d	-	-	-	-	-	-	-0.05	0.03
Day_L	-	-	-	-	-	-	**0.32****	**0.29****
G_rad	-	-	-	-	-	-	**0.38****	**0.33****
Soil	-	-	-	-	-	-	**0.44****	**0.37****
Pe	-	-	-	-	-	-	**0.44****	**0.42****
Evap	-	-	-	-	-	-	**0.40****	**0.38****
RH	-	-	-	-	-	-	**-0.27****	**-0.36****
CldAmt	-	-	-	-	-	-	**-0.27****	**-0.29****
Tmed_10	-	-	-	-	-	-	-0.21	-0.12
Rain_10	-	-	-	-	-	-	0.17	0.16
2018								
	Alnus	***Betula***	**Cupressaceae**	***Fraxinus***	***Quercus***	***Pinus***	**Poaceae**	**Urticaceae**
Tmax	-0.13	-0.15	0.02	**-0.44***	**-0.52****	0.21	-0.05	-0.23
Tmin	-0.05	0.24	0.12	-0.03	**-0.63****	-0.24	0.23	-0.05
Tmin	-0.10	-0.02	0.06	-0.36	**-0.65****	0.10	-0.07	-0.21
Gmin	0.09	0.15	0.12	0.04	**-0.53****	-0.21	0.25	0.01
Rain	-0.06	0.11	0.03	0.16	0.15	-0.19	0.15	-0.03

Pres	0.11	-0.25	-0.03	-0.29	-0.11	**0.43****	**-0.34****	-0.07
Wind_s	**0.37***	0.21	-0.02	-0.19	0.15	-0.32	**0.26****	**0.15****
Wind_d	-0.21	-0.35	0.10	**-0.66****	-0.05	**-0.50***	**0.44****	-0.02
Day_L	-0.12	-0.18	-0.19	**-0.57***	-0.02	0.13	**-0.24***	-0.03
G_rad	-0.04	-0.17	-0.07	**-0.64****	-0.07	0.21	-0.21	0.04
Soil	-0.14	-0.16	0.05	-0.44	**-0.66****	**0.40***	-0.15	-0.11
Pe	0.19	-0.12	0.00	**-0.52***	**-0.26***	0.25	-0.07	-0.02
Evap	0.24	-0.06	0.00	**-0.55****	-0.21	0.20	0.00	0.03
RH	-0.23	0.11	0.05	**0.53****	0.18	**-0.11****	-0.15	0.15
CldAmt	0.07	0.15	0.14	**0.46***	-0.04	-0.10	0.23	0.09
Tmed_10	0.04	-0.32	0.05	-0.38	**-0.71****	0.28	0.04	**-0.60****
Rain_10	-0.05	**0.40*****	**0.04****	**0.48***	**0.65****	-0.26	-0.01	**-0.17***
2019								
	Alnus	***Betula***	**Cupressaceae**	***Fraxinus***	***Quercus***	***Pinus***	**Poaceae**	**Urticaceae**
Tmax	**0.73****	**0.29*****	-0.02	**0.34****	-0.15	0.05	0.19	0.01
Tmin	0.45	-0.05	**-0.21****	-0.02	-0.14	-0.18	-0.02	-0.25
Tmin	**0.66****	**0.21*****	-0.13	**0.21***	-0.16	-0.06	0.10	-0.15
Gmin	0.39	-0.17	**-0.30****	-0.16	-0.14	-0.18	-0.04	**-0.25***
Rain	-0.33	-0.30	**-0.25***	-0.14	-0.01	-0.27	-0.21	**-0.48***
Pres	**0.62****	**0.25***	**0.16****	-0.10	-0.26	**0.32***	**0.42***	**0.43****
Wind_s	-0.03	-0.03	-0.04	-0.19	**0.06***	-0.17	**-0.33***	**-0.35****
Wind_d	**-0.51***	0.08	-0.09	-0.12	0.00	0.14	0.06	-0.11
Day_L	0.02	**0.40*****	0.05	**0.21***	0.00	0.05	0.26	0.17
G_rad	**0.26***	**0.30***	**-0.14***	**0.28***	0.03	0.06	0.32	**0.30****

Soil	**0.62****	-0.02	**-0.22****	**0.21***	-0.25	0.01	0.17	0.17
Pe	**0.56****	**0.31***	**-0.15***	**0.34****	-0.01	0.02	0.28	0.20
Evap	**0.61****	**0.32***	**-0.17****	**0.34****	0.03	0.03	0.28	**0.26***
RH	**-0.54****	**-0.35***	-0.09	-0.18	-0.16	-0.17	**-0.31***	**-0.25***
CldAmt	0.02	-0.20	**-0.09***	-0.09	0.03	-0.09	-0.12	-0.11
Tmed_10	**0.42***	-0.36	**-0.34****	-0.22	-0.33	**-0.47****	**-0.22***	**-0.49****
Rain_10	-0.06	-0.11	**-0.29****	-0.22	0.00	**-0.68****	-0.24	**-0.23***
2020								
	Alnus	***Betula***	**Cupressaceae**	***Fraxinus***	***Quercus***	***Pinus***	**Poaceae**	**Urticaceae**
Tmax	-0.07	-0.06	-0.04	-0.05	**-0.54***	**0.21****	0.50	**0.42****
Tmin	-0.49	0.22	-0.19	0.16	0.04	**0.35***	0.54	0.15
Tmin	-0.37	0.18	-0.12	0.13	-0.27	**0.26****	0.62	**0.37****
Gmin	-0.15	0.12	-0.21	0.09	0.01	0.32	-0.07	0.03
Rain	0.02	0.26	-0.25	0.22	0.24	-0.17	-0.37	-0.09
Pres	-0.35	-0.12	0.16	-0.14	-0.35	0.36	0.62	-0.05
Wind_s	0.26	0.06	-0.07	0.19	**0.35***	-0.04	-0.67	**-0.33***
Wind_d	-0.12	-0.12	-0.21	-0.37	0.02	0.17	0.07	-0.06
Day_L	0.27	-0.15	0.17	0.03	**-0.34***	-0.46	0.52	0.13
G_rad	0.28	-0.20	0.10	0.07	**-0.34***	-0.20	0.60	0.03
Soil	-0.23	-0.10	-0.06	0.06	-0.18	**0.31***	0.44	**0.53****
Pe	0.12	-0.14	**0.04***	-0.10	**-0.49***	-0.15	0.55	0.07
Evap	0.17	-0.05	**0.05***	0.02	-0.36	-0.12	0.55	0.00
RH	-0.25	0.25	-0.22	0.29	0.44	-0.12	-0.59	-0.01
CldAmt	-0.15	0.26	-0.15	0.07	0.26	**0.55***	-0.52	-0.26
Tmed_10	0.10	-0.63	-0.22	-0.65	**0.47****	0.20	**-0.31***	**0.49****
Rain_10	**-0.42***	0.48	-0.40	0.47	-0.27	**-0.79***	0.07	-0.20

**significance at the 95% level, **significance at the 99% level*

A summary of monthly meteorological conditions is also provided in Table 3.3, illustrating the varying weather experienced between the sampling years. Two meteorological extremes were experienced during 2018. A significant cold-spell was experienced during February-March with daily temperatures plummeting to as low as -5 °C. Conversely, in June of the same year, very dry and hot weather was experienced for the location, with daily temperatures reaching highs of 26.5 °C and cumulative rainfall amounts not exceeding 5 mm. In comparison, the weather conditions experienced during 2017, 2019 and 2020 were more stable.

2019 experienced periods of heavy rainfall particularly in May and Autumn from August-November and a mild February with max temperatures reaching an average of 15.6 °C, the highest of all the sampling years. Above-average levels of rainfall were recorded in February 2020 which was later followed by a very dry April and May and then significant amounts of rain in July.

Table 3.3: Descriptive monthly summary of meteorological parameters

2017						
	Tmax	**Tmin**	**Tmed**	**Rain**	**Day_L**	**Soil**
Jan	11.9	-4.8	5.7	21.9	1.9	5.4
Feb	12.9	-3.9	6.2	41.6	1.8	5.8
Mar	16.3	-1.7	7.7	67.2	4.1	8.0
Apr	16.5	-1.2	8.0	10.0	3.3	10.2
May	23.2	-1.5	11.6	43.5	7.2	14.8
Jun	26.3	3.7	14.4	86.4	5.4	16.9
Jul	24.2	6.0	15.0	42.2	5.4	17.3
Aug	21.8	4.9	14.6	73.2	3.9	15.8
Sep	18.9	4.5	12.4	82.3	4.3	13.1
Oct	19.5	0.8	11.2	47.8	2.4	11.4
Nov	14.1	-0.5	6.5	81.5	2.9	6.9
Dec	13.6	-4.8	5.3	63.1	1.9	4.8
2018						
	Tmax	**Tmin**	**Tmed**	**Rain**	**Day_L**	**Soil**
Jan	13.1	-3.2	5.3	93.1	2.4	4.4
Feb	12.0	-4.9	3.4	28.5	3.9	3.5
Mar	11.9	-5.1	4.3	94.8	2.6	3.8
Apr	18.8	-2.1	8.1	68.9	4.8	8.8
May	22.2	0.4	11.4	19.1	7.2	14.6
Jun	26.5	3.8	14.5	4.8	9.0	19.8
Jul	26.7	5.2	16.1	40.0	5.9	20.2
Aug	25.1	3.9	15.3	48.0	3.9	16.9
Sep	23.0	0.4	12.2	43.8	4.5	13.4
Oct	19.2	-4.7	9.3	42.6	3.9	9.8
Nov	15.3	1.1	8.2	131.2	1.7	7.3
Dec	13.4	0.8	7.7	81.0	1.0	6.6
2019						
	Tmax	**Tmin**	**Tmed**	**Rain**	**Day_L**	**Soil**
Jan	11.3	-5.8	5.1	26.8	1.5	5.2
Feb	15.6	-3.8	7.0	30.5	4.0	6.1
Mar	16.8	-2.1	7.3	92.5	4.3	7.3
Apr	21.7	-2.0	8.0	74.6	4.1	9.4
May	20.9	-0.8	10.2	33.4	4.5	12.8

Jun	22.7	2.0	12.5	82.9	5.3	15.0
Jul	24.9	4.4	15.9	41.0	5.4	18.9
Aug	22.3	7.8	15.4	91.9	5.6	16.7
Sep	20.9	3.4	13.0	104.6	4.8	14.2
Oct	16.4	-1.4	9.1	77.2	3.7	9.3
Nov	13.4	-2.4	6.0	173.0	1.4	6.2
Dec	13.8	-2.9	5.9	57.7	1.9	4.8
2020						
	Tmax	**Tmin**	**Tmed**	**Rain**	**Day_L**	**Soil**
Jan	14.2	-2.5	6.3	36.0	2.1	5.0
Feb	13.4	-2.3	5.8	130.4	3.6	4.8
Mar	15.0	-3.9	5.8	31.8	4.5	6.2
Apr	19.4	-2.5	8.5	12.8	6.3	11.2
May	21.5	-2.6	10.9	9.3	9.5	15.6
Jun	25.0	3.8	13.4	69.6	4.3	16.0
Jul	23.1	5.0	14.4	98.9	3.4	16.0
Aug	24.0	3.8	14.7	87.1	3.1	16.4
Sep	22.7	0.9	12.8	60.9	4.8	13.8
Oct	15.2	0.3	9.5	80.6	3.9	9.5
Nov	16.0	-1.2	8.2	48.1	2.4	7.9
Dec	14.2	-4.4	4.9	83.1	2.1	4.4

In efforts to provide a more detailed meteorological comparison with the pollen data collected during the campaign (especially for the years where little correlation was observed), the main pollen seasons of each major pollen type were further divided into PRP and PSP and compared to meteorological conditions. And are illustrated in Tables 3.4 and 3.5. Although varying degrees of correlation were seen depending on the pollen type and year in question, several general trends were observed.

Table 3.4: Spearman´s rank correlation coefficients between daily PRP 2017-2020 Dublin pollen data and meteorological parameters.

2017								
	Alnus	***Betula***	**Cupressaceae**	***Fraxinus***	***Quercus***	***Pinus***	**Poaceae**	**Urticaceae**
Tmax	-	-	-	-	-	-	**0.83****	**0.75***
Tmin	-	-	-	-	-	-	**0.59***	**0.66***
Tmed	-	-	-	-	-	-	**0.82****	**0.77****
Gmin	-	-	-	-	-	-	0.57	0.57
Rain	-	-	-	-	-	-	-0.64	-0.75
Pres	-	-	-	-	-	-	**0.60****	**0.62****
Wind_s	-	-	-	-	-	-	-0.40	-0.04
Wind_d	-	-	-	-	-	-	-0.08	-0.21
Day_L	-	-	-	-	-	-	**0.19***	**0.16****
G_rad	-	-	-	-	-	-	**0.49****	**0.48****
Soil	-	-	-	-	-	-	**0.80****	**0.64****
Pe	-	-	-	-	-	-	**0.59****	**0.70****
Evap	-	-	-	-	-	-	**0.39***	**0.64****
RH	-	-	-	-	-	-	**-0.46***	**-0.40***
CldAmt	-	-	-	-	-	-	**0.07***	**0.04****
Tmed_10	-	-	-	-	-	-	**0.75***	**0.48***
Rain_10	-	-	-	-	-	-	-0.04	0.43
2018								
	Alnus	***Betula***	**Cupressaceae**	***Fraxinus***	***Quercus***	***Pinus***	**Poaceae**	**Urticaceae**
Tmax	0.22	-0.31	0.13	0.17	-0.44	0.07	0.34	0.02
Tmin	-0.19	**0.49***	**0.32****	0.64	-0.39	-0.30	0.34	0.06
Tmed	-0.14	0.09	**0.25***	0.29	-0.50	-0.05	0.34	0.08
Gmin	-0.13	0.52	0.24	**0.78***	-0.16	-0.27	0.29	0.02
Rain	-0.25	-0.64	-0.02	-0.29	0.01	-0.02	0.00	0.32
Pres	-0.09	0.71	0.20	0.16	-0.12	**0.22***	**-0.45****	0.19
Wind_s	-0.08	0.14	0.02	0.07	0.38	-0.26	**0.21***	-0.14

Wind_d	**-0.24***	-0.43	-0.03	**-0.73***	0.10	-0.30	**0.54****	0.11
Day_L	-0.26	0.14	0.01	-0.42	0.07	0.04	-0.03	-0.21
G_rad	-0.18	-0.09	0.04	-0.56	0.00	0.09	0.01	-0.35
Soil	-0.40	0.12	**0.39****	0.19	-0.52	**0.24***	0.26	**-0.41***
Pe	-0.30	-0.03	0.24	-0.23	-0.20	0.16	0.31	-0.45
Evap	-0.31	0.09	0.21	-0.26	-0.15	0.12	0.35	-0.44
RH	0.40	0.03	-0.03	0.39	-0.29	**-0.20****	-0.45	0.36
CldAmt	0.19	-0.09	0.04	-0.49	-0.17	0.00	-0.21	0.06
Tmed_10	-0.06	0.09	-0.08	0.29	0.11	0.04	0.05	0.15
Rain_10	0.09	0.54	**0.47***	**0.45***	**0.69****	0.10	**0.57***	0.20
CldAmt	0.21	0.43	**0.17***	-0.05	0.23	-0.02	-0.49	**0.59****
2019								
	Alnus	***Betula***	**Cupressaceae**	***Fraxinus***	***Quercus***	***Pinus***	**Poaceae**	**Urticaceae**
Tmax	**0.90****	**0.33***	**0.78****	0.15	0.24	**0.71***	0.83	-0.05
Tmin	0.58	0.17	-0.29	-0.19	0.02	0.16	0.16	**-0.29***
Tmed	**0.86****	**0.48****	0.12	0.02	0.18	**0.70***	0.80	-0.23
Gmin	0.52	-0.14	-0.34	-0.32	-0.06	0.03	0.12	**-0.27***
Rain	-0.13	-0.44	-0.53	-0.10	-0.21	-0.45	**-0.18***	**-0.48***
Pres	**0.57***	**0.50***	**0.72****	-0.15	-0.02	0.36	0.33	**0.51****
Wind_s	0.08	-0.28	-0.35	-0.29	**0.15***	-0.07	0.08	**-0.33****
Wind_d	-0.36	0.28	-0.35	-0.29	-0.06	0.04	0.49	-0.10
Day_L	-0.08	0.12	0.21	-0.01	0.31	0.25	0.64	0.19
G_rad	0.25	0.18	0.30	0.16	**0.33***	0.35	0.78	**0.33***
Soil	**0.84****	**0.34***	0.20	0.16	0.26	**0.74****	0.66	0.14
Pe	**0.55***	**0.41***	-0.10	0.12	**0.33***	0.41	0.84	0.20
Evap	**0.64****	0.30	0.07	0.12	**0.39****	0.44	0.71	0.27
RH	**-0.52***	-0.21	-0.04	0.21	-0.38	-0.11	-0.67	**-0.25***
CldAmt	0.21	0.02	-0.12	-0.04	-0.18	-0.11	-0.42	-0.11
Tmed_10	**0.19****	-0.15	0.21	-0.43	0.06	0.25	0.26	**-0.47****
Rain_10	**0.35***	0.02	-0.15	-0.17	**0.14****	-0.05	**-0.32****	**-0.31****
2020								

	Alnus	*Betula*	Cupressaceae	*Fraxinus*	*Quercus*	*Pinus*	Poaceae	Urticaceae
Tmax	-0.07	-0.06	-0.04	-0.05	**-0.54***	**0.21****	0.50	**0.42****
Tmin	-0.49	0.22	-0.19	0.16	0.04	**0.35***	0.54	0.15
Tmed	-0.37	0.18	-0.12	0.13	-0.27	**0.26****	0.62	**0.37****
Gmin	-0.15	0.12	-0.21	0.09	0.01	0.32	-0.07	0.03
Rain	0.02	0.26	-0.25	0.22	0.24	-0.17	-0.37	-0.09
Pres	-0.35	-0.12	0.16	-0.14	-0.35	0.36	0.62	-0.05
Wind_s	0.26	0.06	-0.07	0.19	**0.35***	-0.04	-0.67	**-0.33***
Wind_d	-0.12	-0.12	-0.21	-0.37	0.02	0.17	0.07	-0.06
Day_L	0.27	-0.15	0.17	0.03	**-0.34***	-0.46	0.52	0.13
G_rad	0.28	-0.20	0.10	0.07	**-0.34***	-0.20	0.60	0.03
Soil	-0.23	-0.10	-0.06	0.06	-0.18	**0.31***	0.44	**0.53****
Pe	0.12	-0.14	**0.04***	-0.10	**-0.49***	-0.15	0.55	0.07
Evap	0.17	-0.05	**0.05***	0.02	-0.36	-0.12	0.55	0.00
RH	-0.25	0.25	-0.22	0.29	0.44	-0.12	-0.59	-0.01
CldAmt	-0.15	0.26	-0.15	0.07	0.26	**0.55***	-0.52	-0.26
Tmed_10	0.10	-0.63	-0.22	-0.65	**0.47****	0.20	**-0.31***	**0.49****
Rain_10	**-0.42***	0.48	-0.40	0.47	-0.27	**-0.79***	0.07	-0.20

**significance at the 95% level, **significance at the 99% level*

Table 3.5: Spearman´s rank correlation coefficients between daily PSP 2017-2020 Dublin pollen data and meteorological parameters.

2017								
	Alnus	***Betula***	**Cupressaceae**	***Fraxinus***	***Quercus***	***Pinus***	**Poaceae**	**Urticaceae**
Tmax	-	-	-	-	-	-	**0.53****	**0.50****
Tmin	-	-	-	-	-	-	0.11	0.13
Tmed	-	-	-	-	-	-	**0.41****	**0.38****
Gmin	-	-	-	-	-	-	-0.01	0.03
Rain	-	-	-	-	-	-	**-0.65***	**-0.51***
Pres	-	-	-	-	-	-	**0.67****	**0.39****
Wind_s	-	-	-	-	-	-	**-0.33***	**-0.16***
Wind_d	-	-	-	-	-	-	-0.05	0.06
Day_L	-	-	-	-	-	-	**0.32****	**0.31****
G_rad	-	-	-	-	-	-	**0.33****	**0.29****
Soil	-	-	-	-	-	-	**0.54****	**0.33****
Pe	-	-	-	-	-	-	**0.38****	**0.37****
Evap	-	-	-	-	-	-	**0.35****	**0.33****
RH	-	-	-	-	-	-	-0.20	**-0.36***
CldAmt	-	-	-	-	-	-	**-0.30****	**-0.33****
Tmed_10	-	-	-	-	-	-	-0.23	-0.20
Rain_10	-	-	-	-	-	-	0.01	0.11
2018								
	Alnus	***Betula***	**Cupressaceae**	***Fraxinus***	***Quercus***	***Pinus***	**Poaceae**	**Urticaceae**
Tmax	-0.27	0.11	-0.09	**-0.75***	**-0.43***	-0.45	**-0.34***	-0.05
Tmin	-0.04	0.42	0.06	-0.17	**-0.59****	-0.36	0.17	0.23
Tmed	-0.18	0.13	-0.05	-0.65	**-0.59****	-0.40	-0.41	0.12
Gmin	0.09	0.28	0.11	-0.23	**-0.54****	-0.13	0.33	0.25
Rain	0.03	0.07	0.04	0.28	0.07	**0.14***	**0.66****	0.08
Pres	0.20	-0.25	-0.08	-0.49	0.13	0.43	0.08	-0.03
Wind_s	**0.51****	0.34	-0.01	-0.20	-0.02	0.34	**0.73****	**0.12****

Wind_d	0.04	-0.01	0.20	-0.36	**-0.27***	-0.35	0.06	0.18
Day_L	-0.10	-0.04	**-0.30***	-0.62	0.00	-0.14	**-0.46****	-0.04
G_rad	-0.13	0.03	-0.23	-0.68	-0.02	-0.12	**-0.45****	-0.08
Soil	-0.16	0.13	-0.08	-0.53	**-0.55****	-0.51	**-0.43****	-0.08
Pe	0.05	0.20	-0.18	-0.47	-0.19	-0.08	**-0.48****	-0.15
Evap	0.11	0.28	-0.18	-0.43	-0.16	-0.11	**-0.44***	-0.11
RH	-0.20	-0.37	0.08	0.26	0.22	**-0.53****	0.31	0.14
CldAmt	0.12	-0.03	0.26	0.60	-0.03	-0.08	**0.44***	0.16
Tmed_10	0.12	0.14	-0.07	-0.25	**-0.65****	**-0.42***	**-0.84****	-0.34
Rain_10	0.03	-0.18	0.05	**0.31***	**0.59****	**0.51***	**0.73****	-0.12
2019								
	Alnus	***Betula***	**Cupressaceae**	***Fraxinus***	***Quercus***	***Pinus***	**Poaceae**	**Urticaceae**
Tmax	0.30	**0.66****	-0.01	**0.46***	-0.36	0.23	-0.13	**0.59***
Tmin	0.05	0.09	**-0.21****	-0.04	0.21	0.17	-0.26	0.23
Tmed	0.11	**0.65****	-0.11	0.37	-0.12	0.28	-0.25	0.36
Gmin	-0.01	0.01	**-0.32****	-0.10	0.19	0.14	-0.24	-0.01
Rain	-0.60	-0.28	-0.18	-0.17	0.47	-0.02	-0.31	-0.35
Pres	**0.46***	0.09	**0.11***	-0.04	**-0.67****	0.15	**0.56****	-0.32
Wind_s	0.11	0.01	-0.11	-0.07	-0.07	0.07	**-0.35***	-0.51
Wind_d	**-0.61***	0.13	-0.07	0.09	-0.05	**0.32***	-0.01	-0.40
Day_L	0.14	**0.57****	0.08	0.36	-0.51	-0.08	0.17	-0.07
G_rad	0.30	0.43	-0.02	0.28	-0.43	-0.05	0.28	0.03
Soil	0.03	**0.53***	-0.14	0.26	**-0.57****	0.14	-0.04	**0.63***
Pe	0.40	**0.59****	-0.03	**0.40***	-0.39	0.02	0.20	0.20
Evap	0.42	**0.61***	-0.03	**0.42***	-0.44	0.05	0.21	0.06
RH	**-0.63***	**-0.54****	-0.07	-0.37	0.32	-0.11	**-0.35***	-0.22
CldAmt	-0.32	-0.34	-0.04	-0.15	0.34	0.08	-0.10	-0.06
Tmed_10	0.25	-0.13	**-0.33****	-0.26	**-0.70****	**-0.19****	**-0.65****	-0.42
Rain_10	-0.10	-0.04	-0.25	-0.40	0.40	**-0.76****	-0.14	**0.69***
2020								
	Alnus	***Betula***	**Cupressaceae**	***Fraxinus***	***Quercus***	***Pinus***	**Poaceae**	**Urticaceae**

Tmax	-0.07	-0.10	-	-0.13	**0.22***	0.47	0.27	0.47
Tmin	0.19	-0.05	-	-0.49	-0.46	0.12	**-0.15***	0.30
Tmed	0.09	-0.09	-	-0.44	-0.14	**0.43***	0.08	0.49
Gmin	0.22	0.05	-	-0.29	**-0.40****	-0.11	**-0.20***	0.23
Rain	-0.07	0.00	-	-0.25	**-0.40***	-0.22	-0.20	-0.07
Pres	-0.06	0.25	-	0.23	**0.33****	0.31	0.21	-0.02
Wind_s	0.09	**0.62****	-	0.19	-0.05	0.04	-0.14	0.20
Wind_d	0.04	-0.25	-	-0.26	**-0.11****	-0.22	0.17	0.19
Day_L	-0.18	0.60	-	0.62	**0.54****	0.52	**0.32***	0.07
G_rad	-0.24	0.38	-	0.28	**0.52****	**0.52***	**0.39***	0.05
Soil	-0.03	-0.57	-	-0.24	**0.27****	0.46	0.10	**0.57****
Pe	-0.18	0.36	-	0.22	**0.51****	**0.50***	**0.45****	-0.04
Evap	-0.22	**0.41***	-	0.34	**0.51****	**0.55***	**0.43***	-0.03
RH	-0.03	-0.48	-	-0.26	**-0.61****	-0.40	-0.34	**0.27***
CldAmt	0.12	**-0.72****	-	-0.86	**-0.51****	-0.55	-0.15	0.14
Tmed_10	-0.14	-0.27	-	-0.16	-0.47	-0.07	**-0.43****	0.18
Rain_10	-0.36	0.56	-	0.55	**-0.70****	-0.29	-0.09	-0.35

**significance at the 95% level, **significance at the 99% level*

Examination of the PRP highlighted the importance of temperature and sun duration in pollen production and release. The majority of pollen types exhibited significant positive correlations with temperature variables (air or soil), sun and global radiation in at least one of their PRPs. However, during particularly dry or warm periods, the potential strain on pollen-producing plants can be seen – possibly suggesting drought-like/heat-stress conditions, this can be exhibited as negative correlations with temperature/sun parameters (like what was observed for *Quercus* pollen during the 2018 MPS). The same can be said for the PRP concentrations of *Quercus* pollen 2020, which also exhibited notable negative correlations with sun, global radiation and potential evapotranspiration. Although predominant negative correlations were observed for relative humidity and rain during the PRPs, there were times during the 2018 and 2019 sampling years when a notable positive correlation with average rainfall over the previous 10 days was observed, potentially hinting at the importance of rain before pollen release and again during times of dry weather.

On occasion, similar correlations extended to the PSP, with temperature and sun duration often continuing to play a role in pollen release and later the probable resuspension of pollen. In times of prolonged dry weather, a negative correlation was observed for sun duration and temperature. The PSPs generally show an increased dependence on wind-speed, both leading to an increase and decrease in several pollen types over the campaign. The increasing influence of evaporation was also observed, perhaps also indicating the likelihood of pollen resuspension after

peak days. In the case of the Cupressaceae pollen season of 2020, the PSP was classified as 1 day long and as such no correlations could be obtained.

3.3.4 Geographical origin of major pollen types

To better understand the transport of airborne pollen grains over Dublin, the ZeFir source receptor model was applied. Wind pollination is a significant transport mechanism for a wide variety of pollen types (Dowding, 1987). The resulting wind rose diagrams reveal details about the geographic origins of pollen. Recently, similar methods have been applied to evaluate the temporal variability and geographic origin of ambient bioaerosols (Estève et al., 2018; Markey et al., 2022a, 2022b; Martínez-Bracero et al., 2022; Sarda-Estève et al., 2020, 2019).

Results are depicted as a wind rose plot where sectors are shaded according to the joint probability of the wind originating from that direction. The term "Joint probability" (Figure 3.8) is used to describe the distribution and statistical probability of the prevailing winds experienced during the sampling period. A scale of wind speed in kilometres per hour is shown as white gridlines that cross through the wind rose plot, with the inner circle equalling 8 km/h, followed by 16 km/h, 24 km/h, and 32 km/h. The model results showed that prevailing winds at Dublin originate from a south-westerly direction sector at speeds between 8 and 24 km/h (Figure 3.8).

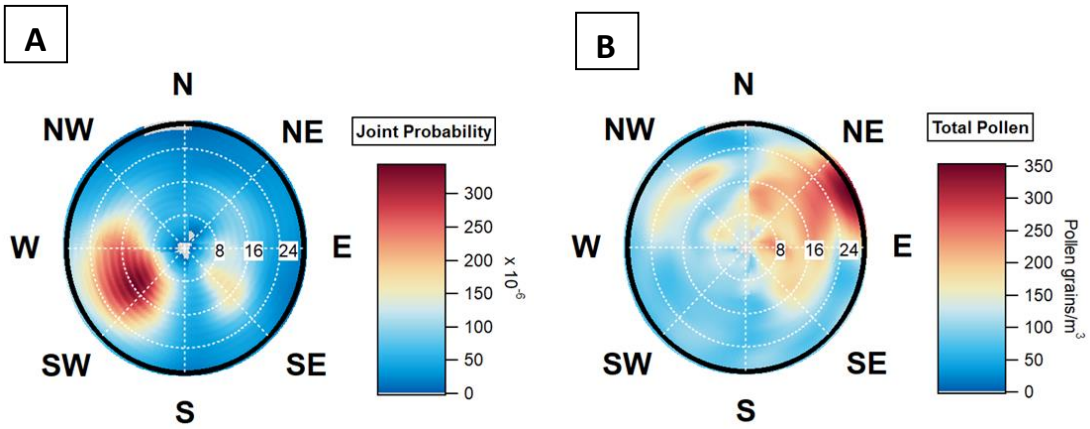

Figure 3.8: Wind rose of (A) prevailing winds during sampling period and (B)origin of total pollen concentration at the Dublin site. The white gridlines represent a wind speed scale in kilometres per hour (8 km/h, 16 km/h, 24 km/h, 32 km/h).

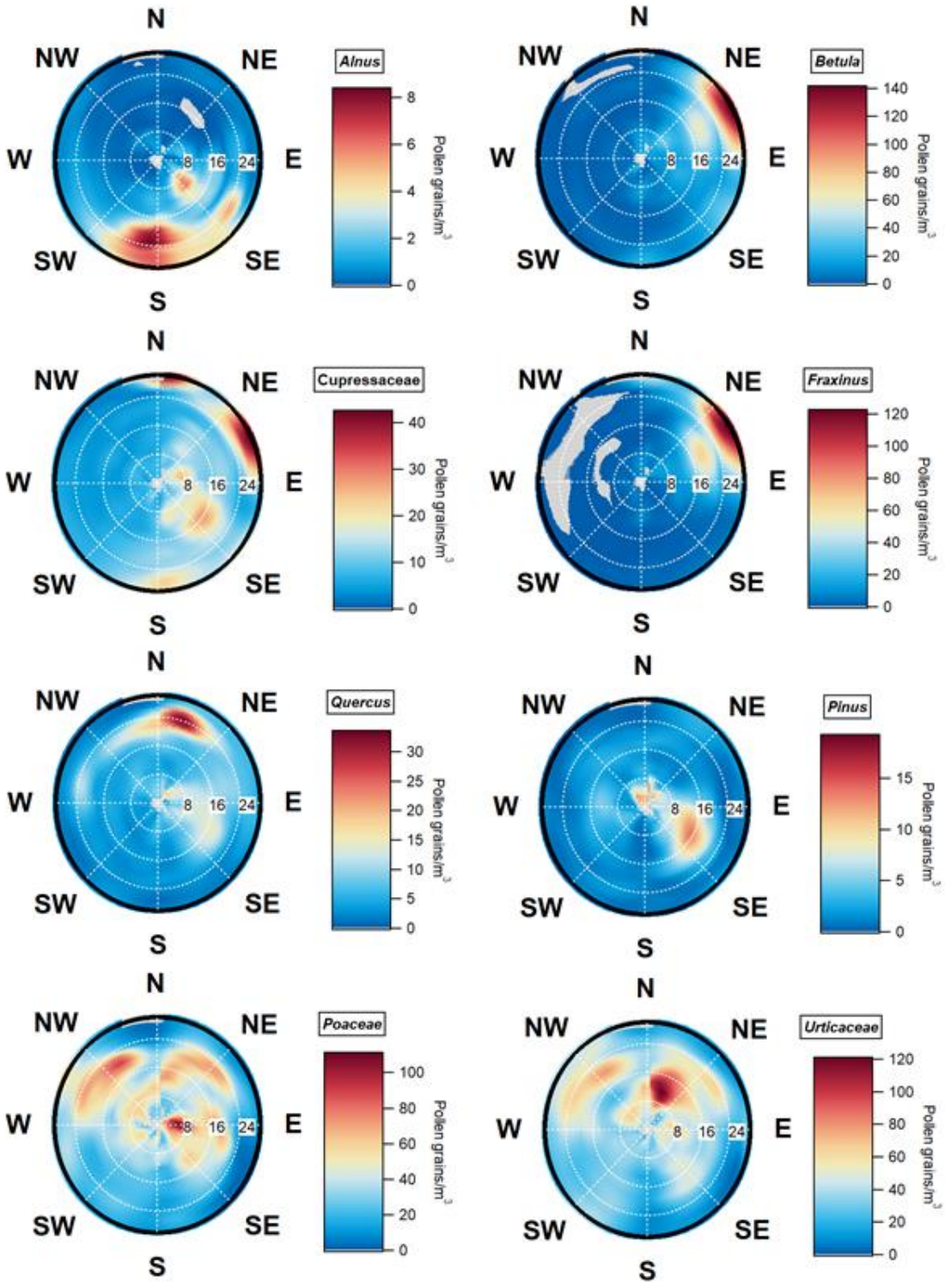

Figure 3.9: Origin of Alnus, Betula, Cupressaceae, Fraxinus, Quercus, Pinus, Poaceae and Urticaceae pollen concentrations at Dublin. The colour scale represents the estimated concentration (Pollen grain/m^3) while the white gridlines represent a wind speed scale in kilometres per hour (8 km/h, 16 km/h, 24 km/h, 32 km/h).

Total pollen was shown to originate from nort-east/east directions which differs significantly from the prevailing wind direction. The same analysis was also carried out for the major pollen types, as illustrated in Figure 3.9. The model results indicate that the main origin for *Alnus* pollen is from a south to south-easterly direction with varying wind speeds from less than 8 to greater than 24 km/h. Although higher concentrations were associated with higher wind speeds from the south. The main origins for both *Betula* and *Fraxinus* pollen were from the northeast/east sectors at strong wind speeds greater than 16 km/h. Cupressaceae pollen illustrated multiple sources in both the northern and north-eastern sectors at high wind speeds greater than 24 km/h. Other minor sources were also noted from a south-easterly direction at a range of wind speeds, this was also seen for *Quercus* pollen. However, the majority of *Quercus* pollen seemed to originate from a northerly direction at wind speeds between 16 and 32 km/h. *Pinus* pollen originated from several locations at particularly low wind speeds surrounding the area and then additionally from the southeast at wind speeds less than 24 km/h. Both Poaceae and Urticaceae pollen showed multiple sources – due to the widespread presence of these plants within the city. However, a strong easterly presence at low wind speeds (<8 km/h) was shown for Poaceae, while Urticaceae pollen exhibited a northerly origin at higher wind speeds between 8 and 16 km/h.

The varying wind speeds and directions associated with the differing pollen types provide greater insight into the geographical origins of different pollen types. To aid in the determination of possible local sources a landcover map for Dublin was also examined (Figure 3.10). Potential southern sources of tree pollen such as *Alnus* and grass pollen include the grasslands and forests that lie to the south of the city – this represents a fraction of the Wicklow mountains and national park. Several green urban areas are also present around the sampling site, including the Phoenix park which is seen as the large urban green area situated to the west of the city centre. Additional urban parks exist close to the sampling site that are not captured by the resolution of the Corine land cover. These include St. Kevin's Park which is directly to the east of the sampling site, the Iveagh Gardens, to the southeast and St. Stephens Green and Merrion Square to the northeast. All of these are within 2 km of the sampling site, representing several likely sources for the variety of pollen types investigated.

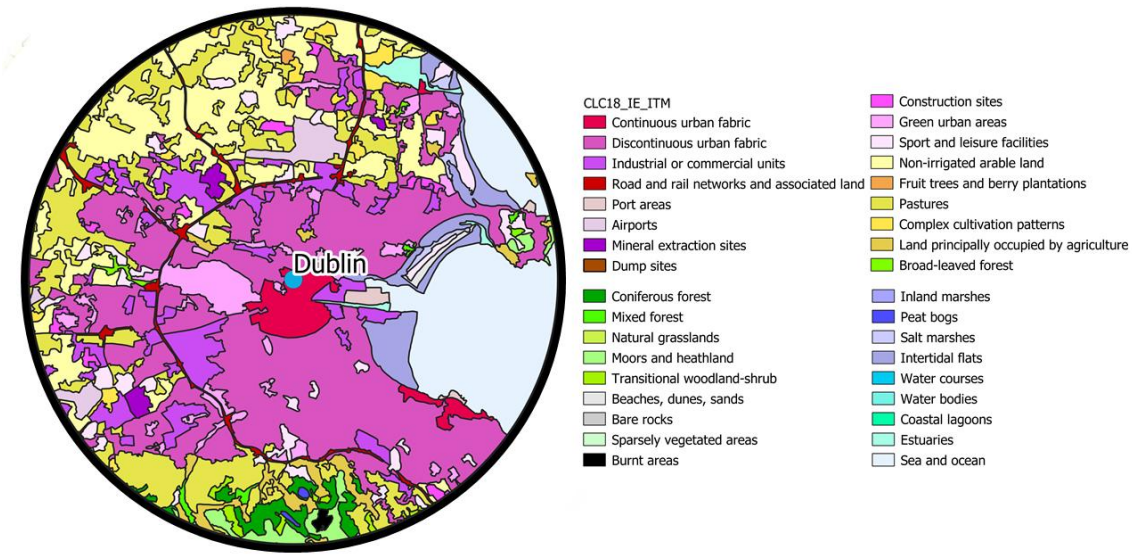

Figure 3.10: Land cover map of the immediate 30km surrounding the Dublin sampling site

3.3.5 Comparison between urban and rural sites (2018-2019)

A more detailed comparison between the two sites has been previously published in (Markey et al., 2022a), this section represents a summarised analysis. The relationship between the two sites was assessed by examining the correlation between the different pollen types, displayed in Table 3.6. Significant positive correlations were noted for *Betula*, Cupressaceae, *Fraxinus*, *Pinus* and Urticaceae for both years. Significant positive correlations were only observed for *Alnus* and *Quercus* during the 2019 season and for Poaceae and Total pollen during the 2018 season. In the case of *Alnus* pollen, the lack of correlation seen for 2018 can be attributed to a delay in sampling at the Carlow site which did not commence until the 18th of April. This led to the *Alnus* season of 2018 in Carlow going largely undocumented.

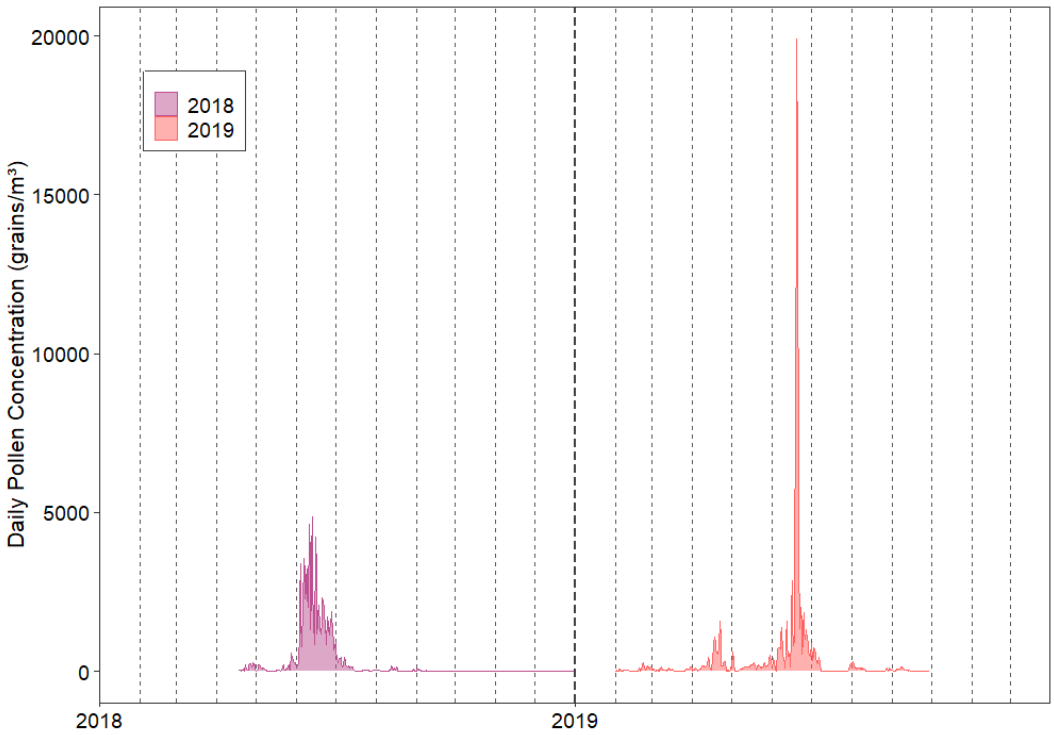

Figure 3.11: Time-series of total pollen concentrations from 2018 -2019 (Carlow)

Table 3.6: Spearman correlations between pollen concentrations in Carlow and Dublin

Major Pollen	2018	2019
Alnus	-0.01	**0.64****
Betula	**0.58***	**0.72****
Cupressaceae	**0.42****	**0.49****
Fraxinus	**0.49****	**0.65****
Pinus	**0.48****	**0.47****
Quercus	0.31	**0.61****
Poaceae	**0.68****	0.61
Urticaceae	**0.71****	**0.61****
Total Pollen	**0.79****	0.41

**significance at the 95% level, **significance at the 99% level*

Although similar diurnal bihourly trends are observed in Figure 3.12(A), an obvious point of contention between the two sites was noted by comparing the annual time-series for Carlow (2018-2019) shown in Figure 3.11 to those previously shown for Dublin (Figure 3.3); the magnitude of pollen concentrations experience at the two sites varied considerably. The mean APIn determined

for Dublin during the 2018-2019 sampling period was 34,217 Pollen * day/m^3. Concentrations at Carlow were significantly higher with an average APIn of 78,389 Pollen * day/m^3 recorded. The deviations in pollen concentration are mainly attributed to considerably higher Poaceae concentrations recorded in Carlow. This can be seen in Figure 3.12 (B), where the biggest deviation between the monthly concentrations can be seen for June. Although Dublin experienced lower annual concentrations, a greater variety in pollen taxa was recorded. There were 26 additional pollen types recorded in Dublin than there were in Carlow (Figure 3.12 (C)). The diversity in pollen concentration at the Carlow site was mainly dominated by Poaceae (70%), Urticaceae (12%), *Betula* (5%), *Quercus* (2%), *Fraxinus* (1%) and *Pinus* (1%).

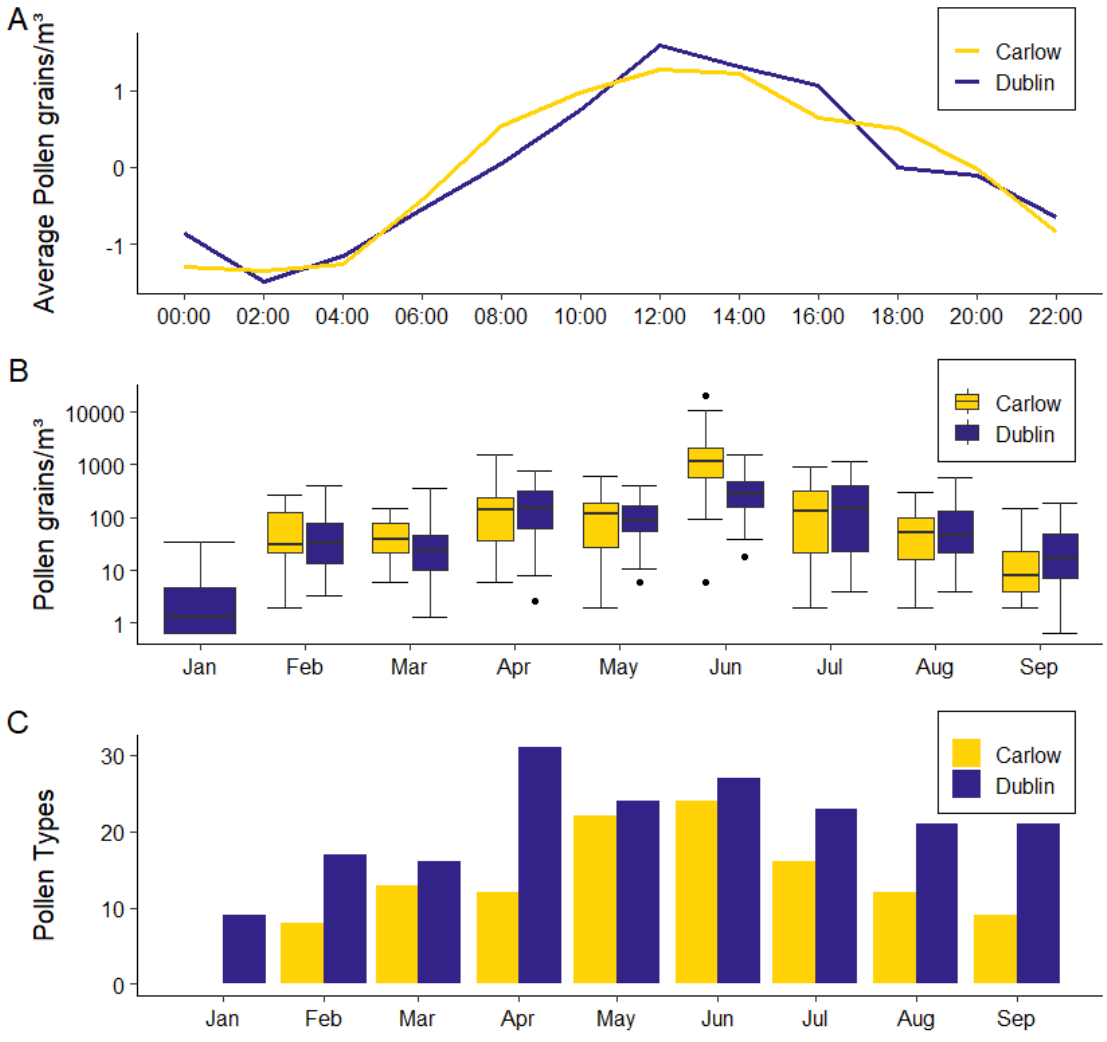

Figure 3.12: Comparison plots between Dublin (Blue) and Carlow (Yellow): (A) Average bihourly diurnal distribution (B) Log transformed distribution of daily pollen concentrations and (C) Average variation in the number of pollen types recorded each month.

3.4 Discussion

3.4.1 Pollen trends and seasonal features

Over the sampling period (2017-2020) a wide variety of pollen types and trends were recorded, generating valuable information regarding the most common pollen taxa and their seasonal changes in Dublin. The bimodal behaviour of the Dublin pollen season can be summarised as commencing with the release of early flowering Betulaceae (*Corylus* and *Alnus*) pollen in late January, coming to a peak in spring with the release of *Betula* and *Fraxinus* pollen followed by a lull in pollen concentration in May, before the primary peak in June as a result of high Poaceae concentrations. The summer peak in Poaceae is succeeded by Urticaceae pollen which in its decline brings the pollen season to an end in late-September/mid-October. This general pollen season trend is comparable to similar aerobiological studies conducted in the United Kingdom (J. Emberlin et al. 1990, 1993, 2007) but is significantly different from those conducted in Mediterranean (Camacho, 2015; Galán et al., 1995; Giner et al., 1999; Puljak et al., 2016; Rodríguez et al., 2015; Subiza et al., 1995) and Nordic climates (Nilsson and Persson, 1981; Przedpelska-Wasowicz et al., 2021).

The prevalence of *Betula* and Poaceae pollen during spring and summer peak periods, respectively, represents the two predominant allergenic pollen taxa observed during the campaign. This can be extended to include pollen originating from other trees within the Betulaceae family such as *Corylus* and *Alnus*. Both Poaceae and Betulaceae are well known for their clinical relevance across Europe in causing allergies (Burbach et al., 2009). Sensitizations have been previously found within the Irish population (Bousquet et al., 2007; Heinzerling et al., 2005), although more up-to-date sensitization tests are required to fully understand the severity and relevance of these aeroallergens to the current population.

The average bihourly diurnal distribution for Dublin also showed similarities to other literature studies. The average daily distribution for Dublin was dominated by a single afternoon peak, peaking at midday. The data was scaled every 24 hours prior to this analysis to reduce the influence of high concentrations of Poaceae pollen. Otherwise, Poaceae pollen would have drastically influenced the trend, which has previously been shown (Markey et al., 2022a). Alternatively, the diurnal distribution herein is more representative of the entire pollen season. Diurnal variations for the most abundant pollen types were also investigated, many of which exhibited a similar afternoon peak such as *Alnus*, *Betula*, Cupressaceae and *Pinus*. Whereas Poaceae and Urticaceae pollen show a slightly later peak between 14:00 and 16:00 and *Fraxinus* at 18:00. The majority of these individual pollen daily trends show similarities to other diurnal studies conducted throughout Europe (Aboulaich et al., 2013; Fernández-Rodríguez et al., 2014a; Kluska et al., 2020; Kolek et al., 2021; Norris-Hill and Emberlin, 1991; R. G. Peel et al., 2014; Spieksma et al., 1985; Yang et al., 2003). This is particularly true for other roof-top studies such as that by Kolek

et al., 2021, many of the rooftop diurnal trends depicted in this study closely mimic those seen for Dublin with only very slight variations.

As an extension of the original study (Markey et al., 2022a), this chapter represents the longest Irish aerobiological study, to-date. Prior to this, traditional aerobiological surveys of Ireland were limited to two summer pollen studies conducted in 1977-1978 in Galway (McDonald, 1980; McDonald and O'Driscoll, 1980) and more recent introductory fungal spore campaigns also conducted in Dublin at the same sampling site (Martínez-Bracero et al., 2022). Neither of these studies was devised to provide any long-term or seasonal details on the pollen season in Ireland. This led to the initial publication of the Markey et al., 2022a study, whereas that study focused more on the comparison between urban and rural sampling sites, this chapter has been extended to include additional 2019 and 2020 data as well as examining more precise influences of meteorological impacts on induvial pollen season stages.

Given the scarcity of previous studies on this topic in Ireland, the few that have been conducted were examined for similarities and differences. The summer-time Galway studies from the late 1970's (McDonald, 1980; McDonald and O'Driscoll, 1980) could be directly compared to the data collected during the equivalent summer months in Dublin (and Carlow). Similar peak periods of both Poaceae and Urticaceae pollen were observed. However, significant concentrations of other pollen such as *Rumex* and *Chenopodium* were also recorded in these studies. Although the presence of these pollen taxa was recorded, the magnitude of which they were present does not directly coincide with concentrations sampled in 1970's Galway. It is possible that these summertime variations could suggest regional variations in pollen within Ireland, however, the true nature of this can only be fully realised once modern-day campaigns are conducted.

Comparisons can also be made between the updated Dublin pollen calendar and similar work conducted by Adams-Groom et al. (2020), who recently published details on the seasonal statistics of allergenic pollen taxa and created a regional pollen calendar for Northern Ireland. The updated Dublin pollen calendar shows marked differences from its original instalment (Markey et al., 2022a) with several pollen taxa showing longer periods of occurrence. This comes as a result of extended sampling throughout 2019 and 2020. The simplified approach of the updated calendar is also more in line with the work presented by Adams-Groom et al. (2020), showing only abundant or important pollen taxa. The presented Northern Irish regional calendar is in many ways comparable to that of the Dublin pollen calendar.

On average the season start-dates and end-dates of the pollen taxa discussed by Adams-Groom et al. (2020) did not deviate much from those seen for Dublin. Generally, the season starts for *Fraxinus*, *Betula*, *Quercus* and Poaceae all commence between ~ 1 week and 10 days earlier than those documented in the North of Ireland. Urticaceae on the other hand started later in Dublin. Seasonal end dates differed more substantially with the end dates for the *Quercus* season differing

by almost 2 months (extending further in Dublin). The average APIn stated for each pollen type was also exceeded by several degrees in Dublin. The majority of these differences can be extended to differing sampling years, slight variations due to different season calculation methods as well as changes in land cover. However, looking at the overall trends in the pollen calendar, peak periods of the differing taxa tend to coincide with their Dublin counterparts for the majority of taxa.

Following the 2020 season the Dublin monitoring site was relocated to the current site at the Met Éireann facility (4 km from former site) due to closure of the TU Dublin Kevin street campus. Due to limitations in availability of sampling locations within the city as well as financial, time and labour constraints required to carry out multiple point monitoring in Dublin, only one Dublin site could be operated at a time. Due to setbacks due to COVID restrictions and changes in sampling locations, additional efforts are required to fully compare and contrast the pollen trends between the sites to identify notable spatial variations within the city. The vast majority of aerobiological studies have continued to use one Hirst volumetric sampler (at roof level) per city, even in relatively large cities (Werchan et al., 2017). Traditionally, pollen data collected using a volumetric sampler at >10m has been shown and is widely believed to be representative for a 30km area (Pashley et al., 2009; Rojo et al., 2019). Nevertheless several studies have examined the potential changes in spatial variation of pollen concentrations in urban areas using multiple Hirst samplers (Arobba et al., 2000; Cariñanos et al., 2002; Fernández-Rodríguez et al., 2014a; Fornaciari et al., 1996; Frisk et al., 2022; Gonzalo-Garijo et al., 2006; Katelaris et al., 2004; Nowak et al., 2012; Simoleit et al., 2017; Velasco-Jiménez et al., 2013; Werchan et al., 2017).

These studies jointly concluded that multiple sampling locations throughout a city show similarities in the general seasonal trends and pollen taxa recorded, however, differences arise due to proximity to local sources (Werchan et al., 2017). Many of these investigations and their findings also suffer from other uncertainties in sampling height. A study by Werchan et al., 2017 aimed to limit these impacts by distributing 14 gravimetric samplers across the city of Berlin at consistent sampling heights. Notable spatial and temporal variations in pollen sedimentation due to the presence of local sources near sampling sites were noted. This variation could equate to different health implications for allergy sufferers. This paper suggests that in larger cities such as Berlin (approximately 8 times larger than the city of Dublin) at least 2 samplers should be deployed at various locations across the city. This is particularly important for the monitoring of Poaceae pollen, which can show considerable spatial variations throughout urban areas even if the effects are limited to several hundred metres from the pollen source (Skjøth et al., 2013a; Werchan et al., 2017). In the case of the Dublin sampling site, further assessment of pollen data from the relocated site is required before an accurate suggestion of how many samplers should be used to more precisely monitor pollen over the city can be made.

3.4.2 Comparison of rural and urban sites

For the 2018-2019 seasons, sampling at both the Dublin (urban) and Carlow (rural) sites were compared. This is explored in greater detail in the Markey et al., 2022a study, but a summarised adaption is provided here. A direct comparison of the APIn for total pollen between the sites illustrated that generally, Carlow experienced higher concentrations of pollen (for both years), mainly driven by exponentially higher Poaceae pollen concentrations recorded during the summer months. This can be expected as the land cover surrounding the Carlow site is dominated by rural grasslands (Markey et al., 2022a). However, the magnitude of the Poaceae pollen recorded at the rural site is also largely dictated but the proximity of the sampler to the ground (2-3 m) when compared to the Dublin sampler (20 m) and resulting counts. The effect of varying sampler heights has been widely documented in the literature (Aulirantio-Lehtimäki et al., 1991; Fernández-Rodríguez et al., 2014b; Kolek et al., 2021; Rojo et al., 2020, 2019; Xiao et al., 2013), many of which have found that grass and other herbaceous pollen concentration are inversely proportional to sampler height (Aulirantio-Lehtimäki et al., 1991; Kruczek et al., 2017; Spieksma et al., 2000). This explains why the concentrations of Poaceae and total pollen did not exhibit a significant correlation between the two sites for the 2019 season (Table 3.6).

The current standard method for pollen monitoring using the Hirst has suggested that the sampler be positioned 10-20 m without direct influence of neighbouring buildings (Galán et al., 2014). However, this is not always possible in isolated rural areas such as with Carlow although efforts were made to raise the device above the level of surrounding foliage. Measurements at ground level are not encouraged as roof-top levels allow for improved regional area monitoring allowing for the best spatial and temporal resolution achievable (de Weger et al., 2013). This conclusion has been met with controversy with some arguing that ground level measurements should be considered to truly depict the real conditions experienced by the individual, especially in urban areas (Bastl et al., 2023). Conflicting results remain throughout literature. Several recent studies have highlighted that ground level exposure can vary throughout different environments with the individual experiencing increased levels of pollen exposure, especially from herbaceous pollen (de Weger et al., 2020). An urban study by de Weger et al., 2020 found increased spatial variation, higher concentrations and earlier detection were recorded at ground level but still correlated with rooftop concentrations. Local ground level sources were attributed to these changes.

When local emissions are not an issue rooftop levels are found to be a good proxy for inhaled pollen concentrations (Peel et al., 2013). On occasion street level analysis in urban areas has even been shown to experience significantly lower grass pollen concentrations than roof-top level concentrations (Robert George Peel et al., 2014). Studies utilising crowd sourced data illustrated that overall, higher agreement with symptom development with rooftop levels were seen than for ground level (Bastl et al., 2019). The local and anecdotal impact of ground level urban monitoring has therefore been deemed unsuitable for long-term regional monitoring, forecasting models, and clinical

studies (de Weger et al., 2013). Therefore, future sites established in Ireland should aim to further elevate monitoring devices when roof-top sampling is not achievable, especially in rural areas, to avoid impacts from local sources such as those seen for Carlow.

Studies investigating the variations in sampler height also noted fewer significant differences in determining arboreal pollen concentrations (Leuschner, 1999; Rantio-Lehtimäki et al., 1991; Soldevilla et al., 1995).Throughout this campaign certain tree pollen types such as *Alnus*, Cupressaceae and *Quercus* pollen were more abundant at the urban site. This can partially be attributed to the surrounding land cover. Although the aforementioned land cover map of Dublin shows little detail on many of the urban green spaces and broad leaf forest areas within the city, Dublin has twice as much surface area occupied by urban green spaces, broadleaved forests and mixed forests than the rural site (Maya-Manzano et al., 2021). Dublin also recorded a greater variety in pollen type diversity with pollen types such as *Platanus*, *Ulmus*, *Fagus*, Ericaceae, *Mercurialis*, *Forsythia*, *Hedera*, *Populus*, and Ranunculaceae which were not identified in Carlow.

The presence of these pollen types can be explained by the common use of ornamental plants within urban green spaces (Velasco-Jiménez et al., 2020). The presence and higher concentrations of *Platanus*, *Castanea*, *Ulmus*, *Fagus*, *Populus*, *Aesculus* and Ericaceae pollen seen in Dublin relative to Carlow can be explained by the ornamental use of these tree types in the city (Ningal et al., 2010; Xie, 2018). The same applies to the higher concentrations of Cupressaceae and *Quercus* pollen. The distribution and allergic impact of urban pollen, particularly tree pollen, has received increased attention in recent years (Cariñanos et al., 2019, 2014; Cariñanos and Marinangeli, 2021; Gonzalo-Garijo et al., 2006; Maya Manzano et al., 2017; Sousa-Silva et al., 2021). The benefits of urban parks, greenspace and street trees are many; ranging from improving air quality (Fang and Ling, 2005), noise reduction (Fang and Ling, 2005), and biodiversity (Kapoor, 2017) as well as being linked to enhancing the general health and wellbeing of residents (Javadi, 2021). This has led to the expansion and promotion of urban greenspaces across Europe in recent decades. Dublin is no different; since 2016 a Dublin city tree strategy has been in place to provide the city with a diversity and abundance of healthy, attractive trees (Snyder et al., 2016).

However, the presence of certain ornamental species in urban areas has been shown to have given rise to new and growing pollen sensitisations in cities (Cariñanos and Casares-Porcel, 2011). Despite recommendations to limit and reduce the impact of allergenic plants in the planning of urban greenspaces, few regulations have been passed to correct this (Cariñanos and Marinangeli, 2021). In efforts to provide a greater awareness and insight into the risk posed by urban flora, particularly certain trees, a number of recent studies have attempted to update and verify the allergenic potential of some of the most common urban trees (Cariñanos et al., 2019; Cariñanos and Marinangeli, 2021). Several of these pollen taxa perceived to represent an agreed moderate-to-high allergenic potential were observed in considerable quantities at the Dublin sampling site, including *Alnus*, *Betula*, *Castanea*, Cupressaceae, *Platanus*, *Quercus*, *Tilia* and *Ulmus*.

Dublin also experienced higher concentrations of pollen associated with coastal and riverside areas such as Juncaceae. Juncaceae has been well associated with coastal regions from both an aerobiological (El-Amier, 2015; Fall, 1994) and ecological (Fontana, 2005) perspective. Ecological surveys of the coastal regions of Dublin have corroborated the presence of such foliage along the coastal regions of Dublin (Doogue et al., 2004). The aesthetic appeal of urban gardens and greenspaces likely resulted in the addition of several varieties of herbaceous pollen types that were absent from the rural sampling location, many of which were only observed in small quantities including Ranunculaceae, *Forsythia* and *Sambucus*. *Hedera* was also unique to the Dublin sampling location, this is likely due to the presence of decorative ivy plants present on many of the historical buildings located in Dublin city centre, close to the sampling site. Interestingly a drastic increase in these pollen types associated with wall growth such as *Hedera* and *Mercurialis* saw substantial increases in concentrations in 2020 most likely due to the COVID pandemic – possibly as a result of reduced maintenance of these public ruins as a result of lockdowns.

All in all, the similarities in seasonal trends observed between Dublin (2017-2020), Carlow (2018-2019), the previously published finding for the summer of 1977-1978 for Galway (McDonald, 1980; McDonald and O'Driscoll, 1980) and seasonal statistics for Northern Ireland (Adams-Groom et al., 2020) suggests that general pollen trends for certain pollen taxa appear to be somewhat comparable across Ireland. More widespread monitoring over comparable sampling years is needed to further investigate this.

3.4.3 Influence of meteorological conditions on pollen concentrations - MPS

Several factors can influence the airborne concentration of pollen grains, this includes both the production/release of the pollen and the dispersal and transportation (Galán et al. 1995; Volkova et al. 2016). Therefore, Spearman's correlation analysis was performed to determine the predominant influential meteorological parameters on pollen concentration during the MPS, PRP and PSP. The trends and strengths of the relationships between the concentrations of major pollen types and meteorological conditions showed strong deviations from year to year, illustrating the complex nature that exists between the two. The majority of pollen types studied decreased in concentration significantly during 2018, followed by high concentrations in 2019, both of these trends can be explained by examining the meteorological conditions experienced. During February-March of 2018 a snowstorm nicknamed "Storm Emma" struck the east coast of Ireland. The worst conditions were experienced during the 28th of February to the 4th of March; including considerable snowfall and air and soil temperatures plummeting 5-10 degrees below normal (Government of Ireland and Met Éireann, 2019). These conditions are very rare thanks to the temperate climate of Ireland. As a result the pollen season recorded during 2018 deviated from expected and was found to more closely mimic

trends seen for countries that normally experience cooler early-spring conditions, such as the Nordic countries (Emberlin et al. 2002; Nilsson and Persson 1981; Przedpelska-Wasowicz et al. 2021).

Early spring temperatures have been shown to act as deciding factors in plant development and pollen production (Matyasovszky et al., 2015). The unusual cold spell experienced in 2018 led to a significant reduction in arboreal pollen release in late March as with the Poaceae pollen release in summer. Similar trends attributed to cold springtime conditions have previously been recorded elsewhere (Emberlin et al., 2002; Kasprzyk and Borycka, 2019; Makra et al., 2012). One such investigation by Emberlin et al. (1999) recorded a similar trend between the soil temperature in early spring and the magnitude of grass pollen released the following summer in the UK. This further corroborated the lack of correlation seen for many tree pollen types in 2018 and accounts for the increased Poaceae pollen concentrations seen in 2019.

Fraxinus is the only exception to this 2018-2019 trend, with a stark decrease in concentrations seen in 2019. This significant drop can result for a number of reasons. For instance, Ireland was experiencing an "Ash Dieback" (ADB) epidemic during the sampling period, which can influence the production and release of pollen (Teagasc, 2019). The impact of ADB on pollen concentration is somewhat conflicting with both reductions (Evans, 2019) and increases (Gassner et al., 2019) in *Fraxinus* pollen concentrations being recorded. It is possible that other factors such as mast years could also lead to deviations in *Fraxinus* pollen concentrations. Many trees experience a variation in reproductive efforts over several years known as masting (Dahl et al., 2013). Literature shows that *Fraxinus* trees can simply experience periods of significantly lower pollen production once every few years. It is possible that 2019 represents one such inactive period (Gassner et al., 2019) and is not a result of ADB.

Spearman correlation analysis highlighted the differing importance of conditions on pollen concentrations throughout the sampling years. Although great degrees of variation were observed, many of the pollen types showcased strong positive association with temperature during their MPS, the importance of which has been recorded extensively in literature (Aboulaich et al., 2013; Emberlin et al., 1993; Frenguelli et al., 1991; Helfman-Hertzog et al., 2023; Khwarahm et al., 2014; Norris-Hill, 1997). However, the opposite was also observed during periods of high temperature or prolonged dry spells. This is most notably seen for *Quercus* pollen during 2018/2020. During both years, the *Quercus* MPS coincided with dry and warm conditions during the summer months of 2018 and late spring of 2020. It is possible that the dry and warm conditions seen during these times led to heat stress and reduced pollen release, which corroborates findings from previous studies illustrating similar trends for both tree and herbaceous pollen during dry conditions (Emberlin and Norris-Hill, 1991; Knaap et al., 2010).

Generally, trends for relative humidity and rainfall were observed to negatively correlate with several of the major pollen concentrations. This trend of decreasing pollen concentrations with

increasing relative humidity and rainfall is well established in literature (Janati et al., 2017) and is largely associated with particle-deposition and washout effects and the inhibition of anthesis of several pollen species (Bruffaerts et al., 2018; Janati et al., 2017; Kluska et al., 2020; Puc and Puc, 2004; Ribeiro et al., 2003). Low relative humidity is important in the wind-mediated detachment of pollen grains from anthers, as to achieve this the pollen grains must be dry (Emberlin, 2009). However, on occasion, it was found that pollen concentrations during MPSs were positively associated with the average rain concentration of the previous 10 days. This suggests that rainy days preceding pollen release may act as a trigger of pollen release (Khwarahm et al., 2014).

It was observed that sun duration and global radiation also had a fluctuating impact on pollen concentrations. Depending on the pollen type and year in question, the MPS was either positively or negatively influenced by sun and radiation. The additive effect of sun duration and global radiation for pollen release has been well documented in literature (Gioulekas et al., 2004; González-Fernández et al., 2021; Khwarahm et al., 2014), especially for grass and herb pollen types (Çakir and Doğan, 2020; de La Guardia et al., 1998; Myszkowska, 2012). Whereas the negative influence can be attributed to the previously discussed likelihood of heat stress.

3.4.4 Influence of meteorological conditions on pollen concentrations – PSP and PRP

Even the pre-season conditions can be interpreted to explain certain seasonal trends recorded. One such case is the notable lack of a predominant Poaceae peak during the 2020 season. Although a peak concentration was recorded on 07/06/2020, there were several comparable peak days (shown in Appendix A Figure A1), varying from previous years when one dominant peak day was observed. In addition, the Poaceae season length was substantially longer in 2020 than in other years. Although little correlation can be seen for Poaceae during the 2020 season (MPS, PRP in particular), this trend can be explained following the unseasonable dry conditions during the late spring/early summer. Such conditions have been well documented to limit the flowering intensity of herbaceous pollen resulting in a longer season devoid of a predominant peak (Dahl et al., 2013; Galán et al., 1995; González Minero et al., 1998).

Previously, correlation analysis between monthly total pollen concentrations and meteorological conditions was conducted for Ireland (Markey et al., 2022a), highlighting the potential influence of weather during the PRP and PSP of several pollen taxa. To more specifically examine how the relationship between meteorological conditions and pollen concentrations changes throughout a MPS, the same Spearman correlation analysis was applied to the PRP and PSP of each major pollen's MPS. Pollen concentrations during the PRP are mainly seen to be driven by temperature parameters which promote the onset of anthesis and pollen release, while the PSP is influenced by parameters that continue the pollen season either by facilitating extended release of pollen or by other mechanisms such as resuspension (Helfman-Hertzog et al., 2023; Mesa et al.,

2003). Typically literature studies tend to echo the same consistent findings; the PRP can show a significant positive correlation with temperature, and sunshine duration and a negative correlation with rainfall and relative humidity, whereas, the PSP often illustrates the opposite effects as temperature dependence generally decreases following peak pollen dates (Helfman-Hertzog et al., 2023; de La Guardia et al., 1998; Pérez-Badia et al., 2013; Piotrowska and Kaszewski, 2012). However, these findings were not always seen during this campaign.

In the case of the Dublin campaign, temperature was seen to strongly influence the PRP for many tree, grass and herbaceous pollen types. This behaviour is well documented, highlighting the important role of temperature in initiating the onset of pollen release (Emberlin et al., 2002; Khwarahm et al., 2014; Piotrowska and Kaszewski, 2012). However, unlike many other literature studies, this relationship often extended into the PSP with many pollen types maintaining this positive relationship with temperature (except for 2018). This suggests that rising temperatures following the peak-day promoted the release of pollen as well as resuspension. These findings corroborate similar trends observed for *Betula* and Poaceae pollen in the UK (Khwarahm et al., 2014). The result implies that maximum air temperature, on the day of measurement, exerts a strong control on pollen count through pollen release and resuspension mechanisms. For 2018, *Fraxinus*, *Quercus* and Poaceae showed negative correlations with PSP temperature recordings. This is largely attributed to a commonly witnessed PSP trend of declining pollen concentrations with increasing temperature (Khwarahm et al., 2014)

Sunshine duration is yet another parameter that has been shown previously to promote pollen release during the PRP of herbaceous pollen (de La Guardia et al., 1998). However, a notable lack of correlation with temperature and sunshine was observed for the Poaceae PRP, removing the peak day from this dataset led to strong positive correlations with these variables. This possibly suggests that the days surrounding the peak day of the Poaceae MPSs may act differently than the PRP and PSP as seen previously by (Smith and Emberlin, 2005) for Poaceae counts in the UK.

Rainfall and relative humidity also led to a decrease in airborne pollen concentrations during PRP and PSP for several major pollen types which is consistent with previous findings (de La Guardia et al., 1998). However, the opposite was also observed for average rain concentrations over the previous 10 days during the PRP and PSP, and rain during the PSP of *Pinus* and Poaceae in 2018. In the case of the positive correlation during the PRP, this is indicative of the relationship between rainfall and the opening of anthers and subsequent pollen release (Hoebeke et al., 2018; Newnham et al., 2013). On average, a stronger positive correlation with rainfall parameters was seen for the PSP. This could still be influenced by the mechanism of rainfall and humidity promoting anther opening etc. in the case of average rain concentrations over the previous 10 days. However, a strong positive correlation was also observed for the PSP of Poaceae in 2018 which is linked to the dry and warm conditions experienced leading to a reduction in Poaceae pollen due to heat stress and pollen production continuing following the return of rain and moisture.

3.4.5 Wind analysis of major pollen concentrations

The importance of wind speed and direction on pollen concentrations has been credited in Ireland since initial studies were conducted (McDonald, 1980; McDonald and O'Driscoll, 1980). Although positive and negative correlations were observed for windspeed and several major pollen types during the MPS, the influence of wind was stronger during the PRP and PSP. Windspeed is an important parameter that is essential for facilitating the release of arboreal pollen from catkins (M. Sofiev et al., 2013). This accounts for the positive correlation seen between several PRP concentrations of tree pollen and windspeeds. Aside from this observation, there was no other consistent correlation between windspeeds with a great degree of variation observed for different times of the seasons, years, and pollen types. Generally, it can be assumed that positive correlations with wind speed are linked with the release of pollen from anthers or transport of pollen to the sampling area from other areas, whereas a negative correlation could be characteristic of the removal of pollen from the sampling area (Khwarahm et al., 2014).

To further evaluate the impact of wind speed and direction on the transportation and spatiotemporal variation of observed pollen concentration, the geographical origins of total and specific pollen types were also investigated for the Dublin sampling location. This is similar to previous work carried out by Markey et al., 2022a. Possible sources of long- and short-range transport can be evaluated by examining Figure 3.9.

Betula, Fraxinus and Cupressaceae pollen were seen to predominantly originate from a Nort-easterly direction at high wind speeds. A recent study regarding the spatial and temporal variations in the distribution of birch trees and *Betula* pollen in Ireland has shown that high concentrations of *Betula* over both Dublin and Carlow originate from air masses coming from the UK (Maya-Manzano et al., 2021). This corroborates the origin of *Betula* pollen although the same may apply to the *Fraxinus* and Cupressaceae. However, it is important not to disregard the influence of local sources which have been shown to contribute up to 70% of the pollen variance of one city (Bogawski et al., 2019; Rojo et al., 2015). Directly northeast of the sampling site is St. Stephen's Green Park, although limited tree surveys exist highlighting the presence of many trees including *Betula* and *Fraxinus*, no Cupressaceae trees are registered (OPW, 2023) although they do exist within the park as well and the surrounding urban area (Xie, 2018). Urticaceae and *Quercus* pollen showed strong associations from the north-to-north east which could also relate to nearby sites such as the botanic gardens, situated to the north of the site. Poaceae and Urticaceae pollen showed multiple possible sources – likely as a result of multiple local and further sources around the city. Both illustrated a north-westerly source at high wind speeds which could be connected to the Phoenix park which has a variety of tree and plant diversity (Gaughran and Stout, 2020)

In addition, high concentrations of *Alnus* pollen appeared to be originating from a south-westerly and south-easterly direction. Other pollen such as Cupressaceae and *Pinus* also showcased similar south easter trends, to a lesser extent. It is possible that pollen originated from forests and pastures located south of the City, as shown by the landcover analysis. Other major sources likely include the Wicklow Mountains National Park (south of Dublin), previously discussed by Maya-Manzano et al. (2021).

Even though the emission of pollen close to the sampling site is largely driven by the imminent meteorological conditions, the inclusion of findings from the ZeFir source receptor models suggests the influence of pollen originating from other sources further from the site. Future work could focus on HYSPLIT back-trajectory analysis to determine the specific origin of these air-masses, similar to the work that has been done previously by Maya-Manzano et al., 2021 for birch pollen. However, in addition to this it is important to consider the representativeness of the analysed meteorological data when examining these sources. It is less likely that the majority of meteorological data used here will correlate with these distant sources. As a result, it is important to consider the connection between different regional meteorological data and pollen dispersion. This connection has been well documented (Mikhail Sofiev et al., 2013). In a study by Tampieri et al., 1977, *Castanea* pollen transport and dispersion was measured using pollen and meteorological data collected from three separate sites. The inclusion of additional monitoring points within Dublin and the neighbouring areas could therefore aid in determining the impact of pollen dispersion from possible sources discussed above using the ZeFir models and land-cover data.

Although several significant correlations could be noted and explained between various pollen taxa and meteorological parameters. There was a strong degree of diversity witnessed between the different years, seasonal periods, locales, and pollen types. Much longer European studies that have encompassed decades of data have been able to highlight particular trends for pollen taxa and various weather conditions (Hoebeke et al., 2018). In comparison, the shorter monitoring campaign conducted herein was greatly influenced by annual variations. As monitoring continues in Dublin and elsewhere in Ireland more consistent and apparent trends will likely emerge.

3.5 Conclusion

The monitoring of pollen at the Dublin site revealed key characteristics around the dominant and allergenic pollen taxa that exist here, as well as their seasonal and diurnal trends. The pollen season in Dublin is largely bimodal in appearance with a peak in spring dominated by *Betula* and *Fraxinus* pollen, and a second more intense summer peak appearing in mid-June because of high Poaceae concentrations. Early-year pollen commences in late January with the release of *Corylus* and *Alnus* pollen, with late-season pollen being dominated by Urticaceae and other herbaceous pollen before coming to an end in late-September/mid-October. Several allergenic pollen taxa were also recorded

in high annual concentrations, especially *Betula* and Poaceae pollen. The further analysis of this data can be used to forecast periods of allergenic exposure which would greatly aid allergy sufferers within the city. Preliminary prediction tools were constructed in the form of an updated pollen calendar for Dublin – to aid allergy sufferers throughout the year.

Differences between urban and rural sites were exposed. The urban site in Dublin showed a greater diversity in pollen taxa as a result of ornamental use of plants and trees throughout the city, whereas, the rural site experienced significantly higher pollen concentrations, particularly during the summer months. This was equated to rural grasslands and pastures surrounding the rural site and sampler height. The increase of potentially allergenic ornamental tree use within the city was also apparent from surveying the ambient pollen data recorded. It is possible that in years to come that the allergenic potential of such trees could burden the public as has been shown in other countries. As such, documented pollen records might prove a valuable resource.

The driving meteorological forces behind pollen production and release were also investigated, showing variating depending on year and pollen type. Overall, temperature showed a positive influence on pollen release with rainfall and relative humidity leading to a decrease in the release and deposition of airborne pollen. The PRP and PSP were also investigated – highlighting the differences in the impact of meteorology throughout the pollen season. PRPs showed a strong association with factors that promote initial pollen release while PSPs were influenced by conditions that promoted extended-release and resuspension.

Wind analysis was further expanded to examine the possible spatiotemporal origins of major pollen types in relation to landcover analysis. Possible local sources originating from nearby green sites as well as long-range sources such as from the Wicklow mountains and further sources from the UK were also discussed.

In conjunction with the previously published work (Markey et al., 2022a), this chapter represents the only in-depth analysis of pollen trends in Dublin and elsewhere in Ireland since the late 1970's.

3.6 Future work

During the relocation of the TU Dublin campus, followed by the subsequent transferral of the research team to Dublin City University, the Hirst sampler was moved and now resides at the Met Éireann headquarters in Glasnevin. There remains several seasons of data that require completion and processing. Future work will aim to complete this task as well as comparing the pollen seasonal trends between the old and new sampling sites (4 km apart). The two sites represent opposite sides of the city. The former site was very much in the centre of the city while the current site is closer in proximity to the National Botanic Gardens of Dublin and might experience a greater diversity in pollen. As such, future work will focus on assessing any variations in pollen trends, concentrations

and taxa to determine if multiple samplers around Dublin city could more accurately account for spatial changes in pollen exposure.

In addition to this, future work will continue to maintain the currently active sampling sites around the country as well as establishing several others. Now that the Carlow sampling site has been retired, it is likely that future sampling locations will include a representative midlands station as well as the further monitoring of other cities such as Galway. Following this, extensive comparisons can be carried out between the varying locations of the Irish pollen network as well as the further development of prediction tools and forecasting models (preliminary work of which is covered in Chapter 4).

References

Aboulaich, N., Achmakh, L., Bouziane, H., Trigo, M.M., Recio, M., Kadiri, M., Cabezudo, B., Riadi, H., Kazzaz, M., 2013. Int. J. Biometeorol. 57, 197–205.

Adams-Groom, B., Ambelas Skjøth, C., Selby, K., Pashley, C., Satchwell, J., Head, K., Ramsay, G., 2020. Allergy 75, 1492–1494.

Aerts, R., Bruffaerts, N., Somers, B., Demoury, C., Plusquin, M., Nawrot, T.S., Hendrickx, M., 2021. Landsc. Urban Plan. 207, 104001.

Arobba, D., Guido, M.A., Minale, P., Montanari, C., Placereani, S., Pracilio, S., Troise, C., Voltolini, S., Negrini, A.C., 2000. Aerobiologia (Bologna). 16, 233–243.

Aulirantio-Lehtimäki, Helander, M.L., Pessi, A.-M., 1991. Aerobiologia (Bologna). 7, 129–135.

Bastl, M., Bastl, K., Dirr, L., Berger, M., Berger, U., 2023. Allergo J. Int. 32, 162–166.

Bastl, M., Bastl, K., Karatzas, K., Aleksic, M., Zetter, R., Berger, U., 2019. World Allergy Organ. J. 12, 100036.

Basu, B., 2021. Development of soil and land cover databases for use in the Soil Water Assessment Tool from Irish National Soil Maps and CORINE Land Cover Maps for Ireland. pp. 1–19.

Bogawski, P., Borycka, K., Grewling, Ł., Kasprzyk, I., 2019. Sci. Total Environ. 689, 109–125.

Bousquet, P.J., Hooper, R., Kogevinas, M., Jarvis, D., Burney, P., Chinn, S., Luezynska, C., Vermeire, P., Kesteloot, H., Bousquet, J., Nowak, D., Prichard, J., de Marco, R., Rijcken, B., Anto, J.M., Alves, J., Boman, G., Abramson, M., Kutin, J., van Bastelaer, F., Neukirch, F., Liard, R., Pin, I., Pison, C., Taytard, A., Magnussen, H., Erich Wichmann, H., Heinrich, J., Gislason, T., Gislason, H.D., Prichard, J., Phil, D., Allwright, S., MacLeod, D., Bugiani, M., Bucca, C., Romano, C., de Marco, R., Cascio, V. Lo, Campello, C., Marinoni, A., Cerveri, I.,

Casali, L., Kremer, A.M., Crane, J., Lewis, S., Gulsvik, A., Omenaas, E., Sunyer, J., Burgos, F., Tech, R., Castellsague, J., Roca, J., Soriano, J., Tobias, A., Muniozguren, N., Ramos-Gonzalez, J., Capelastegui, A., Castillo, J., Rodriguez-Portal, J., Martinez-Moratalla, J., Almar-Marqnes, E., Maldonado-Pérez, J., Pereira, A., Sfinchez-Ramos, J., Quiros, R., Huerta, I., Payo-Losa, F., Boman, G., Janson, C., Björnsson, E., Rosenhall, L., Norrman, E., Lundbgck, B., Lindholm, N., Plaschke, P., Ackermann-Liebrich, U., Künzli, N., Perruchoud, A., Burr, M., Layzell, J., Russell Hall, B., Harrison, B., Stark, J., Sonia Buist, A., Vollmer, W.M., Osborne, M.L., 2007. Clin. Exp. Allergy 37, 780–787.

Bruffaerts, N., De Smedt, T., Delcloo, A., Simons, K., Hoebeke, L., Verstraeten, C., Van Nieuwenhuyse, A., Packeu, A., Hendrickx, M., 2018. Int. J. Biometeorol. 62, 483–491.

Burbach, G.J., Heinzerling, L.M., Edenharter, G., Bachert, C., Bindslev-Jensen, C., Bonini, S., Bousquet, J., Bousquet-Rouanet, L., Bousquet, P.J., Bresciani, M., Bruno, A., Canonica, G.W., Darsow, U., Demoly, P., Durham, S., Fokkens, W.J., Giavi, S., Gjomarkaj, M., Gramiccioni, C., Haahtela, T., Kowalski, M.L., Magyar, P., Muraközi, G., Orosz, M., Papadopoulos, N.G., Röhnelt, C., Stingl, G., Todo-Bom, A., Von Mutius, E., Wiesner, A., Wöhrl, S., Zuberbier, T., 2009. Allergy Eur. J. Allergy Clin. Immunol. 64, 1507–1515.

Büttner, G., Feranec, J., Jaffrain, G., Mari, L., Maucha, G., Soukup, T., 2004. EARSeL eProceedings 3, 331–346.

Çakir, N., Doğan, C., 2020. Turk. J. Botany 44, 526–538.

Camacho, I.C., 2015. Ann. Agric. Environ. Med. 22, 608–613.

Cariñanos, P., Casares-Porcel, M., 2011. Landsc. Urban Plan. 101, 205–214.

Cariñanos, P., Casares-Porcel, M., Quesada-Rubio, J.M., 2014. Landsc. Urban Plan. 123, 134–144.

Cariñanos, P., Grilo, F., Pinho, P., Casares-Porcel, M., Branquinho, C., Acil, N., Andreucci, M.B., Anjos, A., Bianco, P.M., Brini, S., Calaza-Martínez, P., Calvo, E., Carrari, E., Castro, J., Chiesura, A., Correia, O., Gonçalves, A., Gonçalves, P., Mexia, T., Mirabile, M., Paoletti, E., Santos-Reis, M., Semenzato, P., Vilhar, U., 2019. Int. J. Environ. Res. Public Health 16.

Cariñanos, P., Marinangeli, F., 2021. Urban For. Urban Green. 63.

Cariñanos, P., Sánchez-Mesa, J.A., Prieto-Baena, J.C., Lopez, A., Guerra, F., Moreno, C., Domínguez, E., Galan, C., 2002. J. Environ. Monit. 4, 734–738.

Cristofori, A., Cristofolini, F., Gottardini, E., 2010. Aerobiologia (Bologna). 26, 253–261.

CSO, 2012. Population Density and Area Size by Towns by Size, Census Year and Statistic [WWW Document]. URL https://data.cso.ie/

CSO, 2016. Census 2016 [WWW Document]. URL

https://www.cso.ie/en/census/census2016reports/

D'Amato, G., Cecchi, L., Bonini, S., Nunes, C., Annesi-Maesano, I., Behrendt, H., Liccardi, G., Popov, T., Van Cauwenberge, P., 2007. Allergy Eur. J. Allergy Clin. Immunol. 62, 976–990.

Dahl, Å., Galán, C., Hajkova, L., Pauling, A., Sikoparija, B., Smith, M., Vokou, D., 2013. The Onset, Course and Intensity of the Pollen Season, in: ThereSofiev, M., Bergmann, K.-C. (Eds.), Allergenic Pollen. Springer Netherlands, Dordrecht, pp. 29–70.

Donnelly, A., Misstear, B., Broderick, B., 2015. Atmos. Environ. 103, 53–65.

Doogue, D., Tiernan, D., Visser, H., 2004. Ecological Study of the Coastal Habitats in County Fingal, Phase I & II.

Dowding, P., 1987. Int. Rev. Cytol. 107, 421–437.

El-Amier, Y.A., 2015. Egypt. J. Basic Appl. Sci. 2, 132–138.

Emberlin, J., 2009. Allergy Allerg. Dis. Second Ed. 1, 942–962.

Emberlin, J., Detandt, M., Gehrig, R., Jaeger, S., Nolard, N., Rantio-Lehtimäki, A., 2002. Int. J. Biometeorol. 46, 159–170.

Emberlin, J., Mullins, J., Corden, J., Jones, S., Millington, W., Brooke, M., Savage, M., 1999. Clin. Exp. Allergy 29, 347–356.

Emberlin, J., Norris-Hill, J., 1991. Aerobiologia (Bologna). 7, 49–56.

Emberlin, J., Norris-Hill, J., Bryant, R.H., 1990. Grana 29, 301–309.

Emberlin, J., Savage, M., Jones, S., 1993. Clin. Exp. Allergy 23, 911–918.

Emberlin, J., Smith, M., Close, R., Adams-Groom, B., 2007. Int. J. Biometeorol. 51, 181–191.

Estève, R.S., Baisnée, D., Guinot, B., Petit, J.-E., Sodeau, J., O'Connor, D., Besancenot, J.-P., Thibaudon, M., Gros, V., 2018. Remote Sens. 10, 1932.

Evans, M.R., 2019. R. Soc. Open Sci. 6.

Fall, P.L., 1994. Arct. Alp. Res. 26, 383–392.

Fang, C.F., Ling, D.L., 2005. Landsc. Urban Plan. 71, 29–34.

Fernández-Rodríguez, S., Tormo-Molina, R., Maya-Manzano, J.M., Silva-Palacios, I., Gonzalo-Garijo, Á., 2014a. Aerobiologia (Bologna). 30, 173–187.

Fernández-Rodríguez, S., Tormo-Molina, R., Maya-Manzano, J.M., Silva-Palacios, I., Gonzalo-Garijo, Á., 2014b. Aerobiologia (Bologna). 30, 257–268.

Fontana, S.L., 2005. J. Biogeogr. 32, 719–735.

Fornaciari, M., Bricchi, E., Frenguelli, G., Romano, B., 1996. Aerobiologia (Bologna). 12, 219–227.

Frenguelli, G., Spieksma, F.T.M., Bricchi, E., Romano, B., Mincigrucci, G., Nikkels, A.H., Dankaart, W., Ferranti, F., 1991. Grana 30, 196–200.

Frisk, C.A., Apangu, G.P., Petch, G.M., Adams-Groom, B., Skjøth, C.A., 2022. Sci. Total Environ. 814.

Gadermaier, G., Hauser, M., Ferreira, F., 2014. Methods 66, 55–66.

Galán, C., Ariatti, A., Bonini, M., Clot, B., Crouzy, B., Dahl, A., Fernandez-González, D., Frenguelli, G., Gehrig, R., Isard, S., Levetin, E., Li, D.W., Mandrioli, P., Rogers, C.A., Thibaudon, M., Sauliene, I., Skjoth, C., Smith, M., Sofiev, M., 2017. Aerobiologia (Bologna). 33, 293–295.

Galán, C., Emberlin, J., Domínguez, E., Bryant, R.H., Villamandos, F., 1995. Grana 34, 189–198.

Galán, C., Smith, M., Thibaudon, M., Frenguelli, G., Oteros, J., Gehrig, R., Berger, U., Clot, B., Brandao, R., 2014. Aerobiologia (Bologna). 30, 385–395.

Gassner, M., Schmid-Grendelmeier, P., Clot, B., 2019. Allergo J. Int. 28, 289–298.

Gaughran, A., Stout, J., 2020. Biodiversity Audit at Áras an Uachtaráin - Final Report.

Giner, M.M., García, J.S.C., Sellés, J.G., 1999. Int. J. Biometeorol. 43, 51–63.

Gioulekas, D., Balafoutis, C., Damialis, A., Papakosta, D., Gioulekas, G., Patakas, D., 2004. Int. J. Biometeorol. 48, 128–136.

González-Fernández, E., Álvarez-López, S., Piña-Rey, A., Fernández-González, M., Rodríguez-Rajo, F.J., 2021. Forests 12.

González Minero, F.J., Candau, P., Tomás, C., Morales, J., 1998. Allergy Eur. J. Allergy Clin. Immunol. 53, 266–274.

Gonzalo-Garijo, M.A., Tormo-Molina, R., Muñoz-Rodríguez, A.F., Silva-Palacios, I., 2006. J. Investig. Allergol. Clin. Immunol. 16, 37–43.

Government of Ireland, Met Éireann, 2019. Storm Emma, Ireland.

Grinn-Gofroń, A., Strzelczak, A., Przestrzelska, K., 2015. Ann. Agric. Environ. Med. 22, 6–10.

Gross, J., Ligges, U., 2015. nortest: Tests for Normality.

Heinzerling, L., Frew, A.J., Bindslev-Jensen, C., Bonini, S., Bousquet, J., Bresciani, M., Carlsen, K.H., Van Cauwenberge, P., Darsow, U., Fokkens, W.J., Haahtela, T., Van Hoecke, H., Jessberger, B., Kowalski, M.L., Kopp, T., Lahoz, C.N., Lodrup Carlsen, K.C., Papadopoulos, N.G., Ring, J., Schmid-Grendelmeier, P., Vignola, A.M., Wöhrl, S., Zuberbier, T., 2005. Allergy Eur. J. Allergy Clin. Immunol. 60, 1287–1300.

Helfman-Hertzog, I., Galán, C., Levetin, E., Kutiel, H., Hefer, T., 2023. Grana.

Henry, R., Norris, G.A., Vedantham, R., Turner, J.R., 2009. Environ. Sci. Technol. 43, 4090–4097.

Hirst, J.M., 1952. Ann. Appl. Biol. 39, 257–265.

Hoebeke, L., Bruffaerts, N., Verstraeten, C., Delcloo, A., De Smedt, T., Packeu, A., Detandt, M., Hendrickx, M., 2018. Aerobiologia (Bologna). 34, 139–155.

Janati, A., Bouziane, H., del Mar Trigo, M., Kadiri, M., Kazzaz, M., 2017. Aerobiologia (Bologna). 33, 517–528.

Jato, V., Rodríguez-Rajo, F.J., Alcázar, P., De Nuntiis, P., Galán, C., Mandrioli, P., 2006. Aerobiologia (Bologna). 22, 13–25.

Javadi, R., 2021. Build. Environ. 202, 108039.

Kapoor, M., 2017. Univers. J. Plant Sci. 5, 1–9.

Kasprzyk, I., 2003. Aerobiologia (Bologna). 19, 113–120.

Kasprzyk, I., Borycka, K., 2019. Int. J. Biometeorol. 63, 1651–1658.

Kasprzyk, I., Uruska, A., Szczepanek, K., Latałowa, M., Gaweł, J., Harmata, K., Myszkowska, D., Stach, A., Stępalska, D., 2004. Aerobiologia (Bologna). 20, 141–151.

Katelaris, C.H., Burke, T. V., Byth, K., 2004. Ann. Allergy, Asthma Immunol. 93, 131–136.

Khwarahm, N., Dash, J., Atkinson, P.M., Newnham, R.M., Skjøth, C.A., Adams-Groom, B., Caulton, E., Head, K., 2014. Int. J. Biometeorol. 58, 529–545.

Kluska, K., Piotrowicz, K., Kasprzyk, I., 2020. Agric. For. Meteorol. 291, 108042.

Knaap, W.O. Van Der, Leeuwen, J.F.N. Van, Svitavska, H., Pidek, I.A., Kvavadze, E., Chichinadze, M., Giesecke, T., Oberli, F., Kalnin, L., Pardoe, H.S., Tinner, W., Ammann, B., 2010. 285–307.

Kolek, F., Plaza, M.P., Charalampopoulos, A., Traidl-Hoffmann, C., Damialis, A., 2021. Atmos. Environ. 267, 118774.

Kruczek, A., Puc, M., Wolski, T., 2017. Grana 56, 71–80.

de La Guardia, C.D., Alba, F., Girón, F., Sabariego, S., 1998. Grana 37, 298–304.

Leuschner, R.M., 1999. Aerobiologia (Bologna). 15, 143–147.

Makra, L., Matyasovszky, I., Páldy, A., Deák, Á.J., 2012. Grana 51, 215–227.

Markey, E., Clancy, J.H., Martínez-Bracero, M., Maya-Manzano, J.M., Smith, M., Skjøth, C., Dowding, P., Sarda-Estève, R., Baisnée, D., Donnelly, A., McGillicuddy, E., Sewell, G.,

O'Connor, D.J., 2022a. Aerobiologia (Bologna). 38, 343–366.

Markey, E., Hourihane Clancy, J., Martínez-Bracero, M., Neeson, F., Sarda-Estève, R., Baisnée, D., McGillicuddy, E.J., Sewell, G., O'Connor, D.J., 2022b. Sensors 22, 8747.

Martinez-Bracero, M., Markey, E., Clancy, J.H., McGillicuddy, E.J., Sewell, G., O'Connor, D.J., 2022. Atmosphere (Basel). 13, 308.

Martínez-Bracero, M., Markey, E., Clancy, J.H., Sodeau, J., O'Connor, D.J., 2022. Atmosphere (Basel). 13, 313.

Matyasovszky, I., Makra, L., Csépe, Z., Sümeghy, Z., Deák, Á.J., Pál-Molnár, E., Tusnády, G., 2015. Theor. Appl. Climatol. 122, 181–193.

Maya-Manzano, J.M., Skjøth, C.A., Smith, M., Dowding, P., Sarda-Estève, R., Baisnée, D., McGillicuddy, E., Sewell, G., O'Connor, D.J., 2021. Agric. For. Meteorol. 298–299, 108298.

Maya Manzano, J.M., Tormo Molina, R., Fernández Rodríguez, S., Silva Palacios, I., Gonzalo Garijo, Á., 2017. Landsc. Urban Plan. 157, 434–446.

McDonald, M.S., 1980. Grana 19, 53–56.

McDonald, M.S., O'Driscoll, B.J., 1980. Clin. Exp. Allergy 10, 211–215.

Mesa, J.A.S., Smith, M., Emberlin, J., Allitt, U., Caulton, E., Galan, C., 2003. Aerobiologia (Bologna). 19, 243–250.

Myszkowska, D., 2012. Acta Agrobot. 63, 85–96.

Newnham, R.M., Sparks, T.H., Skjøth, C.A., Head, K., Adams-Groom, B., Smith, M., 2013. Int. J. Biometeorol. 57, 391–400.

Nilsson, S., Persson, S., 1981. Grana 20, 179–182.

Ningal, T., Mills, G., Smithwick, P., 2010. Irish Geogr. 43, 161–176.

Norris-Hill, J., 1997. Aerobiologia (Bologna). 13, 91–97.

Norris-Hill, J., Emberlin, J., 1991. Grana 30, 229–234.

Nowak, M., Szymańska, A., Grewling, Ł., 2012. Postep. Dermatologii i Alergol. 29, 156–160.

O'Connor, D., Markey, E., Maya-manzano, J.M., Dowding, P., Donnelly, A., Sodeau, J., 2022. Pollen Monitoring and Modelling (POMMEL).

O'Connor, D.J., Sadyś, M., Skjøth, C.A., Healy, D.A., Kennedy, R., Sodeau, J.R., 2014. Aerobiologia (Bologna). 30, 397–411.

OPW, 2023. Flora and Fauna [WWW Document]. Tree Popul. St Stephens Green Park. URL

https://www.ststephensgreenpark.ie/flora-and-fauna/

Orlandi, F., Oteros, J., Aguilera, F., Ben Dhiab, A., Msallem, M., Fornaciari, M., 2014. Environ. Sci. Process. Impacts 16, 1716–1725.

Pablos, I., Wildner, S., Asam, C., Wallner, M., Gadermaier, G., 2016. Curr. Allergy Asthma Rep. 16.

Pashley, C.H., Fairs, A., Edwards, R.E., Bailey, J.P., Corden, J.M., Wardlaw, A.J., 2009. Aerobiologia (Bologna). 25, 249–263.

Peel, R.G., Hertel, O., Smith, M., Kennedy, R., 2013. Ann. Allergy, Asthma Immunol. 111, 548–554.

Peel, Robert George, Kennedy, R., Smith, M., Hertel, O., 2014. Int. J. Biometeorol. 58, 1317–1325.

Peel, R. G., Ørby, P. V., Skjøth, C.A., Kennedy, R., Schlünssen, V., Smith, M., Sommer, J., Hertel, O., 2014. Biogeosciences 11, 821–832.

Pérez-Badia, R., Bouso, V., Rojo, J., Vaquero, C., Sabariego, S., 2013. Aerobiologia (Bologna). 29, 419–428.

Petit, J.E., Favez, O., Albinet, A., Canonaco, F., 2017. Environ. Model. Softw. 88, 183–187.

Picornell, A., Recio, M., Ruiz-Mata, R., García-Sánchez, J., Cabezudo, B., Trigo, M. del M., 2020. Int. J. Biometeorol. 64, 1637–1647.

Piotrowska, K., Kaszewski, B.M., 2012. Acta Agrobot. 64, 39–50.

Przedpelska-Wasowicz, E.M., Wasowicz, P., Áskelsdóttir, A.Ó., Guðjohnsen, E.R., Hallsdóttir, M., 2021. Aerobiologia (Bologna). 37, 507–524.

Puc, M., Puc, M.I., 2004. Ann. Agric. Environ. Med. 237–244.

Puljak, T., Mamić, M., Mitić, B., Hrga, I., Hruševar, D., 2016. Aerobiologia (Bologna). 32, 709–723.

R Development Core Team, 2020. R Found. Stat. Comput. 10, https://www.R-project.org.

Rantio-Lehtimäki, A., Koivikko, A., Kupias, R., Mäkinen, Y., Pohjola, A., 1991. Allergy 46, 68–76.

Ribeiro, H., Cunha, M., Abreu, I., 2003. Aerobiologia (Bologna). 19, 21–27.

Rodríguez, S.F., Adams-Groom, B., Palacios, I.S., Caeiro, E., Brandao, R., Ferro, R., Garijo, Á.G., Smith, M., Molina, R.T., 2015. Aerobiologia (Bologna). 31.

Rojo, J., Oteros, J., Pérez-Badia, R., Cervigón, P., Ferencova, Z., Gutiérrez-Bustillo, A.M., Bergmann, K.C., Oliver, G., Thibaudon, M., Albertini, R., Rodríguez-De la Cruz, D., Sánchez-Reyes, E., Sánchez-Sánchez, J., Pessi, A.M., Reiniharju, J., Saarto, A., Calderón, M.C.,

Guerrero, C., Berra, D., Bonini, M., Chiodini, E., Fernández-González, D., García, J., Trigo, M.M., Myszkowska, D., Fernández-Rodríguez, S., Tormo-Molina, R., Damialis, A., Kolek, F., Traidl-Hoffmann, C., Severova, E., Caeiro, E., Ribeiro, H., Magyar, D., Makra, L., Udvardy, O., Alcázar, P., Galán, C., Borycka, K., Kasprzyk, I., Newbigin, E., Adams-Groom, B., Apangu, G.P., Frisk, C.A., Skjøth, C.A., Radišić, P., Šikoparija, B., Celenk, S., Schmidt-Weber, C.B., Buters, J., 2019. Environ. Res. 174, 160–169.

Rojo, J., Oteros, J., Picornell, A., Ruëff, F., Werchan, B., Werchan, M., Bergmann, K.C., Schmidt-Weber, C.B., Buters, J., 2020. Atmosphere (Basel). 11.

Rojo, J., Rapp, A., Lara, B., Fernández-González, F., Pérez-Badia, R., 2015. Sci. Total Environ. 538, 672–682.

Sarda-Estève, R., Baisnée, D., Guinot, B., Mainelis, G., Sodeau, J., O'connor, D., Besancenot, J.P., Thibaudon, M., Monteiro, S., Petit, J.E., Gros, V., 2020. Int. J. Environ. Res. Public Health 17, 1–25.

Sarda-Estève, R., Baisnée, D., Guinot, B., Sodeau, J., O'Connor, D., Belmonte, J., Besancenot, J.-P., Petit, J.-E., Thibaudon, M., Oliver, G., Sindt, C., Gros, V., 2019. Remote Sens. 11, 1671.

Simoleit, A., Werchan, M., Werchan, B., Mücke, H.G., Gauger, U., Zuberbier, T., Bergmann, K.C., 2017. Allergo J. Int. 26, 155–164.

Skjøth, C.A., Ørby, P. V., Becker, T., Geels, C., Schlünssen, V., Sigsgaard, T., Bønløkke, J.H., Sommer, J., Søgaard, P., Hertel, O., 2013a. Biogeosciences 10, 541–554.

Skjøth, C.A., Šikoparija, B., Jäger, S., EAN-Network, 2013b. Pollen Sources, in: Allergenic Pollen. Springer Netherlands, Dordrecht, pp. 9–27.

Skjøth, C.A., Smith, M., Šikoparija, B., Stach, A., Myszkowska, D., Kasprzyk, I., Radišić, P., Stjepanović, B., Hrga, I., Apatini, D., 2010. Agric. For. Meteorol. 150, 1203–1210.

Smith, M., Emberlin, J., 2005. Clin. Exp. Allergy 35, 1400–1406.

Snyder, G., Callahan, P.K.I., Carville, J., Dennis, J., Funk, A., Nelson, I., Nicholson, D., Becker, R.J., Berry, R., Blackburn, C., 2016. Dublin City Tree Strategy 2016 - 2020.

Sofiev, Mikhail, Belmonte, J., Gehrig, R., Izquierdo, R., Smith, M., Dahl, Å., Siljamo, P., 2013. Airborne Pollen Transport, in: Allergenic Pollen. Springer Netherlands, Dordrecht, pp. 127–159.

Sofiev, M., Siljamo, P., Ranta, H., Linkosalo, T., Jaeger, S., Rasmussen, A., Rantio-Lehtimaki, A., Severova, E., Kukkonen, J., 2013. Int. J. Biometeorol. 57, 45–58.

Soldevilla, C.G., Alcázar-Teno, P., Domínguez-Vilches, E., Villamandos de la Torre, F., Garcia-Pantaleon, F.I., 1995. Aerobiologia (Bologna). 11, 105–109.

Solomon, W.R., 1969. J. Allergy 44, 25–36.

Sousa-Silva, R., Smargiassi, A., Kneeshaw, D., Dupras, J., Zinszer, K., Paquette, A., 2021. Sci. Rep. 11, 1–13.

Spieksma, F.T.M., van Den Assem, A., Collette, B.J.A., van Den Assem, A., 1985. Grana 24, 99–108.

Spieksma, F.T.M., Van Noort, P., Nikkels, H., 2000. Aerobiologia (Bologna). 16, 21–24.

Subiza, J., Jerezb, M., Jiméneza, J.A., Narganes, M.J., Cabrera, M., Varela, S., Subiza, E., 1995. J. Allergy Clin. Immunol. 96, 15–23.

Tampieri, F., Mandrioli, P., Puppi, G.L., 1977. Agric. Meteorol. 18, 9–20.

Teagasc, 2019. Teagasc leads the fight against Ash Dieback [WWW Document]. URL https://www.teagasc.ie/news--events/news/2019/teagasc-leads-the-fight-a.php (accessed 4.16.20).

The Irish National Meteorological Service [WWW Document], 2023. URL https://www.met.ie/climate/available-data/daily-data (accessed 9.12.23).

Vallverdú, A., Asturias, J.A., Arilla, M.C., Gómez-Bayón, N., Martínez, A., Martínez, J., Palacios, R., 1998. J. Allergy Clin. Immunol. 101, 363–370.

Velasco-Jiménez, M.J., Alcázar, P., Cariñanos, P., Galán, C., 2020. Urban For. Urban Green. 49, 126600.

Velasco-Jiménez, M.J., Alcázar, P., Domínguez-Vilches, E., Galán, C., 2013. Aerobiologia (Bologna). 29, 113–120.

de Weger, L.A., Bergmann, K.C., Rantio-Lehtimäki, A., Dahl, Å., Buters, J., Déchamp, C., Belmonte, J., Thibaudon, M., Cecchi, L., Besancenot, J.-P., Galán, C., Waisel, Y., 2013. Impact of Pollen, in: Allergenic Pollen. Springer Netherlands, Dordrecht, pp. 161–215.

de Weger, L.A., Molster, F., de Raat, K., den Haan, J., Romein, J., van Leeuwen, W., de Groot, H., Mostert, M., Hiemstra, P.S., 2020. Sci. Total Environ. 741, 140404.

Wei, T., Simko, V., Levy, M., Xie, Y., Jin, Y., Zemla, J., Freidank, M., Cai, J., Protivinsky, T., 2021. corrplot: Visualization of a Correlation Matrix.

Werchan, B., Werchan, M., Mücke, H.G., Gauger, U., Simoleit, A., Zuberbier, T., Bergmann, K.C., 2017. Environ. Monit. Assess. 189.

Werchan, M., Werchan, B., Bergmann, K.C., 2018. Allergo J. Int. 27, 69–71.

Xiao, X., Fu, A., Xie, X., Kang, M., Hu, D., Yang, P., Liu, Z., 2013. Int. Arch. Allergy Immunol.

160, 143–151.

Xie, C., 2018. Fresenius Environ. Bull. 27, 8695–8708.

Yang, Y.-L., Huang, T.-C., Chen, S.-H., 2003. Taiwania 48, 168–179.

Chapter 4: Pollen Modelling

4.1 Introduction

Ambient pollen data can be utilised in a range of various applications, the most prominent being to improve the warning and treatment of allergy sufferers and those at risk of experiencing adverse respiratory health effects due to pollen exposure. Data can be shared with relevant stakeholders (medical professionals, agricultural sectors, meteorological services etc.) to improve the diagnosis and treatment of allergic conditions, to identify and prevent the spread of invasive plant species and diseases as well as improving pollen forecast services. The most rudimentary application of pollen monitoring data is to construct a pollen calendar (Oh, 2018). As seen in Chapter 3, a pollen calendar is a simple prediction tool composed of a graphical representation of at least 5 years of pollen season data for a specific location (Galán et al., 2017). The pollen calendar uses previous seasonal trends to estimate when periods of high pollen exposure will likely occur. However, more resolved predictions can be made by developing observational-based models by coupling the historical pollen records with relevant meteorological parameters.

Given the previous lack of monitoring data, Irish pollen forecasts are currently determined by the University of Worcester using UK data and issued by Met Éireann (Irish meteorological service). This might not fully represent the pollen concentrations experienced by the Irish public. According to one report, the pollen found in a specific location is only representative of a surrounding area of 30 km (Katelaris et al., 2004). This is not a suitable or representative long-term approach for the Irish public and so site-specific models for Ireland need to be developed. However, thought must be given to the specific pollen models developed. As seen in Chapter 3, there were over 60 pollen taxa classified throughout the 2017-2020 monitoring campaign. To aid allergy sufferers, it is often more practical to develop models that target specific allergenic pollen classes that pose a critical risk to the public.

The 12 most allergenic taxa as defined by the COST Action ES0603 are *Alnus*, *Ambrosia*, *Artemisia*, *Betula*, Chenopodiaceae, *Corylus*, Cupressaceae, *Olea*, *Platanus*, Poaceae, *Quercus* and Urticaceae, the allergenic potential of which have been well covered in literature (Skjøth et al., 2013). Some studies have shown that sensitisation to grasses and Betulaceae pollen (Bousquet et al., 2007; Heinzerling et al., 2005; Nae et al., 2021) does exist among the Irish population. However, these studies have typically encompassed a wide variety of other known allergens such as dust and animal dander. Specific studies focusing on other pollen types (Bousquet et al., 2007; Heinzerling et al., 2005) are lacking and need to be further explored to assess the impact of potentially allergenic pollen from an Irish perspective. Among European studies, the highest degree of sensitisation towards specific pollen types is against pollen grains from grasses and the Betulaceae family. Clinically relevant sensitisation rates to grass pollen exceeds 50% for the UK with arboreal pollens from the Betulaceae contributing to sensitisation rates of between approximately 10-20% (Burbach et al., 2009). Due to similarities in biodiversity and climate, comparable trends are expected for Ireland.

Although grass pollen remains the prevalent allergenic pollen for Ireland, it is possible and likely that sensitisation to certain tree pollen taxa, particularly those from the Betulaceae family, will increase in years to come. Ireland, at present, would be considered a relatively under-forested country. As a result, afforestation efforts in Ireland are currently progressing at one of the highest rates in Europe (Buscardo et al., 2008). A number of regulatory schemes have promoted the afforestation of many grassland areas in Ireland. Initially, such plans were proposed to improve biodiversity and more recently to improve the genetic quality of Irish trees (Teagasc, 2022) and combat climate change (Department of Agriculture Food and the Marine, 2020). Several of these plans specifically apply to certain trees in the Betulaceae family such as *Alnus* and *Betula* and have been in operation since the late 1990's (Teagasc, 2022). A recent, study by J. M. Maya-Manzano *et al.*, 2021 has shown that *Betula* pollen concentrations over Ireland have increased in the last 40 years as a result of the concomitant increases in the fraction of birch trees in forest areas as well as the ornamental use of birch trees in urban areas and their reaching maturity. Increasing concentrations of tree pollen have often been followed by an increase in sensitisation. A Swiss study (Frei and Leuschner, 2000) found that over a 30 year period, *Corylus* and *Betula* pollen concentrations increased notably while herbaceous pollen concentrations remained relatively stable. This was met with increased rates of tree pollen allergies, concluding that tree pollen allergy had become more important in comparison to grass and herb pollen allergies (Frei and Leuschner, 2000). Increasing sensitisation to Betulaceae pollen over the years has also been found in other European countries such as Sweden (Warm et al., 2013), Denmark (Warm et al., 2013) and Finland (Movérare et al., 2006).

Therefore, this chapter aims to investigate and develop several model types and methods for the forecasting of daily Poaceae and *Betula* pollen using the aforementioned 2017-2020 pollen data collected within Dublin. SVM, RF and ANN models were created using the Dublin monitoring data for both classification and regression purposes, MLR models were also developed for comparison. The combination (Novo-Lourés et al., 2023; Nowosad et al., 2018; Voukantsis et al., 2010b) and individual use of these modelling techniques has received much attention and regard in previous literature studies, leading to their selection. In addition, Poaceae and *Betula* represent 2 of the top 4 most documented pollen types for forecasting studies, with Poaceae being the single most documented (Vélez-Pereira et al., 2021). Numerous studies have evaluated the potential of ANN (Lops et al., 2020; Muzalyova et al., 2021; Puc, 2012; Rodríguez-Rajo et al., 2010; Sánchez-Mesa et al., 2002; Sánchez Mesa et al., 2005; Voukantsis et al., 2010b, 2010a), SVM (Bogawski et al., 2019; Du et al., 2017; Liu et al., 2017), RF (Lo et al., 2021; Navares and Aznarte, 2017a, 2017b; Nowosad, 2016), and MLR and other standard regression models (Aboulaich et al., 2013; Janati et al., 2017; Piotrowska, 2012; Robichaud and Comtois, 2017; de Weger et al., 2014; Zhang et al., 2015) for the prediction of Poaceae and *Betula* concentrations and seasonal trends. Although many of these studies encompass numerous years/decades of data that is currently not available for Dublin, there are several

studies which have constructed models using a more comparable number of annual datasets (Emmerson et al., 2022; Lops et al., 2020; Nowosad et al., 2018).

Different aerobiological networks and studies have also previously proposed several different classification threshold values of allergenic pollen concentration for use in forecasting models. These include Poaceae and/or *Betula* pollen thresholds in Denmark (Kiotseridis et al., 2013), Sweden (Becker et al., 2021; Steckling-Muschack et al., 2021), Italy (Brighetti et al., 2014), Spain (Galán et al., 2007), UK (Osborne et al., 2017) etc. However, these values can vary and change as they have been found to strongly depend on certain regional conditions such as vegetation and climate (de Weger et al., 2013). As forecasts currently come from the UK for Ireland and the two countries share similar climates, the UK threshold values for Poaceae and *Betula* were selected for this study. In addition to this, a more simplistic threshold based on the consensus that allergenic responses in individuals generally begin at Poaceae/*Betula* levels over 30 grains/m^3 (Corsico, 1993; Navares and Aznarte, 2017a) was also used.

4.2 Methods

4.2.1 Pollen and meteorological data collection

In line with methods discussed in Chapters 2-3, Pollen monitoring was conducted continuously over the course of several pollen seasons (May 2017-October 2020) at the previously established Dublin site (Old TU Dublin Campus) using a volumetric Hirst sampler. MPS Poaceae and *Betula* pollen data were used in the construction of preliminary forecast models.

Similarly, meteorological data used was sourced from the Met Éireann website ("The Irish National Meteorological Service," 2023) for the Dublin Airport weather station.

A series of phenological parameters were also considered, including growing degree days (GDD) and previous days' pollen concentrations.

A list of considered Meteorological and phenological parameters for model construction is provided in Table 4.1, below.

Table 4.1: Model input variables

Variable Class	Input Variables	Abbreviations
Pollen Inputs	• Pollen concentration of the previous 1 day (grains/m^3) • Average Pollen concentration of previous 7 days (grains/m^3) • Average Pollen concentration of previous 10 days (grains/m^3)	• Poaceae1/ *Betula*.1 • Poaceae.7/ *Betula*.7 • Poaceae.10/ *Betula*.10
Phenological Inputs	• Growing degree days (Base Temperature= 2-10°C)	• GDD_2 – 10
Meteorological Inputs	• Maximum Temperature (°C) • Minimum Temperature(°C) • Mean Temperature (°C) • Rainfall (mm) • Rainfall of previous day (mm) • Wind direction (Deg) • Wind speed (Knots) • Mean CBL pressure (hPa) • Cloud cover • Sunshine duration (hours)	• Tmax • Tmin • Tmed • Rain • Rain_1 • Wind_d • Wind_s • Pres • Cld_Amt • Day_L

	• Grass minimum temperature (°C) • Global Radiation (J/cm^2) • Relative humidity (%) • Mean soil temperature (°C) • Evapotranspiration (mm) • Potential evapotranspiration (mm) • Average Rainfall of previous 7 days (mm) • Average Mean Temperature of previous 7 days (°C) • Average Rainfall of previous 10 days (mm) • Average Mean Temperature of previous 10 days (°C)	• Gmin • Radiation • Rh • Soil • Evap • Pe • Rain_7 • Tmed_7 • Rain_10 • Tmed_10

4.2.2 Data processing

Data variables were first examined for the presence of collinearity, which has been found to impact both regression and classification models (Chan et al., 2022; Daoud, 2018; Næs and Mevik, 2001). Multicollinearity arises when a linear relationship (or correlation) exists between two or more independent variables in a dataset (Chan et al., 2022). This causes the standard error of the coefficients to increase – making some variables appear to be insignificant when they are in fact significant (Daoud, 2018). To remove parameters that are experiencing multicollinearity, variance inflation factor (VIF) and tolerance (TOL) were calculated and evaluated. VIF is the reciprocal of TOL. Any parameter with a VIF>10 and TOL <0.11 was removed in a stepwise manner prior to model construction and deemed to be collinear. These values are popular thresholds used in air quality (Ebrahimi-Khusfi et al., 2021). VIF has been used extensively at this limit, or in some cases lower, for several aerobiological studies (Cariñanos et al., 2020; Sadyś et al., 2015; Vélez-Pereira et al., 2019; Zhang et al., 2015).

4.2.3 Regression models and classification models

Regression models refer to an algorithm that predicts a numeric output (concentration) that, in this case, can be compared directly with the observed and recorded ambient Poaceae/*Betula* concentrations (grains/m^3). Whereas, classification models compute a classifier rather than a quantitative regression result, fitting results into one of several pre-trained classes (Low, Medium, High etc.). Two classification threshold levels were used for both Poaceae and *Betula* classification models. These include a rough threshold of 30 grains/m^3, over which is deemed high, and under

which is deemed low (30T). The second threshold used comes from those used in the UK (UKT) by both the University of Worcester and the UK Met Office, which is fitting since current Irish forecasts coming from the UK are also using these levels (Adams-Groom et al., 2020; Osborne et al., 2017).

In both cases, the models were trained with 80% of the collected data and tested with the remaining 20%

Random Forest (RF)

RF is an ensemble approach and consists of a combination of tree predictors (Breiman, 2001). It is a supervised learning approach that combines the average prediction of a number of randomised individual decision trees. This random nature of the approach surpasses the ability of classical regression trees by resisting overfitting. One added strength of using the RF model is that they are able to measure variable importance via model training, providing a list in order of most influential (Navares and Aznarte, 2017a). RF models were computed using the randomForest (Breiman et al., 2022) and Caret (Max et al., 2023) packages in R.

RF models were also used to evaluate the relative importance of model variables by measuring the Mean decrease in Gini (MDG) for classification models and the Increase in Node Purity (INP) for regression models. MDG measures how much a particular model feature contributes to reducing Gini impurity when making splits within the RF (Calle and Urrea, 2011). Gini impurity measures the likelihood of misclassification, with lower values equating to better splits within the RF.

The concept of INP refers to the ability of each variable to reduce the impurity of a node when making splits within the RF. The concept of node impurity is closely linked to error metrics such as MSE. An increase in node purity corresponds to a decrease in MSE. The INP metric is computed for each individual tree, and subsequently averaged across all trees within the RF. The variables exhibiting the highest INP values will possess the greatest significance (González et al., 2015).

Support Vector Machines (SVM)

SVM are a type of mathematical algorithm originally proposed by Vapnik, 2000 that maps input variables into a high-dimensional feature space so that the data can be separated and categorised. Typically for pollen forecasting, the radial basis function (RBF) kernel is used (Novo-Lourés et al., 2023). SVM models were constructed using the e1071 (Meyer et al., 2022) and caret (Max et al., 2023) packages in R.

Artificial Neural Networks (ANN)

ANN are forecasting algorithms designed to mimic the information flow of the human brain. It is composed of an input (model parameters) and output layers (result), as well as 1 or many hidden layers in between. ANN models were constructed using the neuralnet (Fritsch et al., 2019) and caret (Max et al., 2023) packages in R

Multiple Regression

Whereas the other model types were used in both regression and classification capacity, multiple regression (MLR) is used exclusively for regression purposes. MLR is an extension of linear regression. Linear regression models are generally composed of one dependent and one independent variable. Multiple regression on the other hand accounts for one dependent variable and more than two independent variables. In this study, MLRs were developed using a backwards-stepwise approach from the MASS package (Ripely et al., 2023) in R.

Combined Regression models

Both mean and median results of combined regression models were also investigated.

Evaluation Metrics

Several metrics were calculated to evaluate and compare the performance of each regression model, these included: the coefficient of determination (R^2), Spearman/Pearson correlation coefficient (r), root mean square error (RMSE), symmetric mean absolute percentage error (SMAPE), mean absolute error (MAE). The interpretation of R^2 values was carried out to assess the degree of linear association between the predicted and observed results. Spearman rank and Pearson correlation coefficients (r) were also computed. Literature states that there is no definitive consensus stating which parameters should be used to evaluate model performance in the prediction of exact daily pollen concentrations (Šikoparija et al., 2018), with papers often using both Pearson and Spearman correlation and a range of other metrics (Csépe et al., 2020). Similar to the r^2, Pearson correlation measures the degree of linear association between a set of variables, on the other hand, Spearman correlation coefficients measure the strength of monotonic relationships. Whereas the RMSE, MAE, and SMAPE were used to assess the degree of errors that existed between the predicted and observed results.

In the case of classification models, model accuracy, sensitivity, specificity and kappa values are considered for evaluation. Model accuracy refers to the percentage of correct classifications made in comparison to the actual observed values. For a given threshold value the sensitivity values measure the proportion of values above the threshold that were correctly classified. Conversely, the

specificity represents the proportion of values correctly classified below the threshold (Navares and Aznarte, 2017a). Cohen's kappa evaluation provides detail on the measure of inter-rater agreement (de Weger et al., 2014), ie. Kappa calculates the probability that the classifications determined by two evaluators will overlap (Novo-Lourés et al., 2023).

4.2.4 Feature selection

Hyperparameter

Hyperparameters for RF and ANN models were determined through grid search analysis of provided vector possibilities, similar to work completed by (Navares and Aznarte, 2017a). This was carried out using the tune function of the caret package (Max et al., 2023) in R. This was completed for both the number of nodes within a hidden layer for ANN development (using a range of values as suggested by (Rodríguez-Rajo et al., 2010)), and for mtry and ntree parameters for RF development. For SVM hyperparameters, such as cost function and gamma the tune.svm function was used from within the e1071 package (Meyer et al., 2022) in R.

Model inputs

Feature selection of model variables is an integral part of data science and is often overlooked in aerobiological studies in favour of popularly used variables from other similar literature works. Model parameter selection is often a dubious task and model developers often struggle to isolate the most important parameters and remove redundant ones. The random forest model is more robust to possessing numerous features and can include them in the model (Lo et al., 2021). In effort to further explore this area of research, a popular feature selection method was deployed. Boruta (BOR) analysis was utilised in the development of both SVM and ANN classification and regression models.

BOR is a wrapper method based on the RF classifier capable of sorting features based on importance (this was also examined). The method creates shadow features alongside the actual model features. For each inputted model feature, the BOR function creates a corresponding shadow variable. A shadow variable is a copy of the true model feature but with its values shuffled randomly (Bulot et al., 2023). Therefore, these shadow variables act as a benchmark of importance for the true model features. Actual model features are classified as relevant only if their importance measurement surpasses that of the maximum shadow variables (Chen et al., 2020).

In this study, important model features were determined by using the BORUTA in R (Kursa, 2022). An example of a BOR result plot (for Poaceae regression models) is provided below.

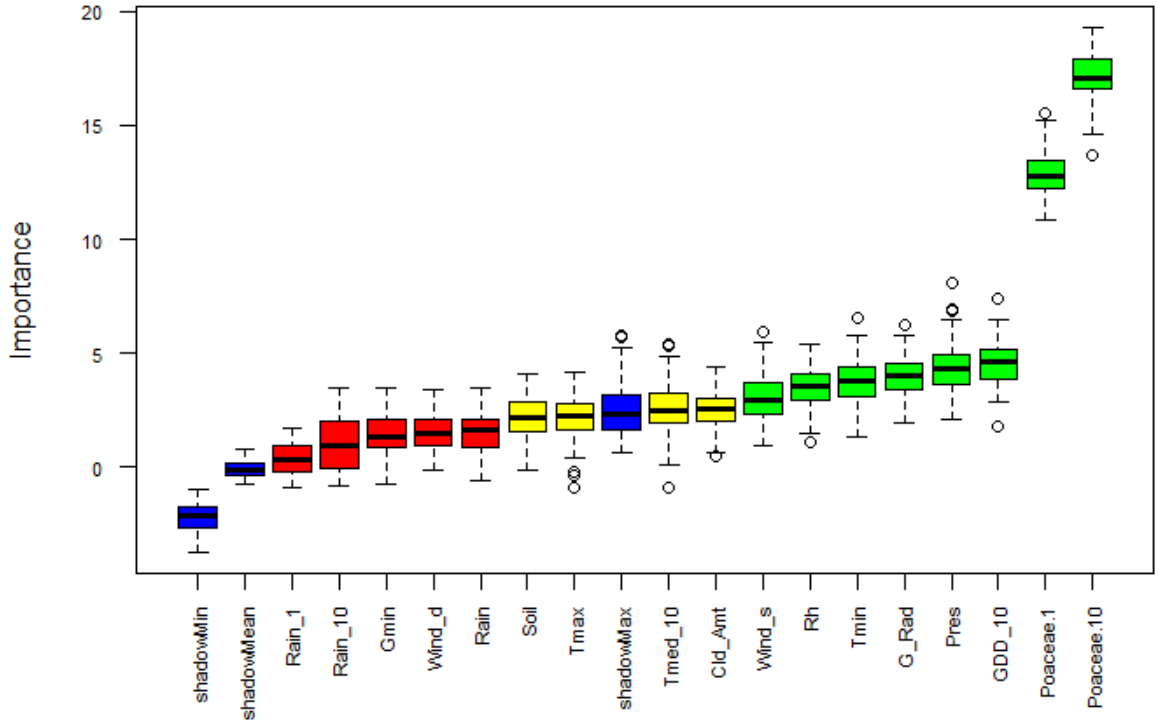

Figure 4.1: BORUTA result plot for Poaceae regression analysis

Green boxes represent variables that were determined to be more "important" than the shadow variables. Yellow is classified as tentative (has importance similar to their best shadow attributes), red is rejected (as less important) and blue represents the shadow variables. During this investigation, BOR models refer to models in which only important and tentative parameters are kept prior to development.

4.3 Results

4.3.1 Poaceae models – Regression

Several regression models were created for the prediction of Poaceae concentration in Dublin using the pollen data collected throughout the 2017-2020 monitoring campaign. The performances of the differing models were compared using r^2, r (Pearson and Spearman), RMSE, MAE and SMAPE. The results of each model are provided in Table 4.2, below.

Table 4.2: Poaceae regression model performance

Model	r^2	r (Pearson)	r (Spearman)	RMSE	MAE	SMAPE
RF	0.27	0.52	0.39	75.03	60.07	1.01
SVM	0.11	0.33	0.50	63.61	43.78	0.97

SVM-BOR	0.036	0.19	0.51	70.68	46.16	0.93
ANN	0.02	0.14	0.43	69.53	42.31	0.85
ANN-BOR	0.03	0.17	0.54	78.82	42.87	0.83
MLR	0.05	0.22	0.46	99.36	77.21	1.27
Mean	0.06	0.25	0.55	65.12	41.94	0.77
Median	0.05	0.22	0.53	66.89	42.55	0.80

Overall, the regression models did not tend to accurately account for all peak periods encountered during the test dataset and the inclusion of the added BOR feature selection did not appear to improve model performance. RF and SVM models were found to perform the best by describing the highest degree of variance, with r^2 values of 0.27 and 0.11 determined, respectively. Spearman rank correlation was also calculated to examine the monotonic relationship that exists between the observed and predicted results. In this instance, the mean of the predicted results from the RF, MLR, SVM and ANN models relayed the increasing and decreasing trend of the observed results best. Comparisons of the differing forecast models are illustrated in Figures 4.2 and 4.3. In the case of RF and SVM, the best model with the highest r^2 and lowest RMSE was selected for the comparison plots.

It can be observed that the models somewhat mimic the observed concentration of Poaceae pollen. However, some issues are apparent. The prediction models are often unable to accurately predict periods of high pollen concentrations, often experiencing a lag of 1 day. When pollen concentrations were seen to increase, all models inaccurately predicted the same rise 1 day later. This is most apparent for the primary peak in Poaceae concentration observed on the 15th of July which was not predicted by any of the regression models to increase until the 16th. However, not all models inaccurately predicted all peak days, the ANN model was able to predict the peaks observed on the 12th, 19th and 21st of July – owing to its high Spearman correlation. No other model accurately predicted these peak periods. To further investigate this lagged trend, -1-day lagged models were also examined in efforts to capture the peak periods accurately, but these models also suffered from the same delay. Dependency on the previous day's concentration was initially suspected to be strongly influencing the model results (owing to the high importance of Poaceae.1 seen from BOR and RF analysis), however, upon removing this variable from the test dataset, a lag still remained. Therefore, this lagged prediction likely resulted from insufficient training dataset size and relevance.

In general, the mean and median models performed better than the majority of the regression models with lower RMSE, MAE, SMAPE errors encountered and Spearman correlation coefficients

of >0.5 calculated, however, r^2 values were still considerably lower than the RF models, despite having lower error readings.

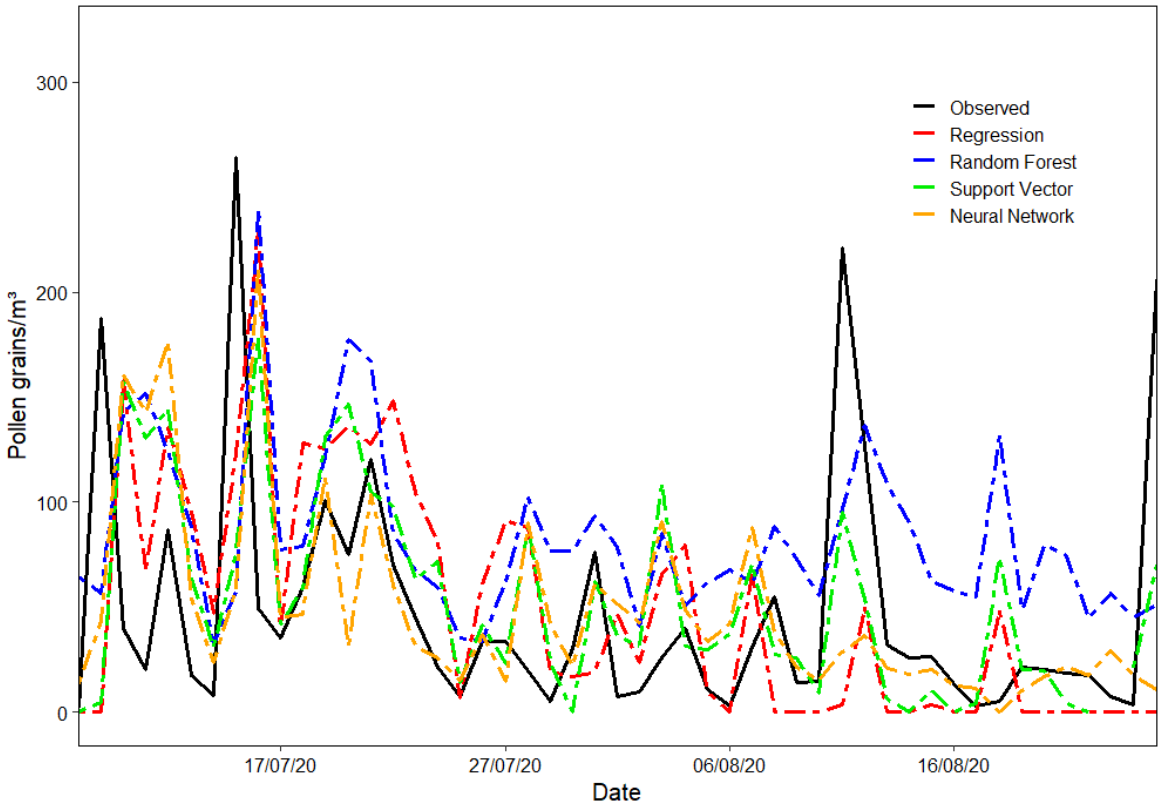

Figure 4.2: Comparison of regression models (MLR, RF, SVM, ANN) for prediction of daily Poaceae pollen concentrations

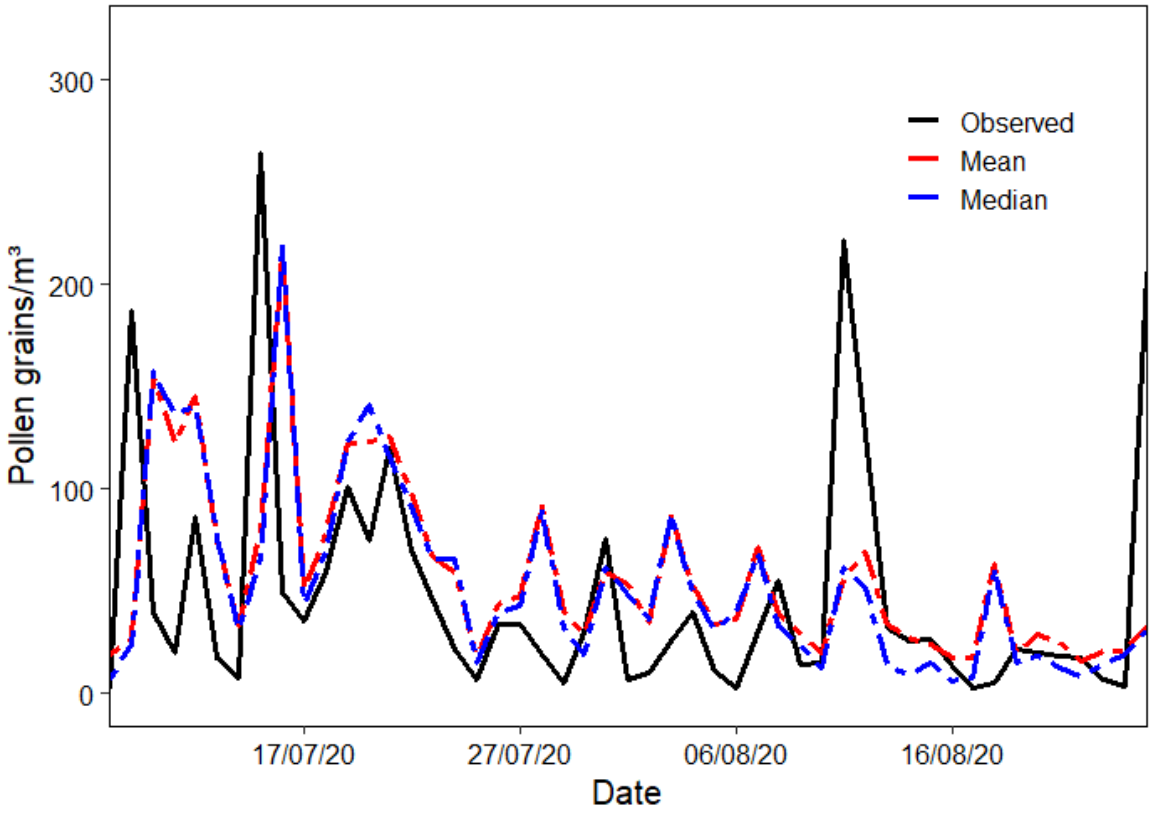

Figure 4.3: Comparison of Mean and Median regression model results for prediction of daily Poaceae pollen concentrations

Since the random forest model had the highest value for r^2, the variable importance of the different model parameters was further investigated and shown in Figure 4.4(A). It was found that the average Poaceae concentration of the previous 10 days was the single most important variable. This was followed by the Poaceae concentration observed the previous day, the average temperature of the previous 10 days, wind speed and pressure. For comparison purposes, the BOR results were also examined, as shown in Figure 4.4(B). In this case, Poaceae concentration of the previous 1 and 10 days (average), pressure and wind speed were again seen as important. However, the average temperature of the preceding 10 days was not, with increased importance also seen for GDD above 10°C, radiation, minimum temperature, and relative humidity.

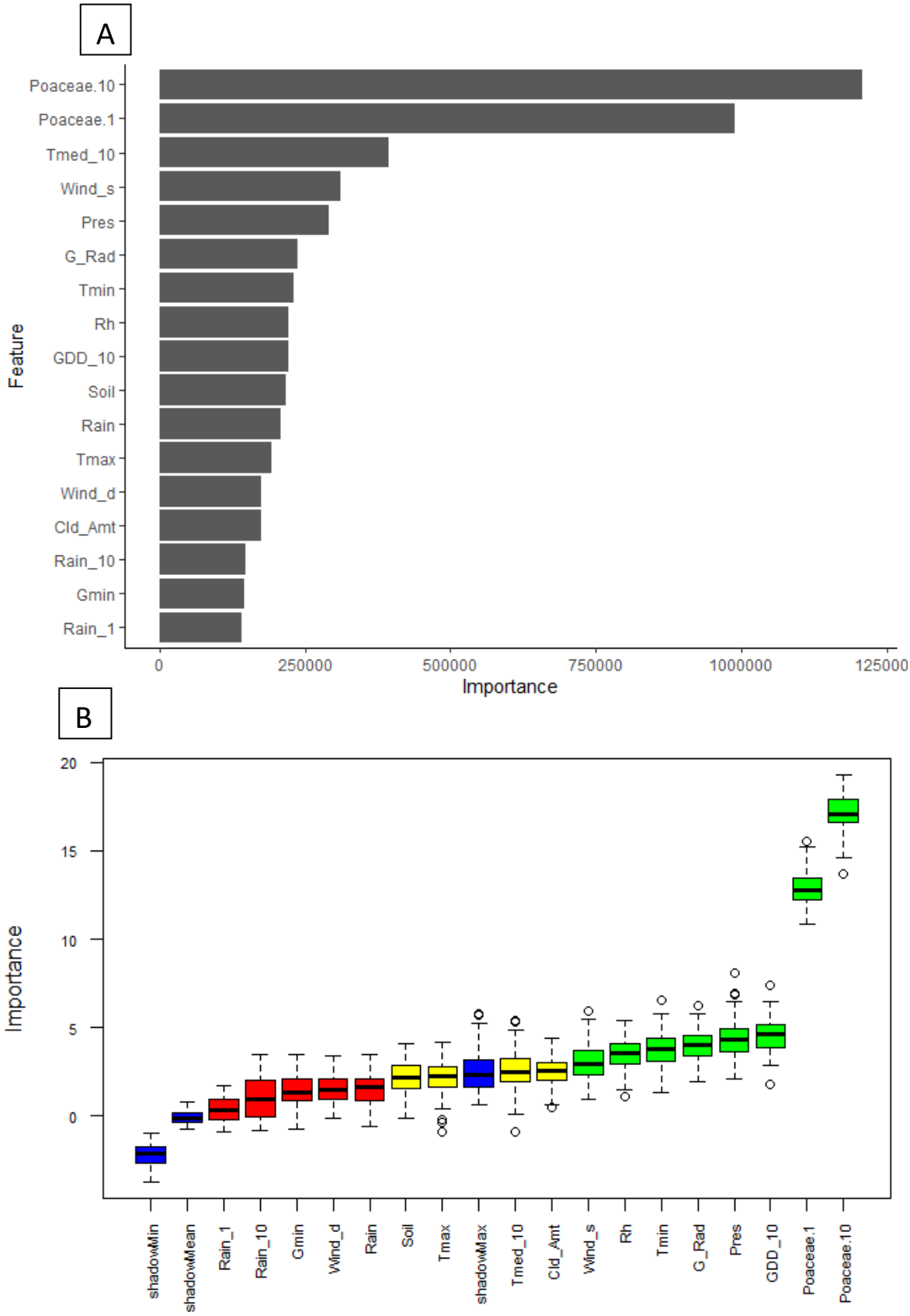

Figure 4.4: Variable importance of model parameters indicated by (A) RF model and (B) BOR feature selection methods - Poaceae

4.3.2 Poaceae models – Classification

A series of RF, SVM and ANN classification models were also developed for Poaceae pollen. These were constructed using two sets of Thresholds:

(i) 30T: Low >=0, High >=30 (Rough threshold based on allergic responses – literature)

(ii) UKT: Low >=0, Medium >=30, High >=50, Very High >=150 (UK Met office)

In this case, a set of different parameters were used to evaluate model performance as a classifier result is predicted. Model accuracy, kappa, sensitivity, and specificity were used to compare the different model performances. A summary of 30T and UKT models is described in tables 4.3 and 4.4 below.

Table 4.3: Model Accuracy and Kappa of Poaceae classification models

Model and Threshold	**Accuracy**	**Kappa**
RF 30	0.63	0.27
RF UK	0.53	0.24
SVM 30	0.67	0.36
SVM UK	0.47	0.21
SVM-BOR 30	0.67	0.35
SVM-BOR UK	0.61	0.35
ANN 30	0.63	0.28
ANN UK	0.55	0.27
ANN-BOR 30	0.63	0.26
ANN-BOR UK	0.59	0.19

Table 4.4: Model Sensitivity and Specificity of Poaceae classification models

Model and Threshold	**Sensitivity**	**Specificity**
RF 30	0.59	0.68
RF UK: LOW	0.67	0.68
RF UK: MEDIUM	0.00	0.80
RF UK: HIGH	0.69	1.00
RF UK: VERY HIGH	0.43	0.91
SVM 30	0.61	0.81
SVM UK: LOW	0.58	0.74
SVM UK: MEDIUM	0.00	1.00
SVM UK: HIGH	0.89	0.55
SVM UK: VERY HIGH	0.00	0.96
SVM-BOR 30	0.63	0.77
SVM-BOR UK: LOW	0.71	0.78
SVM-BOR UK: MEDIUM	0.00	0.80
SVM-BOR UK: HIGH	0.44	0.97
SVM-BOR UK: VERY HIGH	0.00	0.92
ANN 30	0.58	0.75
ANN UK: LOW	0.88	0.26
ANN UK: MEDIUM	0.00	0.97
ANN UK: HIGH	0.44	0.93
ANN UK: VERY HIGH	0.00	0.98
ANN-BOR 30	0.62	0.64
ANN-BOR UK: LOW	1.00	0.21
ANN-BOR UK: MEDIUM	0.00	1.00
ANN-BOR UK: HIGH	0.33	0.98
ANN-BOR UK: VERY HIGH	0.00	0.98

The 30T models often performed better than their UKT counterparts with an increase in accuracy ranging from 6-20%. Unlike the previous models, BOR feature selection often led to an increase in model performance. From examining the accuracy and kappa readings it was found that SVM models performed the best for both threshold types, with the standard SVM model reaching an accuracy of 67% with a kappa of 0.36 for 30T and the SVM-BOR model reaching an accuracy of 61% with a kappa of 0.35 for UKT. The ability of these models to accurately classify results into the designated thresholds can be further examined from their sensitivity and specificity values.

Essentially high sensitivity values can be equated to low false negative rates whereas a high specificity can be equated to a low false positive rate.

In the case of the SVM model for 30T, a sensitivity of 0.61 and a specificity of 0.81 were observed and although these reasonably outperform several of the other 30T models, it is apparent that the model is, to some degree, impacted by false negatives. This can be further witnessed from examination of the confusion matrix, shown in Figure 4.5. In this case, the model is unable to correctly assign all low value days to the low classifier, with only half being assigned correctly. On the other hand, the model performs well in predicting days classified as high.

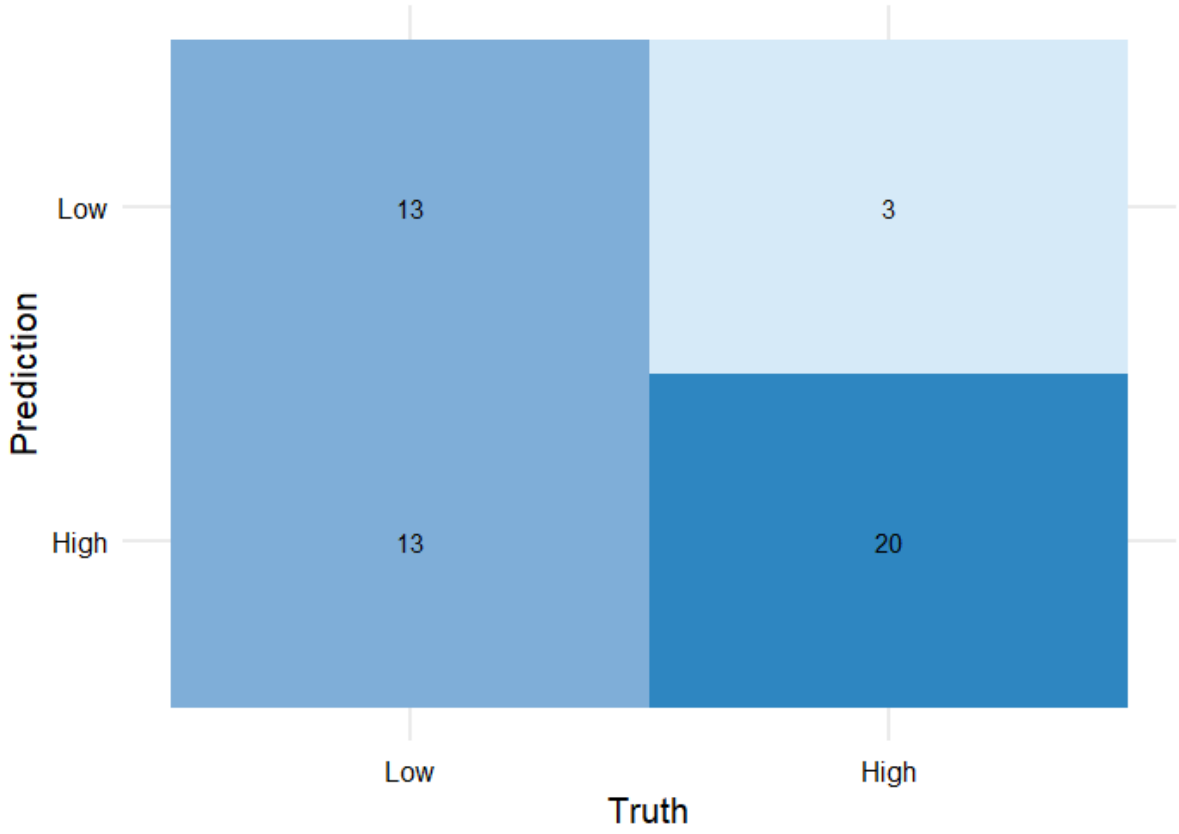

Figure 4.5: Confusion matrix of SVM Poaceae model (30T)

In the case of the SVM-BOR model for the UKT, multiple sensitivity and specificity values are provided for the 4 assigned classes. Although relatively high specificity values were found, sensitivity values were unable to be computed for both the medium and very high classes, giving a result of 0. This arises when there are no positive results predicted for that class. From further examination of the confusion matrix (Figure 4.6), it can be observed that although the model rather accurately predicts the low and high classes, it struggled to correctly determine days of medium and very high concentration, with none of these two classes correctly identified. The other UKT models all failed to correctly account for these classes, as can be seen in their confusion matrix results – provided in Appendix B (Figures B1-B18).

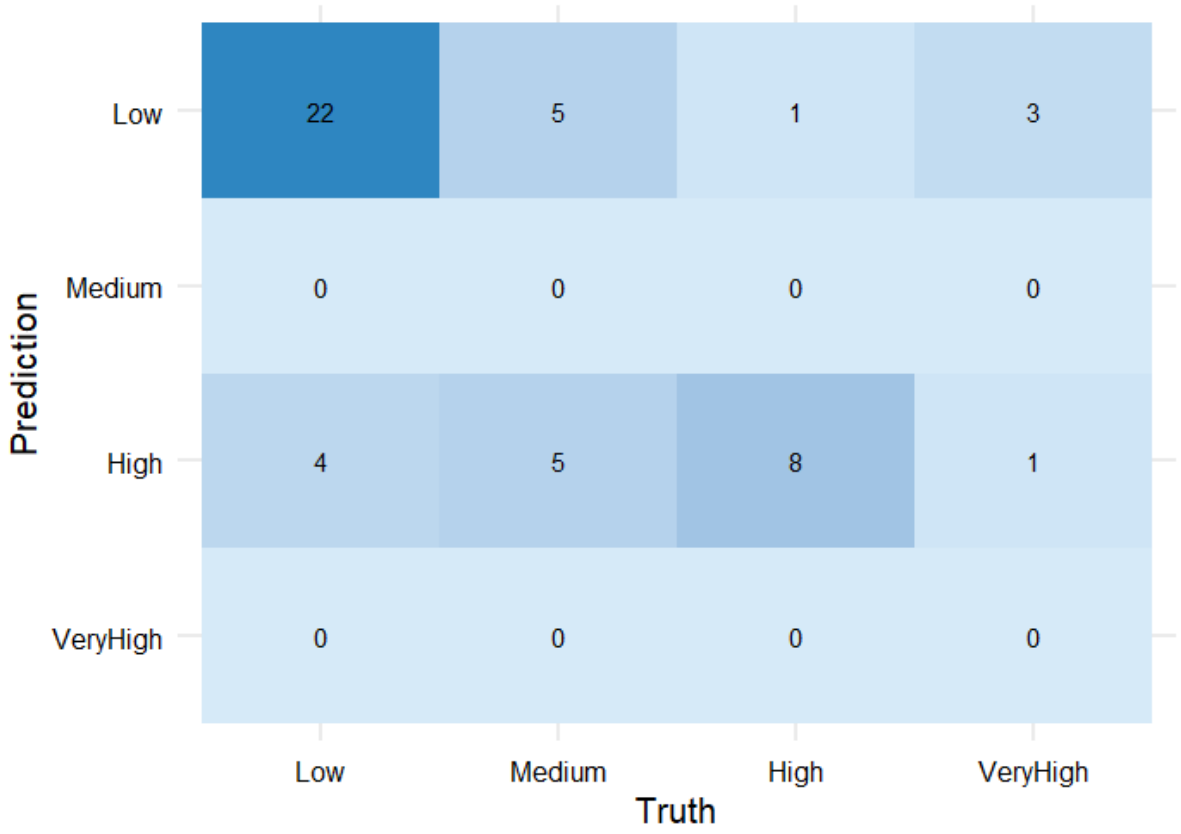

Figure 4.6: Confusion matrix of SVM-BOR Poaceae model (UKT)

Feature importance was also examined using both RF importance ratings and BOR results plot for feature selection, the results of which are summarised in Figures 4.7 and 4.8 for all threshold types. For the 30T model, RF identified Poaceae concentrations of the previous day as the most important variable, followed by average Poaceae concentrations over the previous 10 days, radiation, GDD over 10°C, relative humidity and maximum temperature. BOR feature selection also identified the importance of these parameters. In the case of the UKT models, the RF measure of importance again identified the impact of previous day and average 10-day Poaceae concentrations, radiation, GDD above 10°C, relative humidity, with the addition of pressure and absence of maximum temperature. BOR further corroborated these findings also highlighting the importance of rainfall and maximum temperature.

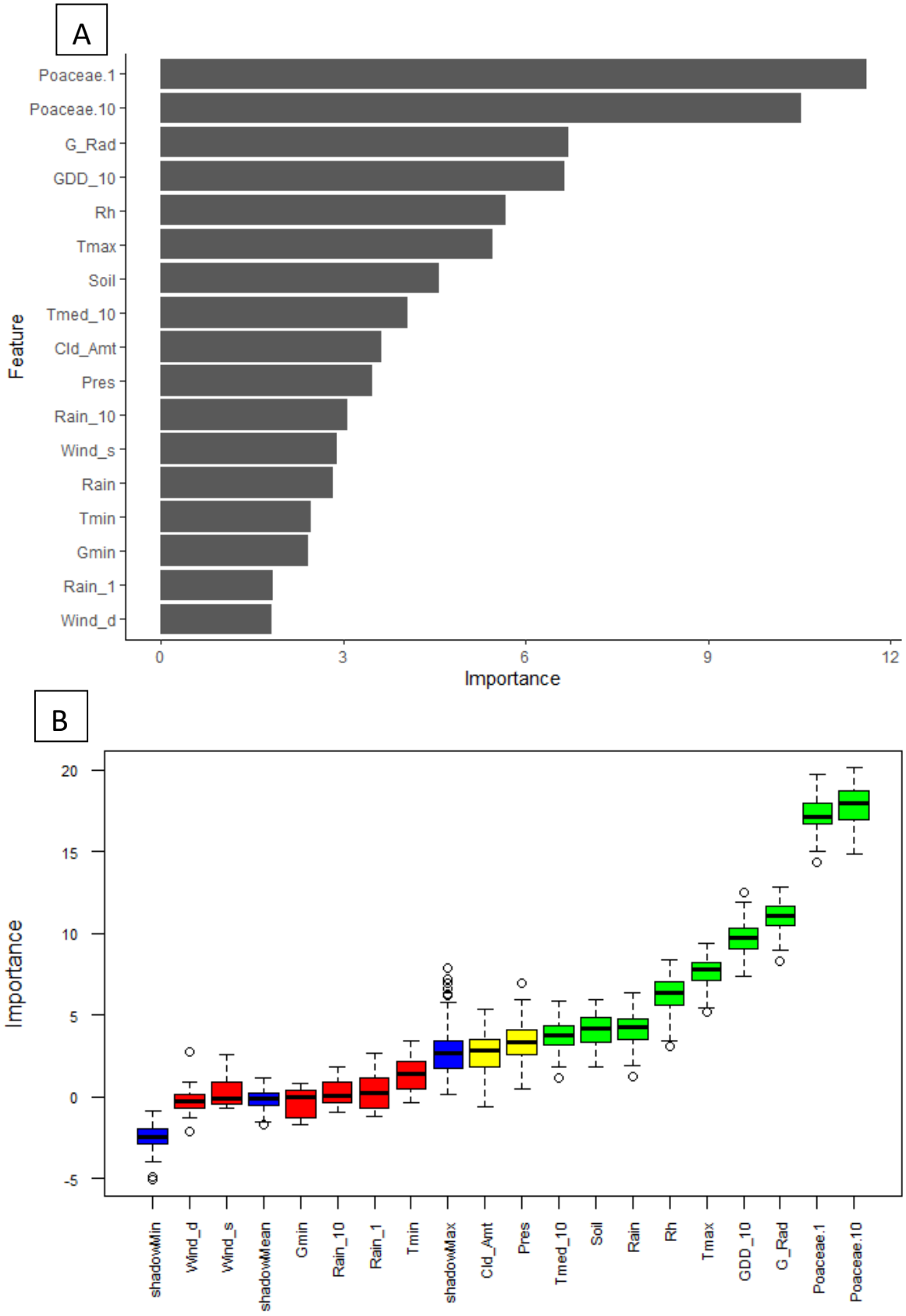

Figure 4.7: Variable importance of model parameters indicated by (A) RF model and (B) BOR feature selection methods for 30T models - Poaceae

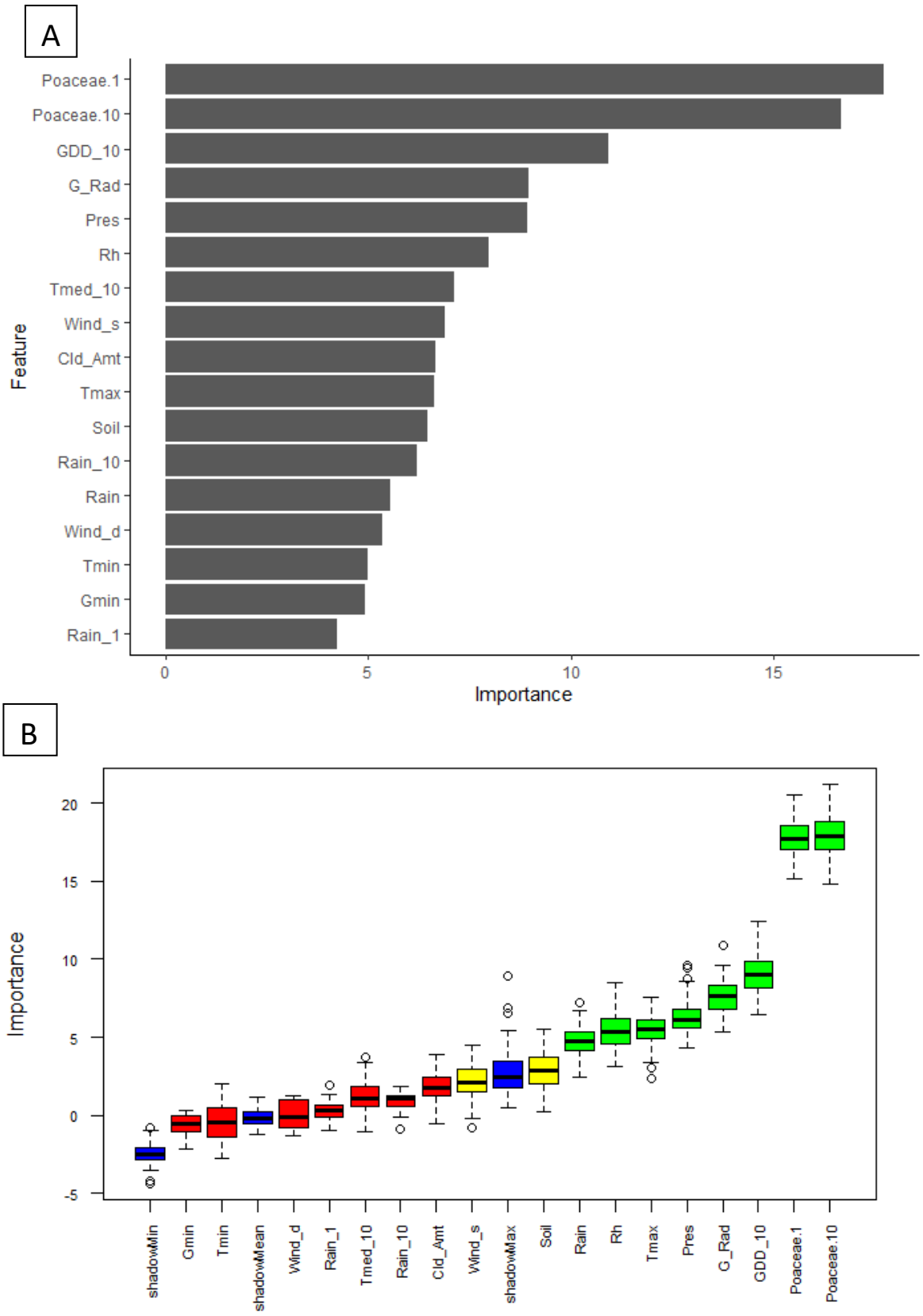

Figure 4.8: Variable importance of model parameters indicated by (A) RF model and (B) BOR feature selection methods for UKT models - Poaceae

4.3.3 *Betula* models – Regression

The same types of regression models were also developed and applied to predict the daily concentrations of *Betula* pollen in Dublin. r2, r (Pearson and Spearman), RMSE, MAE and SMAPE results of each model are summarised in Table 4.5.

Table 4.5: *Betula* regression model performance

Model	**r^2**	**r (Pearson)**	**r (Spearman)**	**RMSE**	**MAE**	**SMAPE**
RF	0.31	0.56	0.42	168.13	109. 18	0.98
SVM	0.37	0.61	0.31	169.13	102.25	1.18
SVM-BOR	0.41	0.64	0.23	162.86	95.58	1.08
ANN	0.05	0.22	0.33	182.03	125.75	1.05
ANN-BOR	0.22	0.47	0.34	163.33	103.88	0.93
MLR	0.25	0.50	0.44	165.34	101.30	0.99
Mean	0.34	0.58	0.37	160.37	95.70	0.93
Median	0.41	0.64	0.46	156.05	91.55	0.92

Although the regression models for *Betula* tended to perform statistically better than the Poaceae regression models, it was seen that they did not accurately account for the main peak period, experiencing the same 1-day lag as seen before (Figure 4.9). The test data depicts a peak in *Betula* concentration on the 20th of April, whereas the models tended to predict a delayed peak on the 21st of April. Mimicking the same lag experienced by the Poaceae regression models. However, the addition of BOR feature selection did improve model performance, leading to increases in r^2 and decreases in error readings. SVM-BOR and median combined regression models were found to perform the best by describing the highest degree of variance, with r^2 values of 0.41 and the lowest of all error values. Average and median combined models were calculated from the models of each type with the highest r^2 and lowest errors. The median of the predicted results from the RF, MLR, SVM-BOR and ANN-BOR models ultimately predicted the *Betula* daily concentrations the best, outperforming the SVM-BOR model on the grounds of errors calculated. Comparisons of the differing forecast models are illustrated in Figure 4.9 and 4.10.

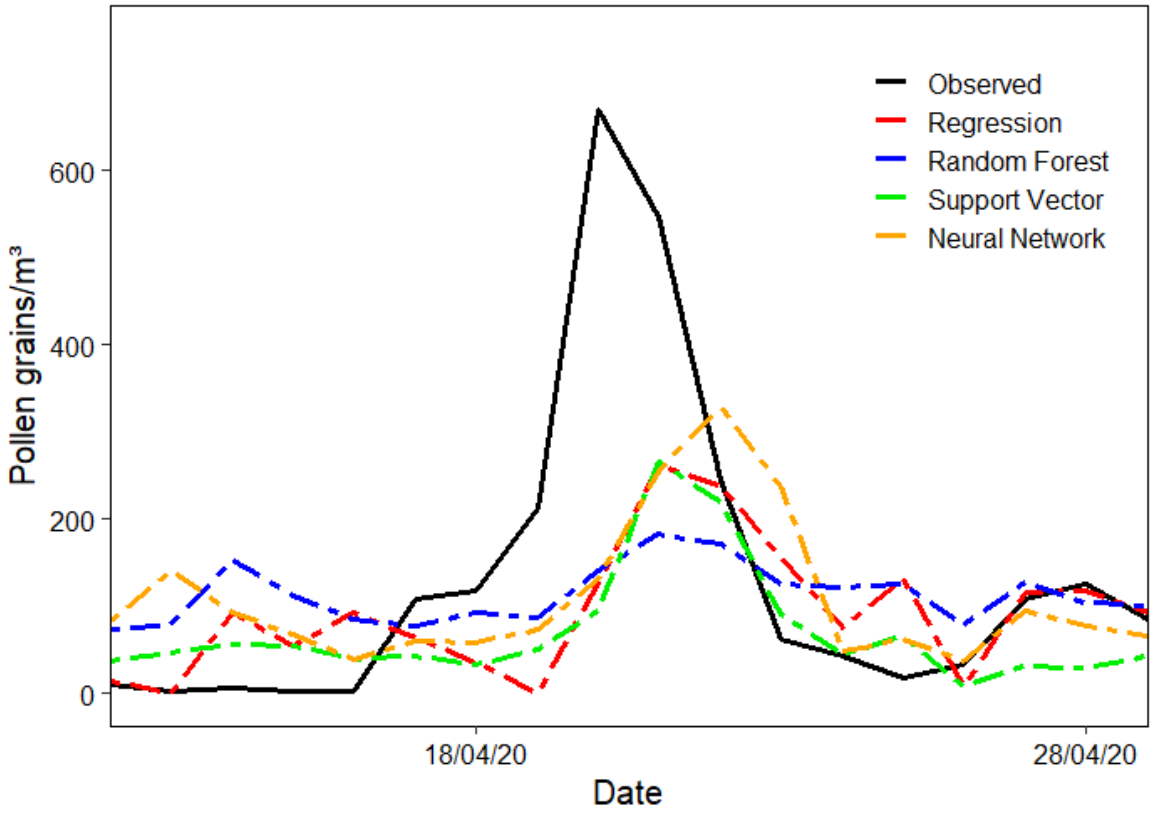

Figure 4.9: Comparison of regression models (MLR, RF, SVM-BOR, ANN-BOR) for prediction of daily Betula pollen concentrations

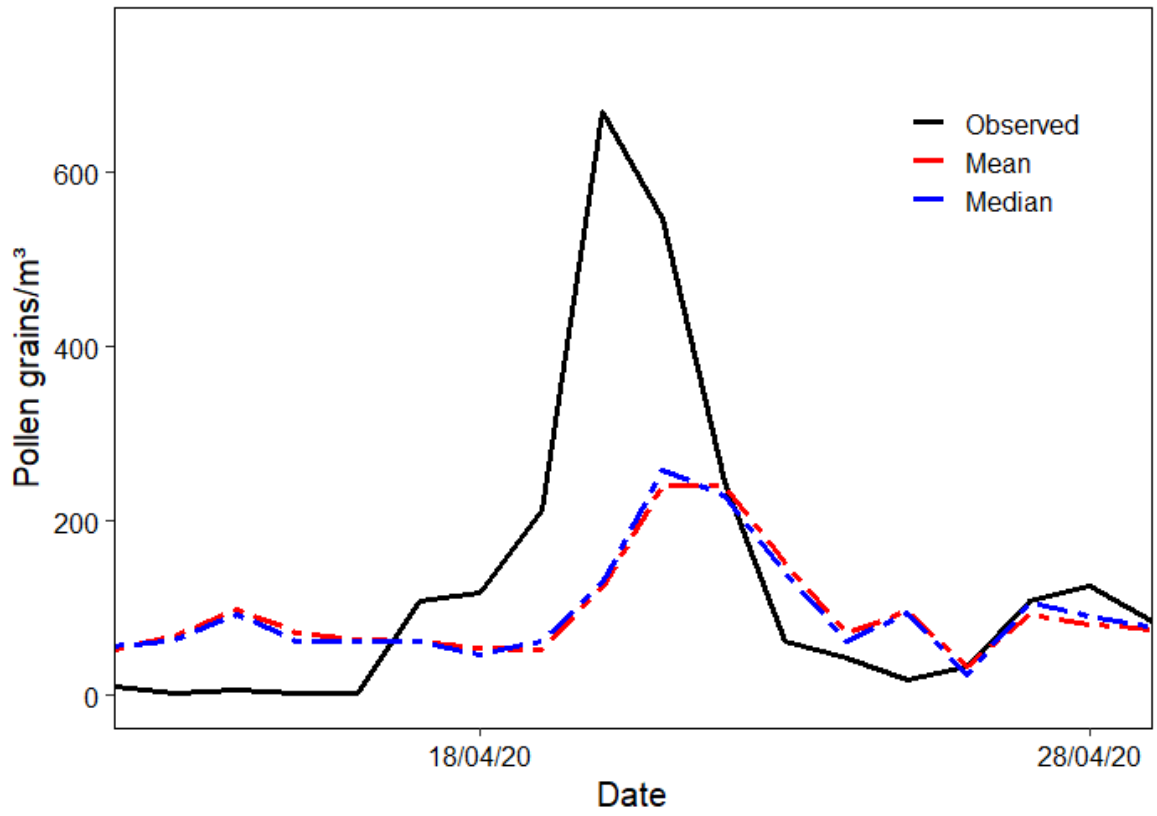

Figure 4.10: Comparison of Mean and Median regression model results for prediction of daily Betula pollen concentrations

Variable importance of the different model parameters was further investigated by examining the RF importance ratings and BOR feature selection shown in Figure 4.11. It was found that the average *Betula* concentration of the previous day was the single most important variable in the RF ranking. This was followed by the GDD above 2°C, the average temperature of the previous 10 days, maximum temperature, pressure, average rainfall over the previous 10 days, sunshine duration and relative humidity. For comparison purposes, the BOR results were also examined, further corroborating the importance of several of these parameters with the addition of GDD above 10°C and the tentative exclusion of relative humidity and rejection of sun duration.

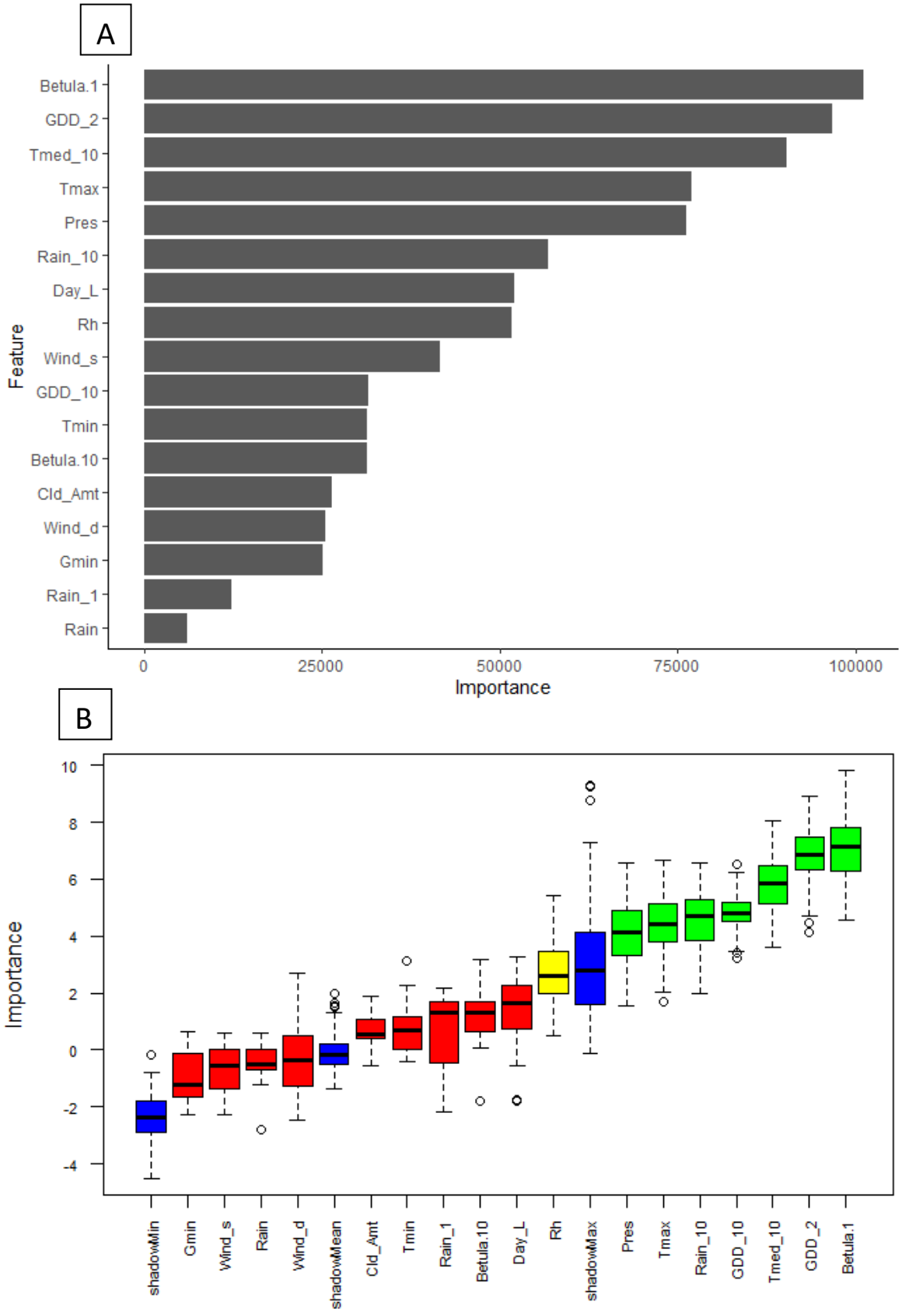

Figure 4.11: Variable importance of model parameters indicated by (A) RF model and (B) BOR feature selection methods - Betula

4.3.4 *Betula* models – Classification

Several RF, SVM and ANN classification models were also developed for *Betula* pollen. These were constructed using two sets of thresholds:

(i) 30T: Low >=0, High >=30 (Rough threshold based on allergic responses – literature)

(ii) UKT: Low >=0, Medium >=40, High >=80, Very High >=120 (UK Met office)

The different classification models were assessed by reviewing several metrics including model accuracy, kappa, sensitivity and. A summary of 30T and UKT models is described in tables 4.6 and 4.7.

Table 4.6: Model Accuracy and Kappa of Betula classification models

Model and Threshold	**Accuracy**	**Kappa**
RF 30	0.67	0
RF UK	0.39	0.23
SVM 30	0.61	-0.11
SVM UK	0.44	0.30
SVM-BOR 30	0.67	0
SVM-BOR UK	0.5	0.21
ANN 30	0.56	-0.2
ANN UK	0.44	0.23
ANN-BOR 30	0.61	-0.11
ANN-BOR UK	0.67	0.50

Table 4.7: Model Sensitivity and Specificity of Betula classification models

Model and Threshold	**Sensitivity**	**Specificity**
RF 30	0.67	0
RF UK: LOW	0.67	0.67
RF UK: MEDIUM	0.22	1.00
RF UK: HIGH	0.25	0.71
RF UK: VERY HIGH	1.00	0.88
SVM 30	0.64	0.00
SVM UK: LOW	0.29	0.91
SVM UK: MEDIUM	1.00	0.56
SVM UK: HIGH	0.40	0.85
SVM UK: VERY HIGH	0.50	1.00
SVM-BOR 30	0.67	0.00
SVM-BOR UK: LOW	0.44	1.00
SVM-BOR UK: MEDIUM	0.00	0.89
SVM-BOR UK: HIGH	0.00	0.72
SVM-BOR UK: VERY HIGH	1.00	0.88
ANN 30	0.63	0.00
ANN UK: LOW	1.00	0.55
ANN UK: MEDIUM	0.00	1.00
ANN UK: HIGH	0.4	1.00
ANN UK: VERY HIGH	0.75	0.92
ANN-BOR 30	0.65	0.00
ANN-BOR UK: LOW	1.00	0.73
ANN-BOR UK: MEDIUM	0.00	1.00
ANN-BOR UK: HIGH	0.40	0.92
ANN-BOR UK: VERY HIGH	1.00	0.93

On average, the majority of classification models for both thresholds performed worse than their Poaceae counterparts although the ANN-BOR UKT model performed slightly better than the best Poaceae UKT model. The most accurate model was witnessed for the UKT, this was also seen when evaluating the kappa values. Cohen's kappa statistic compares the observed accuracy of results to expected accuracy (random chance), a low value indicates no difference between the two, whereas a high value indicates a strong difference, and a negative value is interpreted as disagreement. The majority of kappa values for both the 30T and UKT models are very low, on average much lower than those seen for the Poaceae classification models which themselves were not very high (barely

exceeding 0.3). The only *Betula* model that surpasses this is the ANN-BOR model for the UKT, with a kappa value of 0.50 and an accuracy of 67%.

The 30T models all experienced similar accuracy readings of ~0.6, however, the kappa value indicated that these models performed just as well as random chance. The ability of these models to accurately classify results into the designated thresholds can be further examined from their sensitivity and specificity values. All 30T models exhibit specificity values of 0 – this can be translated as the lack of observed true negatives and that all readings in this class were registered as false positives. From examination of the confusion matrix of the RF model (joint best 30T model along with SVM-BOR), shown in Figure 4.12, it can be observed that issues arose when attempting to classify low levels of *Betula* pollen.

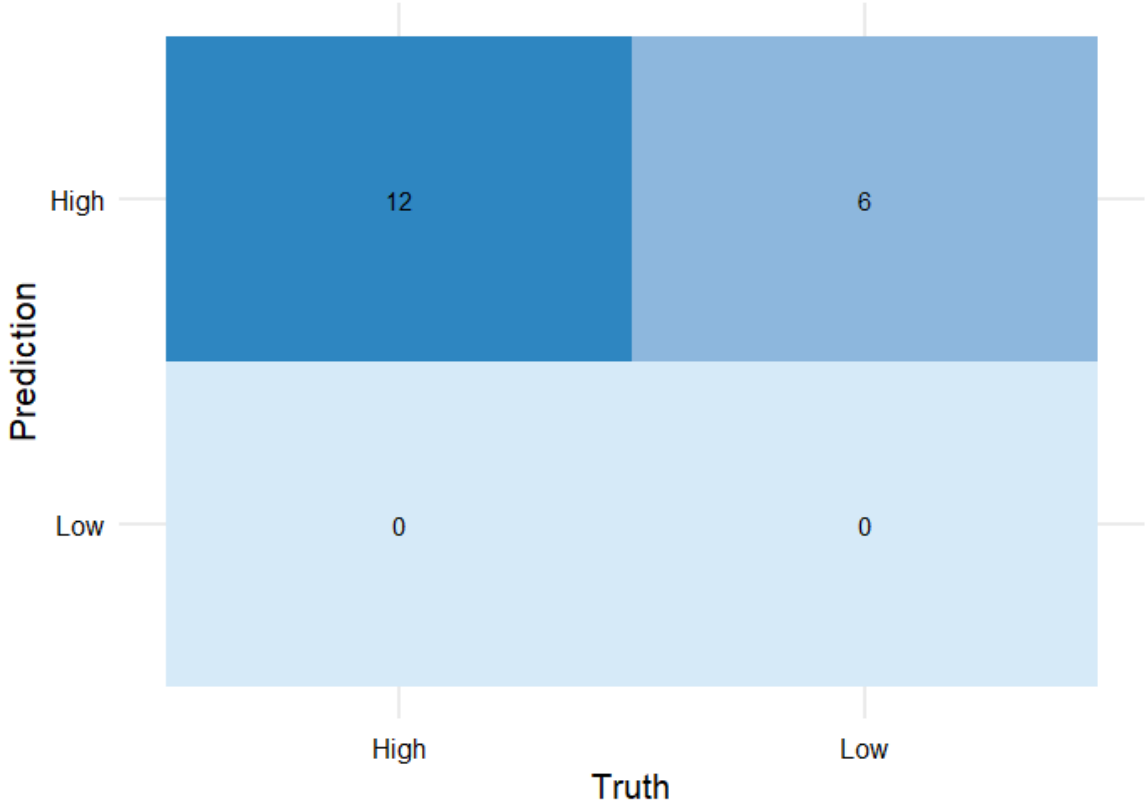

Figure 4.12: Confusion matrix of RF Betula model (30T)

In the case of the best-performing UKT model (ANN-BOR), multiple sensitivity and specificity values were calculated for all assigned classes. Similar to the UKT Poaceae models, the medium class gave a sensitivity value of 0, indicating no positive predicted results as shown in Figure 4.13. From further examination of the confusion matrix, it can be observed that although the model rather accurately predicts the low, high very high classes, it struggled to correctly determine days of medium concentration, leading to several false results. The only UKT model that accurately predicted this level was the SVM model, although this model struggled to assign other classes. All other confusion matrix results are provided in Appendix B (Figures B9-B16).

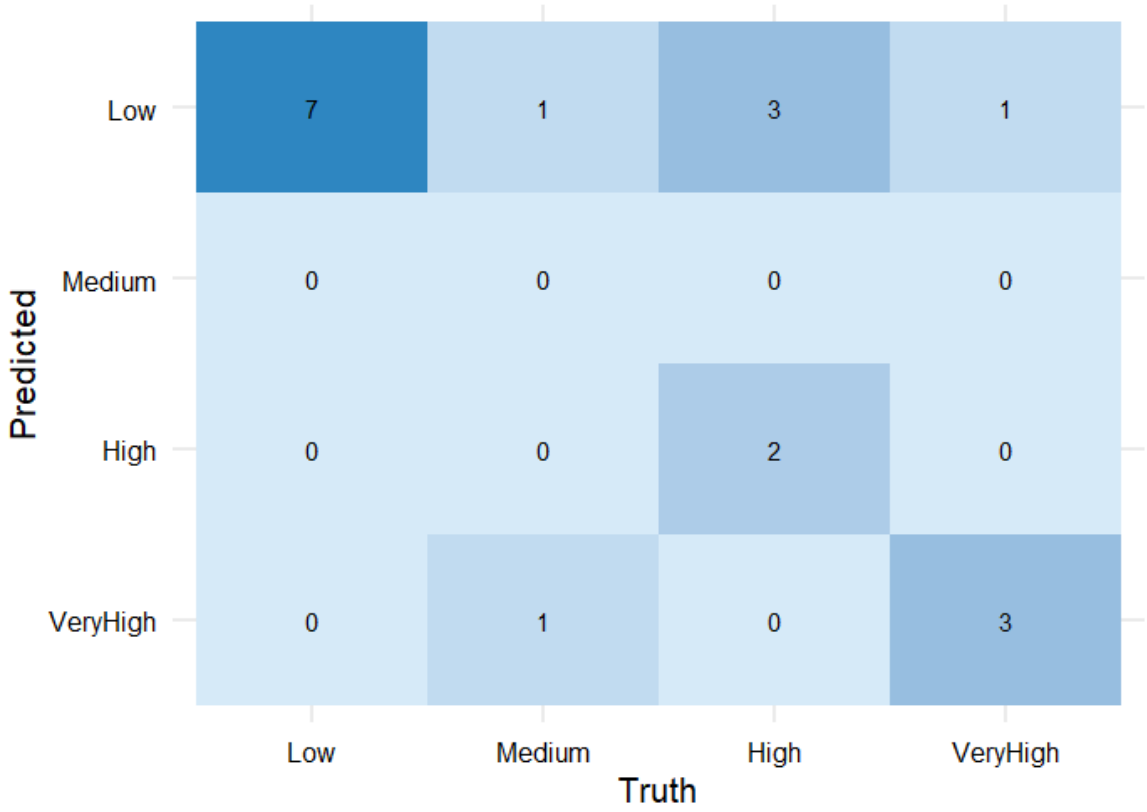

Figure 4.13: Confusion matrix of ANN-BOR Betula model (UKT)

Feature importance was also examined using both RF importance ratings and BOR results plots for feature selection, the results of which are summarised in Figures 4.14 and 4.15 for all threshold types. For the 30T model, RF identified GDD over 2°C as the most important variable, followed by GDD over 10°C, rainfall of the previous day, *Betula* concentrations of the preceding day and wind speed. BOR feature selection also identified the importance of all these parameters. In the case of the UKT models, RF measure of importance again identified the importance of previous day *Betula* concentrations, GDD above 2°C, average temperature of the previous 10 days, maximum temperature, average rainfall over the previous 10 days as well as degrees days above 10°C. The BOR further corroborated these findings for GDD and previous days' *Betula* concentration but classified the average rainfall of the previous day as more important and introduced the importance of the pressure variable while classifying maximum temperature as not important

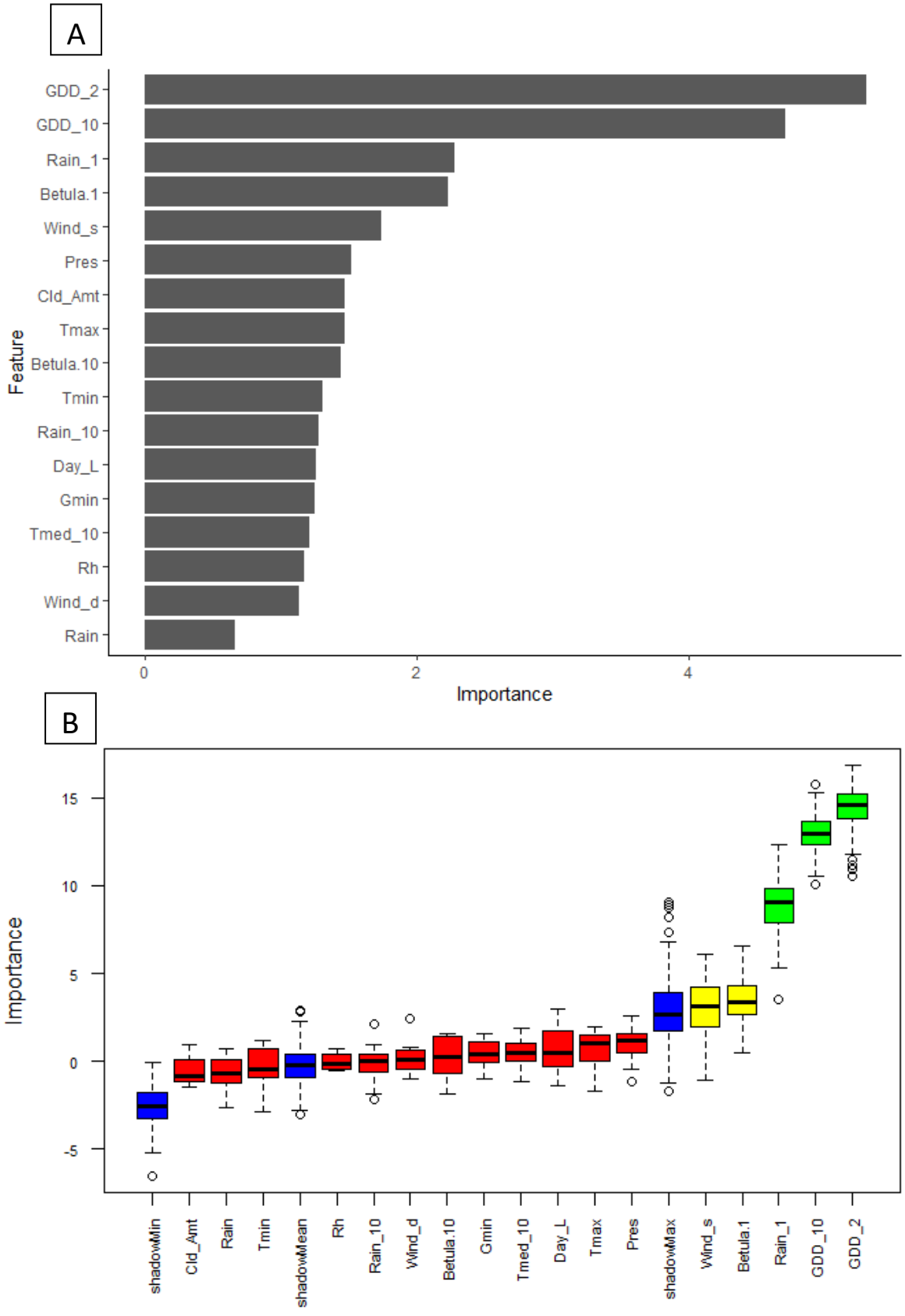

Figure 4.14: Variable importance of model parameters indicated by (A) RF model and (B) BOR feature selection methods for 30T models - Betula

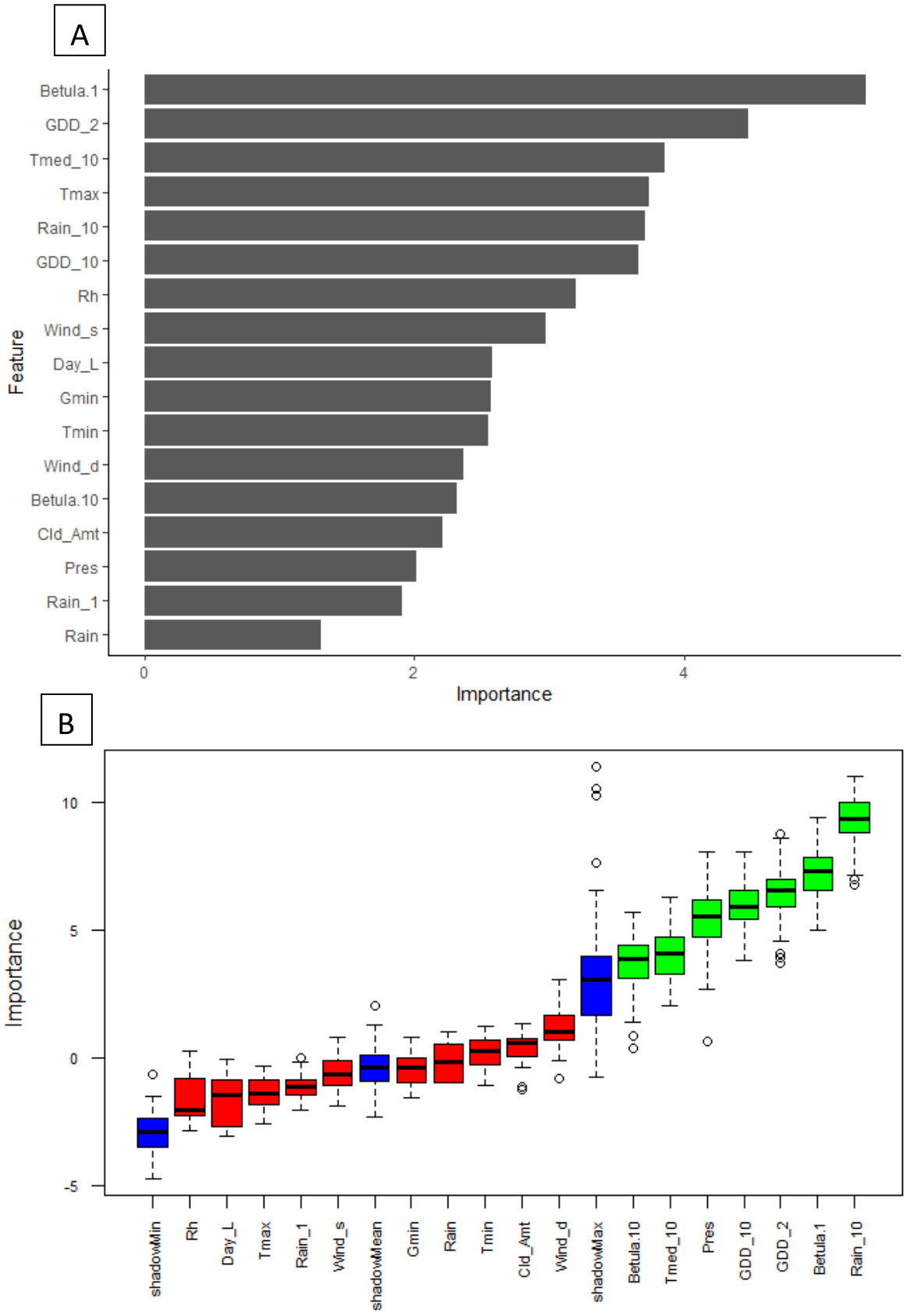

Figure 4.15: Variable importance of model parameters indicated by (A) RF model and (B) BOR feature selection methods for UKT models - Betula

4.4 Discussion

4.4.1 Evaluation of selected models

There are many benefits of monitoring ambient pollen concentrations, such as understanding seasonal/temporal trends and driving factors that promote pollen production and release. However, one of the primary applications of pollen monitoring is to develop pollen forecasting models. This is particularly the case for allergenic pollen taxa that pose risks to the public. In this case, it was decided to develop a number of preliminary regression and classification models to predict daily Poaceae and *Betula* concentrations, which represent the primary allergenic pollen taxa identified in Ireland.

Although modelling efforts before the commencement of this project were non-existent in Ireland, due to the lack of aerobiological studies, there is a unique benefit to this late establishment. The popularity of modelling techniques has varied throughout the decades and was initially dominated by regression methods due to more complex machine learning methods having not been fully established yet (Bringfelt et al., 1982; Galán et al., 1995; Goldberg et al., 1988; Jose María Maya-Manzano et al., 2021; Scheifinger et al., 2013; Vélez-Pereira et al., 2021). As the advent of more sophisticated and machine learning techniques commenced, a gradual decrease in regression techniques was observed. Machine learning methods are now favoured due to their robustness and lack of dependence on linear and normal aerobiological data (Vélez-Pereira et al., 2021). As such, Irish pollen networks are in the unique position to bypass these unfavourable modelling methods which was not possible for other long-established networks whose past modelling advancements were hindered by the computational power/methods available at the time.

Although SVM models have been the least documented in literature, they consistently outperformed several of the other models for the prediction of Poaceae and *Betula*. The best results for the 30T classification of Poaceae pollen were observed for the standard SVM model whereas the SVM-BOR offered the best performance for the UKT classification levels. In the case of *Betula*, SVM-BOR models performed best for *Betula* regression and 30T classification models.

It is generally expected that for locations with limited amounts of ambient pollen data, classification models tend to perform best – making it applicable to the limited data available for Dublin (2017-2020). However, to correctly determine suitable threshold levels for a particular allergenic pollen type, either sensitisation studies (Davies and Smith, 1973; Kiotseridis et al., 2013) and/or comparisons between ambient pollen concentrations and hospital/health data are required (Becker et al., 2021; Steckling-Muschack et al., 2021). However, due to the shortage of aerobiological studies in Ireland, this work has largely gone undone, and the adoption of previously established thresholds was required.

In UKT classification models for Poaceae and *Betula*, a consistent error in classifying medium level pollen concentrations was found, which has been found in similar studies also using RF, ANN and SVM models for the prediction of *Alnus* pollen seasonal trends (Novo-Lourés et al.,

2023). However, in this case, it could have arisen from unbalanced data as *Betula* training/testing data did not have many actual medium level values. Overall, this was the main reason for the majority of sensitivity related issues and is largely linked to the limited amounts of training data. The relatively good results recorded for SVM type models contrasts well with a similar studies conducted by Nowosad *et al.*, 2018, Voukantsis, Niska, *et al.*, 2010 and Novo-Lourés *et al.*, 2023 who found that SVM models were often outperformed by ANN and RF models for the prediction of Betulaceae (including *Alnus* and *Betula*) and Poaceae pollen. Although this is an interesting contrast to several of the well-performing SVM models presented here, it also further corroborates the performance of the RF Poaceae regression and *Betula* ANN-BOR UKT models that substantially outperformed other SVM models. These results could suggest the use of SVM models in pollen forecasting when only several years of data is available – although further study would be needed to corroborate this.

Similar analysis of the same pollen model types for Poaceae, Oleaceae and Urticaceae pollen concentration prediction, was also carried out in Greece. A total of 15 years of continuous data was used in that study (Voukantsis et al., 2010b). Once again, the SVM models for Poaceae were often outperformed by ANN and RF. It was in this case that, although all models performed reasonably well, it was the combined model of all predicted results that performed the best. This is reflective of the median *Betula* regression model seen here, which outperformed the other regression models examined.

Overall, the models constructed here performed reasonably well with the highest r^2 values achieved of 0.27 for Poaceae and 0.41 for *Betula* regression models and accuracies of 61-67% for Poaceae and 67% for *Betula* Classification models. This relatively lower r^2 value for Poacea regression models can partially be attributed to large variances in annual Poaceae pollen concentrations which has been found to impact the forecasting accuracy of such models (Lops et al., 2020). Although the majority of model performances were lower than many literature studies, this study's main goal was to investigate and compare different model types in hopes of establishing preliminary models that can be further improved and built upon as monitoring efforts progress. The r^2 results therefore showed similar ranges to other such preliminary studies (Nowosad et al., 2018).

Previous adaptions of preliminary models for Poaceae, *Betula* and *Alnus* pollen were also developed as part of the EPA POMMEL project (O'Connor et al., 2022). These models also encompassed several years of unpublished data used in the production of the pollen calendar in Chapter 3. In this current adaption, the decision was made to construct pollen models using only the currently available pollen data recorded in Dublin from 2017-2020. This is mainly due to differences in distance between the historical and modern sites ranging from 2-12km, as well as changes within the urban infrastructure and biodiversity of the city between the sampling years. Studies have found that relying on historical data can often overlook and omit changes in pollen seasonality and intensity (Addison-Smith et al., 2021; Anderegg et al., 2021), especially if large inconsistencies exist between the sampling years.

Pollen monitoring sites generate point measurements and, therefore can be considered as an approximation of the real-world situation (Bastl et al., 2023). The resulting observation models are site specific and experience the some of the same uncertainties described in section 3.4.1 relating to spatial and temporal variations. Observational models often cannot be applied to neighbouring regions (Jose María Maya-Manzano et al., 2021). However, it is not always achievable to intricately expand pollen monitoring networks. In such cases mathematical extrapolations and modelling can be used to predict pollen concentration in areas with no sampler using meteorological and landcover data (Lo et al., 2021; Oteros et al., 2019; della Valle et al., 2012). More representative city-wide forecasts can be developed in the future providing the inclusion of additional sampling points throughout the city, if future work shows significant spatial variations between sites due to local sources. As such, this city-wide network could provide more accurate forecasts if urban variations are observed.

4.4.2 Importance of certain model variables

The importance of model variables was also investigated for both regression and classification models. In both Poacea and *Betula* models, the importance of the previous day(s) pollen concentration was highlighted. This has been found in many other literature studies (Emmerson et al., 2022; Janati et al., 2017; Navares and Aznarte, 2017a) providing models with additional data regarding the pollen season and summarising the impact other variables had on pollen release during previous days (Novo-Lourés et al., 2023). The importance of other weather variable such as temperature, sunshine duration, relative humidity and wind speed were also noted and their importance to pollen release was also explained in previous chapters and extensively throughout literature (Fernández-Rodríguez et al., 2016; Laaidi, 2001). However, one interesting finding was the apparent influence of GDD in both Poaceae and *Betula* models, the inclusion of which has been highlighted previously (Lo et al., 2021; Nowosad, 2016). In the case of *Betula*, the dependence of model performance on GDD above 2°C, often trumped that of the previous day's pollen concentration. This high rank can be explained by the temperature stimulation needed by such trees before pollen release which requires consecutive daily temperatures above a certain base temperature (Dahl et al., 2013). A period of chilling followed by GDD above a certain temperature is also required to trigger the flowering phase of grasses (García-Mozo, 2017) adding credence to the importance placed on GDD above 10°C for the Poaceae models.

4.4.3 Feature selection

The forecasting of ambient pollen concentrations is reliant on the representable variables and the computational power available. Meteorological conditions, historical pollen records, air quality measurements, phenological observations as well as air-mass trajectory/transport parameters are all

but a broad classification of parameters that can be included or considered when creating a forecast model. As models become more complex and sophisticated it is important to consider the magnitude of inputs. High dimensional data often leads to complex models with a multitude of redundant relationships and uncertainty, not to mention the computational increase needed to run this algorithm (Navares and Aznarte, 2019). Feature selection is a popular method within data science that aims to aid and improve model performance by removing redundant variables (Kapadia and Jariwala, 2022; Li et al., 2017; Venkatesh and Anuradha, 2019). Although this might not be a big issue for the current model system, it might well become an issue in the future and might already be one for more seasoned aerobiological datasets elsewhere. Very few literature studies provide much detail on the feature selection process carried out (Navares and Aznarte, 2019, 2017b; Voukantsis et al., 2010b) with many using any available parameter (Brighetti et al., 2014), and those that do, often duplicate variables used in other studies or use "simple human judgement" (Emmerson et al., 2022).

The BOR feature selection method has gained popularity in other areas of data science (Chen et al., 2020) and ambient monitoring. Recently, the use of this method has been shown to improve the modelling of tropospheric ozone using ANN (Kapadia and Jariwala, 2022) and in the use of low-cost particulate matter sensors (Bulot et al., 2023). As a result, BOR was further extended to use in aerobiological studies during this investigation. The addition of the BOR feature selection step did not seem to offer much improvement for the forecasting of Poaceae pollen, only increasing classification model accuracy for SVM and ANN by up to 14 and 4%, respectively, for the UKT models. On the other hand, a more notable increase in performance was found for *Betula* models. Classification models experienced an increase of up to 6% and 23% for SVM and ANN models of both threshold types with regression models also exhibiting a slight increase in r^2. An increase in r^2 of 0.04 for SVM and 0.17 for ANN was noted for regression models, accompanied by a reduction of between 7-19 in RMSE. These preliminary results could indicate BOR as a suitable feature selection method in select aerobiological studies, following further testing.

The vast majority of pollen forecasting studies have evolved thanks to the extensive decades of monitoring data available in many countries. Ireland on the other hand has only commenced continuous monitoring as of 2017. The development of more specific forecast models is largely spurred on by the prevalence of allergic disease and respiratory conditions seen among the Irish public. Similar short-term studies (Emmerson et al., 2022; Lops et al., 2020; Nowosad et al., 2018) however, do exist such as a recent study conducted by Emmerson *et al.*, 2022 which developed several short-term daily airborne grass pollen forecasts in several locations around Australia. These forecasts and monitoring efforts were also motivated by public health concerns, having come into effect following the 2016 thunderstorm asthma event in Victoria (Australia). With such minimal amounts of data, these forecasting methods covering only several years of data can be considered a foundation for future work and will improve with each year and experience (Emmerson et al., 2022). A similar short-term study from the US, covering just 5 years of data also often found that peaks in

observed data were not always correctly predicted leading to the conclusion that in order to do so, the models need to be further trained with more consistent pollen and meteorological data as monitoring continues (Lops et al., 2020).

4.5 Conclusion

As is the case with much Irish aerobiological research – very little has been conducted historically in relation to modelling or forecasting pollen concentrations, with the meteorological service in Ireland getting potentially misrepresentative forecasts from the UK. Developing functional Poaceae and *Betula* forecasting systems for Dublin and other major cities/regions in Ireland is therefore of vital importance and would allow those suffering from allergies/asthma to take the necessary precautions.

In efforts to improve and commence pollen forecasting systems within Ireland, a series of popular regression and classification models were developed using several meteorological and phenological parameters to predict Poaceae and *Betula* pollen concentrations. Although only several years of continuous data are available for model training/testing, it is hoped that this work will instigate the future curation of operational forecasts with the addition of future years of pollen data.

Overall, the models constructed here performed reasonably well with the highest r^2 (and lowest error readings) values achieved of 0.27 for Poaceae RF and 0.41 for *Betula* Median regression models and percentage accuracies of 67/61% for Poaceae SVM (30T) /SVM-BOR (UKT) and 67/67% for *Betula* SVM-BOR (30T) /ANN-BOR (UKT) classification models. Regression models often experienced a lag of 1-day for high peak concentrations. This was found to be attributed to insufficient training data and is hoped to benefit from the future inclusion of monitoring data. As such, at this time, with limited data availability, it is recommended that classification models be used for Dublin.

These models represent some of the first Dublin pollen forecast models ever created (including those previously completed by the author in an EPA project report (O'Connor et al., 2022)). They represent an important preliminary step in aerobiological research in Ireland, as often some of the first application of aerobiological monitoring data is for forecasting purposes due to the valuable nature of the results for allergy sufferers. Furthermore, the inclusion of additional data will only aid in the accuracies of these preliminary models and act as a foundation for future forecasting efforts to build upon.

4.6 Future work

At present coarser predictions (classification models and pollen calendars) might be better for end users given the lack of extensive monitoring data. The inclusion of extended years of data will further improve the performance and applications of these initial models. Other future considerations for

model improvement could include the addition of other predictors such as factorised wind direction and spatial variables. The inclusion of additional staggered temporal variables such as lagged data could also further improve the performance and has been recommended after developing preliminary model methods (Nowosad et al., 2018). As such initial future work will aim to discover and include other representable parameters that are able to capture more variance in pollen data. This will be a big task to undertake, especially when considering other feature selection and model methods that could be used. Due to the influence that pollen from the UK has on the concentration of some allergenic pollen that reaches Dublin (eg. *Betula*), transport models and/or the inclusion of air mass trajectories into models could help to account for this. In addition, due to the varying meteorological impacts noted for different parts of the MPS (explained in Chapter 3), future work would also benefit from creating models that account for pollen concentrations at different times within their season eg. PRP Poaceae/*Betula* models which accounts for pollen release and dispersal and PSP models that account for continued release and resuspension impacts. Additional pollen types and fungal spores could also be investigated for forecasting, including other allergenic Betulaceae pollen (*Alnus* and *Corylus*) and fungal spores of allergenic/agricultural concern such as *Cladosporium* and *Alternaria*. Now that the aerobiological research team in DCU is working closely with collaborators in Met Éireann, additional support will be available from their modelling department, who are currently responsible for the entire island's weather and marine forecasts. This will be an invaluable resource and is likely to propel pollen forecasting advancements in the coming years.

References

Aboulaich, N., Achmakh, L., Bouziane, H., Trigo, M.M., Recio, M., Kadiri, M., Cabezudo, B., Riadi, H., Kazzaz, M., 2013. Int. J. Biometeorol. 57, 197–205.

Adams-Groom, B., Ambelas Skjøth, C., Selby, K., Pashley, C., Satchwell, J., Head, K., Ramsay, G., 2020. Allergy 75, 1492–1494.

Addison-Smith, B., Milic, A., Dwarakanath, D., Simunovic, M., Van Haeften, S., Timbrell, V., Davies, J.M., 2021. Front. Allergy 2, 1–10.

Anderegg, W.R.L., Abatzoglou, J.T., Anderegg, L.D.L., Bielory, L., Kinney, P.L., Ziska, L., 2021. Proc. Natl. Acad. Sci. U. S. A. 118, 1–6.

Bastl, M., Bastl, K., Dirr, L., Berger, M., Berger, U., 2023. Allergo J. Int. 32, 162–166.

Becker, J., Steckling-Muschack, N., Mittermeier, I., Bergmann, K.C., Böse-O'Reilly, S., Buters, J., Damialis, A., Heigl, K., Heinrich, J., Kabesch, M., Mertes, H., Nowak, D., Schutzmeier, P., Walser-Reichenbach, S., Weinberger, A., Korbely, C., Herr, C., Heinze, S., Kutzora, S., 2021. Aerobiologia (Bologna). 37, 633–662.

Bogawski, P., Grewling, Ł., Jackowiak, B., 2019. Sci. Total Environ. 658, 1485–1499.

Bousquet, P.J., Hooper, R., Kogevinas, M., Jarvis, D., Burney, P., Chinn, S., Luezynska, C., Vermeire, P., Kesteloot, H., Bousquet, J., Nowak, D., Prichard, J., de Marco, R., Rijcken, B., Anto, J.M., Alves, J., Boman, G., Abramson, M., Kutin, J., van Bastelaer, F., Neukirch, F., Liard, R., Pin, I., Pison, C., Taytard, A., Magnussen, H., Erich Wichmann, H., Heinrich, J., Gislason, T., Gislason, H.D., Prichard, J., Phil, D., Allwright, S., MacLeod, D., Bugiani, M., Bucca, C., Romano, C., de Marco, R., Cascio, V. Lo, Campello, C., Marinoni, A., Cerveri, I., Casali, L., Kremer, A.M., Crane, J., Lewis, S., Gulsvik, A., Omenaas, E., Sunyer, J., Burgos, F., Tech, R., Castellsague, J., Roca, J., Soriano, J., Tobias, A., Muniozguren, N., Ramos-Gonzalez, J., Capelastegui, A., Castillo, J., Rodriguez-Portal, J., Martinez-Moratalla, J., Almar-Marqnes, E., Maldonado-Pérez, J., Pereira, A., Sfinchez-Ramos, J., Quiros, R., Huerta, I., Payo-Losa, F., Boman, G., Janson, C., Björnsson, E., Rosenhall, L., Norrman, E., Lundbgck, B., Lindholm, N., Plaschke, P., Ackermann-Liebrich, U., Künzli, N., Perruchoud, A., Burr, M., Layzell, J., Russell Hall, B., Harrison, B., Stark, J., Sonia Buist, A., Vollmer, W.M., Osborne, M.L., 2007. Clin. Exp. Allergy 37, 780–787.

Breiman, L., 2001. Mach. Learn. 45, 5–32.

Breiman, L., Cutler, A., Liaw, A., Wiener, M., 2022. Package ‘randomForest’ October: Breiman and Cutler’s Random Forests for Classification and Regression.

Brighetti, M.A., Costa, C., Menesatti, P., Antonucci, F., Tripodi, S., Travaglini, A., 2014. Aerobiologia (Bologna). 30, 25–33.

Bringfelt, B., Engström, I., Nilsson, S., 1982. Grana 21, 59–64.

Bulot, F.M.J., Russell, H.S., Rezaei, M., Johnson, M.S., Ossont, S.J., Morris, A.K.R., Basford, P.J., Easton, N.H.C., Mitchell, H.L., Foster, G.L., Loxham, M., Cox, S.J., 2023. Sensors (Basel). 23, 1–29.

Burbach, G.J., Heinzerling, L.M., Edenharter, G., Bachert, C., Bindslev-Jensen, C., Bonini, S., Bousquet, J., Bousquet-Rouanet, L., Bousquet, P.J., Bresciani, M., Bruno, A., Canonica, G.W., Darsow, U., Demoly, P., Durham, S., Fokkens, W.J., Giavi, S., Gjomarkaj, M., Gramiccioni, C., Haahtela, T., Kowalski, M.L., Magyar, P., Muraközi, G., Orosz, M., Papadopoulos, N.G., Röhnelt, C., Stingl, G., Todo-Bom, A., Von Mutius, E., Wiesner, A., Wöhrl, S., Zuberbier, T., 2009. Allergy Eur. J. Allergy Clin. Immunol. 64, 1507–1515.

Buscardo, E., Smith, G.F., Kelly, D.L., Freitas, H., Iremonger, S., Mitchell, F.J.G., O’Donoghue, S., McKee, A.M., 2008. Biodivers. Conserv. 17, 1057–1072.

Calle, M.L., Urrea, V., 2011. Brief. Bioinform. 12, 86–89.

Cariñanos, P., Ruiz-Peñuela, S., Valle, A.M., de la Guardia, C.D., 2020. Sci. Total Environ. 737,

139722.

Chan, J.Y. Le, Leow, S.M.H., Bea, K.T., Cheng, W.K., Phoong, S.W., Hong, Z.W., Chen, Y.L., 2022. Mathematics 10.

Chen, R.C., Dewi, C., Huang, S.W., Caraka, R.E., 2020. J. Big Data 7.

Corsico, R., 1993. L'asthme allergique en Europe, in: Spieksma, F.T.M., Nolard, N., Frenguelli, G., Van Moerbeke, D. (Eds.), Pollen de l'air En Europe. UCB, Braine-l'Alleud, pp. 19–29.

Csépe, Z., Leelőssy, Mányoki, G., Kajtor-Apatini, D., Udvardy, O., Péter, B., Páldy, A., Gelybó, G., Szigeti, T., Pándics, T., Kofol-Seliger, A., Simčič, A., Leru, P.M., Eftimie, A.M., Šikoparija, B., Radišić, P., Stjepanović, B., Hrga, I., Večenaj, A., Vucić, A., Peroš-Pucar, D., Škorić, T., Ščevková, J., Bastl, M., Berger, U., Magyar, D., 2020. Aerobiologia (Bologna). 36, 131–140.

Dahl, Å., Galán, C., Hajkova, L., Pauling, A., Sikoparija, B., Smith, M., Vokou, D., 2013. The Onset, Course and Intensity of the Pollen Season, in: ThereSofiev, M., Bergmann, K.-C. (Eds.), Allergenic Pollen. Springer Netherlands, Dordrecht, pp. 29–70.

Daoud, J.I., 2018. J. Phys. Conf. Ser. 949.

Davies, R.R., Smith, L.P., 1973. Clin. Allergy 3, 263–7.

Department of Agriculture Food and the Marine, 2020. Afforestation Scheme 2014-2020 [WWW Document]. Afforestation Scheme 2014-2020. URL Improving the genetic quality of Irish Birch and Alder.

Du, J., Liu, Y., Yu, Y., Yan, W., 2017. Algorithms 10.

Ebrahimi-Khusfi, Z., Nafarzadegan, A.R., Dargahian, F., 2021. Ecol. Indic. 125, 107499.

Emmerson, K.M., Addison-Smith, E., Ebert, E., Milic, A., Vicendese, D., Lampugnani, E.R., Erbas, B., Medek, D.E., Huete, A., Beggs, P., Katelaris, C.H., Haberle, S.G., Newbigin, E., Davies, J.M., 2022. Atmos. Environ. X 15, 100183.

Fernández-Rodríguez, S., Durán-Barroso, P., Silva-Palacios, I., Tormo-Molina, R., Maya-Manzano, J.M., Gonzalo-Garijo, Á., 2016. Nat. Hazards 84, 121–137.

Frei, T., Leuschner, R.M., 2000. Aerobiologia (Bologna). 16, 407–416.

Fritsch, S., Wright, M. V., Suling, M., Mueller, S.M., 2019. Package 'neuralnet': Training of Neural Networks.

Galán, C., Ariatti, A., Bonini, M., Clot, B., Crouzy, B., Dahl, A., Fernandez-González, D., Frenguelli, G., Gehrig, R., Isard, S., Levetin, E., Li, D.W., Mandrioli, P., Rogers, C.A., Thibaudon, M., Sauliene, I., Skjoth, C., Smith, M., Sofiev, M., 2017. Aerobiologia (Bologna). 33, 293–295.

Galán, C., Cariñanos, P., Alcázar, T., Domínguez-Vilches, E., 2007. Spanish Aerobiology Network (REA): management and quality manual, Servicio de publicaciones de la Universidad de Córdoba.

Galán, C., Emberlin, J., Domínguez, E., Bryant, R.H., Villamandos, F., 1995. Grana 34, 189–198.

García-Mozo, H., 2017. Allergy Eur. J. Allergy Clin. Immunol. 72, 1849–1858.

Goldberg, C., Buch, H., Moseholm, L., Weeke, E.R., 1988. Grana 27, 209–217.

González, C., Mira-McWilliams, J., Juárez, I., 2015. IET Gener. Transm. Distrib. 9, 1120–1128.

Heinzerling, L., Frew, A.J., Bindslev-Jensen, C., Bonini, S., Bousquet, J., Bresciani, M., Carlsen, K.H., Van Cauwenberge, P., Darsow, U., Fokkens, W.J., Haahtela, T., Van Hoecke, H., Jessberger, B., Kowalski, M.L., Kopp, T., Lahoz, C.N., Lodrup Carlsen, K.C., Papadopoulos, N.G., Ring, J., Schmid-Grendelmeier, P., Vignola, A.M., Wöhrl, S., Zuberbier, T., 2005. Allergy Eur. J. Allergy Clin. Immunol. 60, 1287–1300.

Janati, A., Bouziane, H., del Mar Trigo, M., Kadiri, M., Kazzaz, M., 2017. Aerobiologia (Bologna). 33, 517–528.

Kapadia, D., Jariwala, N., 2022. Model. Earth Syst. Environ. 8, 2183–2192.

Katelaris, C.H., Burke, T. V., Byth, K., 2004. Ann. Allergy, Asthma Immunol. 93, 131–136.

Kiotseridis, H., Cilio, C.M., Bjermer, L., Tunsäter, A., Jacobsson, H., Dahl, Å., 2013. Clin. Transl. Allergy 3, 1–12.

Kursa, M.B., 2022. 1–17.

Laaidi, M., 2001. Int. J. Biometeorol. 45, 1–7.

Li, J., Cheng, K., Wang, S., Morstatter, F., Trevino, R.P., Tang, J., Liu, H., 2017. ACM Comput. Surv. 50.

Liu, X., Wu, D., Zewdie, G.K., Wijerante, L., Timms, C.I., Riley, A., Levetin, E., Lary, D.J., 2017. Environ. Health Insights 11, 117863021769939.

Lo, F., Bitz, C.M., Hess, J.J., 2021. Sci. Total Environ. 773, 145590.

Lops, Y., Choi, Y., Eslami, E., Sayeed, A., 2020. Neural Comput. Appl. 32, 11827–11836.

Max, A., Wing, J., Weston, S., Williams, A., Keefer, C., Engelhardt, A., Cooper, T., Mayer, Z., Ziem, A., Scrucca, L., Hunt, T., Kuhn, M.M., 2023. Package ‘ caret ’ : Classification and Regression Training.

Maya-Manzano, J.M., Skjøth, C.A., Smith, M., Dowding, P., Sarda-Estève, R., Baisnée, D., McGillicuddy, E., Sewell, G., O’Connor, D.J., 2021. Agric. For. Meteorol. 298–299, 108298.

Maya-Manzano, Jose María, Smith, M., Markey, E., Hourihane Clancy, J., Sodeau, J., O´Connor, D.J., 2021. Grana 60, 1–19.

Meyer, D., Dimitriadou, E., Hornik, K., Leisch, F., Weingessel, A., Meyer, D., Weingessel, A., Dimitriadou, E., Hornik, K., Leisch, F., Weingessel, A., Meyer, D., Weingessel, A., 2022. e1071: Misc Functions of the Department of Statistics, Probability Theory Group (Formerly: E1071), TU Wien. R Packag. version 1.7-12.

Movérare, R., Kosunen, T.U., Haahtela, T., 2006. J. Investig. Allergol. Clin. Immunol. 16, 274–278.

Muzalyova, A., Brunner, J.O., Traidl-Hoffmann, C., Damialis, A., 2021. Aerobiologia (Bologna). 37, 425–446.

Nae, A., Hinchion, K., Keogh, I.J., 2021. World J. Otorhinolaryngol. - Head Neck Surg. 7, 338–343.

Næs, T., Mevik, B.H., 2001. J. Chemom. 15, 413–426.

Navares, R., Aznarte, J.L., 2017a. Int. J. Biometeorol. 61, 647–656.

Navares, R., Aznarte, J.L., 2017b. Sci. Total Environ. 579, 1161–1169.

Navares, R., Aznarte, J.L., 2019. Theor. Appl. Climatol.

Novo-Lourés, M., Fernández-González, M., Pavón, R., Espinosa, K.C.S., Laza, R., Guada, G., Méndez, J.R., Fdez-Riverola, F., Rodríguez-Rajo, F.J., 2023. Forests 14.

Nowosad, J., 2016. Int. J. Biometeorol. 60, 843–855.

Nowosad, J., Stach, A., Kasprzyk, I., Chłopek, K., Dąbrowska-Zapart, K., Grewling, Ł., Latałowa, M., Pędziszewska, A., Majkowska-Wojciechowska, B., Myszkowska, D., Piotrowska-Weryszko, K., Weryszko-Chmielewska, E., Puc, M., Rapiejko, P., Stosik, T., 2018. Aerobiologia (Bologna). 34, 301–313.

O'Connor, D., Markey, E., Maya-manzano, J.M., Dowding, P., Donnelly, A., Sodeau, J., 2022. Pollen Monitoring and Modelling (POMMEL).

Oh, J.-W., 2018. Pollen Allergy a Chang. World.

Osborne, N.J., Alcock, I., Wheeler, B.W., Hajat, S., Sarran, C., Clewlow, Y., McInnes, R.N., Hemming, D., White, M., Vardoulakis, S., Fleming, L.E., 2017. Int. J. Biometeorol. 61, 1837–1848.

Oteros, J., Bergmann, K.C., Menzel, A., Damialis, A., Traidl-Hoffmann, C., Schmidt-Weber, C.B., Buters, J., 2019. Atmos. Environ. 199, 435–442.

Piotrowska, K., 2012. Grana 51, 263–269.

Puc, M., 2012. Int. J. Biometeorol. 56, 395–401.

Ripely, B., Venables, B., Douglas, B.M., Hornik, K., Gebhardt, A., Firth, D., 2023. Package 'MASS': Functions and datasets to support Venables and Ripley, ``Modern Applied Statistics with S'' (4th edition, 2002).

Robichaud, A., Comtois, P., 2017. Aerobiologia (Bologna). 33, 529–554.

Rodríguez-Rajo, F.J., Astray, G., Ferreiro-Lage, J.A., Aira, M.J., Jato-Rodriguez, M. V., Mejuto, J.C., 2010. Neural Networks 23, 419–425.

Sadyś, M., Strzelczak, A., Grinn-Gofroń, A., Kennedy, R., 2015. Int. J. Biometeorol. 59, 25–36.

Sánchez-Mesa, J.A., Galan, C., Martínez-Heras, J.A., Hervás-Martínez, C., 2002. Clin. Exp. Allergy 32, 1606–1612.

Sánchez Mesa, J.A., Galán, C., Hervás, C., 2005. Int. J. Biometeorol. 49, 355–362.

Scheifinger, H., Belmonte, J., Buters, J., Celenk, S., Damialis, A., Dechamp, C., García-Mozo, H., Gehrig, R., Grewling, L., Halley, J.M., Hogda, K.-A., Jäger, S., Karatzas, K., Karlsen, S.-R., Koch, E., Pauling, A., Peel, R., Sikoparija, B., Smith, M., Galán-Soldevilla, C., Thibaudon, M., Vokou, D., de Weger, L.A., 2013. Monitoring, Modelling and Forecasting of the Pollen Season, in: Allergenic Pollen. Springer Netherlands, Dordrecht, pp. 71–126.

Šikoparija, B., Marko, O., Panić, M., Jakovetić, D., Radišić, P., 2018. Aerobiologia (Bologna). 34, 203–217.

Skjøth, C.A., Šikoparija, B., Jäger, S., EAN-Network, 2013. Pollen Sources, in: Allergenic Pollen. Springer Netherlands, Dordrecht, pp. 9–27.

Steckling-Muschack, N., Mertes, H., Mittermeier, I., Schutzmeier, P., Becker, J., Bergmann, K.C., Böse-O′Reilly, S., Buters, J., Damialis, A., Heinrich, J., Kabesch, M., Nowak, D., Walser-Reichenbach, S., Weinberger, A., Zamfir, M., Herr, C., Kutzora, S., Heinze, S., 2021. Aerobiologia (Bologna). 37, 395–424.

Teagasc, 2022. Irish Birch and Alder Improvement Programme [WWW Document]. Improv. Genet. Qual. Irish Birch Alder. URL https://www.teagasc.ie/crops/forestry/research/irish-birch-and-alder-improvement-programme/

The Irish National Meteorological Service [WWW Document], 2023. URL https://www.met.ie/climate/available-data/daily-data (accessed 9.12.23).

della Valle, C.T., Triche, E.W., Bell, M.L., 2012. Int. J. Biometeorol. 56, 183–194.

Vapnik, V., 2000. The Nature of Statistical Learning Theory, second. ed. Springer, New York.

Vélez-Pereira, A.M., De Linares, C., Belmonte, J., 2021. Sci. Total Environ. 795.

Vélez-Pereira, A.M., De Linares, C., Canela, M.-A., Belmonte, J., 2019. Int. J. Biometeorol. 63,

1541–1553.

Venkatesh, B., Anuradha, J., 2019. Cybern. Inf. Technol. 19, 3–26.

Voukantsis, D., Karatzas, K.D., Damialis, A., Vokou, D., 2010a. Forecasting airborne pollen concentration of Poaceae (Grass) and Oleaceae (Olive), using Artificial Neural Networks and Genetic algorithms, in Thessaloniki, Greece, in: The 2010 International Joint Conference on Neural Networks (IJCNN). IEEE, pp. 1–6.

Voukantsis, D., Niska, H., Karatzas, K., Riga, M., Damialis, A., Vokou, D., 2010b. Atmos. Environ. 44, 5101–5111.

Warm, K., Lindberg, A., Lundbäck, B., Rönmark, E., 2013. Allergy, Asthma Clin. Immunol. 9, 1–8.

de Weger, L.A., Beerthuizen, T., Hiemstra, P.S., Sont, J.K., 2014. Int. J. Biometeorol. 58, 1047–55.

de Weger, L.A., Bergmann, K.C., Rantio-Lehtimäki, A., Dahl, Å., Buters, J., Déchamp, C., Belmonte, J., Thibaudon, M., Cecchi, L., Besancenot, J.-P., Galán, C., Waisel, Y., 2013. Impact of Pollen, in: Allergenic Pollen. Springer Netherlands, Dordrecht, pp. 161–215.

Zhang, Y., Bielory, L., Cai, T., Mi, Z., Georgopoulos, P., 2015. Atmos. Environ. 103, 297–306.

Chapter 5: Evaluation of a Real-time Fluorescence Sensor for Pollen Detection

5.1 Introduction

With the increasing prevalence of seasonal allergies and the labour-intensive and time-consuming laboratory processes needed to analyse the samples collected by the Hirst device, there is now a greater need for more timely aerobiological data. This has led to the increase in real-time monitoring device, as previously summarised in Chapter 1.

There are currently a wide variety of such devices commercially available that operate using fluorescent and/or optical principals (Tummon et al., 2021a). The use of real-time devices offers several improvements over the traditional Hirst volumetric method. For one, data is typically available at much higher time resolutions in real-time or near-real-time and significantly reduces the intensive preparation, counting and identification processes needed for the Hirst. Through this efficient monitoring and dissemination of airborne pollen data, information can be provided to relevant stakeholders/medical sectors in a timelier manner. This could lead to improvements in the prevention and treatment of allergy-related conditions and thus reduce the burden on health systems (Clot et al., 2020). The inclusion of near-real-time pollen measurements is also expected to improve current forecasting tools (Sofiev, 2019), making more representable forecasts available to medical professionals and allergy sufferers so that immediate care can be taken and periods of high exposure can be avoided. Recently, another unexpected improvement of real-time devices was noted amid the COVID-19 pandemic. During periods of lockdown, it was often difficult to maintain Hirst instruments as a result of restrictions and building closures, an issue that is not seen with automatic instruments as do not require weekly manual resets (Tummon et al., 2021b) and data is often available externally through servers.

The availability and reliability of these automatic techniques give way to other areas of study, that typically, were unachievable for traditional methods, including the analysis of indoor air quality. Real-time devices have the potential to monitor other bioaerosols aside from pollen, such as fungal spores, bacteria and potentially viruses and aerosols exuded by individuals, making it applicable to monitoring air quality and potential contaminants in healthcare and other sterile environments (Fennelly et al., 2023, 2022, 2021; Walshe et al., 2021). Aside from this, such high-resolution data for pollen and other PBAP could also improve research efforts in other fields such as investigating the contribution and impact of PBAP on the hydrological cycle/radiative forcing and agricultural studies studying the spread of invasive plant species and diseases etc.

This chapter outlines the deployment and evaluation of one such device for pollen monitoring. The WIBS-NEO was selected for this campaign. As previously discussed in Chapter 1, the WIBS has been used extensively to monitor ambient bioaerosol concentrations in a range of different outdoor and indoor environments, including several Irish field campaigns and lab studies (Healy et al., 2012a, 2012b, 2014; O'Connor et al., 2013, 2014a). Field studies within Ireland have largely been limited to less complex environments with high bioaerosol concentrations such as

national parks and bio-waste sites. Nevertheless, these studies have highlighted the potential of the WIBS to detect ambient bioaerosols when compared to traditional volumetric sampling methods (O'Connor et al., 2014a). Laboratory studies using the WIBS-4 (now surpassed by the WIBS-NEO) have also illustrated the potential for the WIBS to discriminate between pollen grains and fungal spores, as well as other bioaerosols and aerosols of non-biological origin (Healy et al., 2012a). In efforts to determine the suitability of this device to specifically detect pollen grains in more complex urban environments, the WIBS was deployed at the Dublin sampling site during a sampling campaign in 2019.

5.2 Methods

5.2.1 Site and instrumentation

Monitoring took place over 41 days (from 07/08/2019 12:00 – 16/09/2019 12:00) at the Dublin sampling site, situated on the roof of the former TU Dublin Kevin Street campus in Dublin city centre.

The WIBS-NEO was concurrently located a satisfactory distance away from Hirst volumetric sampler, to allow comparison of the results. The WIBS recorded particle counts and details of both fluorescent and non-fluorescent particles sampled during the campaign. Details regarding a particle's size, shape (AF) and fluorescence intensity in each of the 3 fluorescent channels was recorded. This was later compared to the pollen concentrations optically identified.

More detail on the specific operation of either instrument can be found in Chapter 2 (Methods).

5.2.2 WIBS data analysis

A summary of the operation of the WIBS during this campaign is provided below, more detailed information on the specific monitoring principles deployed by the WIBS is given in Chapter 2. Particles detected by the WIBS-NEO were categorised as fluorescent or non-fluorescent based on a predetermined fluorescent threshold (force trigger mode). The WIBS was placed into forced trigger mode daily to ensure no large variations in baseline fluorescence were detected.

Upon determination of the fluorescent fraction, the particles were further categorised utilising the Perring nomenclature (Perring et al., 2015). This annotation system categorizes fluorescent particles into one of seven types based on their fluorescent characteristics in each channel. These categories consider each channel individually (FL1, FL2 and FL3) and all possible combinations.

Various size and fluorescence filters were applied to WIBS particles to extract a representative fraction of the observed FAPs indicative of pollen grains. A Pearson correlation test was then used to calculate the degree and significance of correlation between the isolated WIBS particles and pollen concentrations registered by the Hirst using the nortest (Gross and Ligges, 2015) and corrplot (Gross and Ligges, 2015) packages within R (R Core Team 2017).

5.2.3 Meteorological and air quality data

Meteorological data was obtained from the Met Éireann website ("The Irish National Meteorological Service," 2023). Dublin Weather data was obtained from the weather station at Dublin Airport (53°21'49" N, 06°20'59'' W). The available parameters were: mean temperature [ºC] (Tmed), maximum temperature [ºC] (Tmax) and minimum temperature [ºC] (Tmin), grass minimum

temperature [ºC], 2 cm above the ground (Gmin), mean 10cm soil temperature [ºC] (Soil), precipitation amount [mm] (Rain), mean cbl pressure [hpa] (Pres), mean wind speed [kt] (Wind_s) and wind direction at max 10 min mean [deg] (Wind_d), global radiation [J/cm^2] (G_rad), sunshine duration [hours] (Day_L), potential evapotranspiration [mm] (Pe), evaporation [mm] (Evap) and relative humidity [%] (Rh). Open access air quality and anthropogenic pollution data including NO_x, NO, NO_2, SO_2, CO, PM2.5 and PM10, was collected at nearby sampling sites at Winetavern Street and Rathmines (PM2.5 only). The Winetavern Street sampling site is situated less than 1km from the sampling site, while the Rathmines site is located 1.6 km away. The air quality data collected from these sites was obtained from the Environmental Protection Agency SAFER open data website (EPA Ireland, 2021).

The normal distribution of the WIBS, Hirst and meteorological/pollution daily data was tested using the Shapiro-Wilk test. The results of which showed that most daily data did not follow a normal distribution. A Spearman correlation test was selected to calculate the degree and the correlation between selected variables using the nortest (Gross and Ligges, 2015) and corrplot (Gross and Ligges, 2015) packages within R (R Core Team 2017).

5.3 Results

5.3.1 Overview of pollen trends

Over the course of the monitoring campaign, the ambient pollen concentrations recorded at the Dublin site were largely dominated by Urticaceae pollen, which represented 78% of the pollen identified. There were some small concentrations of Poaceae pollen also recorded, representing only 11% of the pollen encountered. This is to be expected and is indicative of that time of the year when grass pollen season is ending/finished and herbaceous pollen closes out the remaining end of the annual pollen season. A time-series plot of the pollen trends seen during the campaign is provided in Figure 5.1, below. From examination of these temporal trends, it can be seen that the highest daily concentration was recorded on the 25th of August due to the presence of high ambient Urticaceae concentrations. A second peak was witnessed again on the 29th of August, followed by a series of more minor peaks on the 4th, 7th and finally on the 14th of September. Several early peaks were also observed on the 11th, 15th and 17th of August. Again, the majority of these peaks were seen to be largely driven by Urticaceae pollen. In comparison, the highest daily concentration of Poaceae recorded was seen on the 15th of August. Following this, the overall trend in Poaceae pollen concentration lessened, coinciding with the declining pollen season.

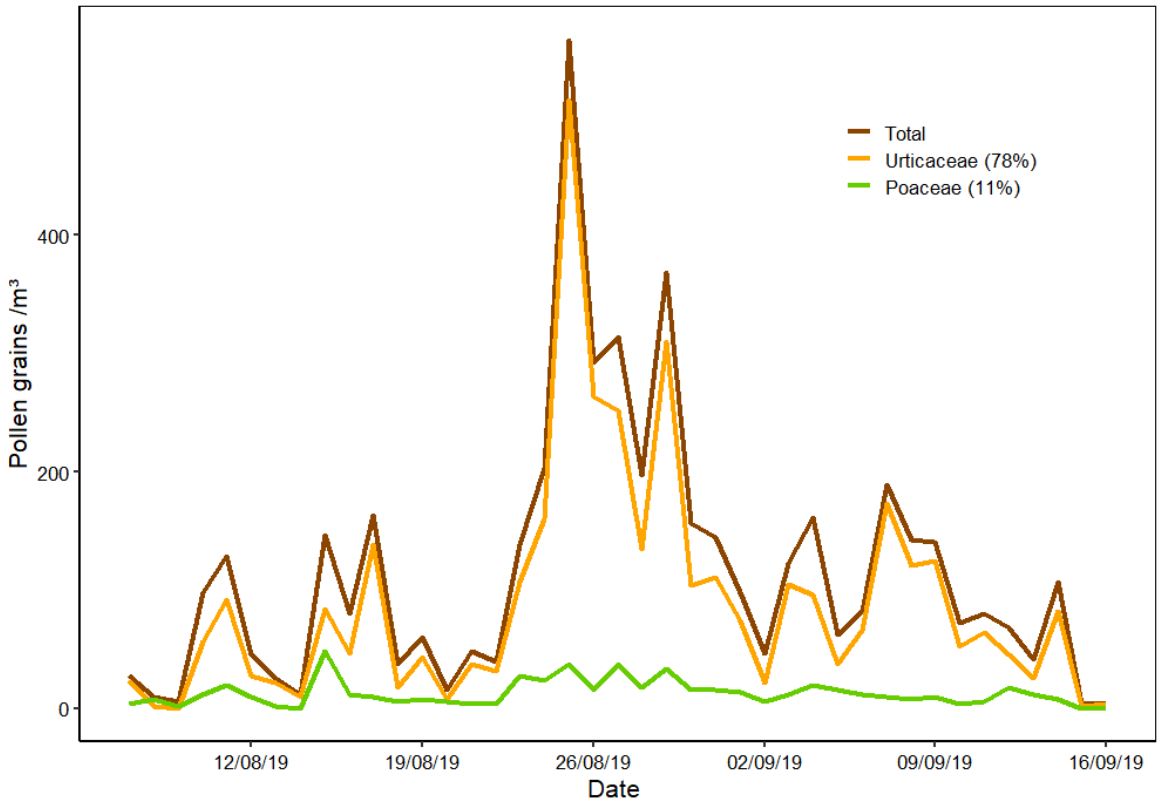

Figure 5.1: Time series of ambient pollen concentrations during the WIBS-NEO campaign

5.3.2 Overview of WIBS particle trends

While pollen concentrations were being monitored by the Hirst, the WIBS-NEO instrument was simultaneously recording the size, shape and fluorescent intensity of airborne particles. Throughout the campaign a total of 47,396,045 particles were sampled. The fluorescent portion of these particles was determined by applying a force trigger threshold/baseline. Initially, the baseline was set to 3 standard deviations greater than the mean fluorescence intensity in each channel (3δ) during force trigger mode. Overall, 86% of particles sampled were classified as non-fluorescent, meaning only 14% of particles sampled exhibited fluorescence above the determined threshold. This fraction is termed FAPs. A time-series of the distribution of fluorescent versus non-fluorescent particles is shown in Figure 5.2. Although the fluorescent particles are considerably outnumbered by non-fluorescent particles, there are two FAP peak periods observed. The first of these occurred on the 20th of August followed by the highest peak on the 25th of August. Two more successive peak periods were also witnessed on the 8th and 14th of September. Although these peaks are representative of all FAPs recorded, including those as small as 0.5 µm in size, the peaks on the 25th of August and 14th of September do coincide with high pollen/Urticaceae concentrations. Diurnal distributions of total FAPs were also investigated (Figure 5.2 (B)), it was found that FAP concentrations peaked in the morning at 8:00, with two less intense peak period also found at 14:00 and 18:00.

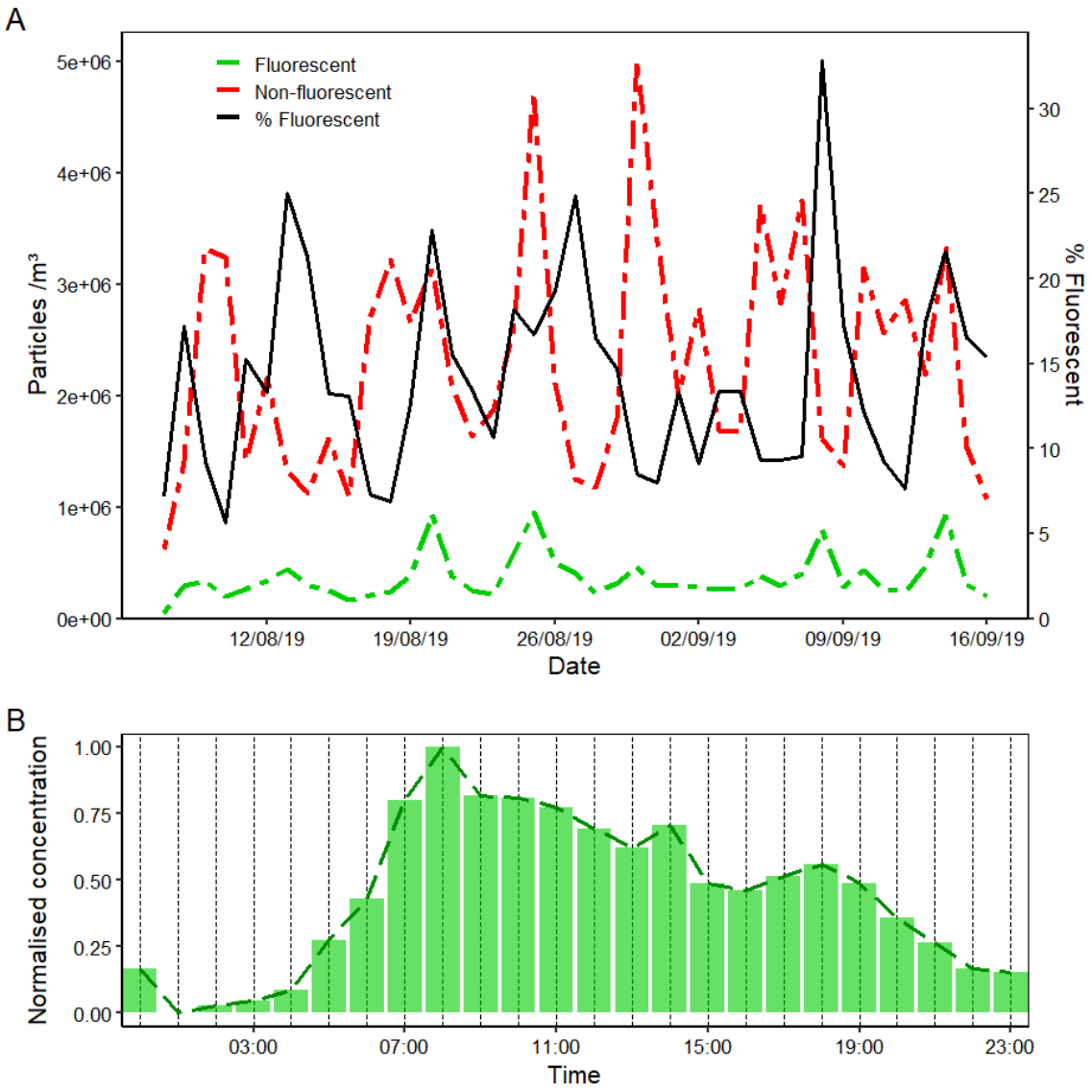

Figure 5.2: (A)Time series of ambient aerosol particles detected by the WIBS-NEO during the monitoring campaign, and (B) normalised diurnal distribution of total FAPs

To further investigate the contributing factors influencing the FAP fraction of WIBS particles, FAPs were further subdivided into distinct categories based on their fluorescence characteristics in each of the 3 channels (FL1, FL2, FL3) (Perring et al., 2015). The contributions to each classification are summarised in Table 5.1. B type particles were found to be the most abundant, followed by BC and ABC particle classes, together these classes represent over 70% of FAPs witnessed. A, C and AB particles were present in lower quantities, while AC type particles contributed negligibly to observed FAPs.

Table 5.1: WIBS particle distribution (% of total FAPs) using Perring nomenclature

Particle Class	**% Contribution**
B	43%
BC	15%
ABC	14%
A	11%
C	9%
AB	7%
AC	<0.5%

To obtain initial estimates of the bioaerosol classes that might be contributing to each FAP class, a more detailed analysis of particle characteristics was conducted. A temporal plot of WIBS particle classes and heatmaps detailing distributions in AF and size are illustrated in Figures 5.3 - 5.5. Over the course of the campaign, it can be observed (Figure 5.3) that the majority of particle classes were dominated by smaller particles, this is especially clear for periods of high B particle concentrations. However, periods of high BC particle concentration are also apparent, especially on the days of the 7th and 14th of September. The majority of particle types were dominated by particles of size less than 10-15 μm, as shown in Figure 5.4, except ABC particles which were seen to contain larger-sized particles. The larger ABC particles greater than 15 μm observed could very well represent the coarser fraction of pollen grains observed, especially Poaceae pollen, which represents one of the bigger pollen types observed during the campaign. B, AB and BC type particles also exhibited notable shifts in particle contributions at larger size and AF ranges (Figure 5.4). Typically, particles with lower AF values are indicative of a spherical morphology whereas larger values are indicative of more obscured shapes, with a value of 100 representing a perfect rod shape.

Many of the particle classes were seen to possess high concentrations of small and diversely shaped particles with some appearing more rod-like in shape than any other sizes. Since the size resolution of the WIBS-NEO can detect particles as small as 0.5μm in size, it is likely much of this AF diversity is the result of bacteria and other small microbes or biological debris. The larger particles also see a shift in AF, this is particularly true for ABC particles, suggesting the presence of inconsistently shaped large particle formations. This could potentially represent a mix of larger bioaerosols, plant debris or clusters of smaller bioaerosols.

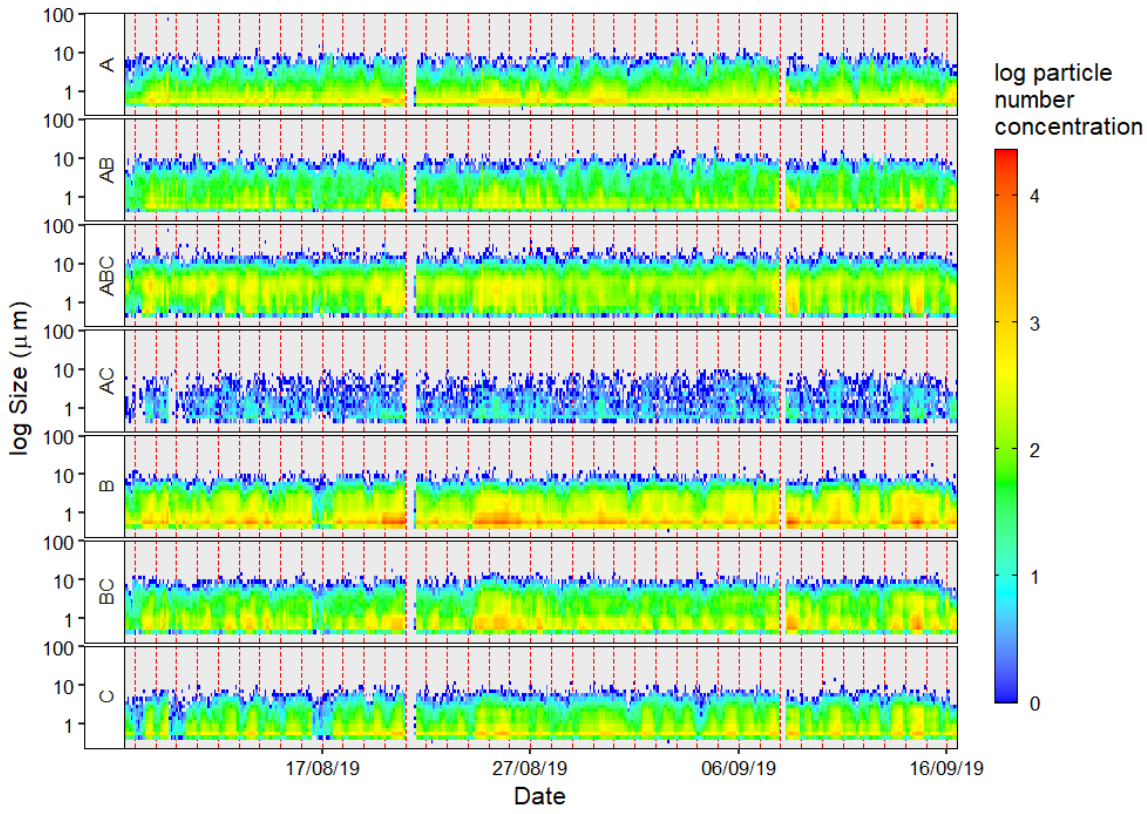

Figure 5.3: Daily temporal trends of WIBS FAPs (each area within the red dotted line illustrates 1 day) with relation to size

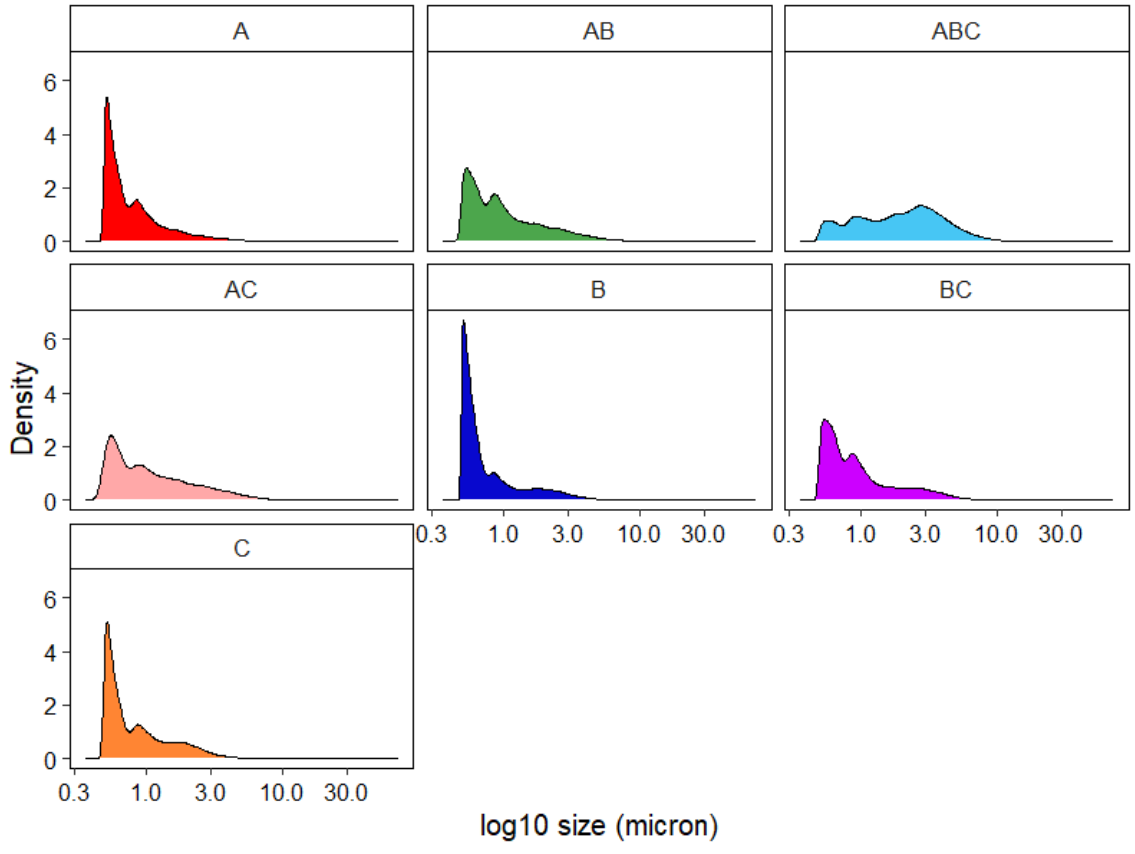

Figure 5.4: Kernel density distribution of WIBS particle sizes

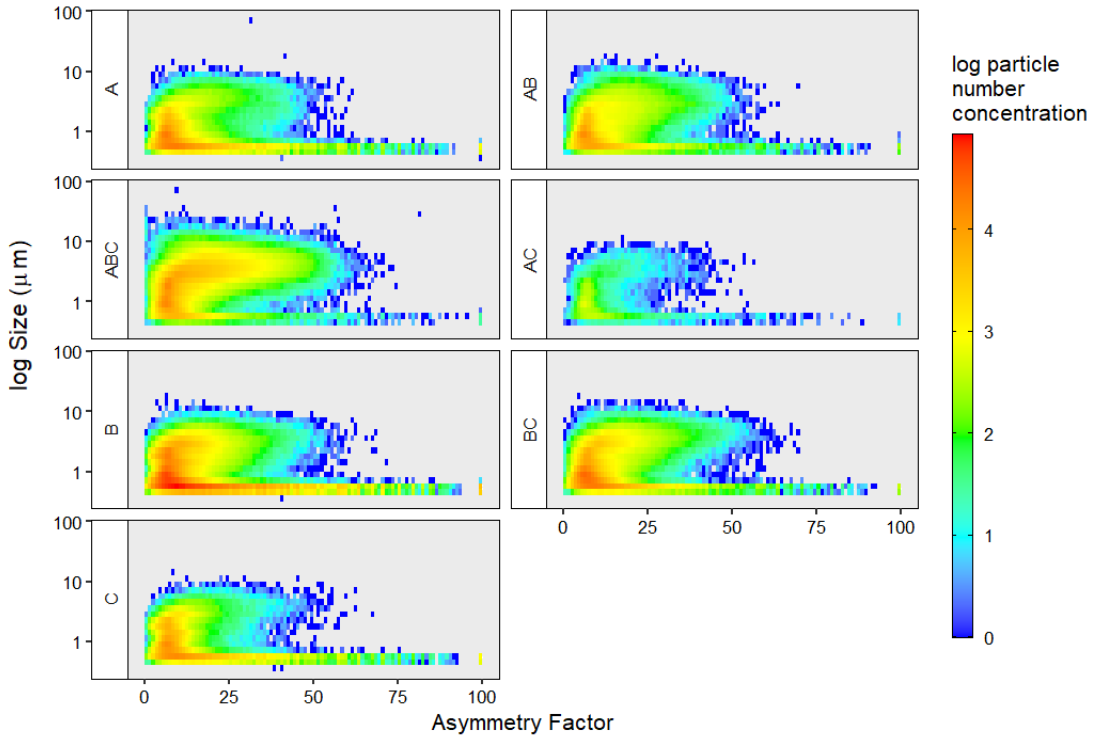

Figure 5.5: Size vs. Asymmetry Factor distribution of WIBS FAP classes

Up to now, there are no clear suggestions as to which class is influenced by pollen concentrations except for that ABC, BC, and AB classes seem to possess particles with larger sizes (especially ABC) as shown in Figure 5.4, with BC and B particles also illustrating selective high temporal concentrations that could coincide with peaks in pollen concentrations. The WIBS can record particles as small as 0.5µm, making it applicable for monitoring other bioaerosols such as bacteria. The Hirst on the other hand is limited by its use of microscopic analysis, limiting it to detection of particles ~2µm in size (Fernández-Rodríguez et al., 2018). The WIBS and Hirst also operate using very different flow rates. The WIBS operates at a flowrate of 0.03 L/min while the Hirst operates at a considerably higher flow of 10 L/min. As a result, differing numbers of FAPs and pollen grains were sampled by the WIBS and Hirst. In efforts to improve the comparison of the two methods, WIBS particles less than 2µm were removed from the collected fluorescent data prior to any additional analyses/comparison to Hirst data. This allows for preliminary comparison to pollen (and fungal spore) concentrations.

Further examination of the average diurnal trends of the classified FAPs provides little supporting information on the possible contributing PBAP fractions. As seen in Figure 5.6, the average hourly trends of the WIBS particles are rather erratic and do not typically converge with the trends observed for pollen. The only exception to this is the slight association between BC particles and Urticaceae pollen. The average diurnal trend for BC particles was also seen to peak in the early morning and continuously during the afternoon.

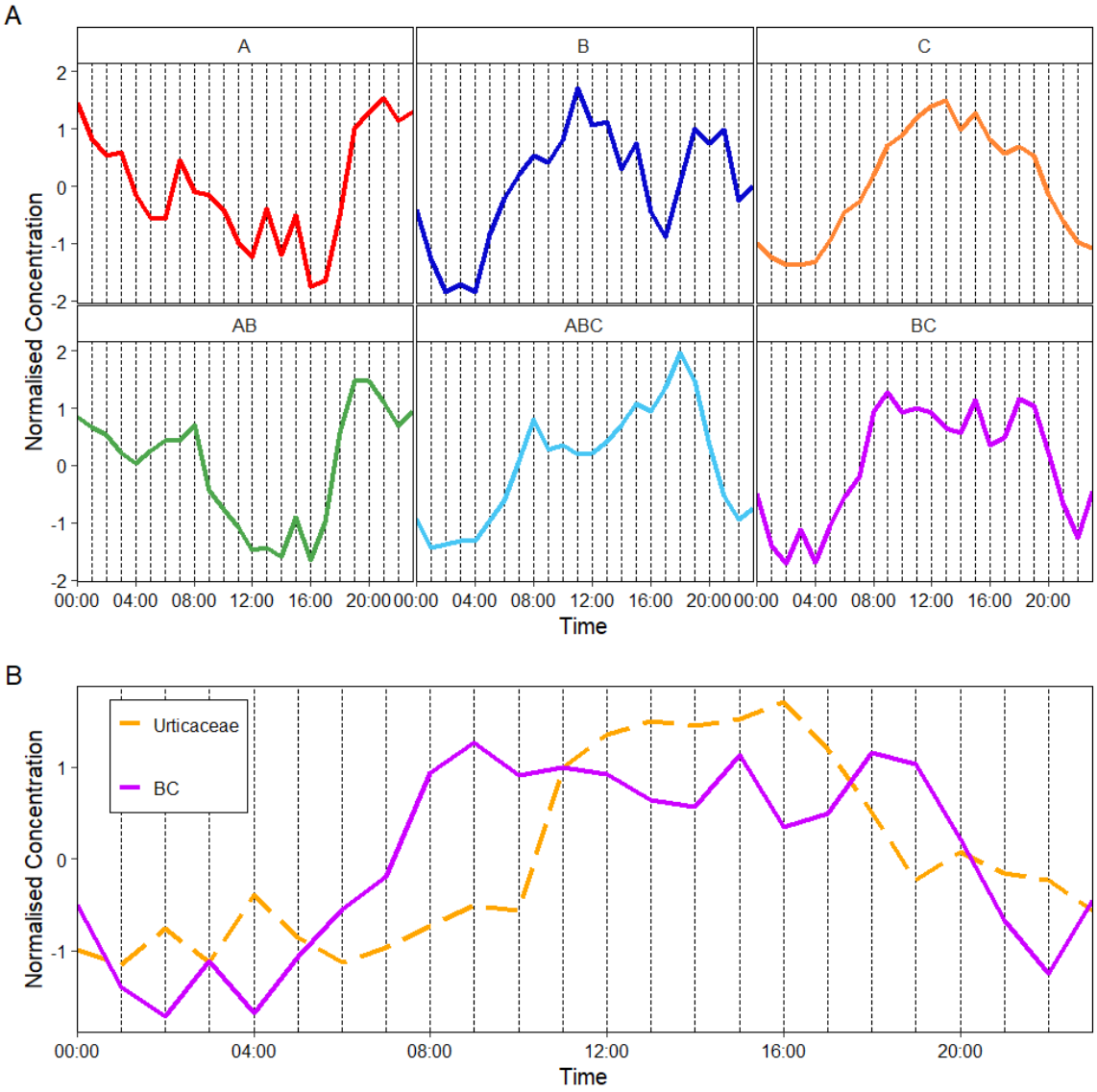

Figure 5.6: (A) Normalised diurnal concentrations of WIBS FAPs >2µm, and (B) comparison of BC and Urticaceae diurnal trends

5.3.3 Comparison of WIBS particle fraction to pollen concentrations

To further improve comparison efforts between Hirst pollen results and WIBS FAPs, additional size and fluorescent filters were applied to isolate these larger particle fractions. This aided in removing potentially interfering biological particles such as bacteria and fungal spores that remain even after removal of less than 2µm. The fluorescent threshold was also subsequently raised to 6σ and 9σ in efforts to remove other less fluorescent interfering particles. Following this, total pollen and Urticaceae concentrations were found to correlate the strongest with BC particles greater than 8µm in size at 6σ, yielding Pearson correlation coefficients (r) of 0.73. This comparison is illustrated in Figure 5.7, below. In the case of Poaceae pollen, no substantial relationship greater than r=0.5 was observed with any of the WIBS particle fractions at any fluorescent threshold. The best correlation

for Poaceae pollen was also observed for BC particles greater than 8µm at 6σ (r=0.54). However, this isolated fraction of BC particles failed to account for many of the peaks in Poaceae. A slight improvement was also seen for slightly larger particles and total pollen concentrations (>10µm, r=0.77 for total pollen) but the particle concentrations were significantly lower indicating the loss of potentially representative bioaerosols and so the size filter of >8µm was favoured.

Overall, increasing the florescent threshold from 3σ to 6σ showed only a slight improvement between the two instruments. Increasing the fluorescent threshold was found to drastically improve the particle number/m^3 seen between the two instruments, removing redundant particles or interferences. However, several deviations remained, the most obvious being the peak in BC particles seen on the 20th of August when pollen concentrations were notably low. This peak illustrates the potential limitations in utilising the WIBS for the selective detection of specific pollen taxa. Although the isolated BC particles do greatly follow the trend of observed pollen, there are unexplained deviations, which may be other biological particles or highly fluorescent interferents. Further increasing the fluorescent threshold from 6σ to 9σ does not improve the correlation between BC particles and Urticaceae pollen at any size range. Increasing the fluorescent thresholds changes the classification pathway of FAPs samples. At the higher threshold, it is observed that some particles previously classified as ABC, are now in the BC class, potentially adding non-pollen-like aerosols to the fraction, thus reducing the correlation seen when compared to the Hirst counts.

Although not covered here, it was found that ABC particles followed the trends seen for many different types of fungal spores, with larger ABC particles also following similar trends. This suggests the larger ABC particles were representative of large clusters of fungal spores rather than individual spores.

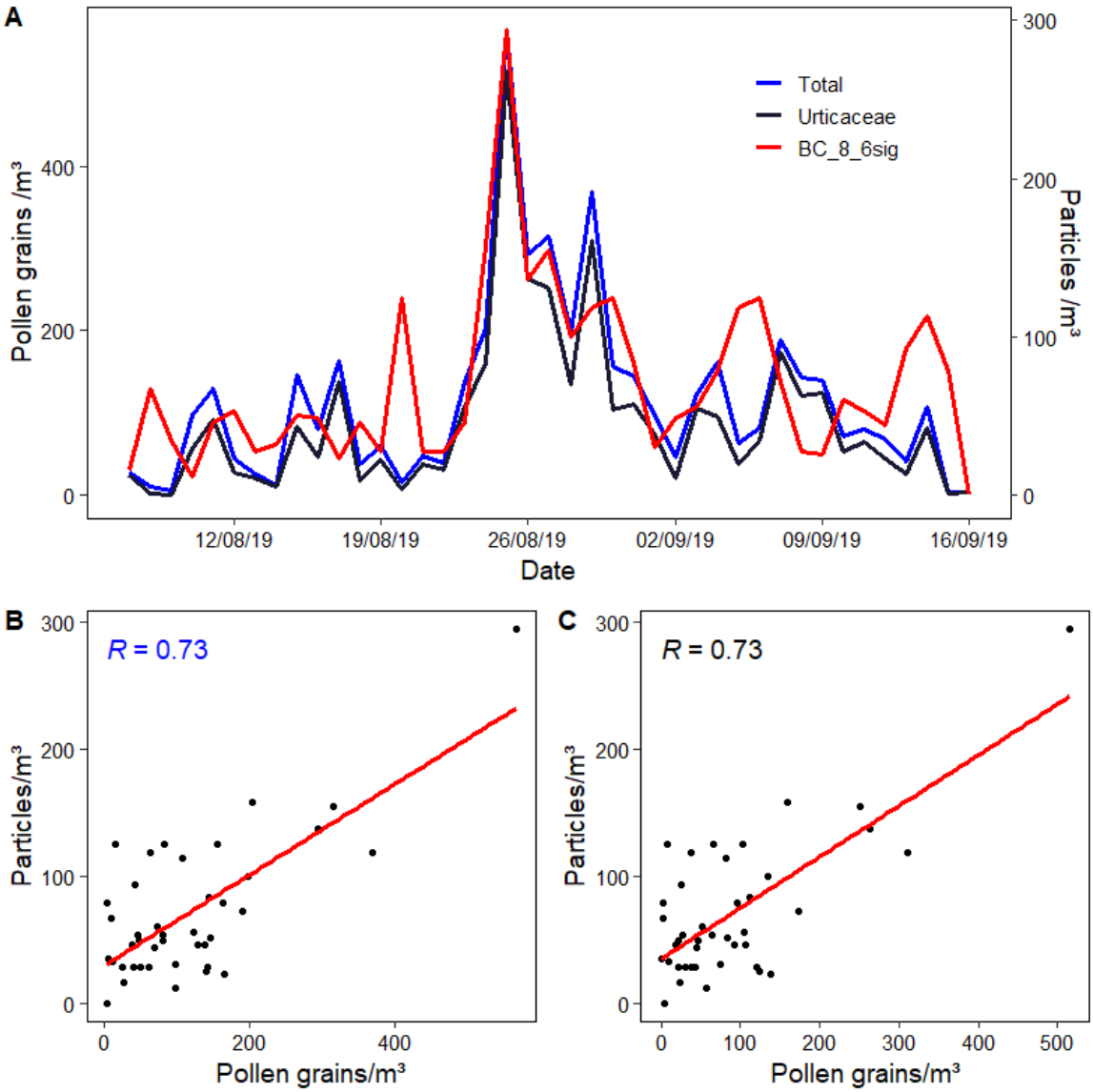

Figure 5.7: (A) Time series of Hirst Pollen counts and WIBS Pollen type particles (Daily) and (B) Hirst Total Pollen counts vs WIBS type particles (Daily) and (C) Hirst Urticaceae Pollen counts vs WIBS type particles (Daily)

Despite the promising results seen for the comparison of WIBS BC particles and pollen concentrations, it was found that this BC class at sizes greater than 8µm was also indicative of other, similarly sized bioaerosols, namely *Alternaria* spores. The isolated BC fraction was found to have a mean size of 10 µm with maximum sizes reaching 20 µm. Although this could suggest the presence of Urticaceae pollen, it is possible that other bioaerosols may also be present. Although the real-time detection of fungal spores is beyond the scope of this thesis, it was found that this fraction also mimicked the temporal trends of *Alternaria*, with the combined concentrations of total pollen and *Alternaria* yielding a higher correlation with a Pearson coefficient of 0.8 (shown in Figure 5.8). This could be driven by the fact that the peak days of pollen and *Alternaria* occurred at similar times. However, at this time it is not possible to differentiate the BC classes further. Efforts were made to distinguish between the pollen and spore-related FAP fractions by use of K-means clustering but to

no avail. This fraction may be representative of both bioaerosol classes and the narrowing shape of *Alternaria* spores and the potential spherical/rumpled shape of the Urticaceae could be representative of the shifts in AF seen for larger BC type particles.

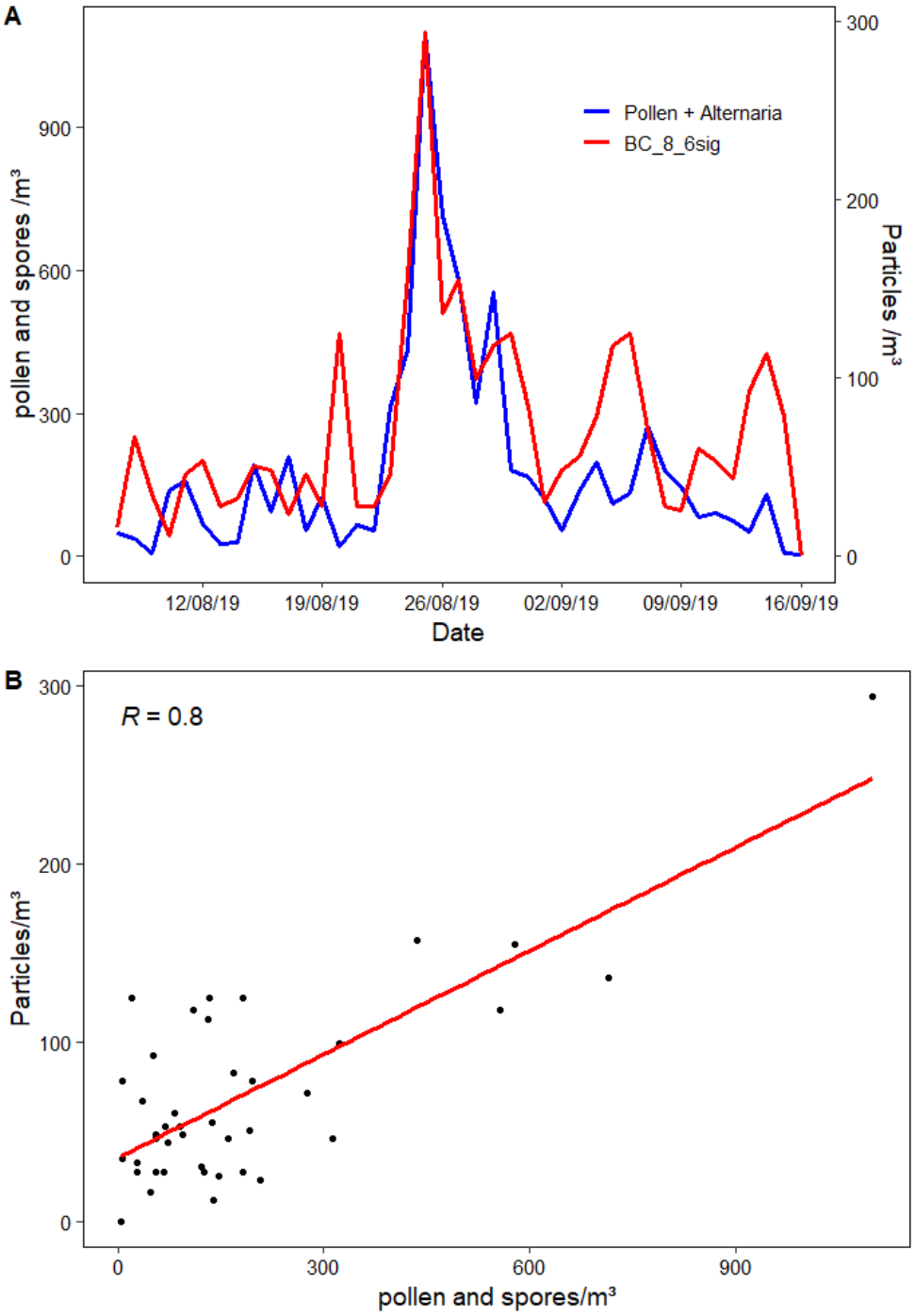

Figure 5.8: (A) Time series of Hirst Total Pollen and Alternaria counts and WIBS BC > 8µm (6σ) type particles (Daily) and (B) regression plot Hirst Total Pollen and Alternaria counts and WIBS BC > 8µm (6σ) type particles (Daily)

5.3.4 Correlation analysis between meteorological parameters/air quality and WIBS particles

To assess the influence varying meteorological and air quality parameters have on the detection of FAPs, Spearman's rank correlation analysis was carried out, the results of which are shown in Table 5.2. The analysis of WIBS classes includes all particle sizes classified at the 3σ threshold.

Table 5.2: Spearman´s rank correlation coefficients between daily WIBS Particle data and meteorological parameters.

	A	**B**	**C**	**AB**	**AC**	**BC**	**ABC**	**FL**	**NF**
Tmax	-0.06	-0.16	-0.13	0.02	-0.1	-0.07	0.04	-0.11	-0.11
Tmed	-0.23	-0.29	**-0.36***	-0.19	**-0.36***	-0.23	-0.2	-0.27	-0.18
Tmin	-0.29	**-0.33***	**-0.43****	**-0.29***	**-0.47****	**-0.28***	**-0.32***	**-0.33***	-0.14
Gmin	**-0.48****	**-0.66****	**-0.67****	**-0.61****	**-0.61****	**-0.57****	**-0.57****	**-0.66****	-0.17
Rain	-0.42	-0.33	-0.49	-0.32	-0.4	-0.22	-0.22	-0.33	-0.28
Pres	0.32	**0.4***	**0.45****	**0.39***	**0.4****	**0.28***	0.16	**0.36***	0.17
Wind_s	-0.19	**-0.39****	**-0.24***	**-0.48****	**-0.43****	**-0.51****	**-0.48****	**-0.4****	0.23
Wind_d	-0.12	-0.1	-0.05	-0.2	-0.1	-0.14	-0.1	-0.11	0.07
Day_L	0.24	0.2	0.25	0.18	0.17	0.1	0.3	0.19	0.12
G_rad	0.04	0	0.06	0	0.04	-0.03	0.24	0.03	-0.05
Soil	-0.26	-0.24	-0.33	-0.14	-0.27	-0.09	-0.03	-0.19	-0.21
Pe	-0.1	-0.22	-0.2	-0.19	-0.17	-0.22	-0.02	-0.19	-0.21
Evap	-0.1	-0.23	-0.18	-0.23	-0.20	-0.26	-0.03	-0.2	-0.12
Rh	-0.09	-0.02	-0.16	0.12	-0.01	0.14	0.1	0.02	-0.14
PM2.5	**0.52****	**0.52****	**0.55****	**0.54****	**0.65****	**0.49****	**0.55****	**0.58****	**0.25****
PM10	**0.60****	**0.43****	**0.49****	**0.49***	**0.56****	**0.43***	**0.36***	**0.48****	**0.34****
NO_X	**0.37***	**0.42***	**0.29****	**0.64****	**0.59****	**0.53****	**0.57****	**0.49****	-0.12
NO	**0.37***	**0.38***	**0.27****	**0.64****	**0.56****	**0.53****	**0.48****	**0.44****	-0.11
NO_2	0.32	**0.37***	**0.25***	**0.58***	**0.54****	**0.49***	**0.53***	**0.45***	-0.14
CO	**0.37***	**0.41****	**0.37****	**0.44***	**0.41****	0.14	**0.48***	**0.39****	0.09
SO_2	**0.37***	**0.41****	**0.37****	**0.44***	**0.41****	0.14	**0.48***	**0.39****	0.09

*significance at the 95% level, **significance at the 99% level

It was observed that the majority of fluorescent WIBS FAP classes exhibited very similar and consistent correlations with several of the meteorological parameters. Significant negative correlation with minimum temperature, grass minimum temperature and wind speed was recorded for B, C, AB, AC, BC, ABC and total fluorescent particles (FL). In addition, a notable positive correlation was observed for FAP classes and pressure. Daily trends and regression of such parameters are shown in Figure 5.9. Although the current analysis extends down to small FAPs, several of these observed correlations remained, even at higher FAP size ranges. It was seen that

even BC particles >8um maintained a significant negative association with windspeed and grass minimum temperature. Days with wind speeds greater than 9 knots led to the highest deviations between sampling methods for all pollen types. This wind speed is the equivalent to a moderate breeze, highlighting the possible environmental limitations of the WIBS in comparison to traditional methods. Upon removal of these days from the analysis (resulting 18-day dataset), the Pearson correlation coefficient (r) between BC particles and Total/Urticaceae pollen increases from 0.73 to ~0.84.

In comparison, few significant correlations were observed for non-fluorescent (NF) particles recorded by the WIBS. Correlation analysis with meteorological and air quality parameters was also extended to ambient pollen concentrations (Appendix C, Table C1). However, few significant correlations were found apart from the expected positive correlation with temperature and sun parameters, followed by negative associations with rain and relative humidity.

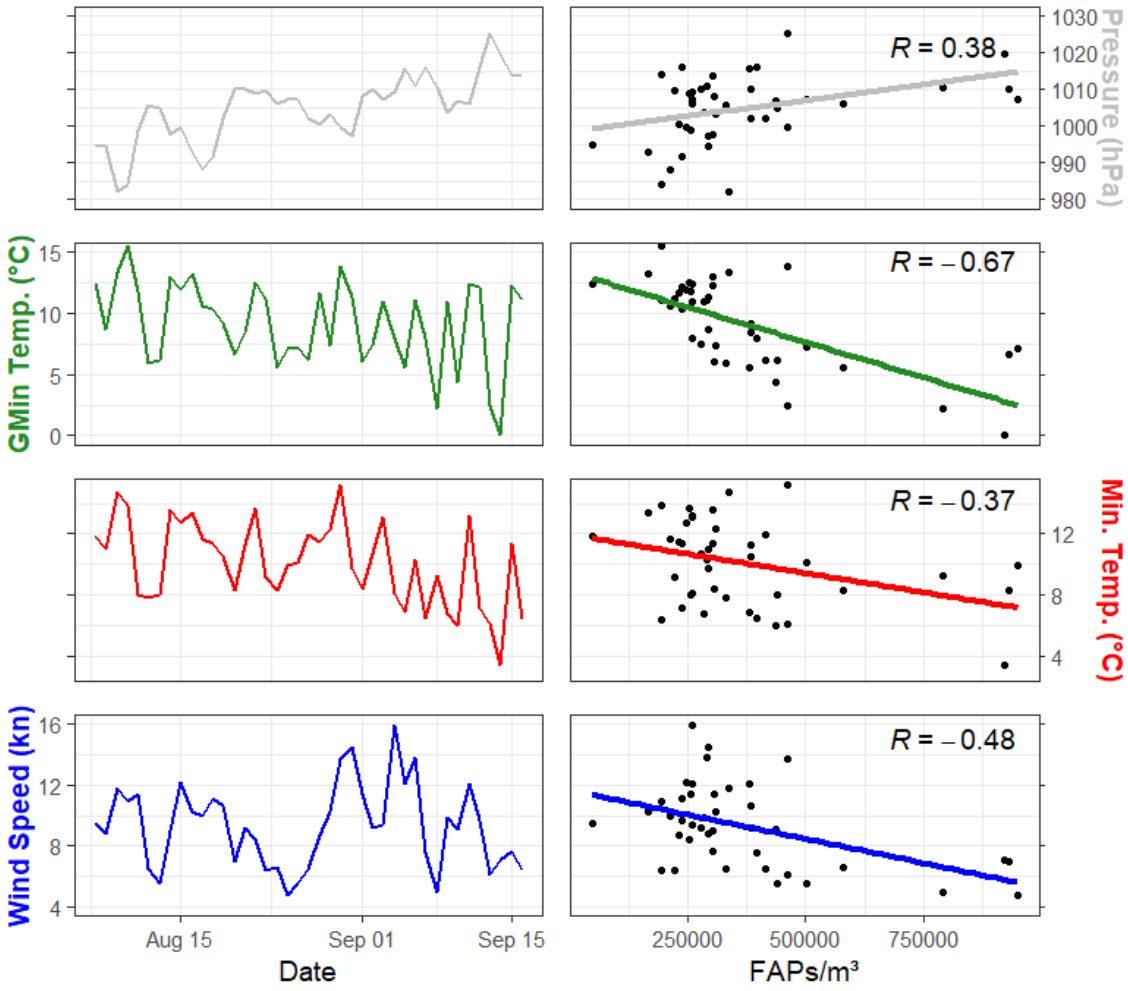

Figure 5.9: Daily trends in FAP and selected meteorological parameters

To investigate the possibility of anthropogenic interferences, due to the urban location of the sampling site, correlation analysis was extended to locally sourced anthropogenic and air quality parameters. The majority of FAP classes showed significant correlation with almost all pollution parameters (NO_X, NO, NO_2, SO_2, CO, PM2.5 and PM10). Although it was expected that the ambient particle concentrations recorded by the WIBS would correlate well with PM2.5 and PM10, as the WIBS samples particles within these size classes, a comparably high correlation was also seen for NO_X. NO_X showed strong correlations to FL1 type particles, particularly AB type particles (r=0.64 at 3σ with no size filtering applied). Increasing fluorescent thresholds to 9σ, could not remove this association with FL1 type particles. Correlation analysis to meteorology was also extended to these air quality parameters (Table 5.3) and it was found that NO_X and its constituents mimicked the strong correlations seen for FAPs. NO_X concentrations exhibited similar negative correlations with minimum temperature and wind speed as well as the positive correlation with pressure, that were seen earlier for FAPs. However, the influence of these anthropogenic sources on WIBS FAPs decreased significantly with increasing particle size. It was found that WIBS FAPs less than 2 µm in size had the highest correlations with these gaseous pollutants. High r (spearman) coefficients of between 0.6-0.7 were observed for NO_X with AB, AC and ABC type particles at this size range. AB particles illustrated the strongest correlation with NO_X (at sizes less than 2 µm) and are presented in Figure 5.10, below.

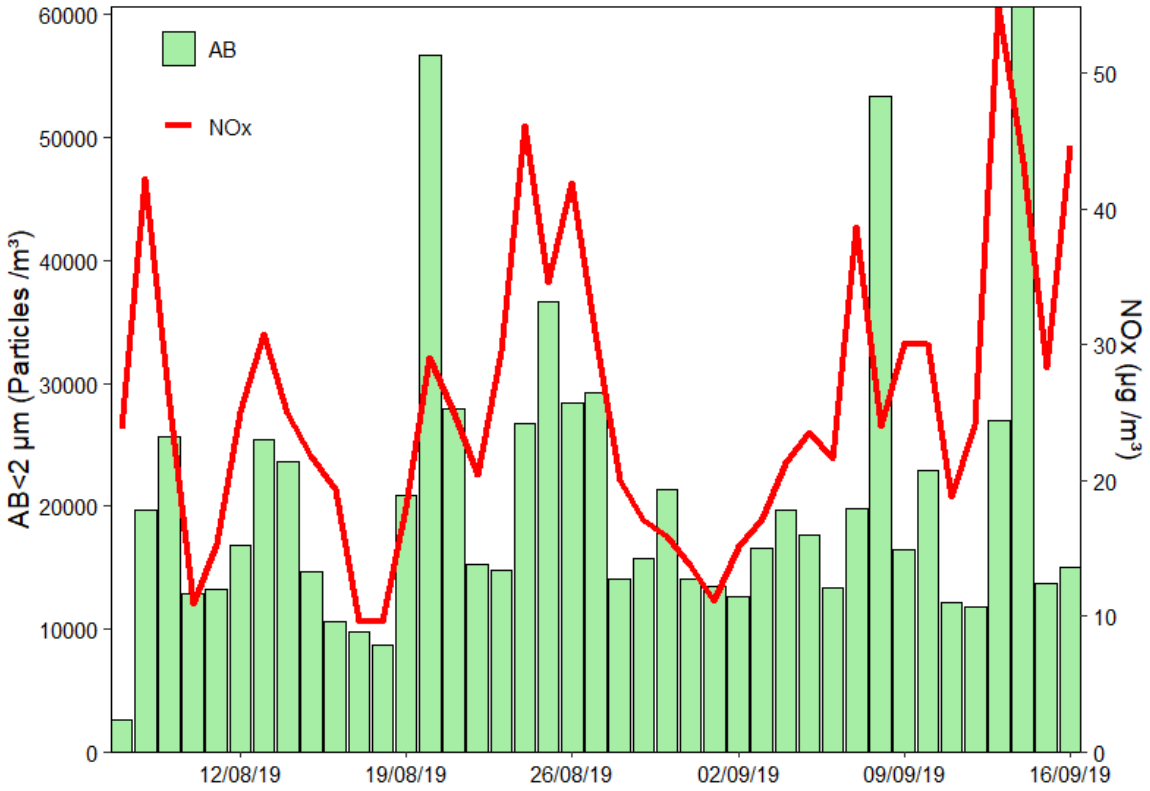

Figure 5.10: NO_X and AB particle time-series analysis

The correlation between NO_X and AB type particles yields an r = 0.7. It can be seen that increases in AB particle concentration are often seen to correspond to increased NO_X concentrations. It is unlikely that these FAPs directly correspond to NO_X itself, as it is a gaseous pollutant and more probably corresponds to combustion-related particulates and/or secondary organic aerosols (SOA), related to the formation and reactivity of NO_X.

Table 5.3: Spearman´s rank correlation coefficients between Air quality and meteorological parameters

	PM2.5	**PM10**	**NO_X**	**NO**	**NO_2**	**CO**	**SO_2**
Tmax	0.13	0.14	0.03	0.04	0.01	0.00	0.00
Tmed	-0.09	-0.08	**-0.35***	**-0.35***	-0.34	-0.20	-0.20
Tmin	-0.20	-0.21	**-0.51****	**-0.51****	**-0.48****	**-0.27***	**-0.27***
Rain	-0.45	-0.53	-0.24	-0.30	-0.20	-0.36	-0.36
Gmin	-0.35	**-0.46****	**-0.41****	**-0.43***	-0.36	-0.22	-0.22
Pres	0.27	0.09	**0.44****	**0.50***	**0.42***	**0.59***	**0.59***
Wind_s	**-0.46****	-0.20	**-0.70****	**-0.62***	**-0.71***	**-0.51***	**-0.51***
Wind_d	-0.40	-0.38	-0.20	-0.13	-0.19*	-0.11	-0.11
Day_L	0.09	0.41	0.22	0.20	0.22	-0.09	-0.09
G_rad	0.01	0.29	0.09	0.06	0.11	-0.32	-0.32
Soil	0.02	0.03	-0.07	-0.16	-0.02	-0.13	-0.13
Pe	-0.09	0.21	-0.21	-0.21	-0.19	**-0.44***	**-0.44***
Evap	-0.12	0.21	-0.23	-0.23	-0.20	**-0.51***	**-0.51***
Rh	0.04	-0.25	0.33	0.23	0.38	0.24	0.24

*significance at the 95% level, **significance at the 99% level

Given the presence of significant positive correlations between PM2.5 and PM10 readings with WIBS FAPs, and considering the ability of the WIBS to measure the sizes of the particles sampled, it was decided to conduct a more comprehensive assessment of the suitability of the WIBS as a monitoring tool for PM2.5 and PM10. To do this a mass density conversion was applied to all individual particles detected by the WIBS, this included fluorescent particles and non-fluorescent particles. For comparison to PM10, WIBS particles were filtered to those that have size measurements less than 10 µm whereas for PM2.5 comparisons a filter of <2.5 µm was applied. A conversion was required to compare the concentrations sampled by the WIBS (particles/m^3) to PM mass readings (µg/m^3), the volume of the particle was determined from its size reading and a single unit density (1g/cm^3) was then applied to find the rough mass of each particle. Once converted, the mass reading of the WIBS particles can be compared to the PM10 and PM2.5 readings as shown in Figures 5.11 and 5.12.

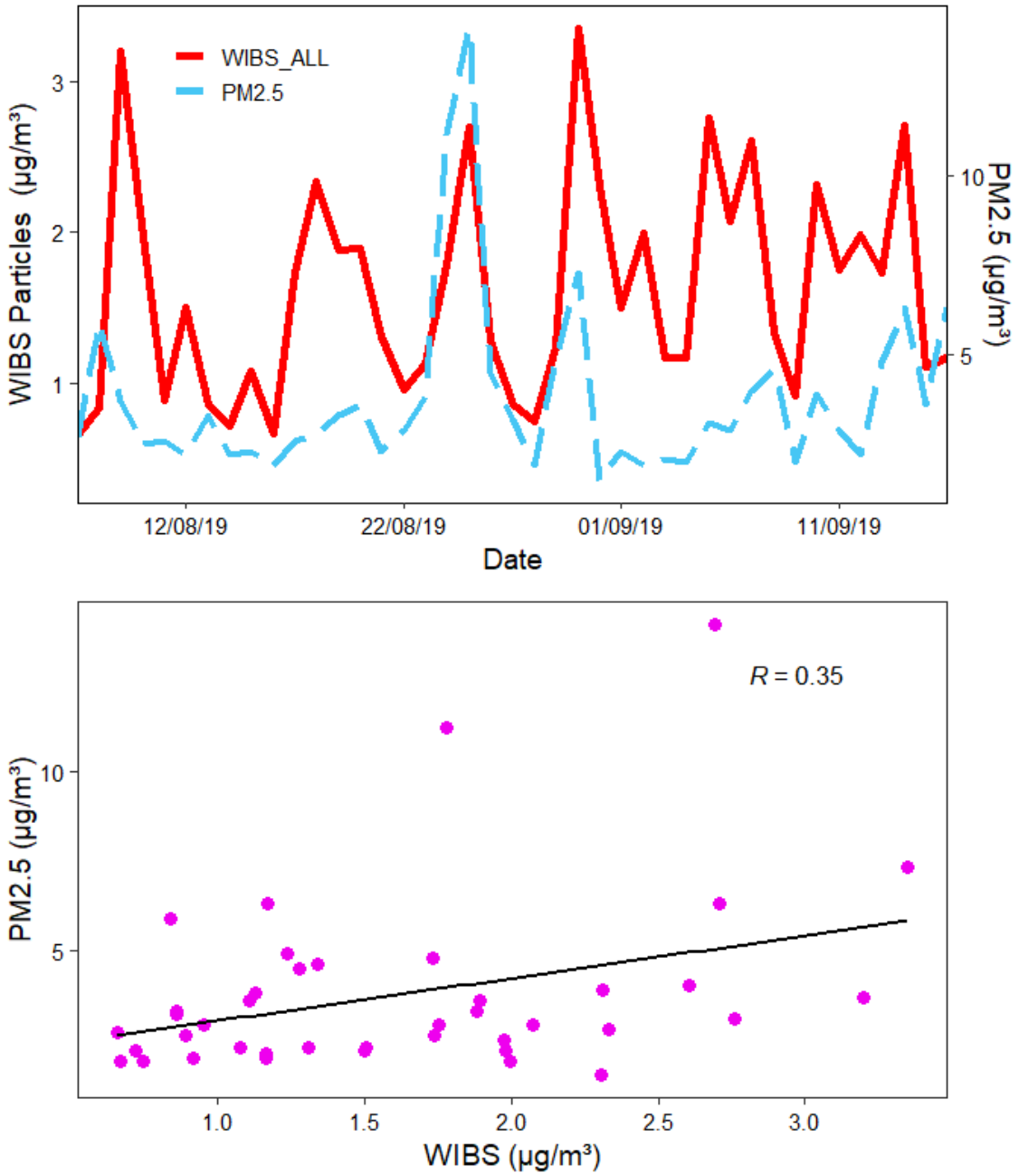

Figure 5.11: Comparison of WIBS particle masses with PM2.5 measurements

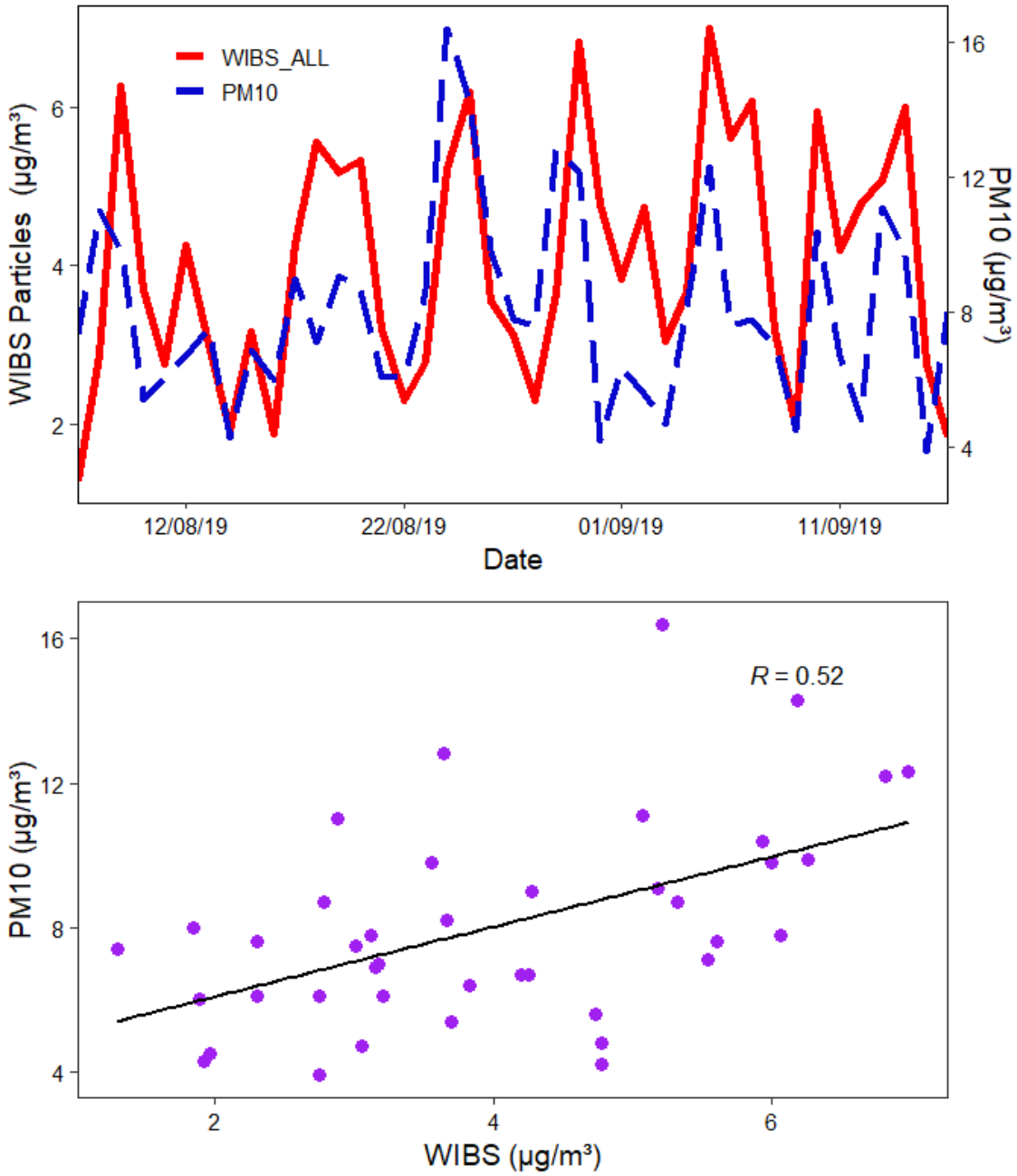

Figure 5.12: Comparison of WIBS particle masses with PM10 measurements

The mass of extracted WIBS particles seemed to follow the general trends of the PM2.5 and PM10 readings. Improved results were noted for PM10 over PM2.5. One considerable point of inflexion between the comparison of ambient PM readings and WIBS particle masses is the notable reduction in mass seen for the WIBS readings, however, this is likely explained by inaccurate unit density values used as well as the differing heights of the samplers. Whereas the WIBS was situated at roof level, PM readings were taken 1-2 km away, closer to ground level. In addition, the WIBS is capable of detecting particles as small as 0.5 µm in size, while the PM10 and PM2.5 monitoring devices can record particles smaller than this. As a result, the WIBS mass conversions for PM2.5 and PM10 can be considered incomplete measurements due to the absence of these smaller particles.

Considering these differences, the WIBS particle masses performed rather well as proxies for PM10 and PM2.5 measurements.

5.4 Discussion

5.4.1 FAP trends observed over the sampling campaign

Over the course of the monitoring campaign, it was found that airborne pollen concentrations were mainly dominated by Urticaceae pollen which is representative of established Irish pollen trends for that time of the year (Markey et al., 2022a). While pollen concentrations were monitored by the Hirst, the WIBS-NEO instrument measure airborne aerosol particles. The concentration of FAPs identified by the WIBS-NEO was found to be considerably higher than those previously found in other Irish campaigns. Previous studies have been conducted at similar times of the year at more pristine rural sites, such as the WIBS campaign conducted by Healy *et al.*, 2014 in 2010 from 02/08/2010 – 02/09/2010 at Killarney National Park. Since urban areas such as Dublin, typically experience lower concentrations of ambient bioaerosols compared to rural areas (due to the notable reduction in plant cover), it would be expected that a higher amount of FAPs would be observed at the rural site. These higher FAP concentrations may be indicative of interfering sources. Although, other factors such as instrument sensitivity, which can vary from WIBS to WIBS as well as from different generations (WIBS-4 to WIBS-NEO) (Forde et al., 2019) should be considered. However, similar trends have been noted previously by Yu et al., (2016) when comparing urban and rural FAP concentrations. This literature study concluded that increases in FAPs could very well be attributed to the presence of combustion-related particles present at the urban site (Yu et al., 2016). The prevalence of potentially anthropogenic/interfering particles is not unexpected at the Dublin site considering the urban location and the declining pollen season.

The FAPS monitored by the WIBS were heavily dominated by B type particles (43%). Although B type particles are representative of some biogenic sources (Savage et al., 2017), it is more commonly linked to anthropogenic sources and other interfering particles (Gabey et al., 2011; Toprak and Schnaiter, 2013; Twohy et al., 2016). This further corroborates the initial suspicions of anthropogenic interferences. Previous studies have cautioned that any atmospheric sampling in which B type particles dominate the fluorescent fraction should be examined carefully for likely interferents (Hernandez et al., 2016). This warning comes as a result of B type particles only marginally contributing to PBAP fractions (Hernandez et al., 2016). BC (15%) and ABC (14%) type particles were the next prevalent FAP types found. Both of these classes have been associated with the presence of airborne PBAP, most notably, pollen grains. Several laboratory and field studies have highlighted the contribution of various pollen types to both BC and ABC categories (Hernandez et al., 2016; Hughes et al., 2020; Markey et al., 2022b; Savage et al., 2017).

The majority of FAP types were dominated by small particles with the exception of ABC, BC and AB particles which were seen to contain larger sizes, this was particularly true for ABC particles. It has been shown that fluorescence intensity and fluorescence type is a function of particle size and as such, larger particles tend to favour the ABC category (Savage et al., 2017). AB type particles showed notable fluorescence in the FL1 channel for both particles present at small size ranges of less than 5µm as well as at the coarser size ranges recorded for the AB fraction (10-18µm). This general trend could be representative of ambient fungal spore concentrations. Fungal spore classification has often been associated with strong FL1 fluorescence (Hernandez et al., 2016; Hughes et al., 2020; O'Connor et al., 2015; Savage et al., 2017). Other types, namely AC were seen to contribute negligibly to the fluorescent fraction (0.3 %). This limited presence of AC particles has been well-documented in previous WIBS studies (Hernandez et al., 2016; Perring et al., 2015; Yu et al., 2016).

Examination of diurnal trends provided little information regarding the potential identity of the contribution of PBAP to FAP classes. The majority of WIBS diurnal trends almost perfectly mirrored those observed by Yu et al. (2016), which were shown to track well with ambient concentrations of black carbon, especially for FL1 classes. This observation adds further credence to the presence of interfering particles at the Dublin site. The only exception to this is the association between BC particles and Urticaceae pollen. The average diurnal trend for BC particles was also seen to peak in the early morning and continuously during the afternoon as observed in Figure 5.6. This trend has been routinely observed for Urticaceae and grass pollen (Kosisky et al., 2010; del Mar Trigo et al., 1996). When compared to the normalised diurnal trend of Urticaceae pollen, BC particles seem to follow a similar trend, accounting for both the minor morning peak and afternoon behaviour.

5.4.2 Evaluation of WIBS instrument for pollen detection

As yet, there is no standard procedure to which to compare real-time monitoring instruments (Pereira et al., 2021). Many studies compare the performance of real-time pollen monitoring instruments to the Hirst as it is traditionally the most widely used pollen monitoring method. However, caution should be taken when comparing such methods due to the uncertainty in measurements produced by the Hirst (Pereira et al., 2021) as well as any differences introduced by the varying operating principles. For fluorescence-based instruments like the WIBS, it has also been speculated that some bioaerosols may fluoresce too weakly to be detected in certain circumstances (Healy et al., 2014). As such, comparisons should be made to the Hirst to assess how real-time instruments function under different ambient conditions and to determine any limitations associated with the real-time method.

A series of size and fluorescent filters were applied to the FAP data in order to isolate pollen-like FAPs. The temporal profiles of these FAPs were then compared to those seen by the Hirst. Following this, it was found that the best association between the WIBS and Hirst instruments for

pollen monitoring was found for BC type particles at the 6σ threshold at sizes larger than 8µm. BC particles were largely classified at size ranges less than 20µm at low AF values less than 9, indicating the detection of spherical particles. The observed size range of this fraction (particles between 9-20 µm in size) is indicative of Urticaceae pollen. The various individual species making up Urticaceae pollen exist in the atmosphere at sizes between 9 and 20 µm (Sorsa and Huttunen, 1975). Although, the main Urticaceae type in Dublin is *Urtica dioica* (15-30 µm) is slightly larger (Healy et al., 2012a) it is possible that this late in the season that Urticaceae pollen may be slightly smaller due to dehydration experienced during dispersion (Pacini, 2000). Particle sizing by the WIBS is based on Mie theory which estimates particle size from the scattering of light assuming particles are spherical. Inaccuracies in sizing can therefore occur as particles become less spherical. In addition to this, Mie theory can vary in accuracy depending on the particle size and wavelength of light used (Kolokolnikov et al., 2019). As such, a slight disparity between the size calculated by the WIBS and that of the actual recorded particle can occur. This explains why slightly smaller particles were seen to correlate the best with Urticaceae pollen. Previous studies have suggested particles with high FL2 and FL3 fluorescence intensities (BC) and lower AF values correlate well with both pollen and fungal spores (Healy et al., 2012a, 2014; Hernandez et al., 2016; O'Connor et al., 2014a; Savage et al., 2017; Sodeau et al., 2019). This fraction could therefore represent smaller pollen grains such as Urticaceae or similar-sized fungal spores, particularly considering the peak in BC particles noted on the 25th of August, coinciding with the highest observed Urticaceae.

However, notable deviations were observed between the two instruments. This can be attributed to the differing operating principles of the instruments. The enhanced flow rate of the Hirst makes it more efficient at sampling faster moving and larger particles, such particles are unaffected and thus under-sampled by the lower flow rate of the WIBS, resulting in under-sampling of certain bioaerosol fractions by the WIBS. Several laboratory studies have investigated the counting efficiency of the WIBS for particles of varying sizes. In both cases, for the WIBS-4 and the WIBS-NEO, a greater sampling efficiency was determined for smaller particles less than 2 µm (Healy et al., 2012b; Lieberherr et al., 2021b). This means the WIBS-NEO could have under sampled larger particles such as pollen which accounts for the slightly lower ambient concentrations seen for the isolated BC particles when compared to ambient pollen concentrations sampled by the Hirst. The Hirst sampler is designed to constantly align itself with the prevailing wind direction. Consequently, it may as a result provide differing estimates of bioaerosol concentrations in comparison to less wind-orientated samplers like the WIBS (Heffer et al., 2005; Miki et al., 2019). This disparity could potentially account for the absence of specific pollen peak periods observed by the WIBS. It is possible also that other biological and chemical interferents are influencing the analysis – resulting in peaks seen by the WIBS that are not observed by the Hirst.

Although the Hirst represents the standardised method to compare the WIBS-NEO to, it is far from ideal, and various studies have identified several uncertainties (Adamov et al., 2021) such

as significant differences between Hirst samplers positioned close together (Tormo Molina et al., 2013), inaccuracies in calculating flowrate (Oteros et al., 2017), sampling efficiency (Käpylä and Penttinen, 1981; Oteros et al., 2017; Rojo et al., 2019; Šikoparija et al., 2011), and human errors when counting (Cariñanos et al., 2000; Galán et al., 2014). The resulting data also suffers from high degrees of uncertainty due to the limited sample area analysed and use of extrapolation (Galán et al., 2014; Šikoparija et al., 2011). This can lead to an overall measurement uncertainty of at least 30% (Adamov et al., 2021; Gottardini et al., 2009). Uncertainties using the WIBS are less known, due to its limited field use in comparison to the Hirst. By comparing the WIBS to a known and standardised method, limitation of its use in various settings can be identified. Despite several literature investigations evaluating the potential of the WIBS to be used as a real-time monitoring device (compared to the Hirst), little discussion is often given on the relative uncertainties that have appeared in relation to this (Healy et al., 2014; Markey et al., 2022b; O'Connor et al., 2014a; Tummon et al., 2021a). This introduces some concerns regarding the readiness of such a device for pollen monitoring. For one, although the majority of pollen grains sampled during the current WIBS-NEO study (Urticaceae) were within the size limits of the device, the coarser fraction of pollen often exceeds the maximum size range of the WIBS-NEO (30-35 µm). This is mirrored in previous studies that have favoured relatively simple ambient environments with only several dominating pollen types of agreeable sizes such as Yew pollen which is typically seen at sizes less than 27 µm (O'Connor et al., 2014a). As such the WIBS is currently incapable of detecting the full spectrum of ambient pollen within the air. This is a particular issue when considering known allergenic pollen types of concern that typically exist above this range such as Japanese cedar and many species of Poaceae.

The current study as well as other works conducted as part of this PhD (Markey et al., 2022b) have shown that even when additional fluorescent emission bands are added to the WIBS, only broad classes of pollen can be detected. Compared to other popular real-time pollen devices such as the Rapid-E, Poleno and BAA500, which have all been shown to be able to relatively accurately differentiate various pollen taxa, the specificity of the WIBS is greatly limited. Literature studies using the BAA500 have yielded multiclass accuracies of over 90% for the identification of 14 different pollen types ranging from arboreal and herbaceous sources, the lowest accuracies were seen for *Populus* (73%) and *Alnus* (64%) pollen (Oteros et al., 2020). The Rapid-E device has also shown promising results, being able to detect and differentiate 5 of 11 pollen taxa with accuracies of over 80% and has shown robustness and reproducibility in varying locations (Šauliene et al., 2019). Similar studies using the Swisens Poleno has also illustrated promising potential for more in-depth pollen monitoring – being able to identify 6 of 8 pollen taxa with an accuracy exceeding 90% (Sauvageat et al., 2020). Compared to these other methods the WIBS is very limited and has been shown to possess further uncertainties regarding the reproducibility between instruments and model iterations. These other real-time methods operate using various principles as discussed in Chapter 1 with classification of pollen taxa being made in real-time using trained machine learning algorithms. Traditionally, WIBS analysis has favoured a more simplistic and unsupervised approach, however

more recent studies have also investigated the possibility of using similar supervised learning methods, however these too focussed on broad classification of pollen versus other bioaerosol classes (Ruske et al., 2017).

Several studies have also collocated and/or compared a number of real-time devices (Lieberherr et al., 2021a; Maya-Manzano et al., 2023; Tummon et al., 2021a). In one such case where WIBS was included in a pollen monitoring campaign comparing various real-time device to each other and to the Hirst. Limitations were put in place to restrict analysis to total pollen due to the limited specificity of instruments such as the WIBS and KH-3000-01 (Tummon et al., 2021a). In this particular literature investigation, no single device outperformed the rest. Varying degrees of agreement were seen between the real-time devices and the Hirst. This was largely attributed their varying abilities to identify different pollen taxa as well as applying classification algorithms that were not originally developed for total pollen (Tummon et al., 2021a). Aside from this total pollen study, the sole use of the LIF principles used by the WIBS can be considered too restrictive for taxa specific pollen monitoring. As a result, future work will focus on further incorporating additional real-time devices such as the Swisens Poleno into the current Irish pollen network. The Swisens Poleno Jupiter offers the combine benefits of LIF and holography for pollen identification and has illustrated some promising initial results (Ruske et al., 2017).

5.4.3 Potential interferents

Although efforts were made to reduce the impact of interferences, evidence of other contributing factors to the BC pollen-type fraction was noted. Efforts were made to remove other interfering bioaerosols by applying a size filter representative of pollen. However, larger bioaerosols such as large fungal spores like *Alternaria* could be also impacting the analysis. Correlation for the isolated BC fraction and *Alternaria* spores was also observed. This introduces additional uncertainty to the connection between the BC fraction and pollen. It is possible that this BC fraction could be representative of both *Alternaria* and Urticaceae pollen as the highest correlation was seen for the sum of *Alternaria* and total pollen concentration with the BC fraction ($r = 0.8$). However, using the current setup there was no way to further differentiate this fraction.

Improved separation could be achieved with the inclusion of additional fluorescent channels such as those previously suggested, for the detection of chlorophyll (O'Connor et al., 2014b, 2011; Pöhlker et al., 2013). The inclusion of such fluorescence detection channels could aid in the differentiation of grass and other herbaceous pollen such as the major pollen types witnessed during this campaign. Although the presence of chlorophyll in photosynthesising plants is well known, the same is not known for pollen grains. Pollen grains lack the presence of chloroplasts making the presence of chlorophyll unexpected. Despite this, several studies have highlighted the presence of chlorophyll fluorescence when examining the autofluorescence and fluorescent lifetimes of grass and

other herbaceous pollen taxa (O'Connor et al., 2014b, 2011; Pöhlker et al., 2013). Therefore the presence of chlorophyll in these pollen grains can exist in the form of freely bound chlorophyll bound to the pollen cell wall or bound to flavoproteins (O'Connor et al., 2014b; Pöhlker et al., 2013) .

Detecting the presence of chlorophyll and other plant specific fluorophores could further differentiate pollen types from other bioaerosols such as fungal spores since fungal spores do not possess chlorophyll. Another campaign conducted under this PhD project assessed just this (Markey et al., 2022b). A modified WIBS instrument was deployed at a semi-urban site in Saclay, France. The WIBS-4 model was modified to include two additional detection bands (FL4 and FL5) targeted to detect the emission maxima of chlorophyll-a fluorescence (~670 nm) across the wavelength range of 600–750 nm using two excitation sources (280 nm and 370 nm). The study found that the addition of the FL4 and FL5 channels allowed for the improved differentiation between tree (R^2 = 0.8), herbaceous (R^2 = 0.6) and grass (R^2 = 0.4) pollen as well as for fungal spores (R^2 = 0.8).

During this modified WIBS study, the inclusion of this additional fluorescent data also improved unsupervised k-mean clustering possibilities. Earlier investigations dismissed the viability of k-means clustering for WIBS data analysis because it often resulted in groups of similar sizes (Robinson et al., 2013). Nevertheless, a recent demonstration of its effectiveness in distinguishing various pollen types using data from a different fluorescence-based bioaerosol sensor has renewed interest in its potential (Swanson and Huffman, 2018). The incorporation of FL4 and FL5 channels introduced supplementary dimensions that could distinguish between FAPs originating from various sources. This potential enhancement suggests that k-means clustering may be a more suitable approach for analysing WIBS data than previously believed, providing additional fluorescent intensity is included. Markey et al., 2022b found that utilising k-means clustering could present a time-efficient alternative that maintains effective differentiation between pollen and fungal spore concentrations, especially when incorporating the FL4 and FL5 channels. However, due to the lack of additional fluorescent data in this current study, k-means clustering attempts were unsuccessful.

Although the emission channels of the WIBS are selected for the specific detection of biomarkers present in bioaerosols, several studies have highlighted potential interferents that can also contribute to the fluorescence signals in these channels (Savage et al., 2017). Generally, these interferences originate from anthropogenic sources, the presence of which would not be unexpected at the urban sampling location in the heart of Dublin city centre. Such interferents include polycyclic aromatic hydrocarbons (PAH), humic-like substances (HULIS), mineral dust, SOAs and black carbon (Savage et al., 2017; Yue et al., 2016). The effects of potentially interfering aerosols can be reduced by increasing the initial fluorescent threshold - from 3σ to 6σ and 9σ. Increasing the fluorescent threshold in this manner has been shown to significantly reduce the interference from non-biological aerosols but not affect the relative fraction of bioaerosols detected by the WIBS (Savage et al., 2017). Interfering particles linked to the anthropogenic emissions of NO_X, CO and

SO_2 were also observed during this campaign. These particles likely came from combustion-related origins or via SOA formation using these gaseous pollutants. However, increasing the fluorescence threshold and size filter was found to reduce the association between the WIBS FAPs and these suspect combustion-related particles. Although these chemical interferences correlated well with WIBS FAPs at sizes smaller than 2 µm, some chemical interferences such as soil, dust and soot particles have been found to produce aerosols of up to 10 µm in size (Gabey et al., 2011). These particles could potentially interfere with the observed BC FAPs, representing peaks that were not accounted for from comparison to aerobiological data.

5.4.4 Influence of meteorology/air quality on detection

Meteorological conditions such as strong wind speeds have been seen to inhibit the ability of the WIBS to successfully sample pollen (O'Connor et al., 2014a). Spearman correlation analysis between WIBS FAPs and meteorological parameters showed a notable negative correlation with wind speeds, further corroborating this finding. As a result, the sampling efficiency of the WIBS is likely to be greatly inhibited by wind speeds. This was found to be true even at larger particle sizes for BC type particles, thus, improved results were observed when days of moderate wind speed were removed from the analysis. This could be explained by the low flow rate of the WIBS being unable to efficiently capture fast-moving aerosols during periods of high wind speeds. A notable negative correlation between temperature and grass minimum temperature during this period could well be indicative of declining pollen concentrations. One reason for this decline in FAPs could also be related to the significant correlation seen between grass minimum temperature, rain and wind speed which are drivers for the transport and deposition of certain bioaerosols (Brągoszewska and Pastuszka, 2018; Davies and Smith, 1974; Hart et al., 1994; Oliveira et al., 2009). A notable positive correlation was also observed for FAPs detected by the WIBS with pressure. Such trends with pressure have been well documented in past literature for a myriad of pollen and fungal spore types (Kruczek et al., 2017; O'Connor et al., 2014c), potentially indicating a degree of contribution by bioaerosols to the FAP fraction.

Since the WIBS measures the intrinsic fluorescence of a particle, it can detect other particles that are not biological in nature. Considering the urban location of the sampling site, the likelihood of chemical interferents is higher than for previous Irish WIBS campaigns which were mainly conducted in less atmospherically diverse environments. NO_X and its derivatives were the more prevalent of these pollutants recorded during the sampling period. The negative correlations between NO_X, minimum temperature and wind speed as well as the positive correlation with pressure have been noted previously (Arain et al., 2009; Harkey et al., 2015), including in a study from 1998 conducted in Dublin (Delaney and Dowding, 1998). NO_X is strongly associated with the production of SOAs and can be used as a proxy for particulate emissions from both car exhausts and homes/industries. The general diurnal trend witnessed for total FAPs sampled by the WIBS (Figure

5.2 (B)) initially illustrated comparable trends to NO_2 emissions recorded for the same year, with peak periods directly coinciding with increasing NO_2 concentrations seen between 7:00-8:00 (Perillo et al., 2022). Following further analysis, a strong correlation was seen for NO_X and FL1 type particles. Previous studies using LIF techniques have shown similar trends for combustion-type particles (Miyakawa et al., 2015; Yu et al., 2016). A study by Miyakawa et al., (2015) showed that the detection of fluorescent aerosols, which possess similar temporal trends to NO_X indicates the presence of PAHs or their derivatives. These particles were shown to interfere with the selective detection of PBAP using UV-LIF methods, even at larger particle size ranges (Miyakawa et al., 2015). As a result, it can be inferred that the collected FAPs are representative of both ambient bioaerosol and anthropogenic aerosol concentrations.

Only a limited number of research studies have explored the WIBS characterisation of known anthropogenic aerosols. In a specific investigation conducted by Savage et al., 2017, various non-biological samples were examined. The study found that soot-type particles primarily displayed A-type fluorescence, while smoke-type samples were predominantly categorised as B-type particles (Savage et al., 2017). The observed strong correlation observed for AB-type particles and combustion-related pollution such as NO_X and its derivates suggests that some FAPs sampled during the campaign exhibit strong resemblances to the smoke and soot particles generated during wood burning, as identified in the research by Savage et al., 2017.

Another similar study conducted by Yu et al., 2016b investigated the impact of combustion-related particles on the real-time detection of fluorescent aerosols using the WIBS-NEO. It was found that when using LIF instruments like the WIBS near polluted sites (such as a busy city centre), fluorescent measurements experience heavy interference from anthropogenic aerosols, notable for combustion particles such as black carbon. Substantial contributions to the FL1 channel were found for combustion-related particles. Therefore, the correlation witnessed here in Dublin between AB particles and combustion-related sources further supports previous results that some FAPs might originate from anthropogenic/combustions processes (Miyakawa et al., 2015; Toprak and Schnaiter, 2013; Yu et al., 2016). Other interfering aerosols not compared to the WIBS in this study due to the absence of co-located monitoring data such as mineral dust, HULIS-like compounds and other SOAs have also been shown to possess fluorescence and could also be contributing to fluorescent fractions of the sampled WIBS particles (Pöhlker et al., 2012; Savage et al., 2017; Toprak and Schnaiter, 2013).

These findings indicate the potential use of the WIBS as a general air quality monitor that can broadly detect anthropogenic and biological aerosols. To further extend this possibility to PM monitoring a density conversion was applied to all WIBS particles (fluorescent and non-fluorescent) and filtered for particles less than 2.5 µm and 10 µm for comparison with PM2.5 and PM10 measurements. Results correlated reasonably well with PM10 and PM2.5 despite the differences in sampling heights and size fractions sampled by the WIBS. The WIBS underestimated the mass of

PM readings, however, this could be a function of height compared to lower-level PM monitoring devices and the sampling ability of the WIBS. Studies have shown that PM measurements are inversely proportional to sampling height (Ding et al., 2005; Yadav et al., 2013). In this scenario, the influence of meteorological and air quality factors on the performance of the WIBS has highlighted the potential of using the WIBS or future versions as a comprehensive air quality monitoring tool. Such a system could have the capacity to identify and potentially categorise both biological and anthropogenic particles.

5.5 Conclusion

This campaign represents the first real-time pollen monitoring study in Dublin city and aims to investigate possible limitations of the real-time sampler used. The WIBS-NEO was deployed from 07/08/2019 to 16/09/2019 to assess its potential to identify and detect atmospheric concentrations in a relatively complex ambient environment. Although a good correlation was observed for total pollen and WIBS BC particles (>8 μm, at 6σ), the presence of other interferences was apparent. Other larger bioaerosols such as *Alternaria* spores were also associated with these particles. Deviations in WIBS FAP trends also indicate the presence of other interfering particles. This analysis shows that the WIBS-NEO is not exclusively capable of differentiating pollen from these interferences. This is largely due to the limited excitation and emission wavebands used by the WIBS instrument. The inclusion of additional fluorescent detection bands and emission sources could aid in this development and has been shown for other urban sites, such as Paris

Analysis of meteorological and air quality data illustrated the importance of certain conditions on FAP production, some of which showed strong similarities to combustion-related interferences which were also studied. The impact of wind speed on the ability of the WIBS to detect some particles was also observed, increasing wind speed was shown to negatively impact the sampling efficiency of the WIBS. This was especially true for smaller particles, although negative correlations with wind speed were also observed for relatively larger particles. This highlights a potential environmental limitation of the WIBS – especially in areas known to be affected by wind. With regards to potentially interfering non-biological interferences, notable correlations with combustion-related sources and PM (PM2.5 and PM10) were observed. Although these findings could forewarn users against future urban deployment of the WIBS due to the apparent influence of anthropogenic emissions, this might also indicate the possibility of the WIBS extending its applications to general aerosol monitoring (bioaerosol and other). However, further testing is required to fully evaluate the true potential of the WIBS to act as an overall air quality monitoring device

5.6 Future work

Ultimately, the WIBS-NEO instrument was not exclusively capable of undoubtedly identifying pollen concentrations from other biogenic and anthropogenic interferences. It is for that reason that future work should experiment with other instrumentation such as more diverse fluorescent instrumentation or holographic instruments. Initially, work with the WIBS-4+ might be able to further evaluate the ability of the WIBS to differentiate between biological and anthropogenic sources. This model differs by the addition of 2 extra detection bands. Similar work has been carried out by the author previously (Markey et al., 2022b). In an upcoming (currently unpublished) work, the WIBS-4+ was examined for its ability to differentiate between biological and anthropogenic aerosols more specifically than what has been done for the WIBS-NEO, in a semi-urban site in Paris. Promising results were found, indicating the additional channels could also aid in detecting similar combustion-related aerosols (such as black carbon) separately from bioaerosols. It would therefore be interesting if the same could be applied/tested in Dublin – to further examine the environmental applications/limitations of the WIBS family of instruments.

In addition to this, the aerobiology team at DCU (working in conjunction with Met Éireann) has recently gained access and full use of a Swisens Poleno Jupiter. Although the aims currently focus on training the Poleno with representable local pollen samples of known taxa. Work is planned to further examine whether the addition/impact of anthropogenic exposure can vary results obtained by the Poleno. A fraction of this possibility will be explored in Chapter 6, however, training studies using the Poleno will offer a more accurate account of anthropogenic impacts on a more diverse fluorescent instrument, while also examining any changes to holographic characteristics.

References

Adamov, S., Lemonis, N., Clot, B., Crouzy, B., Gehrig, R., Graber, M.J., Sallin, C., Tummon, F., 2021. Aerobiologia (Bologna). 5.

Arain, M.A., Blair, R., Finkelstein, N., Brook, J., Jerrett, M., 2009. Can. Geogr. 53, 165–190.

Brągoszewska, E., Pastuszka, J.S., 2018. Aerobiologia (Bologna). 34, 241–255.

Cariñanos, P., Emberlin, J., Galán, C., Dominguez-Vilches, E., 2000. Aerobiologia (Bologna). 16, 339–346.

Clot, B., Gilge, S., Hajkova, L., Magyar, D., Scheifinger, H., Sofiev, M., Bütler, F., Tummon, F., 2020. Aerobiologia (Bologna). 4.

Davies, R.R., Smith, L.P., 1974. Clin. Allergy 4, 95–108.

Delaney, C., Dowding, P., 1998. The relationship between extreme nitrogen oxide (NO(x)) concentrations in Dublin's atmosphere and meteorological conditions. Environ. Monit. Assess.

Ding, G., Chan, C., Gao, Z., Yao, W., Li, Y., Cheng, X., Meng, Z., Yu, H., Wong, K., Wang, S., Miao, Q., 2005. Sci. China, Ser. D Earth Sci. 48, 38–54.

EPA Ireland, 2021. Secure Arcive for Environmental Research Data [WWW Document]. URL https://eparesearch.epa.ie/safer/ (accessed 12.15.21).

Fennelly, M., Gallagher, C., Harding, M., Hellebust, S., Wenger, J., O'Sullivan, N., O'Connor, D., Prentice, M., 2022. J. Dent. 120, 104092.

Fennelly, M., Hellebust, S., Wenger, J., O'Connor, D., Griffith, G.W., Plant, B.J., Prentice, M.B., 2023. J. Hosp. Infect. 131, 54–57.

Fennelly, M., Keane, J., Dolan, L., Plant, B.J., O'Connor, D.J., Sodeau, J.R., Prentice, M.B., 2021. J. Hosp. Infect. 110, 108–113.

Fernández-Rodríguez, S., Tormo-Molina, R., Lemonis, N., Clot, B., O'Connor, D.J., Sodeau, J.R., 2018. Atmos. Environ. 175, 1–14.

Forde, E., Gallagher, M., Walker, M., Foot, V., Attwood, A., Granger, G., Sarda-Estève, R., Stanley, W., Kaye, P., Topping, D., 2019. Atmosphere (Basel). 10, 1–29.

Gabey, A.M., Stanley, W.R., Gallagher, M.W., Kaye, P.H., 2011. Atmos. Chem. Phys. 11, 5491–5504.

Galán, C., Smith, M., Thibaudon, M., Frenguelli, G., Oteros, J., Gehrig, R., Berger, U., Clot, B., Brandao, R., 2014. Aerobiologia (Bologna). 30, 385–395.

Gottardini, E., Cristofolini, F., Cristofori, A., Vannini, A., Ferretti, M., 2009. J. Environ. Monit. 11, 751–755.

Gross, J., Ligges, U., 2015. nortest: Tests for Normality.

Harkey, M., Holloway, T., Oberman, J., Scotty, E., 2015. J. Geophys. Res. Atmos. 120, 11,775-11,797.

Hart, M.L., Wentworth, J.E., Bailey, J.P., 1994. Grana 33, 100–103.

Healy, D.A., Huffman, J.A., O'Connor, D.J., Pöhlker, C., Pöschl, U., Sodeau, J.R., 2014. Atmos. Chem. Phys. 14, 8055–8069.

Healy, D.A., O'Connor, D.J., Burke, A.M., Sodeau, J.R., 2012a. Atmos. Environ. 60, 534–543.

Healy, D.A., O'Connor, D.J., Sodeau, J.R., 2012b. J. Aerosol Sci. 47, 94–99.

Heffer, M.J., Ratz, J.D., Miller, J.D., Day, J.H., 2005. Aerobiologia (Bologna). 21, 233–239.

Hernandez, M., Perring, A.E., McCabe, K., Kok, G., Granger, G., Baumgardner, D., 2016. Atmos. Meas. Tech. 9, 3283–3292.

Hughes, D.D., Mampage, C.B.A., Jones, L.M., Liu, Z., Stone, E.A., 2020. Environ. Sci. Technol. Lett. 7, 409–414.

Käpylä, M., Penttinen, A., 1981. Grana 20, 131–141.

Kolokolnikov, I., Nepomnyashchaya, E., Velichko, E., 2019. J. Phys. Conf. Ser. 1410.

Kosisky, S.E., Marks, M.S., Nelson, M.R., 2010. J. Allergy Clin. Immunol. 125, AB16.

Kruczek, A., Puc, M., Wolski, T., 2017. Grana 56, 71–80.

Lieberherr, G., Auderset, K., Calpini, B., Clot, B., Crouzy, B., Gysel-Beer, M., Konzelmann, T., Manzano, J., Mihajlovic, A., Moallemi, A., O'connor, D., Sikoparija, B., Sauvageat, E., Tummon, F., Vasilatou, K., 2021a. Atmos. Meas. Tech. 14, 7693–7706.

Lieberherr, G., Auderset, K., Calpini, B., Clot, B., Crouzy, B., Gysel-Beer, M., Konzelmann, T., Manzano, J., Mihajlovic, A., Moallemi, A., O'Connor, D., Sikoparija, B., Sauvageat, E., Tummon, F., Vasilatou, K., 2021b. Atmos. Meas. Tech. Discuss. 1–21.

del Mar Trigo, M., Cabezudo, B., Recio, M., Toro, F.J., 1996. Aerobiologia (Bologna). 12, 85–90.

Markey, E., Clancy, J.H., Martínez-Bracero, M., Maya-Manzano, J.M., Smith, M., Skjøth, C., Dowding, P., Sarda-Estève, R., Baisnée, D., Donnelly, A., McGillicuddy, E., Sewell, G., O'Connor, D.J., 2022a. Aerobiologia (Bologna). 38, 343–366.

Markey, E., Hourihane Clancy, J., Martínez-Bracero, M., Neeson, F., Sarda-Estève, R., Baisnée, D., McGillicuddy, E.J., Sewell, G., O'Connor, D.J., 2022b. Sensors 22, 8747.

Maya-Manzano, J.M., Tummon, F., Abt, R., Allan, N., Bunderson, L., Clot, B., Crouzy, B., Daunys, G., Erb, S., Gonzalez-Alonso, M., Graf, E., Grewling, Ł., Haus, J., Kadantsev, E., Kawashima, S., Martinez-Bracero, M., Matavulj, P., Mills, S., Niederberger, E., Lieberherr, G., Lucas, R.W., O'Connor, D.J., Oteros, J., Palamarchuk, J., Pope, F.D., Rojo, J., Šaulienė, I., Schäfer, S., Schmidt-Weber, C.B., Schnitzler, M., Šikoparija, B., Skjøth, C.A., Sofiev, M., Stemmler, T., Triviño, M., Zeder, Y., Buters, J., 2023. Sci. Total Environ. 866.

Miki, K., Kawashima, S., Clot, B., Nakamura, K., 2019. Atmos. Environ. 203, 18–27.

Miyakawa, T., Kanaya, Y., Taketani, F., Tabaru, M., Sugimoto, N., Ozawa, Y., Takegawa, N., 2015. J. Geophys. Res. Atmos. 120, 1171–1185.

O'Connor, D.J., Healy, D.A., Hellebust, S., Buters, J.T.M., Sodeau, J.R., 2014a. Aerosol Sci. Technol. 48, 341–349.

O'Connor, D.J., Healy, D.A., Sodeau, J.R., 2013. Atmos. Environ. 80, 415–425.

O'Connor, D.J., Healy, D.A., Sodeau, J.R., 2015. Aerobiologia (Bologna). 31, 295–314.

O'Connor, D.J., Iacopino, D., Healy, D.A., O'Sullivan, D., Sodeau, J.R., 2011. Atmos. Environ. 45, 6451–6458.

O'Connor, D.J., Lovera, P., Iacopino, D., O'Riordan, A., Healy, D.A., Sodeau, J.R., 2014b. Anal. Methods 6, 1633–1639.

O'Connor, D.J., Sadyś, M., Skjøth, C.A., Healy, D.A., Kennedy, R., Sodeau, J.R., 2014c. Aerobiologia (Bologna). 30, 397–411.

Oliveira, M., Ribeiro, H., Delgado, J.L., Abreu, I., 2009. Int. J. Biometeorol. 53, 61–73.

Oteros, J., Buters, J., Laven, G., Röseler, S., Wachter, R., Schmidt-Weber, C., Hofmann, F., 2017. Aerobiologia (Bologna). 33, 201–210.

Oteros, J., Weber, A., Kutzora, S., Rojo, J., Heinze, S., Herr, C., Gebauer, R., Schmidt-Weber, C.B., Buters, J.T.M., 2020. Environ. Res. 191, 110031.

Pacini, E., 2000. Plant Syst. Evol. 222, 19–43.

Pereira, S.G., Guedes, A., Abreu, I., Ribeiro, H., 2021. Aerobiologia (Bologna). 37, 15–28.

Perillo, H.A., Broderick, B.M., Gill, L.W., McNabola, A., Kumar, P., Gallagher, J., 2022. Sci. Total Environ. 827, 154299.

Perring, A.E., Schwarz, J.P., Baumgardner, D., Hernandez, M.T., Spracklen, D. V., Heald, C.L., Gao, R.S., Kok, G., McMeeking, G.R., McQuaid, J.B., Fahey, D.W., 2015. J. Geophys. Res. Atmos. 120, 1153–1170.

Pöhlker, C., Huffman, J.A., Pöschl, U., 2012. Atmos. Meas. Tech. 5, 37–71.

Pöhlker, C., Huffman, J.A., Pöschl, U., 2013. Atmos. Meas. Tech. 6, 3369–3392.

Robinson, N.H., Allan, J.D., Huffman, J.A., Kaye, P.H., Foot, V.E., Gallagher, M., 2013. Atmos. Meas. Tech. 6, 337–347.

Rojo, J., Oteros, J., Pérez-Badia, R., Cervigón, P., Ferencova, Z., Gutiérrez-Bustillo, A.M., Bergmann, K.C., Oliver, G., Thibaudon, M., Albertini, R., Rodríguez-De la Cruz, D., Sánchez-Reyes, E., Sánchez-Sánchez, J., Pessi, A.M., Reiniharju, J., Saarto, A., Calderón, M.C., Guerrero, C., Berra, D., Bonini, M., Chiodini, E., Fernández-González, D., García, J., Trigo, M.M., Myszkowska, D., Fernández-Rodríguez, S., Tormo-Molina, R., Damialis, A., Kolek, F., Traidl-Hoffmann, C., Severova, E., Caeiro, E., Ribeiro, H., Magyar, D., Makra, L., Udvardy, O., Alcázar, P., Galán, C., Borycka, K., Kasprzyk, I., Newbigin, E., Adams-Groom, B., Apangu, G.P., Frisk, C.A., Skjøth, C.A., Radišić, P., Šikoparija, B., Celenk, S., Schmidt-Weber, C.B., Buters, J., 2019. Environ. Res. 174, 160–169.

Ruske, S., Topping, D.O., Foot, V.E., Kaye, P.H., Stanley, W.R., Crawford, I., Morse, A.P.,

Gallagher, M.W., 2017. Atmos. Meas. Tech. 10, 695–708.

Šauliene, I., Šukiene, L., Daunys, G., Valiulis, G., Vaitkevičius, L., Matavulj, P., Brdar, S., Panic, M., Sikoparija, B., Clot, B., Crouzy, B., Sofiev, M., 2019. Atmos. Meas. Tech. 12, 3435–3452.

Sauvageat, E., Zeder, Y., Auderset, K., Calpini, B., Clot, B., Crouzy, B., Konzelmann, T., Lieberherr, G., Tummon, F., Vasilatou, K., 2020. Atmos. Meas. Tech. 13, 1539–1550.

Savage, N.J., Krentz, C.E., Könemann, T., Han, T.T., Mainelis, G., Pöhlker, C., Alex Huffman, J., 2017. Atmos. Meas. Tech. 10, 4279–4302.

Ŝikoparija, B., Pejak-Ŝikoparija, T., Radiŝić, P., Smith, M., Soldevilla, C.G., 2011. J. Environ. Monit. 13, 384–390.

Sodeau, J., O'connor, D., Feeney, P., Quirke, M., Daly, S., Fennelly, M., Buckley, P., Hellebust, S., McGillicuddy, E., Wenger, J., 2019. Online Bioaerosol Sensing (OLBAS).

Sofiev, M., 2019. Aerobiologia (Bologna). 35, 523–531.

Sorsa, P., Huttunen, P., 1975. Ann. Bot. Fenn. 12, 165–182.

Swanson, B.E., Huffman, J.A., 2018. Opt. Express 26, 3646.

The Irish National Meteorological Service [WWW Document], 2023. URL https://www.met.ie/climate/available-data/daily-data (accessed 9.12.23).

Toprak, E., Schnaiter, M., 2013. Atmos. Chem. Phys. 13, 225–243.

Tormo Molina, R., Maya Manzano, J.M., Fernández Rodríguez, S., Gonzalo Garijo, Á., Silva Palacios, I., 2013. Grana 52, 59–70.

Tummon, F., Adamov, S., Clot, B., Crouzy, B., Gysel-Beer, M., Kawashima, S., Lieberherr, G., Manzano, J., Markey, E., Moallemi, A., O'Connor, D., 2021a. Aerobiologia (Bologna). 0.

Tummon, F., Arboledas, L.A., Bonini, M., Guinot, B., Hicke, M., Jacob, C., Kendrovski, V., McCairns, W., Petermann, E., Peuch, V.H., Pfaar, O., Sicard, M., Sikoparija, B., Clot, B., 2021b. Clin. Transl. Allergy 11.

Twohy, C.H., McMeeking, G.R., DeMott, P.J., McCluskey, C.S., Hill, T.C.J., Burrows, S.M., Kulkarni, G.R., Tanarhte, M., Kafle, D.N., Toohey, D.W., 2016. Atmos. Chem. Phys. 16, 8205–8225.

Walshe, N., Fennelly, M., Hellebust, S., Wenger, J., Sodeau, J., Prentice, M., Grice, C., Jordan, V., Comerford, J., Downey, V., Perrotta, C., Mulcahy, G., Sammin, D., 2021. Front. Public Heal. 9.

Yadav, A.K., Sahoo, S.K., Kumar, A.V., Pandey, G., 2013. Int. Res. J. Environ. Sci. Int. Sci. Congr.

Assoc. 2, 19–24.

Yu, X., Wang, Z., Zhang, M., Kuhn, U., Xie, Z., Cheng, Y., Pöschl, U., Su, H., 2016. Atmos. Chem. Phys. 16, 11337–11348.

Yue, S., Ren, H., Fan, S., Sun, Y., Wang, Z., Fu, P., 2016. Sci. Rep. 6, 1–10.

Chapter 6: Spectroscopic and Surface Analysis of Pollen – A Lab Study

6.1 Introduction

Aerobiology is reliant on the time-consuming and accurate identification of pollen grains which is made worse by the delays incurred by the traditional volumetric Hirst method. This has led to the advent of various real-time devices based on a variety of methods such as image recognition, fluorescence, light scatter or a mixture of all these parameters (Crouzy et al., 2016; Erb et al., 2023; Kawashima et al., 2007; O'Connor et al., 2014c, 2014a; Oteros et al., 2020; Šauliene et al., 2019). Essentially, two criteria exist for the evaluation of such methods: (i) comparable identification quality to traditional methods and (ii) timely output availability (Depciuch et al., 2018). In all cases, these traditional and real-time methods are limited to higher taxonomic levels such as families of pollen, as genus and species-level identification are often not possible. This level of identification offers several drawbacks such as not being able to differentiate between pollen species that are optically inseparable but have differences in allergenicity – such as Urticaceae (Vega-Maray et al., 2006), Cupressaceae (Barberini et al., 2015) and even Poaceae (Jung et al., 2018). Identifying grass pollen at the genus level holds significant importance as it has been shown that different genera can vary in their capacity to induce allergic reactions (Hrabina et al., 2008; Jung et al., 2018; De Weger et al., 2011). As pollen allergies continue to rise and pollen seasons worsen (D'Amato et al., 2007) the identification of allergenic pollen species becomes more vital and thus the identification resolutions of available instruments should increase. Therefore, there is a clear need for more sensitive methods of pollen monitoring (Kraaijeveld et al., 2015). To date, this level of analysis has largely been conducted using various molecular methods and has been shown to greatly improve the possibility of detecting invasive species, plant pathogens as well as specific clinically relevant allergenic species of pollen and fungal spores (Banchi et al., 2020). However, these molecular methods can be costly and require biochemical training and expensive equipment (Zimmerman et al., 2016).

These problems can be solved by Fourier transform infrared spectroscopy (IR). One major advantage of using IR for pollen analysis is the quick analysis and no need for any pre-treatment steps or extractions (Zimmermann, 2018). As previously mentioned in Chapter 2, IR is used to measure the vibrations of different chemical functional groups within a sample. Absorbances at different infrared wavelengths are indicative of vibrational frequencies of different chemical bonds, providing information on the chemical composition of the sample. Vibrational spectroscopic analysis of pollen offers an alternative approach to pollen differentiation by providing detail on a pollen's biochemical 'fingerprint'. The resulting spectra detail the presence of lipids, proteins, carbohydrates, water etc. (Kenđel and Zimmermann, 2020). IR has been used extensively in recent years for the analysis and differentiation of pollen samples and has achieved more accurate classification (species level) than optical microscopy and real-time devices (Depciuch et al., 2018; Diehn et al., 2020; Zimmerman et al., 2016). The detailed compositional changes that are not apparent from microscopic analysis of pollen grains also provide information on environmental conditions experienced by the samples. Spectroscopic studies have highlighted the differing spectral features of pollen exposed to

adverse conditions such as heat stress (Lahlali et al., 2014), urban pollution (Depciuch et al., 2017, 2016; Zhao et al., 2016) as well as differences between the same pollen types sampled from varying locations (Bağcıoğlu et al., 2017; Zimmermann et al., 2017) and different years (Bağcıoğlu et al., 2017).

While changes in pollen chemical composition have been linked to exposure to air pollution and different levels of urbanisation, this work has mainly focussed on the effects of gaseous pollutants. Several studies have investigated the effects of pollution on the IR spectral properties of pollen (Depciuch et al., 2017, 2016; Zhao et al., 2016). These studies have largely focussed on sampling pollen from unpolluted and polluted environments and comparing spectral features – concluding any differences to be the result of anthropogenic exposure. However, the degree of these differences is also likely influenced by changes in location – which has been shown to exist when devoid of pollution exposure. To further investigate the chemical and structural changes that occur to pollen grains following release and transport in a polluted environment, a series of lab studies were conducted. This has focussed on exposing pollen to various gaseous (ozone and car fumes), particulate (ash and dust exposure) and environmental (hydration) conditions and analysing any changes that are noted.

To further examine the changes that can occur under different conditions/environments, samples were also analysed using fluorescent confocal microscopy. This section of the study is aimed at assessing whether changes in pollen fluorescence, as a result of environmental conditions, have the potential to impact current real-time detection methods (that use LIF), such as the Poleno and WIBS. Although initial evaluations of current real-time instruments offer promising results, it is vital to continue to fully understand the capabilities of these technologies in differing environments. Conclusions from the previous real-time chapter (Chapter 5), highlight the potential interferences and limitations of such real-time techniques in adverse and urban environments.

6.2 Methods

6.2.1 Pollen samples

Pollen samples for IR analysis were either purchased from Bonapol or collected from local foliage surrounding the DCU campus/nearby North Dublin area. A detailed description of each pollen used is provided in Table 6.1. Efforts were made to speciate the pollen types being collected, where possible. If any doubts remained, taxonomical identification was made to the genus level (denoted as sp.).

Table 6.1: Pollen samples used in IR analysis and source

Pollen Sample	**Sourced**
Alnus glutinosa (L.) Gaertn.	Collected in Dublin
Betula pendula L.	Collected in Dublin
Corylus sp.	Collected in Dublin
Fraxinus excelsior L.	Bonapol
Lolium perenne L.	Bonapol
Pinus sp.	Collected in Dublin
Plantago lanceolata L.	Bonapol
Platanus x acerifolia (Aiton) Willd.	Bonapol
Quercus robur L.	Bonapol
Taxus baccata L.	Bonapol
Urtica dioica L.	Collected in Dublin

The collection and storage procedures used for both tree and grass/herbaceous pollen samples collected from the Dublin area are discussed in detail in Chapter 2.

For IR and fluorescence analysis of exposed samples, *Betula pendula* samples were chosen for the study. *Betula* pollen was chosen due to its allergenic prevalence across Europe and elsewhere. Considerable quantities could also be collected rather easily compared to other allergenic pollen taxa such as Poaceae. *Betula* pollen was collected near Dowth Avenue (53°21'34.5"N 6°17'13.0"W) in North Dublin at the onset of inflorescence and used for all exposure scenarios.

6.2.2 *Betula pendula* exposure scenarios

Control Pollen

Control pollen refers to the pollen sampled directly from the catkin, devoid of any heat treatment or exposure as per the standard method given in chapter 2.

Hydrated Pollen

A small sample of *Betula* was hydrated using a similar method to Castro et al., 2010 - by placing it on a wet filter paper and incubating for 1 hour at 30°C. The original method proposed a 30-minute incubation period. However, following microscopic analysis of the hydrated sample at the 30-minute mark, it was clear that the sample was not yet fully hydrated and so the incubation time was extended until the *Betula* pollen had a notable full-hydrated appearance.

Dried Pollen

A sample of *Betula* pollen was dried on a filter paper overnight at 30°C to ensure excess water removal with no changes in pollen surface structure or composition, that may arise at higher temperatures.

Pollen exposed to dust/ashes

Pollen samples were exposed to known ash samples generated in the lab/obtained from suppliers. A small sample of pollen followed by a small sample of ash (wood ash, turf ash or coal ash – generated by combustion of known fuel sources) or dust (Saharan dust obtained from Swisens) were added to a small sample tube and agitated for 10 minutes to promote mixing. Following this, the polluted pollen samples were examined under light microscopy to ensure coagulation of particulates had taken place. The removal of unbound ash/dust was aided by sieving smaller particles from the contaminated sample before analysis. To produce pollen grains that the majority of which contained at least 1-2 adsorbed particulates, an excess of dust/ash was required – far exceeding typical ambient concentrations. This was done to ensure the majority of pollen grains tested were representative of a "polluted *Betula* pollen grain" which has been shown to carry on average of 2 ± 1 particles per grain (Choël et al., 2022a).

Pollen exposed to O_3

Samples of unexposed (control) and exposed *Betula pendula* pollen were obtained from collaborators at the University of Lille, France. Pollen originally collected in 2019 was exposed to O_3 at concentrations of 130±5 ppb for 16 hours. In this case, the control pollen used was a pre-exposed sample of *Betula pendula* from Lille.

Pollen exposed to Car exhaust fumes

A sample of *Betula* pollen was also placed into a sample chamber and exposed directly to a petrol car exhaust for 10 minutes. After which the pollen sample was collected and later evaporated at 30 degrees for up to 2 hours to remove any heavy moisture from the sample introduced during exposure – to more accurately mimic ambient exposed pollen.

6.2.3 IR spectroscopy and data analysis

IR spectra were acquired using an ATR IR spectrometer and the resulting spectra were pre-processed using Savitzky Golay EMSC, as previously detailed in Chapter 2.

Pre-processed spectral data were utilised to examine the chemical/compositional similarities among the individual pollen samples (general comparison of different pollen types as well as comparison of control *Betula* pollen to exposed samples), this was done by employing principal component analysis (PCA) and hierarchical clustering (HAC). HAC analysis and dendrograms were constructed using the Euclidean distance matrix measurements and Ward distance (Zimmermann et al., 2015b).

Typically, PCA was applied to non-derivatised data for comparison to average spectra – in order to determine areas of interest from principal component loading values. HAC was then applied to the more complex derivatised data. Although the derivatised spectra can be difficult to visually critique compared to the non-derivatised spectra, they offer several benefits. Derivatisation typically enhances peak resolution and improves sensitivity which can make small spectral differences more apparent and is favoured for clustering. These processing and data analytics steps were adopted from various studies by the Zimmermann research group, who have extensively analysed pollen and fungal spores by IR (Kenđel and Zimmermann, 2020; Zimmermann, 2018; Zimmermann et al., 2015a, 2015b; Zimmermann and Kohler, 2014).

All processing and data analytic steps were carried out using R.

6.2.4 Sample imaging – fluorescence microscopy

Pollen exposed to various conditions was further analysed with a Leica sted super-resolution confocal microscope using a 405nm excitation laser and 410-750 nm emission range. The resulting images were further analysed using ImageJ software by Fiji. A more detailed description of these processes is provided in Chapter 2.

The intensity of autofluorescence of the pollen grain surfaces was calculated as the mean intensity per unit area of the extracted pollen grain using maximum projections from Z-stack images. The fluorescence intensity of each sample type (n=40 pollen grains) was plotted in the form of box plots using R software and ggplot2 package. The normality of sample types was also assessed using

the Shapiro-Wilks test. Overall, all datasets were found to contain at least one variable illustrating non-normal distributions, as a result, non-parametric comparison tests were used to compare the differing sample fluorescence intensities to each other and a control (pure-unexposed pollen) sample. Differences between sample fluorescence were analysed using the Kruskal- Wallis test and followed by a Dunn's test for multiple pairwise comparisons. While the Kruskal-Wallis test is used to determine whether there are statistically significant differences between two or more groups, it does not specifically describe which groups are significantly different from each other. In essence, the Dunn's test can be considered as an extension or a post hoc test to be used following the rejection of a Kruskal-Wallis test and involves performing pairwise comparisons between each independent group to determine which groups are statistically significantly different. In some cases, only two samples could be compared (exposed: (ozone or car exhaust exposed pollen), and unexposed pollen), in this case, the Mann-Whitney U test was used for the pairwise comparison.

6.3 Results and Discussion

6.3.1 Comparison of various pollen taxa by IR spectra

Throughout literature, the use of vibrational spectroscopy for the analysis of the chemical composition of pollen has been well documented. Studies have favoured analysing a wide variety of species and taxa of both pollen and fungal spores (Bağcıoğlu et al., 2017; Baʇcioʇlu et al., 2015; Kenđel and Zimmermann, 2020; Zimmerman et al., 2016; Zimmermann et al., 2015b) as well as individual studies on select pollen types, including Poaceae (Diehn et al., 2020), *Betula* (Depciuch et al., 2018), *Corylus* (Depciuch et al., 2017), *Ambrosia* (Zhao et al., 2016) and *Artemisia* (Depciuch et al., 2016) pollen, from a myriad of locations/environments. Several studies have even utilised IR-microscopy to probe the differences that exist between the composition of differing parts/orientations of individual saccate pollen grains (Zimmermann et al., 2015a). During this current study, an initial replication of such work was carried out to assess the ability of IR analysis to differentiate between 11 of the most common pollen taxa present in the Irish environment and to determine the spectral features responsible for such differentiation.

The IR spectra of each pollen sample were investigated for the presence of various spectral features between 800-1900 cm^{-1}. Within this spectral range, various regions can be attributed to the presence of different components such as lipids, carbohydrates, proteins and sporopollenin units (Zhao et al., 2016). The appearance and general ratios of these signals are the defining features used to differentiate between various pollen types. However, before discussing the regions of importance between the 11 pollen types samples, a general overview of IR band identifications will be covered to highlight typical pollen band allocations. The provided IR spectra for *Quercus robur* will be taken as an example, as seen in Figure 6.1. The *Quercus* sample was chosen for this analysis as it contained a wide variety of spectral bands seen in many of the other arboreal and herbaceous pollen samples.

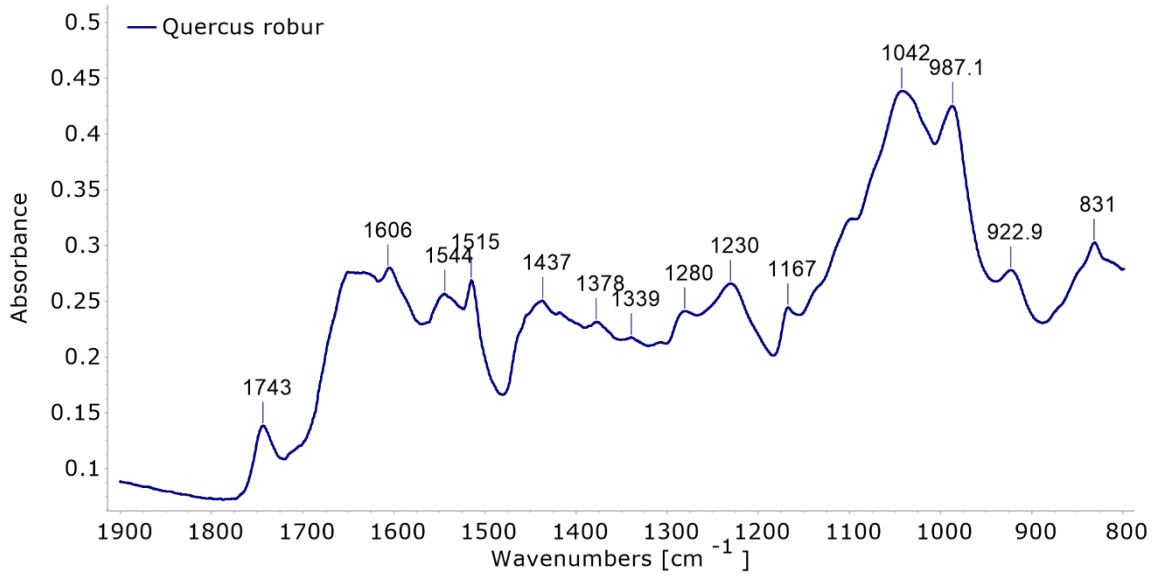

Figure 6.1: IR spectra obtained from the ATR analysis of Quercus robur pollen

The region between 1800-1500 cm^{-1} indicates the presence of C=C and carbonyl groups. The peak seen at 1743 cm^{-1} corresponds to the carbonyl vibration of esters (Lahlali et al., 2014; Pappas et al., 2003), indicating the presence of intracellular lipids (Depciuch et al., 2016; Zimmermann, 2010). The next peak appearing is a broad band seen at 1640-1606 cm^{-1}. This band likely represents multiple overlapping bands resulting from the presence of C=C and carboxylate groups ($-COO^-$) (Pappas et al., 2003; Prdun et al., 2021). However, this band can also be attributed to the presence of proteins via C=O amide stretches and/or H-O-H vibrations (deformation) from water (Ba‡cio‡lu et al., 2015; Mularczyk-Oliwa et al., 2012; Prdun et al., 2021). The next band at 1544 cm^{-1} is likely comprised of N–H bending and C–N stretching from the presence of proteins (Depciuch et al., 2016; Hong et al., 2021; Prdun et al., 2021). The band in the region of 1437 cm^{-1} comes as a result of CH_2 bending and, CH_3 deformations (Bağcıoğlu et al., 2017; Gottardini et al., 2007; Zimmerman et al., 2016) belonging to lipid, protein and carbohydrate fractions (Zimmermann, 2018, 2010). The next band at 1378 cm^{-1} indicates the presence of OH, COH, COO-, CH_3 bending and CH_2 wagging/twisting (Mularczyk-Oliwa et al., 2012), commonly resulting from the presence of sporopollenin in conjunction with several other bands (Ba‡cio‡lu et al., 2015). The band at 1230 cm^{-1} is assigned to the presence of –OH in-plane bending as well as C–O stretching vibrations from ester and amide carboxyl groups (Pappas et al., 2003; Zimmermann, 2010). Several bands can also be indicative of aromatic ring vibrations – mainly seen at 1515, 1167 and 831 cm^{-1} (Zimmermann and Kohler, 2014). The final few bands at 1042 cm^{-1} and 987 cm^{-1}correspond to the stretching vibrations of C–OH and C–O–C groups present in carbohydrates, whereas the bands at 922 cm^{-1} and 830 cm^{-1} are indicative of b-glycosidic bonds and a-glycosidic bonds, respectively (Ba‡cio‡lu et al., 2015; Pappas et al., 2003). As such, this final arrangement of bands can be correlated with the presence of carbohydrates and sugars.

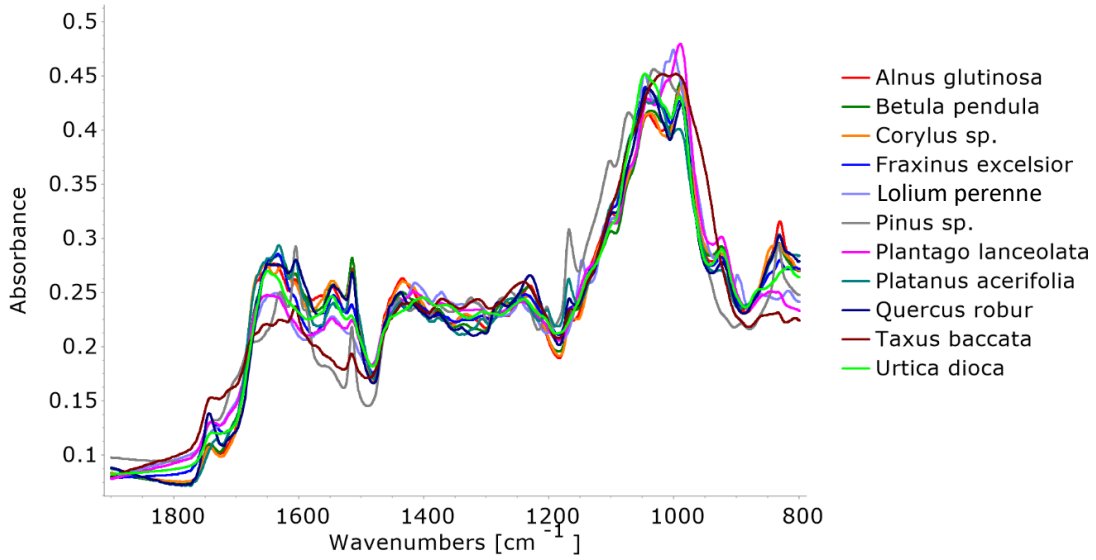

Figure 6.2: Combined spectra of various pollen samples investigated by IR-ATR analysis

The majority of pollen samples investigated contain varying magnitudes of these vibrational bands which can be seen in the combined spectrum shown in Figure 6.2. Analysis of individual pollen taxa can be found in Appendix D (Figure D1 –D11). It can be seen that generally speaking the composition of various pollen species can be considered to be relatively consistent. Although the majority of grouped samples illustrate similar compositional features there are notable differences seen for *Taxus baccata* and *Pinus* pollen. They both illustrate notable absences of bands at ~1540 cm^{-1} which is seen in the majority of other samples. Similar spectral trends have been seen for other *Taxus* (Zimmermann, 2010) and *Pinus* species (Zimmermann et al., 2015a) and are related to changes in protein composition, specifically the amide II band. Additional differences between the spectra of the various pollen types can be further identified by examining the PCA (Figure 6.3) and princip component (PC) loading plots (Diehn et al., 2020). Figure 6.4 shows the loadings of the first and second PCs which explained over 73% of the total variance between the pollen samples. The PCA applied to the IR data reveals that the primary differences between spectra arise from fluctuations in the bands linked to proteins, carbohydrates, and sporopollenin (Kenđel and Zimmermann, 2020).

From an examination of the PCA biplot in Figure 6.3, it can be seen that *Pinus*, *Taxus*, *Lolium*, *Plantago* and *Urtica* pollen all show mostly positive score values with PC1, and the remaining pollen types all show negative values with PC1. In comparison, *Quercus*, *Platanus*, *Pinus* and the majority of *Fraxinus* pollen show positive score values with PC2, with the remaining pollen samples illustrating negative values. Similarities between the pollen samples within the Betulaceae family (*Alnus, Betula* and *Corylus*) were also visible which all show strong negative values with PC1, and neutral values with PC2 and are clustered close together. It has been shown previously that pollen from the same family share common chemical features (Kenđel and Zimmermann, 2020). Similarities are also witnessed for *Platanus* and *Quercus* pollen and to a lesser extent for *Plantago*

and *Lolium* pollen. Loading plots can be used to determine the contributing factors to each PC and have been used in this manner for several pollen analysis studies (Zhao et al., 2016; Zimmermann et al., 2015a, 2015b). According to the loadings plots (Figure 6.4), the most prominent differences (seen as intense peaks) between the spectra exist in the ~1605-1700 cm^{-1} (PC1), ~1500-1600 cm^{-1} (PC1) and 1475 cm^{-1} (PC2) regions which are mainly assigned to differences in protein compositions (Diehn et al., 2020; Kenđel and Zimmermann, 2020). Changes associated with sporopollenin structure were also witnessed for areas close to 1605 cm^{-1} (PC2), 1169 cm^{-1} (PC2) and 833.5 cm^{-1} (PC2). Many of these sporopollenin bands are associated with phenyl ring vibrations (Kenđel and Zimmermann, 2020). Weaker changes in carbohydrate and lipid content were also observed at ~920 cm^{-1} (PC2), ~833.5 cm^{-1} (PC1 and PC2), and ~1741 cm^{-1} (PC1 and PC2) etc. Overall, it can be seen that PC1 mainly led to the differentiation of pollen samples based on protein content and composition, whereas PC2 was more strongly influenced by changes in the sporopollenin structure. Although the exact chemical composition of sporopollenin has yet to be clarified in literature, it is known to be a biopolymer, made of phenylpropanoid sub-units (Blokker et al., 2006), which are linked to UV-B protection. The composition of which is also known to vary depending on species-specific production pathways (Baıcioılu et al., 2015), further corroborating the differential power found in this study.

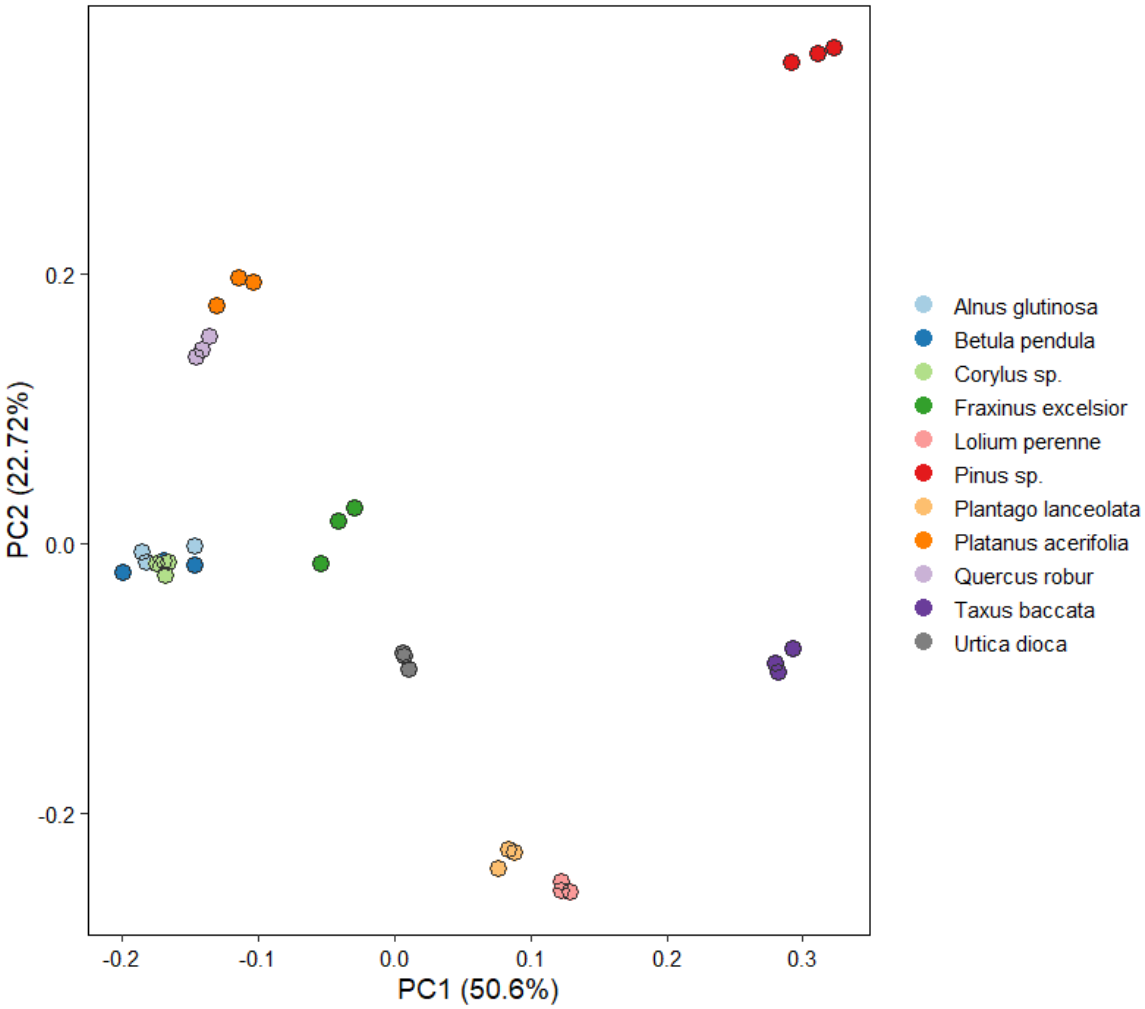

Figure 6.3: PCA biplot of 11 pollen species analysed by IR-ATR analysis

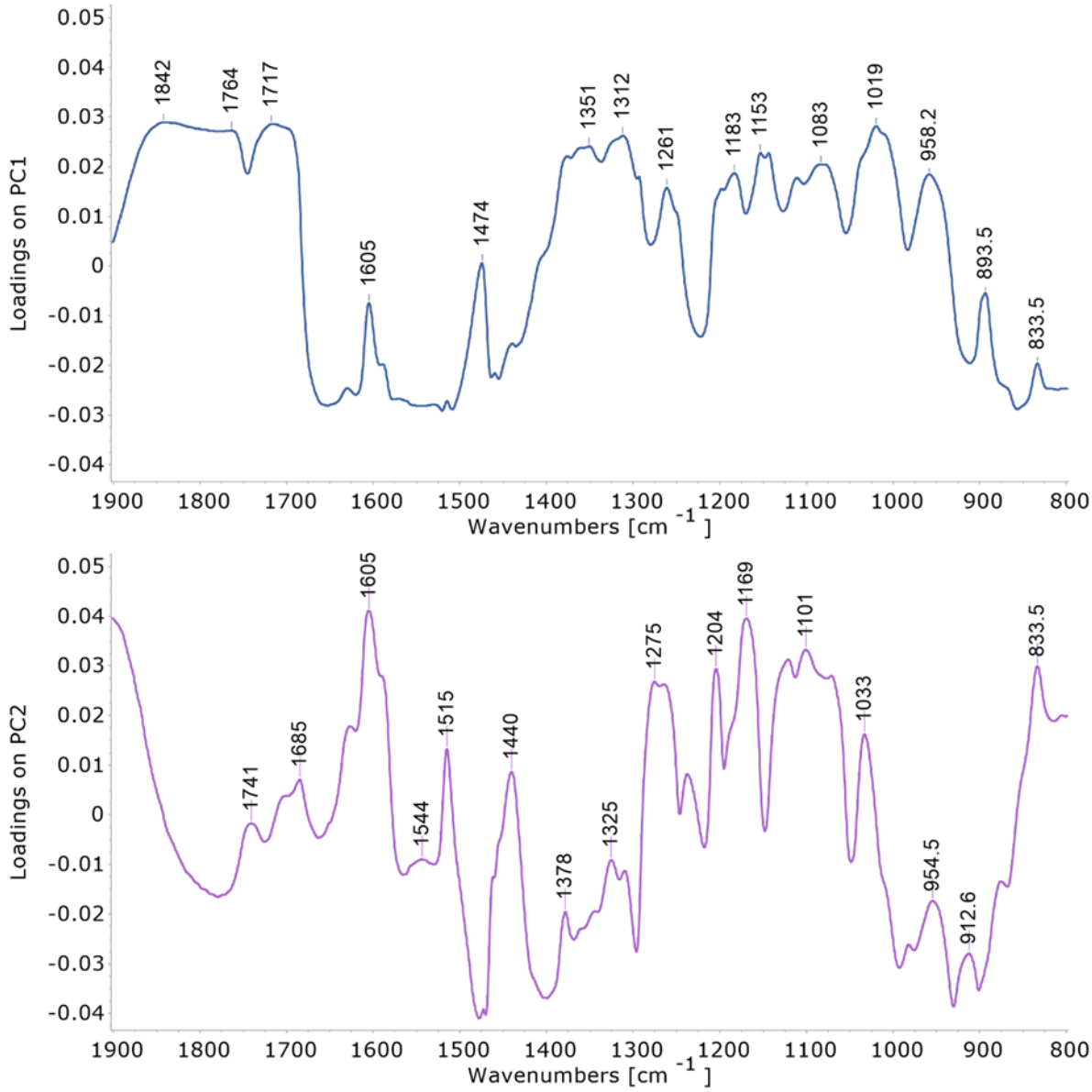

Figure 6.4: PC loadings plot of PC1 and PC2

HAC was also carried out on the spectral data of the differing pollen types to examine similarities and differences of the underlying features. The HAC dendrogram is shown in Figure 6.5 and was constructed using second-derivative spectral data. Good separation between the different pollen types is clear, with all samples clustered accordingly. Similarities can again be seen in the close proximity of the Betulaceae pollen clusters. Ultimately, second derivative data provides a good separation of the different taxonomic pollen samples. However, non-derivatised data was chosen for spectral and PCA/PC loadings analysis due to the ease of comparison and interpretation. This work further supports this method process initially suggested by Zimmermann, Tkalčec, *et al.*, 2015. Overall, IR analysis of common Irish pollen types showed clear separation based on spectral features and slight differences in chemical composition.

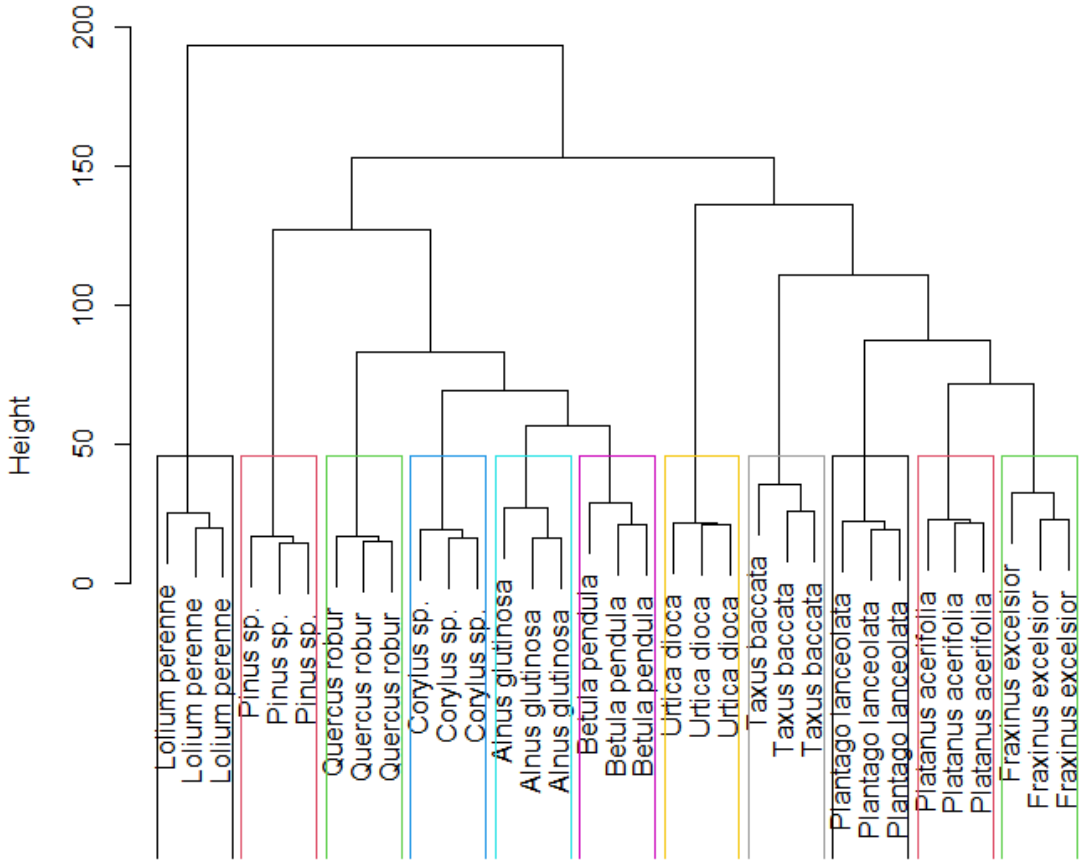

Figure 6.5: HAC dendrogram of second derivative processed spectra of 11 pollen types analysed by IR-ATR

6.3.2 IR analysis of pollen exposed to differing hydration conditions.

Pollen grains undergo various stages of hydration, dehydration and rehydration during their production, release and dispersal. There are 5 main phases in pollen development and each one is subject to changes in hydration (Firon et al., 2012). Pollen initially develops inside the anther, surrounded by a nutrient-rich locular fluid, during which the grain becomes hydrated. This fluid is then either reabsorbed or lost through evaporation prior to anthers opening (Pacini et al., 2006), following this the mature pollen grain undergoes dehydration. As the anther undergoes dehydration, it opens, releasing pollen. Up to this point, the water content of pollen is generally well-covered in literature, although variations to this general process can be expected for plants of differing types and environments (Firon et al., 2012; Pacini et al., 2006). Typically, most pollen species are partially dehydrated prior to anther opening but several species such as Urticaceae and Poaceae remail partially hydrated with no mechanisms to prevent water loss (Dahl et al., 2013). These pollens are often quite spherical in shape a lack furrows (colpi) and may experience wall collapse due to water loss. However, after release of pollen from the anther, the literature becomes less certain as environmental uncertainty is experienced. The hydration state of pollen upon its release is largely dependent on the conditions of its development as well as the environmental conditions faced (Firon

et al., 2012; Lisci et al., 1994; Nepi et al., 2001). Upon release, different pollen can be subject to ambient conditions for different lengths of time. These conditions can have adverse effects on the hydration and composition of pollen grains before they finally reach a stigma and are rehydrated before germination and pollen tube growth.

In this investigation changes induced by different degrees of pollen hydration were investigated. To further explore these changes IR analysis was applied to both a dehydrated and hydrated sample, the resulting spectra are shown in Figure 6.6, below. It was noted that the control pollen was essentially inseparable from the dried pollen sample – indicating the release of dehydrated pollen from the *Betula* catkin. Even secondary derivative HAC analysis failed to differentiate between the two. This section thus focuses on the comparison between dried and hydrated pollen. The similarities between the control and dried samples highlight two main points of interest. For one, this corroborates previous studies highlighting that dehydrated or semi-dehydrated pollen is released from anthers (Firon et al., 2012). The similarities between the two spectra also ensure that the drying process did not generate heat stresses or changes. Heat stress has been shown to affect the protein and lipid composition of pollen grains leading to detrimental impacts on the pollen's viability (Lahlali et al., 2014).

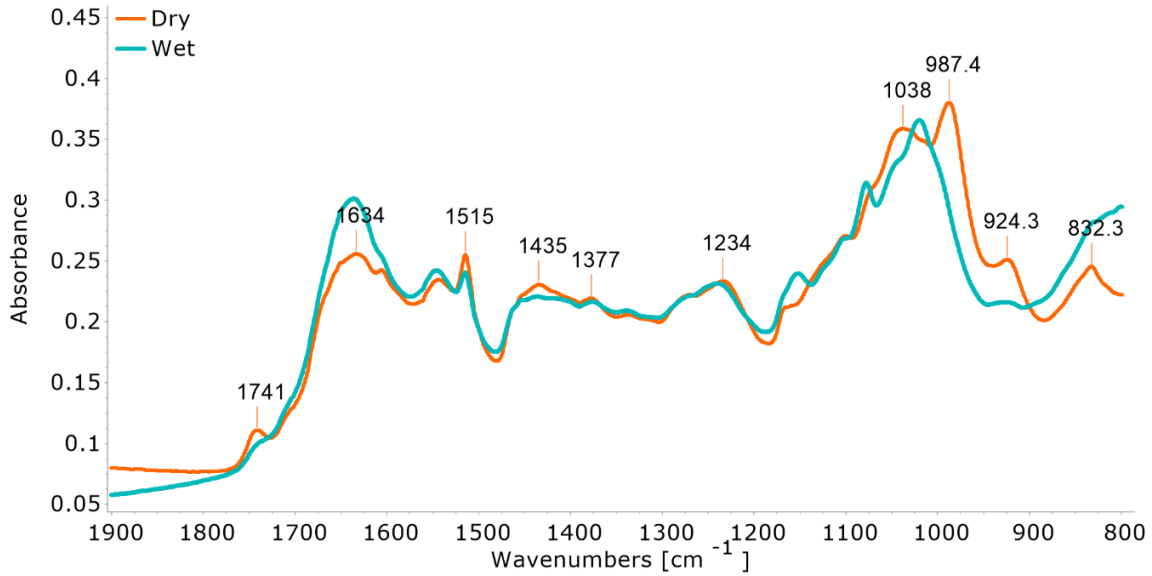

Figure 6.6: IR spectra of Betula pendula pollen samples exposed to varying hydration conditions

Notable differences were seen for the PCA and HAC (Figures 6.7 - 6.8) analysis of the pollen samples investigated. Notable changes in composition are apparent from the examination of the IR spectra. Three main areas of importance are apparent: 1741 cm^{-1}, 1634 cm^{-1} and 830-1200 cm^{-1}. The most prominent being the changes seen at ~1634 cm^{-1}. This band was seen to increase substantially upon hydration. This band area is typically dominated by several functional groups including carboxylate groups and amid stretches, however, due to the nature of the exposure and increases in the intensity of the broad band at 3300-3400 cm^{-1} (not shown in the fingerprint region, noted from

original expanded spectra) this band escalation is a result of increased water content and H-O-H vibrations (deformation) from water (Ba‡cio‡lu et al., 2015; Mularczyk-Oliwa et al., 2012; Pappas et al., 2003; Prdun et al., 2021). A notable decrease in lipid concentration was also noted at ~1741 cm^{-1} for hydrated pollen. This could be the result of adverse adhesion mechanisms that pollen undergoes once hydrated at the stigma. Once adhered to a plant stigma, or in this case a moist environment, the external layer of the exine (containing lips) has been shown to permeate from the surface to attach to the stigma surface (Scott, 1994)(Lahlali et al., 2014). This could have resulted in the reduction of lipids seen here.

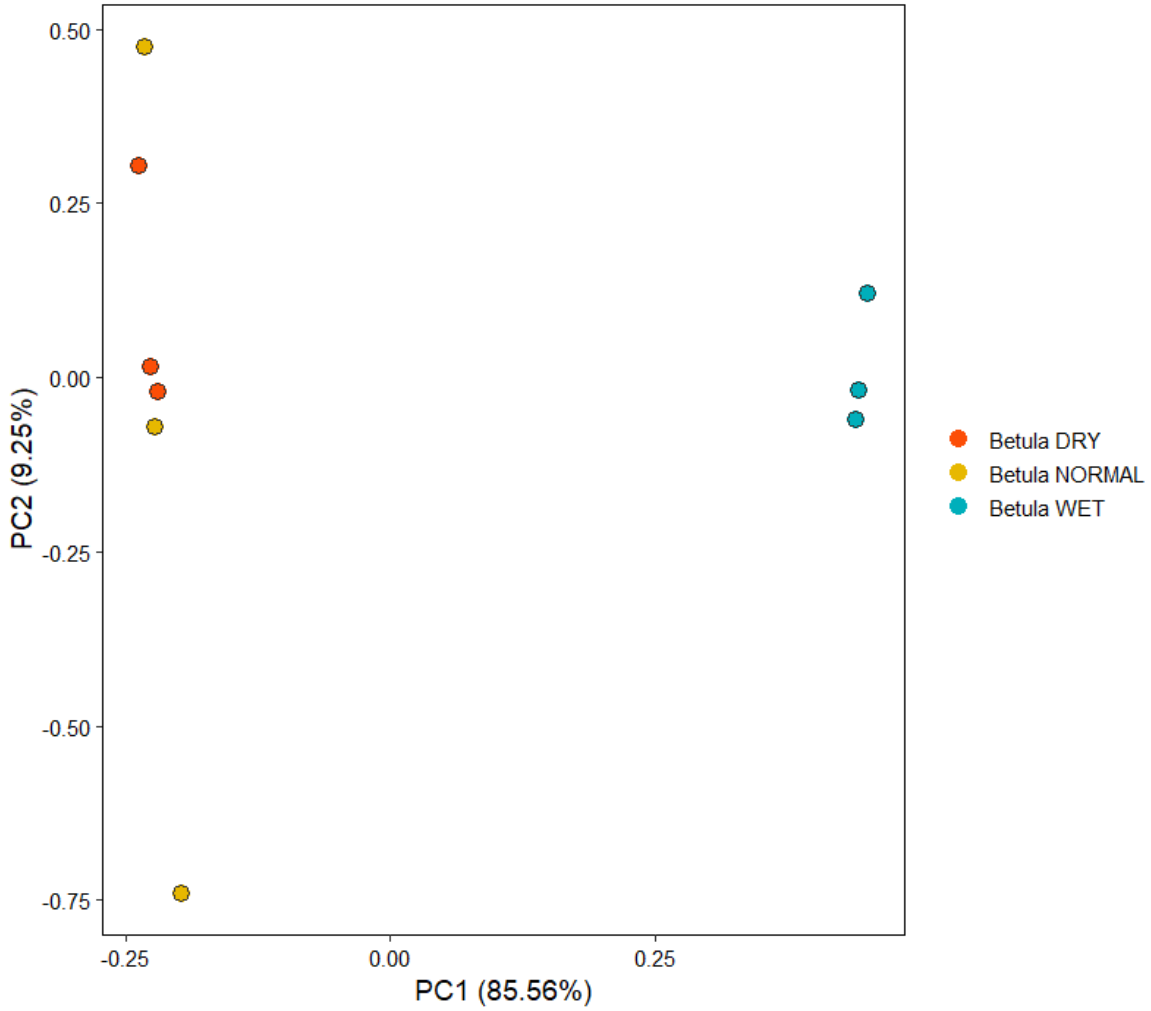

Figure 6.7: PCA biplot of Betula pendula pollen exposed to various hydration conditions analysed by IR-ATR analysis

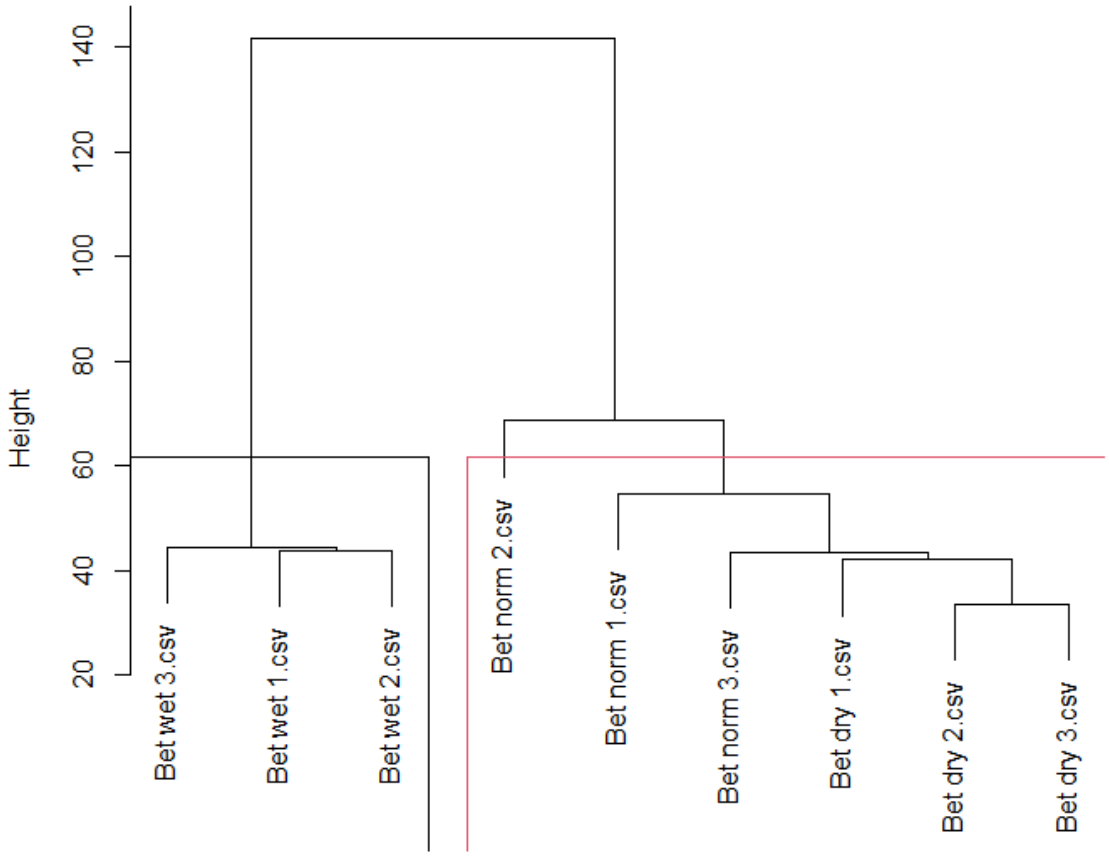

Figure 6.8: HAC dendrogram of second derivative processed spectra Betula pendula pollen exposed to various hydration conditions analysed by IR-ATR analysis

Considerable variance was also witnessed for the 800-1200cm^{-1} region which indicates changes in the polysaccharide content of the pollen. Literature studies have also examined the nutritional changes (especially with regard to carbohydrate reserves) that occur within pollen during various stages of its production, release, hydration/dehydration and gemination (Pacini, 1996; Pacini et al., 2006).Ripe pollen can contain stores of starch, or not. If there is no starch present, this means that starch has been fully hydrolysed to glucose, fructose, sucrose etc. during the final stages of pollen maturation (Pacini et al., 2006). In this case, one might expect to see increased presence of representative bands such as those at ~1032 cm^{-1}, ~1050 cm^{-1} and ~990 cm^{-1} for glucose, fructose and sucrose, respectively (Prdun et al., 2021; Wang et al., 2010). Whereas the presence of bands in the 1175–1140 cm^{-1} region could be the result of glycosidic linkage formation in polysaccharides (Hong et al., 2021; Lammers et al., 2009). Different configurations of glycosidic linkages also result in changes in the 1000–920 cm^{-1} region (Hong et al., 2021). From the analysis of the spectra presented here, it appears as though the dehydrated pollen is dominated by the presence of monosaccharides and disaccharides (Prdun et al., 2021; Wang et al., 2010) indicated by the bands at ~987 and 1038 cm^{-1}. On the other hand, the absence of these bands and increased absorbances at 1020 and 1080 cm^{-1} in the hydrated sample could suggest the presence of polysaccharides such as starch – which has been shown to present a notable absorbance at ~1020 cm^{-1} and ~1080 cm^{-1} (Liu

et al., 2021; Pozo et al., 2018). Changes in the 920-830 cm^{-1} region between the two spectra are linked to different types of glycosidic bonds between the sugar units whereas the band in the dry sample at 922 cm^{-1} are representative of b-glycosidic bonds whereas the increased band intensity of ~830 cm^{-1} of the hydrated sample can be attributed to a-glycosidic bonds (Pappas et al., 2003). The reduction in b-glycosidic bond presence and increase in a-glycosidic bonds further indicates the presence of starch which contains strictly a-glycosidic bonds (Jiang and Zhang, 2013).

This shift in carbohydrate composition could result from changes in pollen activity upon rehydration in wet conditions. Upon rehydration, the metabolism of previously dormant pollen has been shown to reignite (Firon et al., 2012). Depending on storage conditions, pollen can remain viable for at least 3-6 months post-storage (Kadri et al., 2022), the pollen collected here was tested soon after collection with a maximum delay of several weeks. Under dry conditions, pollen has been shown to contain low concentrations of starch and high concentrations of sucrose, such functionalities of which have been linked to membrane protection and protection against desiccation (Firon et al., 2012; Hoekstra et al., 2001). Although levels of hydration in pollen have previously been shown to have little effect on starch concentration (Nepi et al., 2010), the results herein do illustrate some change. Starch can be found within mature pollen as energy reserves or can undergo partial or full hydrolysis before release (Pacini, 1996; Pacini et al., 2006; Speranza et al., 1997; Vesprini et al., 2002). It is possible that the suspect starch polysaccharides became more prominent during hydration due to the metabolism of sugars or through interconversion, which has been shown to occur in pollen (Vesprini et al., 2002).

Alternatively, starch granules are released via the rupturing of pollen grains under certain conditions such as exposure to rain/humidity (Mampage et al., 2022). Although no ruptured/damaged grains were noted upon microscopic analysis of pollen samples, this does not mean some grains did not experience partial/total rupture, releasing SPP such as starch granules, which could have occurred during the compaction of the sample by the ATR method. The presence of ruptured grains could result in contamination of SPP released – potentially accounting for this increased starch-related band. Shifts in carbohydrate composition/intensity have previously been noted for the comparison of intact and ground pollen, perhaps further corroborating the potential of carbohydrate release upon the breaking of external cell walls of the pollen grain (Baıcioılu et al., 2015). Nevertheless, to further corroborate these suspicions and reject the possibilities of other interferences, an investigation was carried out to see if at any point during the rehydration process would pollen become contaminated with starch. However, the equipment used in the process was either made of silica glass or pure cellulose filter papers, which would not result in the increase seen for a-glycosidic bonds as it is insoluble in water and is exclusively bonded through b-glycosidic linkages. The differences in IR spectra seen suggest changes in carbohydrate composition upon re-hydration either through the metabolism of sugars, interconversion to polysaccharide or release of starch granules following cell wall rupture/breakage.

6.3.3 IR analysis of pollen exposed to differing anthropogenic (gaseous) sources.

The severity and rising prevalence of seasonal allergies are further worsened by air pollutants. This includes various gaseous and particulate emissions. Exposure to gaseous pollutants such as NO_x and O_3 has been shown to independently induce airway inflammation as well as enhance allergenic responses (Gruijthuijsen et al., 2006). Exposure to polluted environments has been shown to also result in chemical modifications of pollen grains, with a major focus placed on altering allergen and protein structures/potency (Gruijthuijsen et al., 2006; Ribeiro et al., 2014; Sedghy et al., 2018; Sénéchal et al., 2015)(Zhao et al., 2016). Several studies have investigated such compositional and structural changes in polluted areas using spectroscopic techniques, either by sampling pollen from areas of varying pollutant concentrations (Depciuch et al., 2017, 2016) or by artificially exposing pollen (Pereira et al., 2021; Ribeiro et al., 2017) or plants (Kanter et al., 2013) to gaseous pollutants. During this particular study, the choice was made once again to expose *Betula pendula* samples to various controlled conditions to determine the specific changes introduced by each condition rather than sampling from areas of varying pollution exposure. This was due to the fact that although studies exist doing just this, there are also studies that highlight the interannual and intrasample variation between pollen samples. The variation in pollen composition can be substantial, even between the same species samples or pollen from the same area (Bağcıoğlu et al., 2017).

The pollen samples were exposed to car exhaust fumes and ozone. The European Environmental Agency previously published work detailing the impacts various pollutants have on air quality in Ireland, highlighting PM2.5, NO_x and O_3 as major contributors (Quintyne and Kelly, 2023). According to the Irish Environmental Protection Agency, the leading source of NO_x in Ireland is traffic, whereas the major sources of PM2.5 (and PM10) are fuel combustion as well as diesel emissions (EPA Ireland, 2023). In the case of O_3, Ireland generally has relatively low levels compared to other countries, although this is influenced by transboundary sources. However, in urban areas, O_3 levels are typically lower due to reactions with other pollutants emitted through combustion processes. Considering this, O_3 was still utilised to illustrate potential changes that can be induced via the oxidation of the pollen samples which although less likely to occur due to anthropogenic O_3 sources in urban Ireland, can still occur as a result of exposure to other gaseous pollutants such as

NO_X and from atmospheric O_3 concentrations - which has commonly been used to mimic aerosol aging processes (Santarpia et al., 2012).

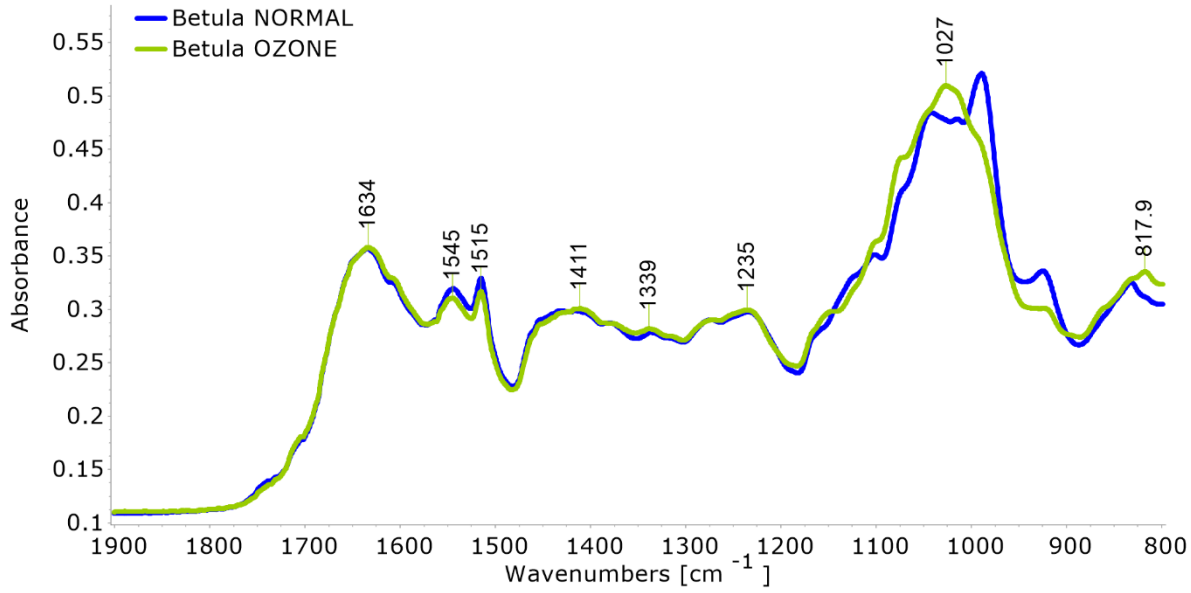

Figure 6.9: IR spectra of Betula pendula pollen samples exposed to varying O_3 conditions

Individual samples of *Betula* pollen were exposed to ozone and car fumes, however, they cannot be compared together since different sources (Dublin and Lille Pollen) were used. Pollen collected from collaborators at the University of Lille was exposed to ozone concentrations of 130±5 ppb for 16 hours and was then analysed by IR-ATR. The resulting spectra are shown in Figure 6.9, above. Several notable differences are apparent, including differences in the 1545, 1515 and 900-1200 cm^{-1} regions. Such findings indicate alterations in protein, protein/sporopollenin and carbohydrate compositions, respectively. These deviations led to the clear distinct separation of pollen samples – evident by the resulting PCA and HAC plots (Figure 6.10 and 6.11). There is a clear divide evident in the PCA plot of the non-derivatised pre-processed spectral data with each sample type showing opposite loading value signs for PC1. The first two PCs explain over 92% of the variance between sample types. Resulting loadings plots only strengthen the association differences clearly seen from the comparison of the two spectra. The second derivative spectra used in the HAC plot also highlight the clear division between the two samples – with no miss classification evident.

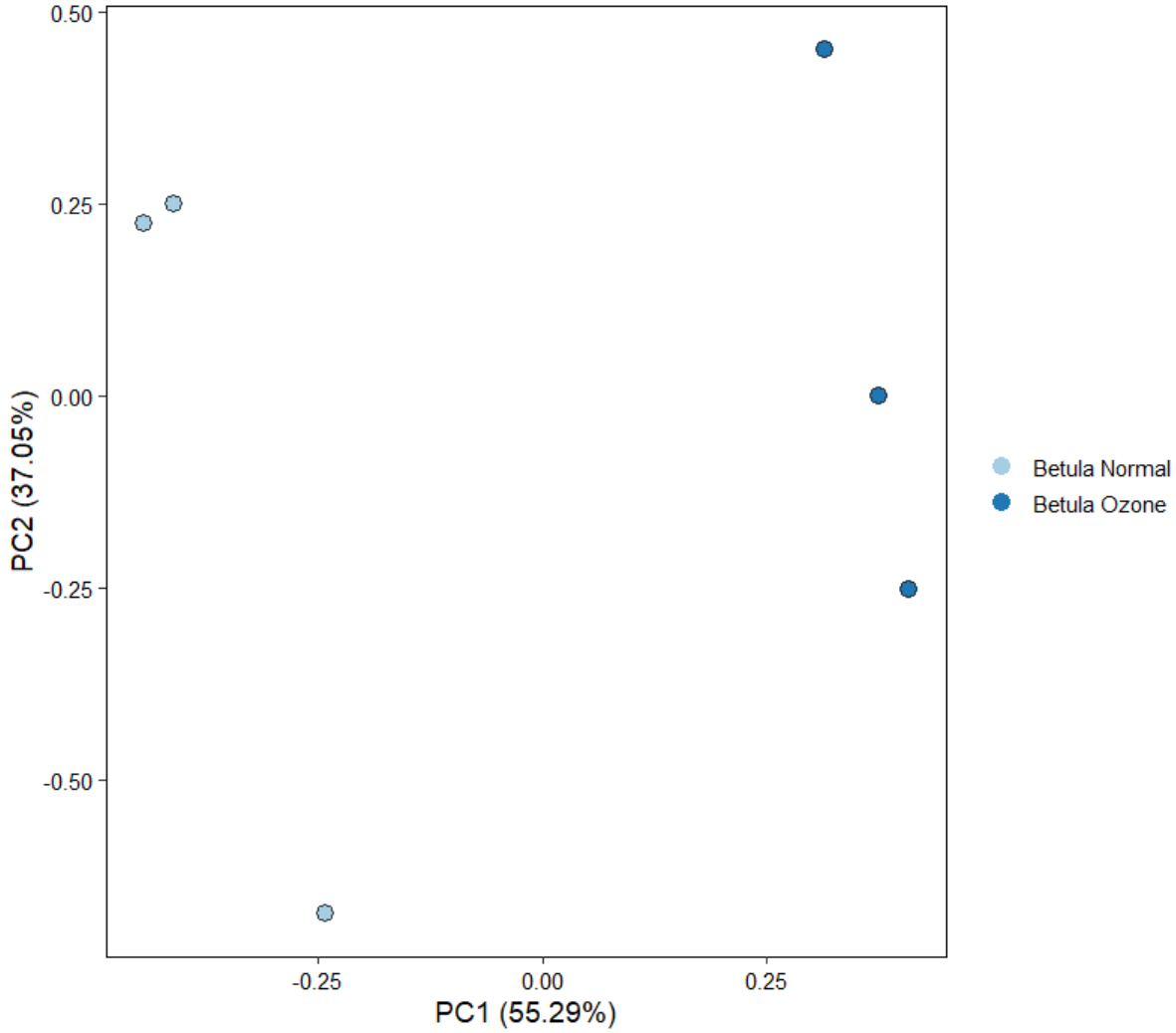

Figure 6.10: PCA biplot of Betula pendula pollen exposed to various O_3 conditions analysed by IR-ATR analysis

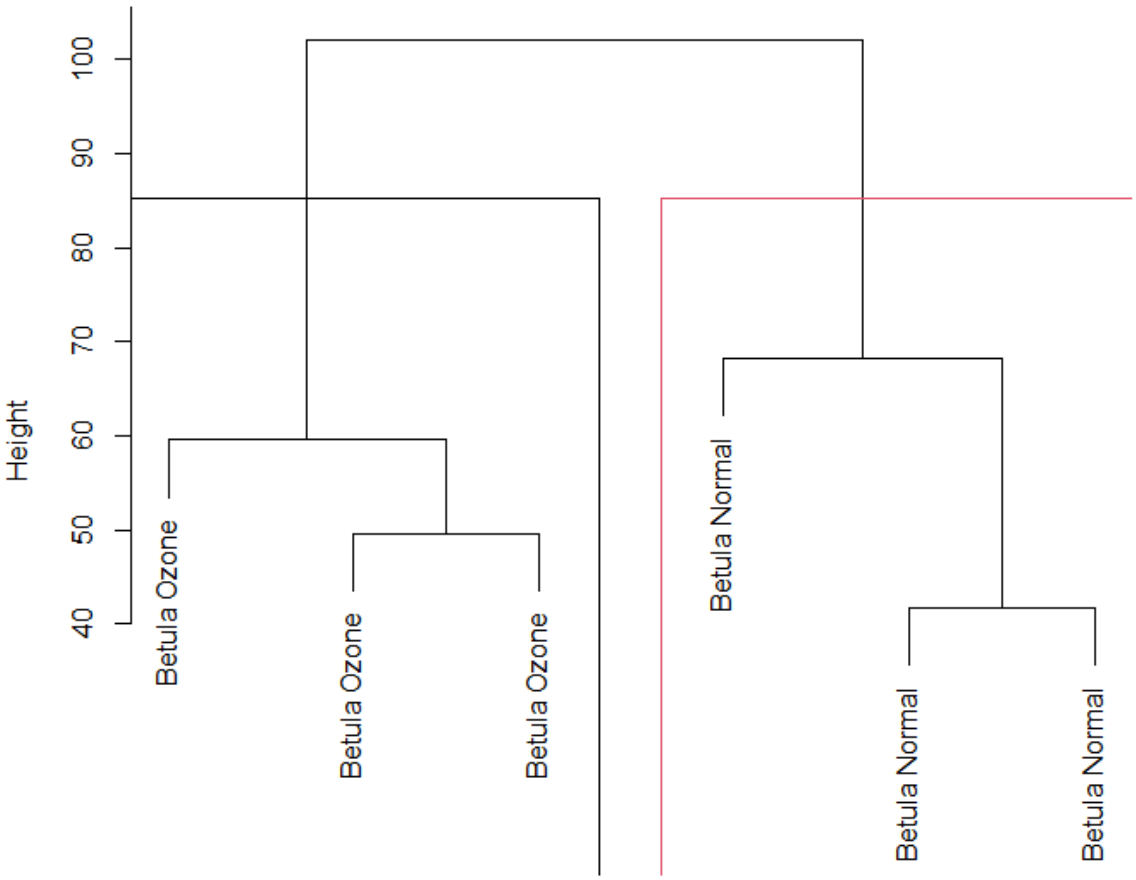

Figure 6.11: HAC dendrogram of second derivative processed spectra Betula pendula pollen exposed to various O_3 conditions analysed by IR-ATR analysis

The increased intensity of protein bands at 1545-1515 cm^{-1} (C-N-H vibration of amide II bond) has previously been found in a similar study by Depciuch *et al.*, 2016, during which *Artemisia* pollen was sampled from several different areas of varying pollution concentrations. The highest absorbance values for proteins in this region were seen for pollen collected from the non-polluted, traffic-free site, corroborating the higher absorbances seen for the unexposed *Betula* pollen. However, as a response to growing under varying conditions, this literature study also noted that the largest differences occur in the protein regions of the spectra between (1600-1700cm^{-1}), these observations were not seen here during this current investigation and are related to the plant's defence mechanisms to adverse anthropogenic conditions experienced prior to pollen production and release (Depciuch *et al.*, 2016). In another study by Depciuch *et al.*, 2017, *Corylus* pollen from various unpolluted and urbanised areas were also compared – again showing noticeable protein changes (1600-1700 cm^{-1}). However, neither of these studies nor other plant exposure studies (Kanter et al., 2013; Zhao et al., 2016) indicate the drastic difference seen here for the presence of carbohydrates – as such these changes are likely linked to the post-influorescence exposure and not to in-vivo exposure of the plants. It is also possible that such changes could have resulted from damage to the pollen cell wall following exposure to O_3 (as was the case with hydrated pollen), although no noticeable damage to the cell wall was seen via microscopic analysis. However, it is possible that fractures existed that were not noticeable at the X400 magnification used. In addition, further

breakage could have occurred during ATR analysis since exposure to oxidising gaseous pollutants has been shown previously to weaken and damage the cell wall of pollen grains (Sénéchal et al., 2015). This could have led to the release of internal cytoplasmic carbohydrates.

A decrease in peak intensity at 980 cm^{-1} coupled with the increase in 1027 cm^{-1} intensity has been noted before in laboratory oxidation tests of spores and pollen. These changes are thus indicative of oxidation processes (Jardine et al., 2015), which can occur upon O_3 exposure (Ribeiro et al., 2014). The decrease in bands at ~980 cm^{-1} can also be related to oxidation and attributed to the loss or destruction of cellulose structures (Domínguez et al., 1998). Cellulose is a common structural component found in the cell walls of many plant cells, including pollen grains where it usually composes part of the cell wall (intine) (Jardine et al., 2015; Zimmermann et al., 2015b). In similar pollen exposure studies of *Platanus* pollen, comparable reduction in amide II bands has been noted with changes found to be more apparent when exposed to both NO_2 and O_3 (Ribeiro et al., 2017). Similar reduction in the 980 cm^{-1} (allocated to glycosidic bonds of carbohydrates) was also noted for ozone exposure (Ribeiro et al., 2017). Changes to the pollen wall composition of four forest tree species, *Betula pendula*, *Corylus avellana*, *Acer negundo* and *Quercus robur* examined by Raman spectroscopy highlighted changes in lipid, protein and sporopollenin as well as the differences in susceptibility of different pollen types to pollutant exposure (Pereira et al., 2021). This suggests that the changes seen here for *Betula pendula* could vary depending on pollen species.

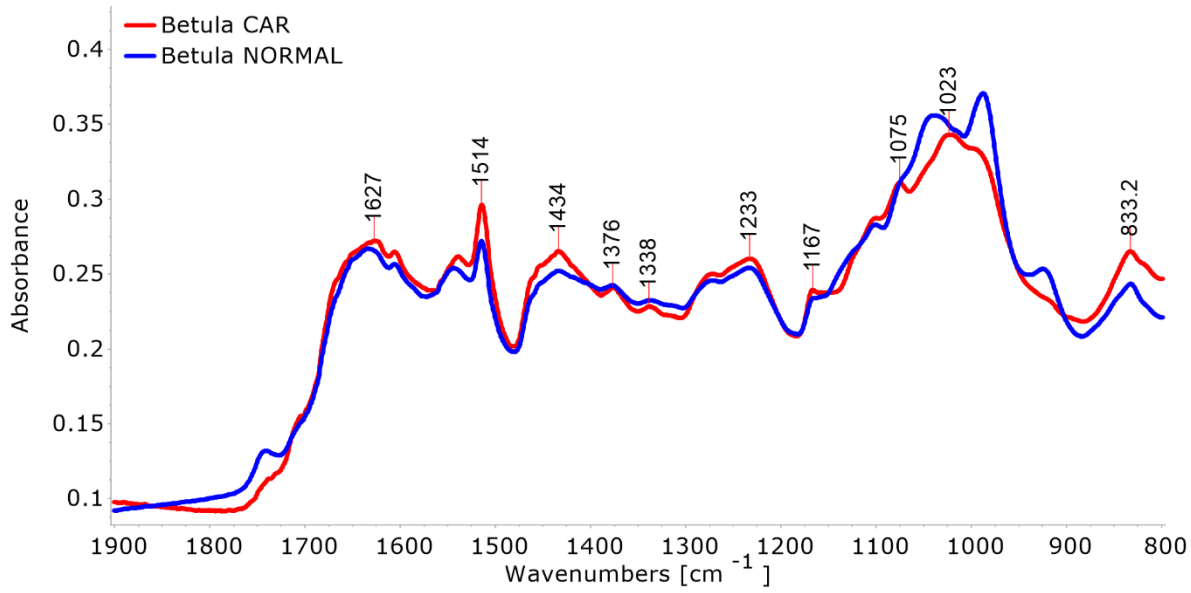

Figure 6.12: IR spectra of Betula pendula pollen samples exposed to car exhaust fumes

Betula pollen exposed to car exhaust fumes characterised by the presence of CO_2, NO_x, CO and particulate matter (Jaworski et al., 2018) was also examined. The resulting spectra are shown in Figure 6.12, above. Several changes such as the reduction in bands at ~920 cm^{-1} ~988 cm^{-1} and 1040 cm^{-1} and the increase in bands at 1023 cm^{-1} and 830 cm^{-1} illustrate much of the same deviations witnessed for the resulting oxidation caused by O_3 exposure. However, additional variation was also

witnessed including the notable increase in bands at ~1627 cm^{-1}, 1514 cm^{-1}, and 1434 cm^{-1} and a decrease in the band at ~1745 cm^{-1}. These notable changes also led to the clear differentiation between exposed and unexposed pollen samples following PCA and HAC analysis as shown in Figures 6.13 and 6.14, with the first two PCs accounting for over 95% of sample variance.

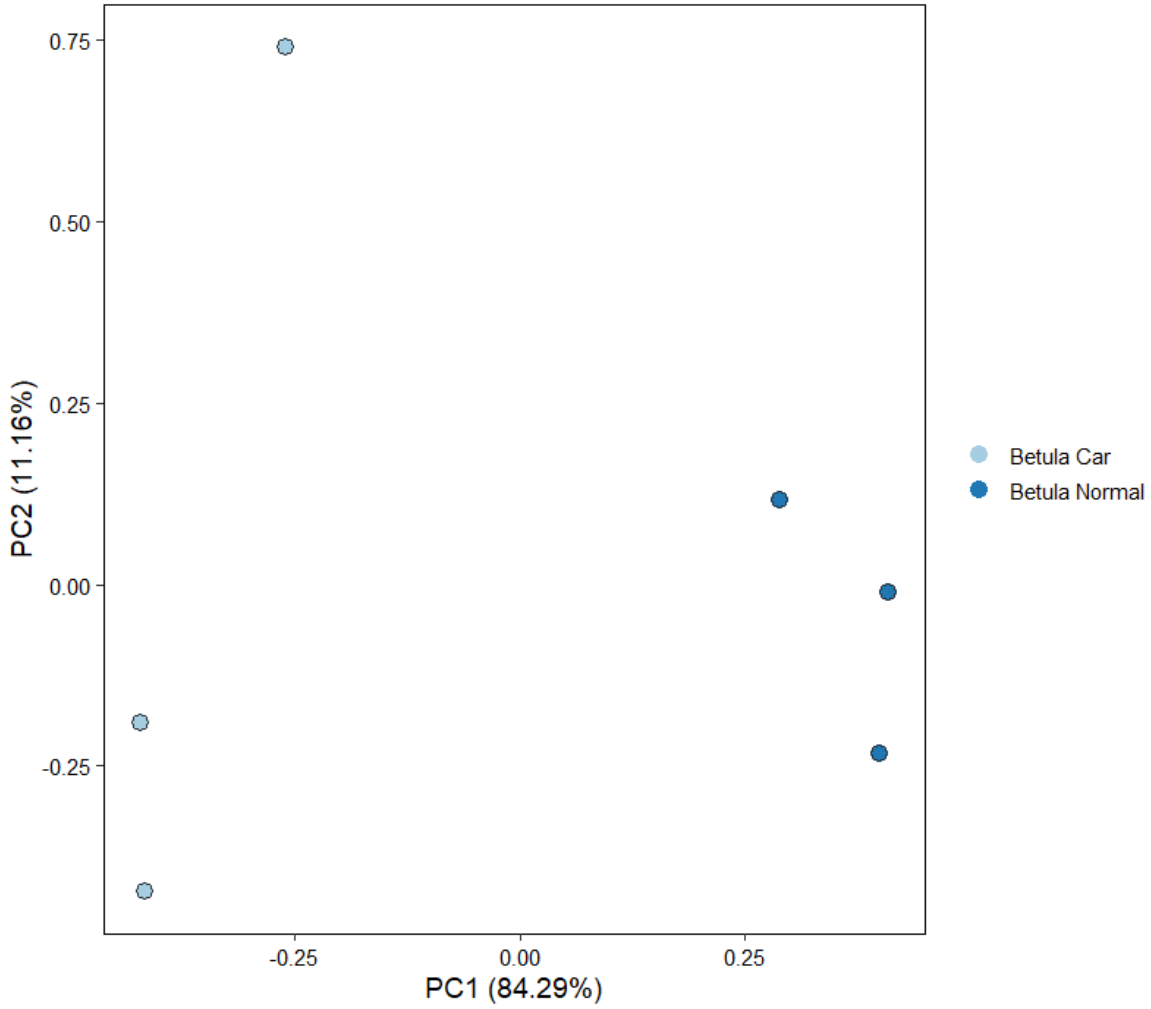

Figure 6.13: PCA biplot of Betula pendula pollen exposed to car exhaust fumes analysed by IR-ATR analysis

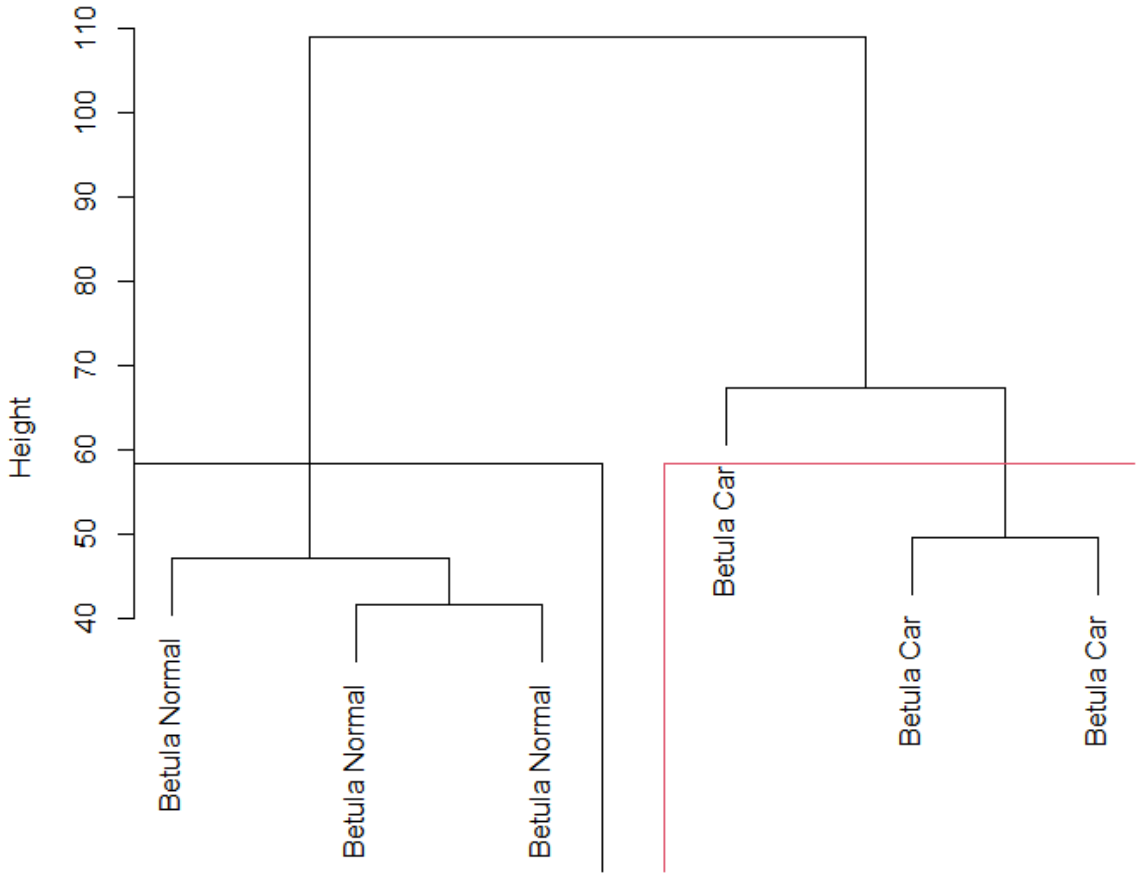

Figure 6.14: HAC dendrogram of second derivative processed spectra Betula pendula pollen exposed to exhaust fumes analysed by IR-ATR analysis

The shift in this 1620-1640 cm^{-1} could occur simply due to changes in hydration and water content (Mularczyk-Oliwa et al., 2012). However, coupled with the changes seen in the ~1514-1550 cm^{-1} range it is likely that there are changes in protein composition/concentration since proteins are mainly characterised by two strong and broad bands at 1640 cm^{-1} (amide I: C = O stretch) and ~1540 cm^{-1} (amide II: NH deformation and C–N stretch) (Baıcioılu et al., 2015). Similar increases in the absorbance of protein bands and decreases in carbohydrate bands have been noted previously for ragweed pollen exposed to elevated levels of NO_2 (Zhao et al., 2016). It has been shown that even at levels below legislative limits for plant health, changes can be induced in the general protein structure of the pollen grains (Ribeiro et al., 2017). Many studies have also investigated the changes in allergenicity of certain pollen allergens following exposure. Conflicting results in protein modification and changes in allergenicity have been well documented in past literature with both increases and decreases in protein content/allergenicity noted for a variety of pollen taxa and conditions (Bist et al., 2004; Chassard et al., 2015; Franze et al., 2005; Gruijthuijsen et al., 2006; Sénéchal et al., 2015; Sousa et al., 2012; Zhao et al., 2016). Variation in protein modifications is largely dependent on pollen type and exposure conditions. Exposure to ambient conditions and anthropogenic sources can lead to protein oxidation and nitration posttranslational modification due to oxidative stress and aging (Reinmuth-Selzle et al., 2014; Ribeiro et al., 2017). These oxidative

stresses have been shown to change protein structure and content – recorded as increases, decreases or no change in protein content (Kanter et al., 2013; Reinmuth-Selzle et al., 2014; Ribeiro et al., 2017). Thus, the oxidation/nitration of protein can be observed as changes in the band at 1640 and 1515-1545 cm^{-1}.

The decrease in absorbance seen at ~1745 cm^{-1} is largely attributed to changes in intracellular lipid concentrations. From a pollen development point of view, lipids play a pivotal role in pollen development, particularly in the development of the exine and later, before release, in the production of the pollen coat from the tapetum (Piffanelli et al., 1998). The presence of lipids on the exterior of the pollen grain serves to protect it from UV damage and dehydration but can also be stored in the form of intracellular lipids which can be used up after the pollen grain is released (Piffanelli et al., 1998; Zimmermann and Kohler, 2014). It has also been shown that heat stress and other environmental factors can further impact and reduce the lipid content of mature pollen (Lahlali et al., 2014; Zimmermann and Kohler, 2014). Lipid modification and a decrease in IR lipid-related bands have also been noted following exposure to air pollution (Kanter et al., 2013). Fatty acid content of pollen grains has been shown to reduce in accordance with proximity/extent of pollution exposure caused by degradation and peroxidation processes (Pukacki and Chałupka, 2003). However, exposure to oxidising pollutants like ozone has also been shown to result in the de-methylation and or de-esterification of pectin (also found in the intine of pollen grains) which has also been shown to contribute to the bands at ~1740cm^{-1} (indicative of the ester group of pectin) (Kanter et al., 2013). Similar behaviour has previously been reported for ragweed pollen, subject to elevated ozone concentrations (Kanter et al., 2013). Exposure to oxidative gaseous compounds like O_3 and NO_2 has also been shown to change the bands observed in the 1410-1450 cm^{-1} region (Ribeiro et al., 2017) which can also be attributed to the presence of lipid components (Baıcioılu et al., 2015; Zimmermann and Kohler, 2014). In the case of a study carried out by Ribeiro *et al.*, 2017, where *Platanus* pollen was artificially exposed to NO_2 and O_3, notable changes were observed for the 1410-1450 cm^{-1} region, showing slight increases in band prominence for polluted samples, similar to what was seen here.

6.3.4 IR analysis of pollen exposed to differing particulate matter (ashes and dust).

Following anther dehiscence, released pollen can come into contact with various forms of PM through its transport and dispersal. Various mechanisms of pollen and particle interactions have recently been suggested, investigated and discussed (Visez et al., 2020). Although catkins (prior to pollen release) can contain adhered particles, this has been found not to transfer PM to the individual grains. Therefore, particle adhesion to individual pollen grains mainly occurs during dispersal (Choël et al., 2022b). Particles that adhere to the surface of pollen grains can interact with pollen allergens often binding to combustion particles – aiding their dispersal and respiratory implications since PM represents a known respiratory allergen in itself (Namork et al., 2006; Solomon, 2002). Many studies

have noted the adhesion of such anthropogenic PM to the pollen grain surface, particularly in urban settings, can occur even under low pollution conditions (Choël et al., 2022a; Visez et al., 2020). Whereas the implication of gaseous pollutants on pollen grain compositions has been well documented in literature (Frank and Ernst, 2016), there exists very few studies doing the same for PM (Choël et al., 2022b, 2022a; Visez et al., 2020).

Particulate matter represents another major contributor to air quality within the Irish environment, PM2.5 and PM10 are dominated by particles resulting from combustion processes such as fossil fuel burning (EPA Ireland, 2023). As such, *Betula pendula* pollen samples were exposed to combustion ashes of three common household fuels used in Ireland, including wood ashes, turf (peat) ashes and coal ashes. To ensure a representative fraction of each exposed sample contained adhered particles within the limits quantitatively determined by Choël, Ivanovsky, *et al.*, 2022 (individual grains on average containing 2± 1 particles), an excess of ashes/dust was mixed with the pollen – this was further evaluated by examining the grains by light microscopy. This was carried out in small reaction tubes by agitation and does not represent atmospherically relevant concentration ratios of pollen and PM. However, this was intended as a proof of principle study and required excesses of contaminant due to the bulk analysis method available (ATR). Saharan dust was also investigated as a possible contamination of the pollen due to the concurrent transport noted in literature (Grewling et al., 2019). The likelihood of this debris reaching Ireland and the British Isles has been noted several times through the decades (Goudie and Middleton, 2001). The resulting IR spectra of the pure ash/dust samples as well as the contaminated pollen samples and ash/dust samples are provided in Figures 6.15-6.19, below (individual ash/dust spectra are shown in Appendix D, Figures D12-D15).

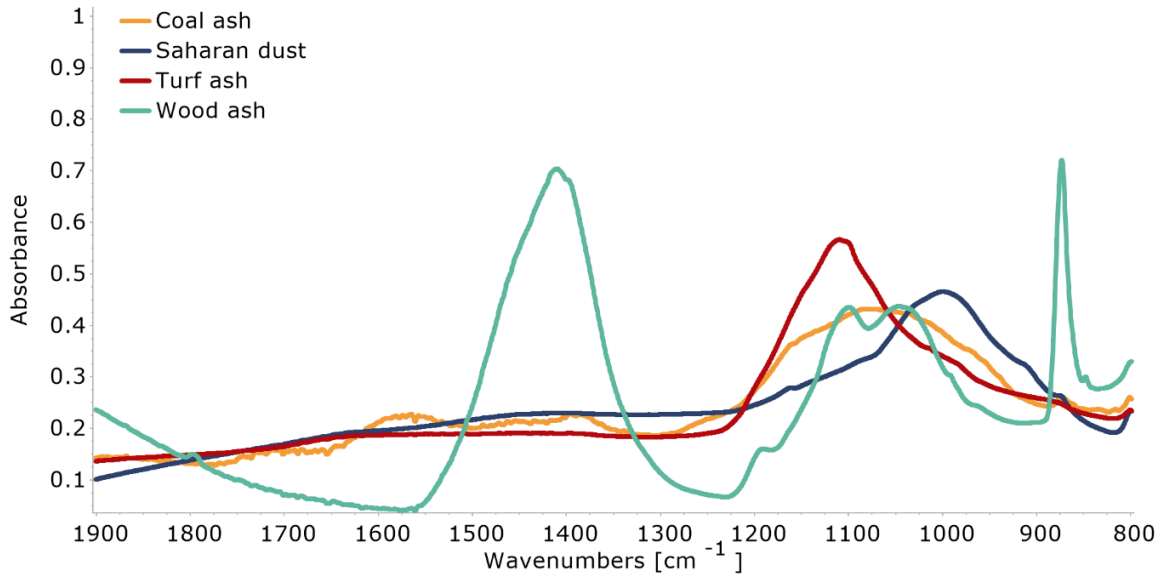

Figure 6.15: IR Spectra of ash and dust samples

Clear distinctions between the various ashes/dust samples are evident. All samples contain a wide band within the 900-1200 cm^{-1} region which is common among typical atmospheric dust

particles (Laskina et al., 2012). The single peak at 1000 cm^{-1} found for Saharan dust is a signature band highlighted previously for the same sample source (Laskina et al., 2012). Coal ashed illustrated several bands at 1070 cm^{-1}, 1396 cm^{-1} and 1565 cm^{-1}. The peak at 1070 cm^{-1} can be attributed to the stretching of silica-containing bonds, whereas the band at 1396 cm^{-1} results from methyl or ethyl group vibrations and the band at ~1565 cm^{-1} arises due to vibrations related to aromatic rings (Lin et al., 2019). The strong peak at 1100 cm^{-1} seen for turf ashes indicates the presence of silicate groups (Anıl et al., 2014). Compared to the other samples, wood ashes appear to be the most complex with several notable bands at 873 cm^{-1}, 1047 cm^{-1}, 1099 cm^{-1} and 1410 cm^{-1}. The strong bands at 1410 cm^{-1} and 873.2 cm^{-1} can be attributed to several possible groups, including aromatic silicon bonds, various mineral bonds such as ammonium-containing compounds as well as aromatic C-H bonds, all of which are present in a host of ambient aerosols including other carbonaceous combustion particles (Barnasan et al., 2021). Upon combining with pollen samples, it is apparent that several of these features are inherited from the ash/dust additives.

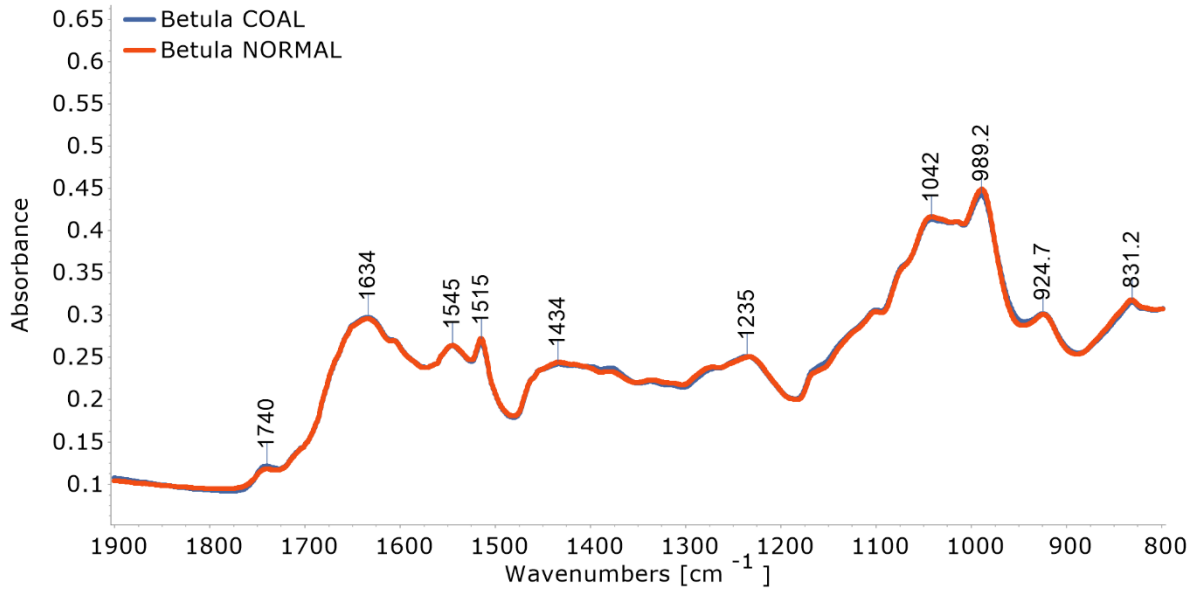

Figure 6.16: IR spectra of contaminated Betula pendula pollen with coal ash

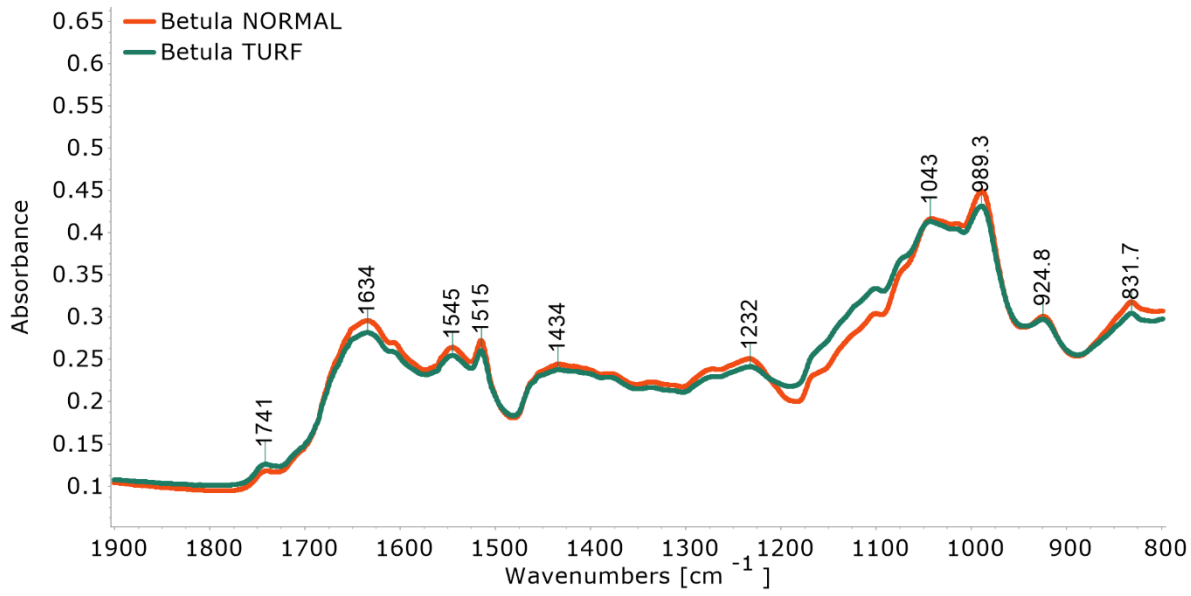

Figure 6.17: IR spectra of contaminated Betula pendula pollen with turf ash

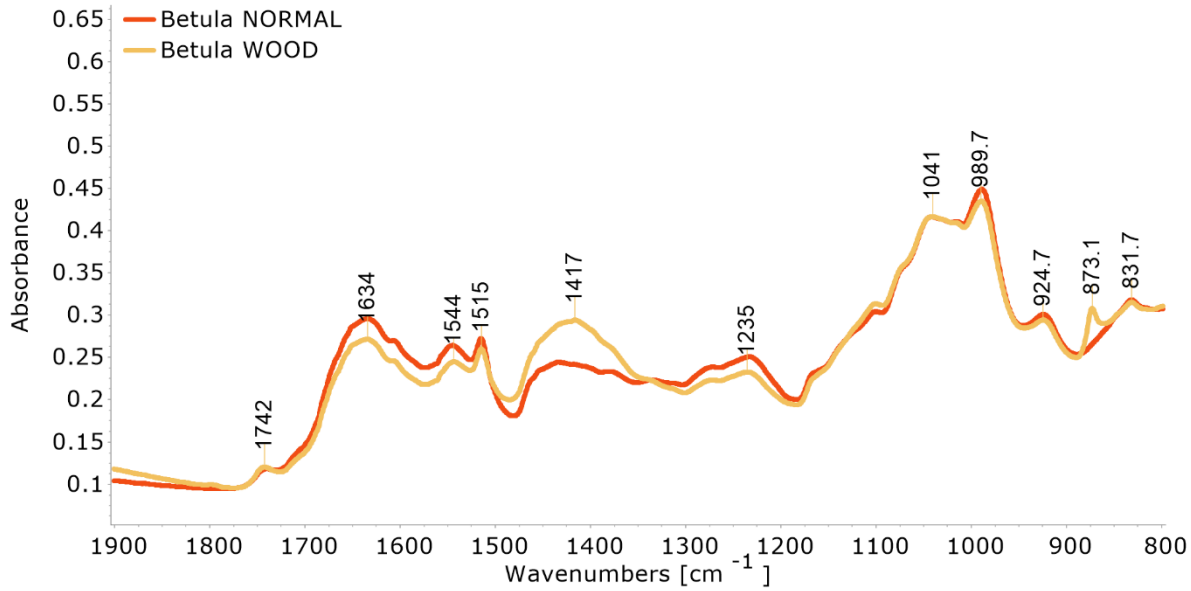

Figure 6.18: IR spectra of contaminated Betula pendula pollen with wood ash

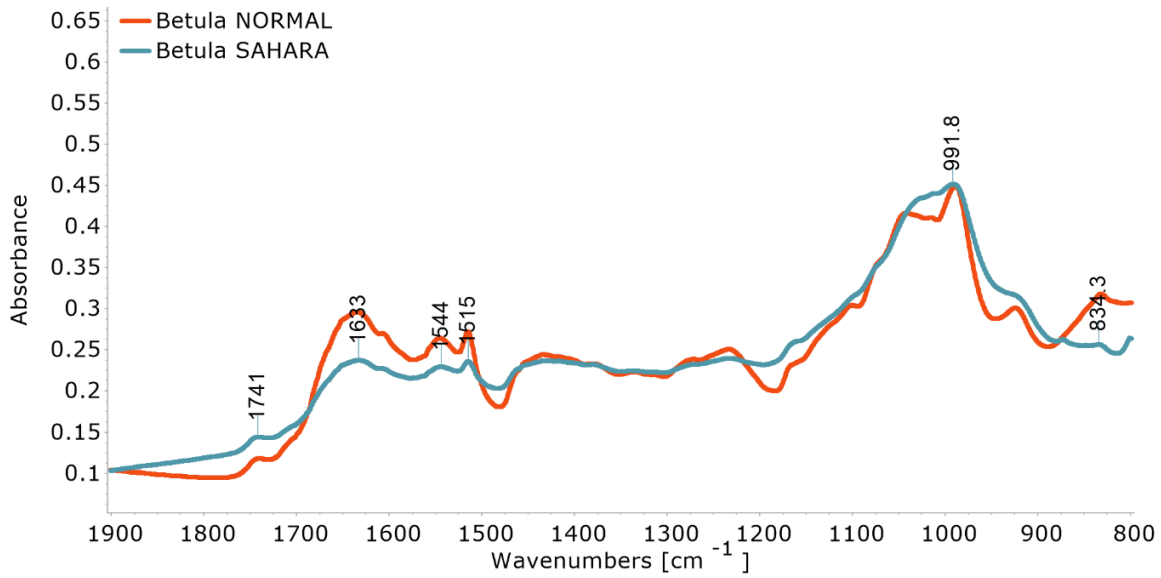

Figure 6.19: IR spectra of contaminated Betula pendula pollen with Saharan dust

The combination of coal ash and pollen contains the least variation from the original pollen sample, whereas the wood ash contaminated sample contains a prominent peak seen at 1417 cm^{-1} as well as a new peak forming for the band seen at 873 cm^{-1}, inherited from the ash samples. Contaminating the pollen sample with Saharan dust led to the broadening of bands seen at ~1000 cm^{-1}, whereas turf ash contamination resulted in a more apparent broad shoulder forming at ~1100 cm^{-1} in the pollen spectra. The similarities between the contaminated samples were further compared to each other and uncontaminated samples using PCA and HAC analysis (Figure 6.20-6.21). The PCA plot illustrates the similarities and differences seen from examination of the spectra. The majority of samples show clear differentiation from one another and from the uncontaminated sample, except for the coal-pollen sample which shows strong similarities. However, upon analysis of the second derivatised spectra (Figure 6.22), enough variance between the two is evident to allow for correct clustering following HAC analysis. This was most apparent at 1745 cm^{-1} and 960 cm^{-1} regions.

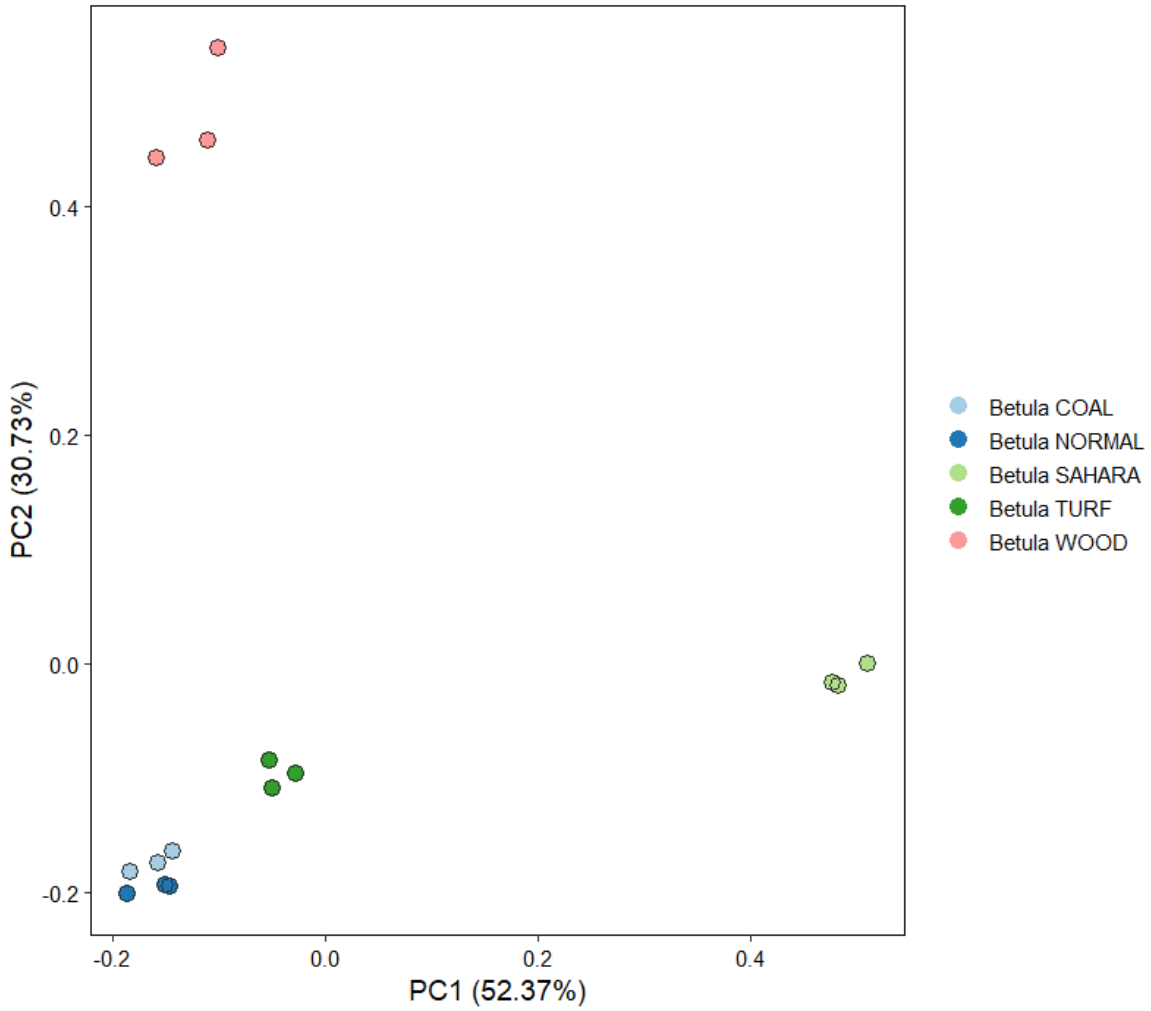

Figure 6.20: PCA biplot of Betula pendula pollen exposed to ashes/dust samples analysed by IR-ATR analysis

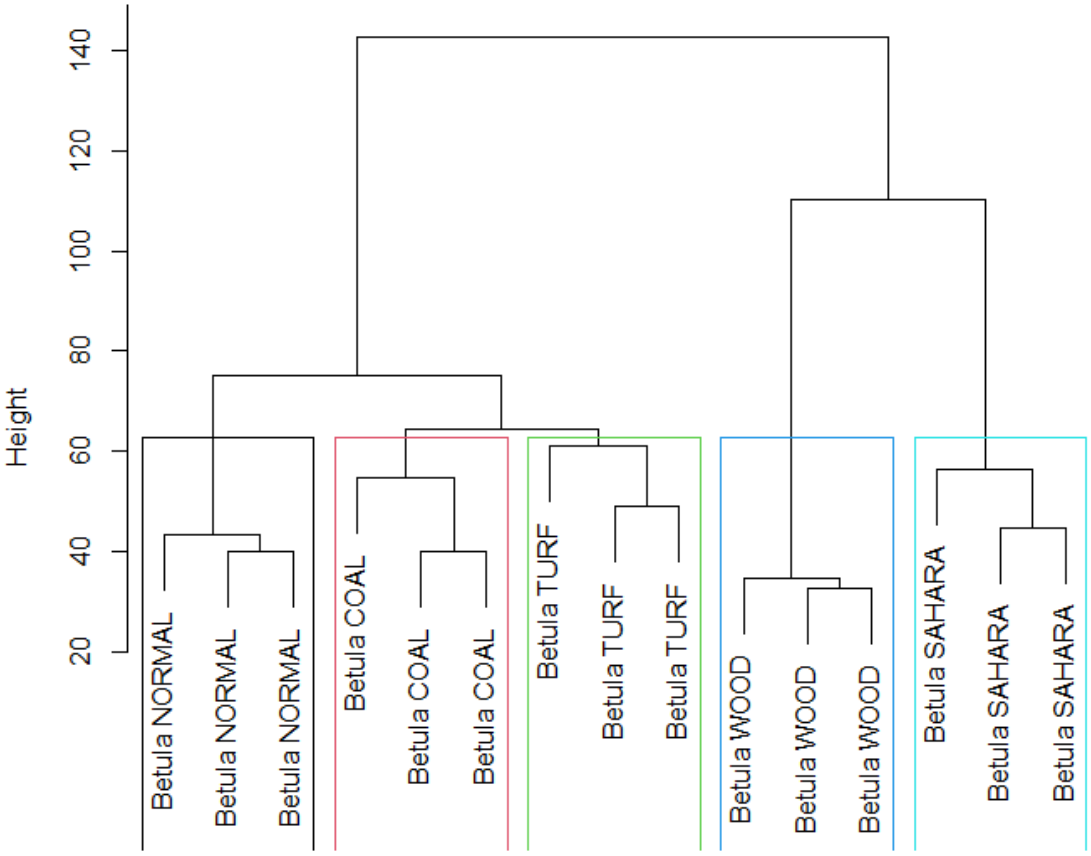

Figure 6.21: HAC dendrogram of Betula pendula pollen exposed to ashes/dust samples analysed by IR-ATR analysis

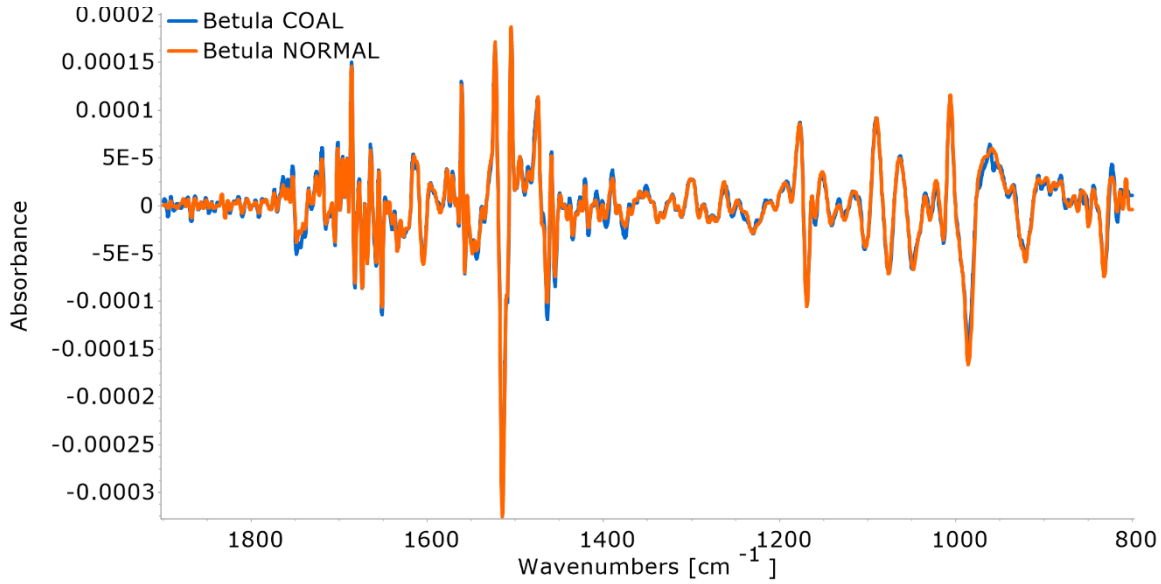

Figure 6.22: IR 2nd derivative spectra of contaminated Betula pendula pollen with coal ash

Overall, the inclusion of dust and ash particles to pollen samples introduced sufficient variance between the samples for them to be categorised as distinctly separate from the original sample. Although this is unlikely to affect the bulk sampling of pollen, if microscopic IR analysis is to traverse into the realm of real-time pollen detection, this is likely to lead to misclassification and

uncertainties – especially in urban environments where these polluted pollen grains could cause heightened allergic and respiratory responses. Therefore, identification of pollen samples via IR spectroscopy can be considered a rather complex task that needs to take into account not only the variability that exists between species, sampling locations and growing conditions (Baʇcioʇlu et al., 2015) but also variations that can occur during dispersal and exposure to air pollutants.

6.3.5 Changes to the overall fluorescence intensity of exposed and control pollen samples

The interest in pollen and bioaerosol autofluorescence has been a topic of popularity for decades. To date many studies have investigated the fluorescent profile of pollen and other bioaerosol classes, determining contributing fluorophores as well as differences that may exist between different bioaerosol classes (Després et al., 2012; Fennelly et al., 2017; Melnikova et al., 1997; O'Connor et al., 2011, 2014b; Pöhlker et al., 2012, 2013). The detection of important bio-fluorophores is what led to the development of LIF real-time devices, aimed at improving the detection of airborne pollen and other biogenic emissions /aerosols.

In the previous sections of this chapter, the chemical composition changes induced via exposure of pollen to varying environmental and anthropogenic conditions were investigated. Whereas these changes were apparent on a vibrational spectroscopic level, the majority of popular new-age and novel real-time detection devices utilise LIF to detect bio-fluorophores that are indicative of various biogenic sources. In order to investigate whether these conditions have the potential to disrupt the detection of pollen from various environments, these samples were also analysed by fluorescent-confocal microscopy. This not only allowed for differentiation between fluorescent intensities but also any physical/structural differences to be noted, since several real-time instruments such as the Poleno (Sauvageat et al., 2020), BAA500 (Oteros et al., 2020) and Pollensense (Buters et al., 2022) are primarily led by the use of holographic imaging/image recognition. This means that the algorithms used to classify airborne pollen grains are heavily dependent on the general shape and size of the grains. Although previous studies separately analysed the potential of anthropogenic aerosols to interfere with LIF type instrumentation such as the WIBS (Savage et al., 2017) and changes in pollen autofluorescence by exposure to various pollutants (Castro et al., 2010; Roshchina, 2003; Roshchina and Karnaukhov, 1999; Roshchina and Mel'nikova, 2001), no study has investigated whether changes in pollen fluorescence can impact the detection using such instrumentation.

In this study, pollen exposed to O_3, car exhaust fumes, various ashes, Saharan dust and varying degrees of hydration (dry vs. wet) were compared to a control sample of unpolluted pollen when autofluorescence was triggered using an excitation wavelength of 405 nm and emission detection band of 410-750 nm. Although selection of excitation wavelength was limited due to

available resources, the detection band was chosen as it encompasses many of the channels used in popular LIF instruments such as the Swisens Poleno, Rapid-E and the WIBS. The Poleno utilises 3 separate excitation wavelengths, one being 405 nm. Although this study is limited by the selection of excitation wavelength, it was designed as a preliminary investigation of whether pollutants shown to alter the chemical composition of the surface of pollen grains would translate to changes in fluorescent characteristics – potentially leading to difficulties in characterisation by LIF.

Boxplots illustrating the differences in fluorescence intensity between samples and conditions are illustrated in Figures 6.23,6.25,6.27 and 6.28. From examination of the boxplots, it can be observed that changes in the fluorescent intensity of the sample varied depending on the conditions used. In the case of O_3 and car exhaust exposure, little deviation in fluorescence intensity was observed when compared to the control samples – despite notable changes in the chemical composition being found prior. More drastic differences were observed for the remaining samples. To determine if any statistically significant differences existed between the exposed pollen samples and control sample Kruskal-Wallis tests followed by a Dunn's tests for multiple pairwise comparisons were carried out as well as Mann-Whitney U tests, the results of which are highlighted in Table 6.2.

Table 6.2: P-values of pairwise comparison tests

Condition	**P-value**
Betula Dry	**0.02***
Betula Wet	**9.74E-04***
Betula Turf	0.52
Betula Wood	**0.04***
Betula Coal	**0.01***
Betula Sahara	**6.82E-11***
Betula Ozone	0.91
Betula Car	0.59

* P-value <0.05 indicated significant differences between the sample and control (unpolluted pollen)

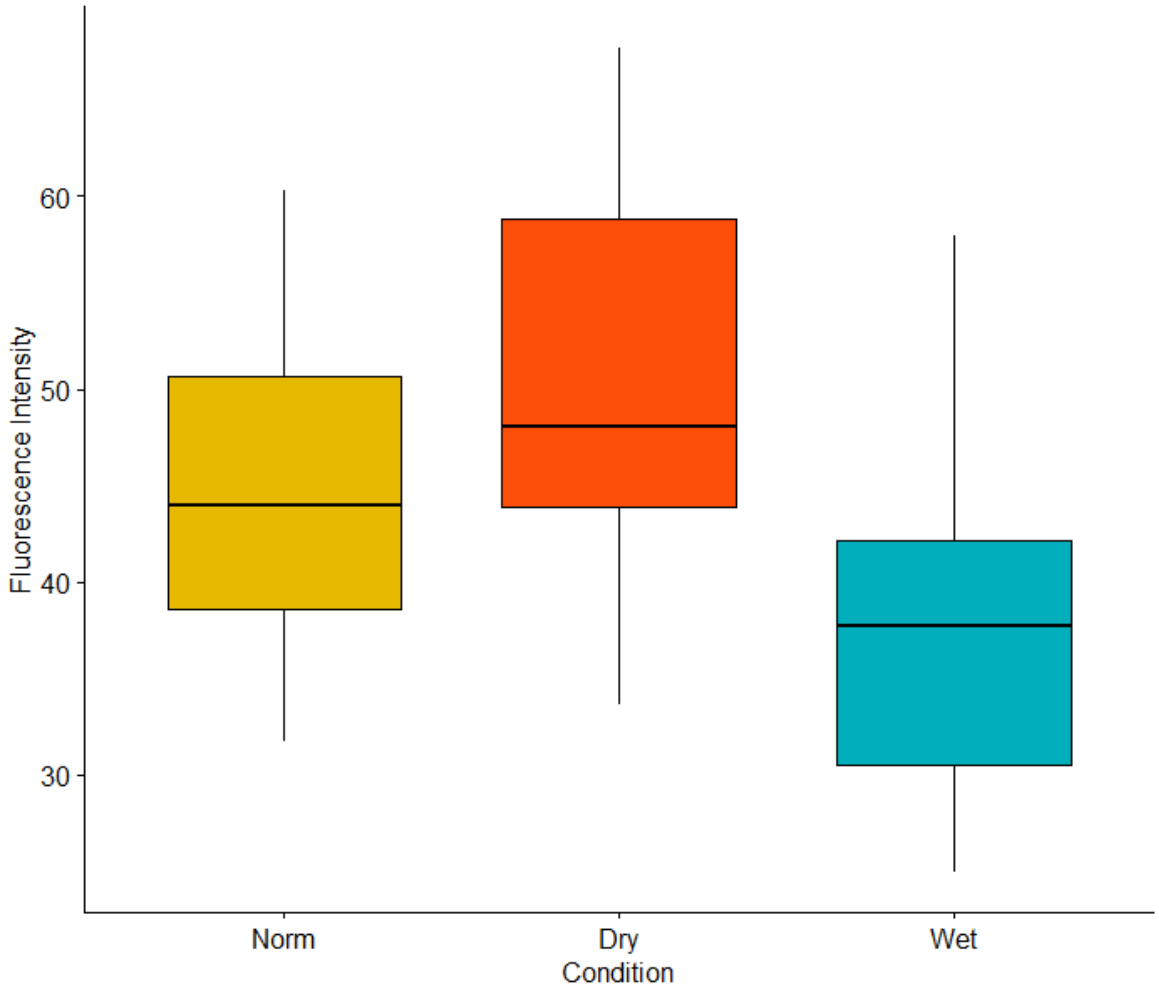

Figure 6.23: Fluorescence intensity ranges for pollen exposed to varying hydration conditions (n=40)

Pollen samples that were hydrated and dried accordingly were analysed in comparison to each other as well as to a control sample. Varying degrees of fluorescence intensity were experienced for each sample as illustrated in Figure 6.23. All three conditions were found to be statistically significant from each other following Kruskal-Wallis and Dunn's post hoc testing. The control sample generally contained pollen grains at varying degrees of drying/hydration since the sieved sample likely contained dehydrated and semi-dehydrated fresh pollen. In comparison, the dried pollen had notably higher fluorescence intensity and dehydrated appearance as shown in Figure 6.24. Conversely, the hydrated sample had a notable decrease in fluorescence intensity and a more rounded and bloated appearance, as well as this, the hydrated sample had a greater affinity for forming large groups of pollen grains whereas the other samples often gave rise to single independent grains. It was, however, apparent that under all conditions a variety of intensity was observed with some pollen grains being brighter or duller than others in the same sample type (Figure 6.24). It is possible that despite stable exposure settings, this intra-variability reflects fluctuations in the water content across each sample group.

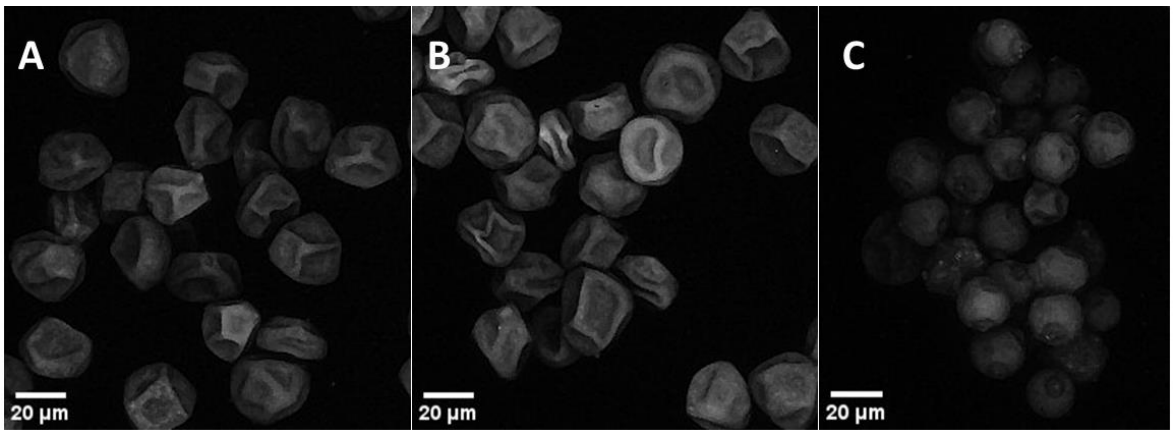

Figure 6.24: Confocal microscopic view of (A) control, (B) dried and (C) hydrated Betula pendula pollen

Similar findings have been noted previously for the hydration of various pollen types. In a similar investigation, pollen from several species was examined by fluorescence microscopy before and after rehydration (Castro et al., 2010). Although different excitation and emission wavelengths were used, there was a notable decrease in fluorescence observed upon re-hydration along with the same changes to the physical structures of pollen. Dried pollen was found to contain a tight formation usually containing furrows and folds, upon rehydration the structure expanded and filled and often became rounder in appearance – further justifying the observations noted here. The decrease in fluorescence seen upon hydration is attributed to the quenching ability of water which has previously been found to occur naturally during rehydration at the stigma as well as upon germination (Audran and Willemse, 1982; Roshchina, 2005). Interestingly, high intensities were still found for the wet pollen – although significantly less so than for the dried or control pollen, this possibly indicates the presence of non-viable pollen grains, which have been found not to experience the same notable decreased in fluorescence (Castro et al., 2010; Roshchina, 2003). The difference between the control and dried pollen set an interesting comparison to the IR analysis, which was not able to distinguish any notable differences in composition. This indicates that even when no notable differences can be determined from chemical analysis – differences in fluorescence may remain.

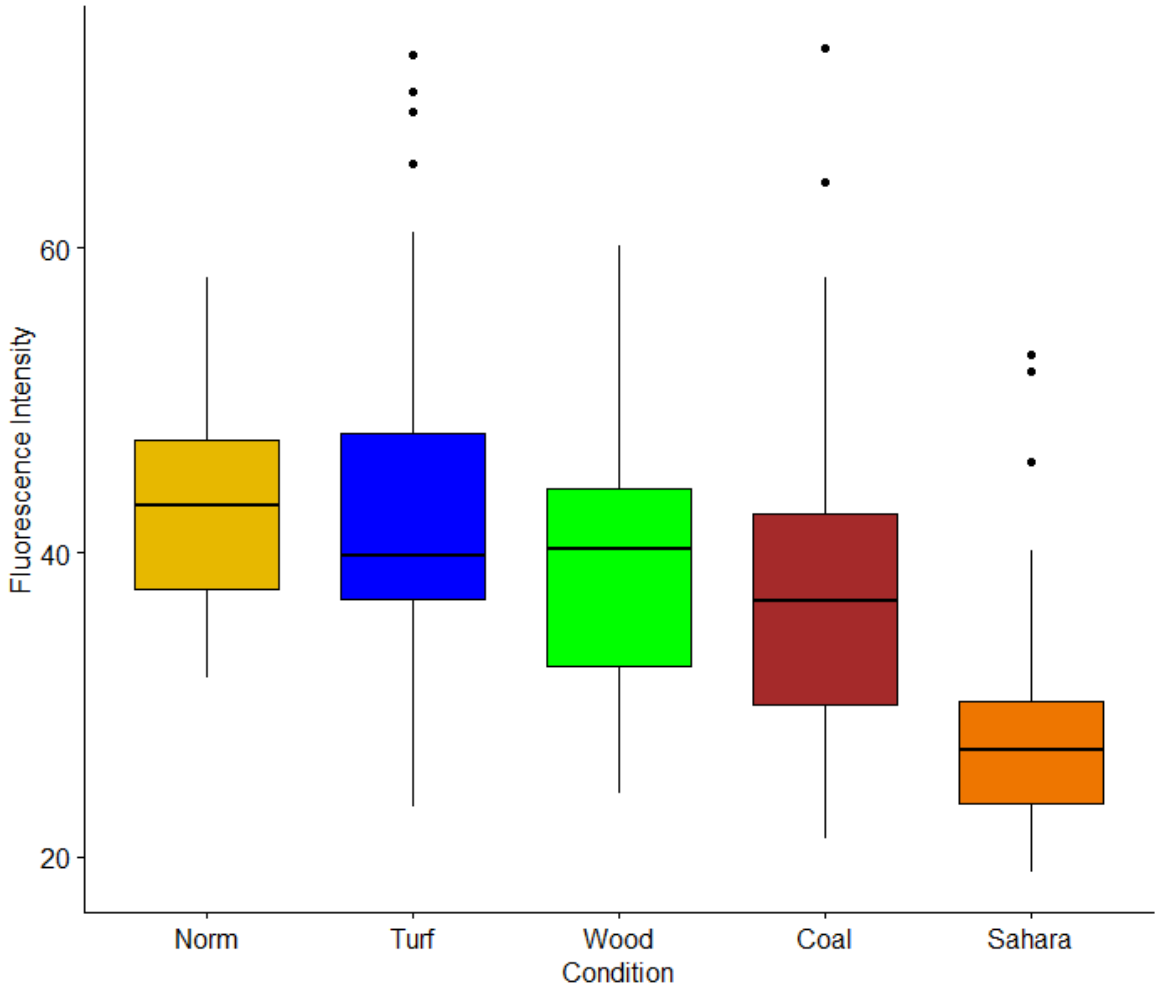

Figure 6.25: Fluorescence intensity ranges for pollen exposed to ashes/dust samples (n=40)

Upon exposure to different types of ashes/dust, a range of fluorescent intensities were observed. All samples except the pollen-turf sample exhibited statistically significant differences from the control pollen. Although the turf-pollen sample was ultimately determined to have comparable average fluorescent intensity to the control pollen, a greater variance in intensity was found. In some cases, the adhesion of turf ash to the pollen grain led to a reduction in fluorescence whereas on other occasions a notable increase was noted. This can be observed in Figure 6.26B where some fluorescent particles from the tuft ash was seen adhered to the pollen. This notable fluorescence of some ashes/soot has been noted previously in an investigation focussing on potentially interfering fluorescent particles that could be misclassified as bioaerosols using the WIBS (Savage et al., 2017). Soot was shown to possibly possess notable fluorescence whereas wood smoke aerosol illustrated a varying degree of fluorescence (Savage et al., 2017). Although the majority of ashes investigated here had a negative impact on pollen fluorescence – this could vary using other excitation wavelengths such as 280 nm and 370 nm (WIBS) since notable fluorescence for dust and soot has been noted previously. A similar study by Pöhlker, Huffman and Pöschl, 2012 examined the autofluorescent behaviour of several bioaerosols and potential interfering aerosols and although soot and dust samples exhibited less intense fluorescence than many of the other samples, the fluorescence

that was noted commonly occurred at lower excitation and emissions than was used here. However, it is still possible that the fluorescence provided by the adhered particles could still be less than that of the pollen – leading to a dulling effect, which was seen for the remaining samples. This was particularly true for the Saharan dust samples as illustrated in Figure 6.26C, the addition of particles on the pollen surface can be noted as dull areas – where the intensity of the pollen grain fluorescence is muted. There is a notable absence of literature studies that investigate the combined effect of pollen grains and adhered particles in terms of fluorescence. However, one study looking at the effects of fullerene particle adhesion to pollen noted a significant decrease in fluorescence, similar to what was observed here, in addition to a decrease in pollen germination (Aoyagi and Ugwu, 2011). This also suggests that perhaps smaller particles similar in size to fullerene particles can also have a notable impact on pollen fluorescence.

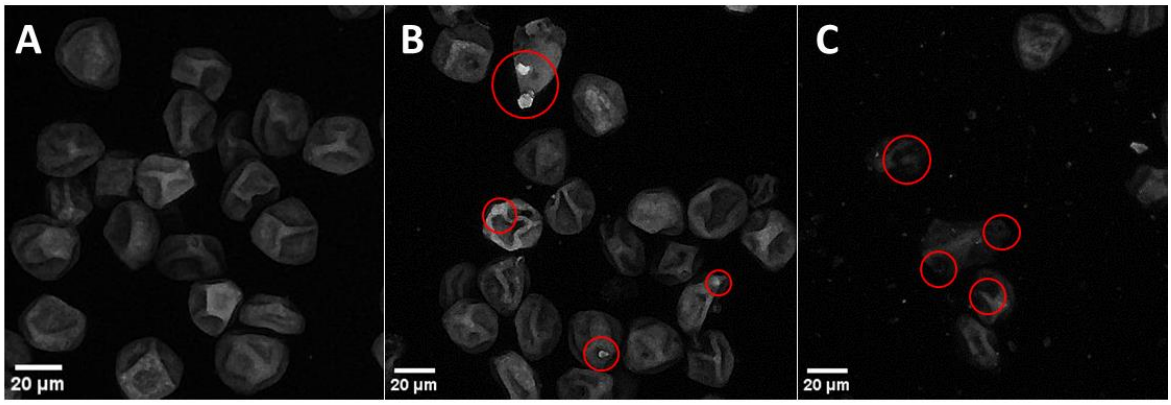

Figure 6.26: Fluorescence microscopic images of (A) control sample, and (B) turf ash and (C) Saharan dust on Betula pendula pollen grains, adhered particles are shown within red circles for clarification

In the case of the pollen exposed to O_3 and car exhaust fumes, little difference in fluorescent intensity was observed. In previous studies, extracts of several pollens were shown to undergo a notable shift in emission maxima following exposure to O_3 (from 530-550 nm to 475-480 nm) (Roshchina and Karnaukhov, 1999; Roshchina and Mel'nikova, 2001). Similar changes have also been observed for other bioaerosol classes including bacteria (Santarpia et al., 2012). Perhaps a si,ilar shift occurred in the current study but was not noted due to the inability to obtain specific fluorescent spectra using the apparatus available. Similar shifts in pollen fluorescence have also been noted for pollen that has been aged for several years as well as pollen exposed to UV light (Roshchina, 2003; Schulte et al., 2008). It is possible that changes occurred in the pollen samples exposed to O_3 and car exhaust fumes (as evident from the IR spectra), however, this was not detected using the available confocal microscope setup. Although the overall fluorescence intensity did not differ between the exposed and unexposed samples, it is likely that if examined using more sophisticated fluorometric devices or even using the varying channels available for bioaerosol classification in the WIBS,

Rapid-E and Poleno, that deviations would be observed if these shifts in fluorescent maxima were to occur.

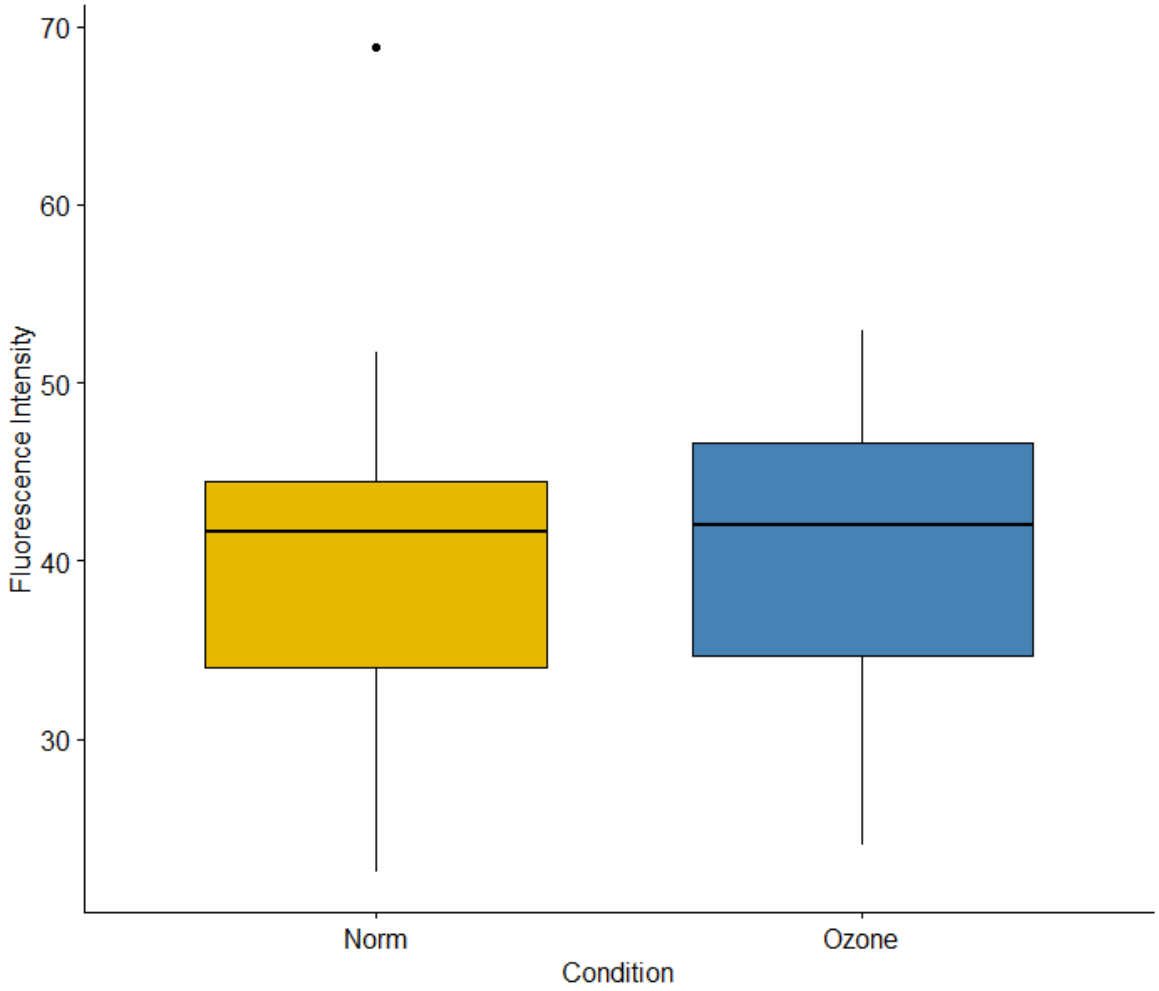

Figure 6.27: Fluorescence intensity ranges for pollen exposed to O_3 (n=40)

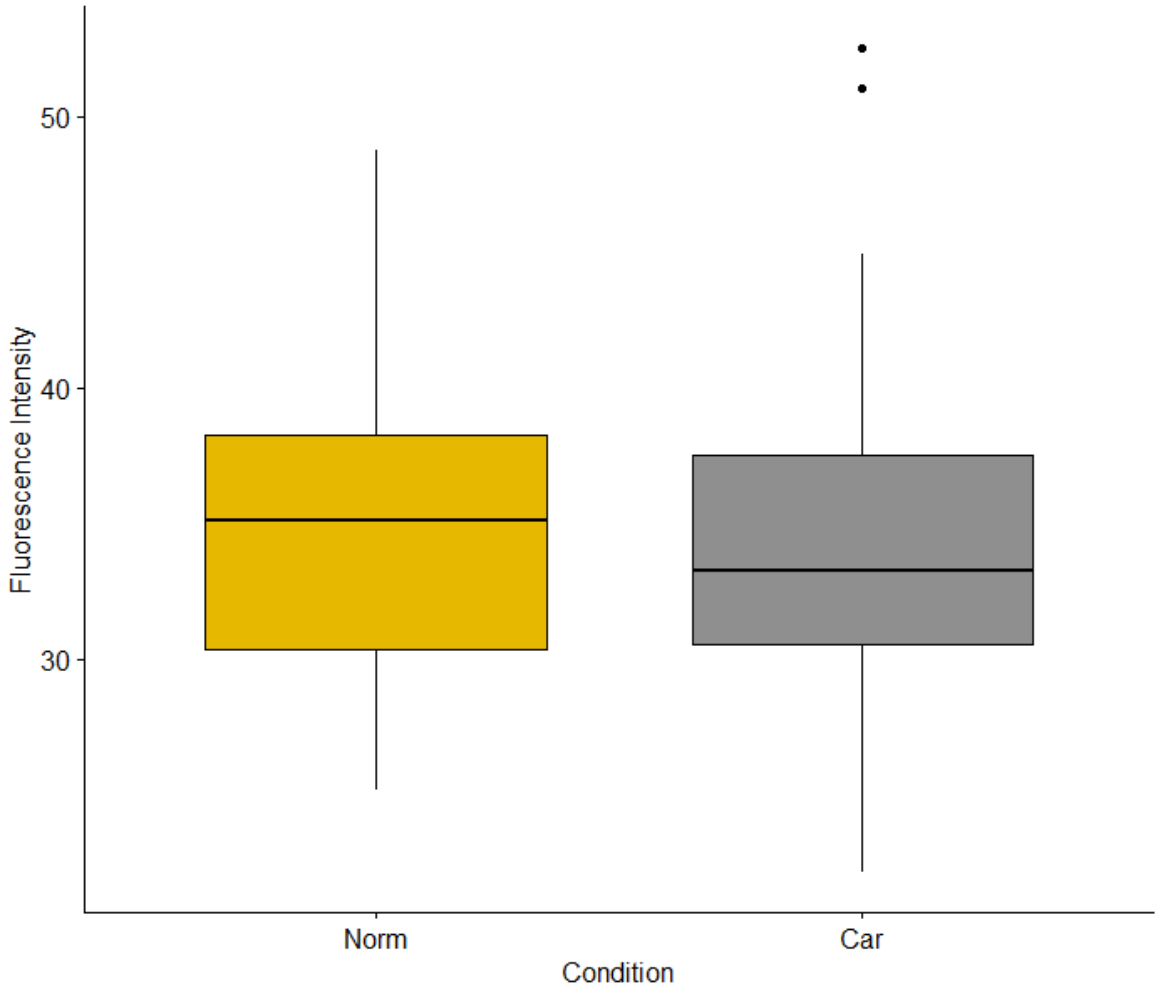

Figure 6.28: Fluorescence intensity ranges for pollen exposed to car exhaust (n=40_)

6.4 Conclusion

Vibrational spectroscopy offers a strong alternative to molecular methods when determining species-specific level identification of ambient pollen types, including the accurate differentiation of 11 of the most common pollen types present within the Irish environment. The power of IR to detect compositional changes to the pollen grains following exposure to varying environmental and anthropogenic conditions was also noted. Changes introduced due to variations in water availability, exposure to gaseous pollutants such as car exhaust and ozone as well as particle adhesion to the pollen surface can all lead to notable changes in pollen composition. This suggests if such methods were ever to be introduced to the real-time detection of ambient pollen concentrations, the potential exists to also examine air quality parameters through the identification of such interferences.

Several of these changes in chemical composition did not translate to changes in overall fluorescence intensity, although this could be due to the fluorescence parameters/equiptment used being unable to detect changes in emission maxima. However, in the case of samples that showed limited compositional changes, making IR differentiation between control and dried pollen difficult,

changes in fluorescence intensity were apparent. This indicates the potential synergy between the two analytical methods. Notable changes in pollen fluorescence intensity were observed for changes in water content as well as the adherence of particulate matter. Although emission spectra were not available, the clear deviations indicate that LIF instrumentation such as the WIBS and potentially the Poleno could be subject to a range of uncertainties when sampling pollen in diverse urban environments. This has previously been noted in this project for the use of the WIBS (as has other preceding literature), however, it is unclear how such conditions could affect the identification efficiency of more complex instruments such as the Poleno.

6.5 Future work

Although the potential to discriminate to a species level has been shown for the analysis of pollen with IR, this was not fully investigated in Dublin. To further assess this potential, IR analysis coupled with molecular methods (currently in place at the Dublin site) could further add credence to this. Notable deviations in the chemical composition of *Betula pendula* following exposure to various conditions were also noted. However, alterations induced in pollen composition are dependent on a range of parameters, including pollen type. Therefore, to determine the susceptibility of different pollen types to different conditions, future work should also include the analysis of a variety of other pollen taxa (following exposure scenarios), particularly those of allergenic concern such as Poaceae.

Much work is intended with regard to the fluorescent implications associated with polluted or contaminated pollen. Many real-time instruments such as the Poleno (recently purchased and currently being trained at the Dublin site) operate on the basis of machine learning algorithms having been trained with known pollen samples. However, although this method is likely to account for fluorescent changes between different pollen types, it may not fully account for changes in pollen fluorescence and morphology following pollen dispersal. Future work could focus on analysing samples of polluted pollen using fluorometers (excitation and emission scans), once a suitable solid sample holder is sourced, to determine specific spectral deviations. Following this, samples could be further examined using the Poleno and/or WIBS to determine if misclassification occurs since these polluted pollens will likely represent more immediate respiratory concern than their unpolluted counterparts. Training using suitably exposed pollen (using typical atmospheric concentrations of pollutants etc.) could aid in this detection and will be further investigated beyond the scope of this project in future studies.

References

Anıl, I., Golcuk, K., Karaca, F., 2014. Water. Air. Soil Pollut. 225.

Aoyagi, H., Ugwu, C.U., 2011. Nanotechnol. Sci. Appl. 4, 67–71.

Audran, J.C., Willemse, M.T.M., 1982. Protoplasma 110, 106–111.

Bağcıoğlu, M., Kohler, A., Seifert, S., Kneipp, J., Zimmermann, B., 2017. Methods Ecol. Evol. 8, 870–880.

Banchi, E., Pallavicini, A., Muggia, L., 2020. Aerobiologia (Bologna). 36, 9–23.

Barberini, S., Della Rocca, G., Danti, R., Zanoni, D., Mori, B., Ariano, R., Mistrello, G., 2015. Eur. Ann. Allergy Clin. Immunol. 47, 149–155.

Barnasan, P., Damdin, B., Sanjaa, B., Munkhtaivan, B., Ariunbold, A., Soninkhuu, J., Budeebazar, A., Aleksandr, A., Kuznetsov, P., 2021. Proc. 5th Int. Conf. Chem. Investig. Util. Nat. Resour. 2, 118–127.

Baıcioılu, M., Zimmermann, B., Kohler, A., 2015. PLoS One 10, 1–19.

Bist, A., Pandit, T., Bhatnagar, A.K., Singh, A.B., 2004. Grana 43, 94–100.

Blokker, P., Boelen, P., Broekman, R., Rozema, J., 2006. Plant Ecol. 182, 197–207.

Buters, J., Clot, B., Galán, C., Gehrig, R., Gilge, S., Hentges, F., O'Connor, D., Sikoparija, B., Skjoth, C., Tummon, F., Adams-Groom, B., Antunes, C.M., Bruffaerts, N., Çelenk, S., Crouzy, B., Guillaud, G., Hajkova, L., Seliger, A.K., Oliver, G., Ribeiro, H., Rodinkova, V., Saarto, A., Sauliene, I., Sozinova, O., Stjepanovic, B., 2022. Aerobiologia (Bologna).

Castro, A.J., Rejon, J.D., Fendri, M., Jimenez-Quesada, M.J., Zafra, A., Jimenez-Lopez, J.C., Rodriguez-Garcia, M.I., Alche, J.D., 2010. Microsc. Sci. Technol. Appl. Educ. 607–613.

Chassard, G., Choël, M., Gosselin, S., Vorng, H., Petitprez, D., Shahali, Y., Tsicopoulos, A., Visez, N., 2015. Environ. Pollut. 196, 107–113.

Choël, M., Ivanovsky, A., Roose, A., Hamzé, M., Blanchenet, A.M., Visez, N., 2022a. J. Aerosol Sci. 161.

Choël, M., Visez, N., Secordel, X., Deboudt, K., 2022b. Aerobiologia (Bologna). 38, 151–162.

Crouzy, B., Stella, M., Konzelmann, T., Calpini, B., Clot, B., 2016. Atmos. Environ. 140, 202–212.

D'Amato, G., Cecchi, L., Bonini, S., Nunes, C., Annesi-Maesano, I., Behrendt, H., Liccardi, G., Popov, T., Van Cauwenberge, P., 2007. Allergy Eur. J. Allergy Clin. Immunol. 62, 976–990.

Dahl, Å., Galán, C., Hajkova, L., Pauling, A., Sikoparija, B., Smith, M., Vokou, D., 2013. The Onset, Course and Intensity of the Pollen Season, in: Allergenic Pollen. Springer Netherlands, Dordrecht, pp. 29–70.

Depciuch, J., Kasprzyk, I., Drzymała, E., Parlinska-Wojtan, M., 2018. Aerobiologia (Bologna). 34, 525–538.

Depciuch, J., Kasprzyk, I., Roga, E., Parlinska-Wojtan, M., 2016. Environ. Sci. Pollut. Res. 23, 23203–23214.

Depciuch, J., Kasprzyk, I., Sadik, O., Parlińska-Wojtan, M., 2017. Aerobiologia (Bologna). 33, 1–12.

Després, V.R., Alex Huffman, J., Burrows, S.M., Hoose, C., Safatov, A.S., Buryak, G., Fröhlich-Nowoisky, J., Elbert, W., Andreae, M.O., Pöschl, U., Jaenicke, R., 2012. Tellus, Ser. B Chem. Phys. Meteorol. 64.

Diehn, S., Zimmermann, B., Tafintseva, V., Bağcıoğlu, M., Kohler, A., Ohlson, M., Fjellheim, S., Kneipp, J., 2020. Anal. Bioanal. Chem. 6459–6474.

Domínguez, E., Heredia, A., Mercado, J.A., Quesada, M.A., 1998. Grana 37, 93–96.

EPA Ireland, 2023. Ireland's environment: Air [WWW Document]. Curr. trends air Qual. URL https://www.epa.ie/our-services/monitoring--assessment/assessment/irelands-environment/air/current-trends-air/#d.en.85983 (accessed 9.29.23).

Erb, S., Graf, E., Zeder, Y., Lionetti, S., Berne, A., Clot, B., Lieberherr, G., Tummon, F., Wullschleger, P., Crouzy, B., 2023. EGU Sph. Prepr. Repos. 1–20.

Fennelly, M., Sewell, G., Prentice, M., O'Connor, D., Sodeau, J., 2017. Atmosphere (Basel). 9, 1.

Firon, N., Nepi, M., Pacini, E., 2012. Ann. Bot. 109, 1201–1213.

Frank, U., Ernst, D., 2016. Front. Plant Sci. 7, 2–5.

Franze, T., Weller, M.G., Niessner, R., Pöschl, U., 2005. Environ. Sci. Technol. 39, 1673–1678.

Gottardini, E., Rossi, S., Cristofolini, F., Benedetti, L., 2007. Aerobiologia (Bologna). 23, 211–219.

Goudie, A.S., Middleton, N.J., 2001. Earth-Science Rev. 56, 179–204.

Grewling, Ł., Bogawski, P., Kryza, M., Magyar, D., Šikoparija, B., Skjøth, C.A., Udvardy, O., Werner, M., Smith, M., 2019. Environ. Pollut. 254.

Gruijthuijsen, Y.K., Grieshuber, I., Stöcklinger, A., Tischlera, U., Fehrenbach, T., Weller, M.G., Vogel, L., Vieths, S., Pöschl, U., Duschl, A., 2006. Int. Arch. Allergy Immunol. 141, 265–275.

Hoekstra, F.A., Golovina, E.A., Tetteroo, F.A.A., Wolkers, W.F., 2001. Cryobiology 43, 140–150.

Hong, T., Yin, J.Y., Nie, S.P., Xie, M.Y., 2021. Food Chem. X 12, 100168.

Hrabina, M., Peltre, G., Moingeon, P., 2008. Clin. Exp. Allergy Rev. 8, 7–11.

Jardine, P.E., Fraser, W.T., Lomax, B.H., Gosling, W.D., 2015. J. Micropalaeontology 34, 139–149.

Jaworski, A., Lejda, K., Mądziel, M., Ustrzycki, A., 2018. IOP Conf. Ser. Mater. Sci. Eng. 421.

Jiang, L., Zhang, J., 2013. Biodegradable Polymers and Polymer Blends, in: Handbook of Biopolymers and Biodegradable Plastics. Elsevier, pp. 109–128.

Jung, S., Estrella, N., Pfaffl, M.W., Hartmann, S., Handelshauser, E., Menzel, A., 2018. PLoS One 13, 1–12.

Kadri, K., Elsafy, M., Makhlouf, S., Awad, M.A., 2022. Saudi J. Biol. Sci. 29, 1085–1091.

Kanter, U., Heller, W., Durner, J., Winkler, J.B., Engel, M., Behrendt, H., Holzinger, A., Braun, P., Hauser, M., Ferreira, F., Mayer, K., Pfeifer, M., Ernst, D., 2013. PLoS One 8.

Kawashima, S., Clot, B., Fujita, T., Takahashi, Y., Nakamura, K., 2007. Atmos. Environ. 41, 7987–7993.

Kenđel, A., Zimmermann, B., 2020. Front. Plant Sci. 11, 1–19.

Kraaijeveld, K., de Weger, L.A., Ventayol García, M., Buermans, H., Frank, J., Hiemstra, P.S., den Dunnen, J.T., 2015. Mol. Ecol. Resour. 15, 8–16.

Lahlali, R., Jiang, Y., Kumar, S., Karunakaran, C., Liu, X., Borondics, F., Hallin, E., Bueckert, R., 2014. Front. Plant Sci. 5, 1–10.

Lammers, K., Arbuckle-Keil, G., Dighton, J., 2009. Soil Biol. Biochem. 41, 340–347.

Laskina, O., Young, M.A., Kleiber, P.D., Grassian, V.H., 2012. J. Geophys. Res. Atmos. 117, 1–10.

Lin, S., Liu, Z., Zhao, E., Qian, J., Li, X., Zhang, Q., Ali, M., 2019. Process Saf. Environ. Prot. 130, 48–56.

Lisci, M., Tanda, C., Pacini, E., 1994. Pollination Ecophysiology of Mercurialis annua L. (Euphorbiaceae), an Anemophilous Species Flowering all Year Round. Ann. Bot.

Liu, X., Renard, C.M.G.C., Bureau, S., Le Bourvellec, C., 2021. Carbohydr. Polym. 262, 117935.

Mampage, C.B.A., Hughes, D.D., Jones, L.M., Metwali, N., Thorne, P.S., Stone, E.A., 2022. Atmos. Environ. X 15, 1–23.

Melnikova, E. V., Roshchina, V. V., Karnaukhov, V.N., 1997. Biofizika 42, 233.

Mularczyk-Oliwa, M., Bombalska, A., Kaliszewski, M., Włodarski, M., Kopczyński, K., Kwaśny, M., Szpakowska, M., Trafny, E.A., 2012. Spectrochim. Acta - Part A Mol. Biomol. Spectrosc. 97, 246–254.

Namork, E., Johansen, B. V., Løvik, M., 2006. Toxicol. Lett. 165, 71–78.

Nepi, M., Cresti, L., Guarnieri, M., Pacini, E., 2010. Plant Syst. Evol. 284, 57–64.

Nepi, M., Franchi, G.G., Padni, E., 2001. Protoplasma 216, 171–180.

O'Connor, D.J., Healy, D.A., Hellebust, S., Buters, J.T.M., Sodeau, J.R., 2014a. Aerosol Sci. Technol. 48, 341–349.

O'Connor, D.J., Iacopino, D., Healy, D.A., O'Sullivan, D., Sodeau, J.R., 2011. Atmos. Environ. 45, 6451–6458.

O'Connor, D.J., Lovera, P., Iacopino, D., O'Riordan, A., Healy, D.A., Sodeau, J.R., 2014b. Anal. Methods 6, 1633–1639.

O'Connor, D.J., Sadyś, M., Skjøth, C.A., Healy, D.A., Kennedy, R., Sodeau, J.R., 2014c. Aerobiologia (Bologna). 30, 397–411.

Oteros, J., Weber, A., Kutzora, S., Rojo, J., Heinze, S., Herr, C., Gebauer, R., Schmidt-Weber, C.B., Buters, J.T.M., 2020. Environ. Res. 191, 110031.

Pacini, E., 1996. Sex. Plant Reprod. 9, 362–366.

Pacini, E., Guarnieri, M., Nepi, M., 2006. Protoplasma 228, 73–77.

Pappas, C.S., Tarantilis, P.A., Harizanis, P.C., Polissiou, M.G., 2003. Appl. Spectrosc. 57, 23–27.

Pereira, S., Fernández-González, M., Guedes, A., Abreu, I., Ribeiro, H., 2021. Forests 12, 88.

Piffanelli, P., Ross, J.H.E., Murphy, D.J., 1998. Sex. Plant Reprod. 11, 65–80.

Pöhlker, C., Huffman, J.A., Pöschl, U., 2012. Atmos. Meas. Tech. 5, 37–71.

Pöhlker, C., Huffman, J.A., Pöschl, U., 2013. Atmos. Meas. Tech. 6, 3369–3392.

Pozo, C., Rodríguez-Llamazares, S., Bouza, R., Barral, L., Castaño, J., Müller, N., Restrepo, I., 2018. J. Polym. Res. 25.

Prdun, S., Svečnjak, L., Valentić, M., Marijanović, Z., Jerković, I., 2021. Foods 10.

Pukacki, P.M., Chałupka, W., 2003. Acta Soc. Bot. Pol. 72, 99–104.

Quintyne, K.I., Kelly, C., 2023. Public Heal. Pract. 6, 100406.

Reinmuth-Selzle, K., Ackaert, C., Kampf, C.J., Samonig, M., Shiraiwa, M., Kofler, S., Yang, H., Gadermaier, G., Brandstetter, H., Huber, C.G., Duschl, A., Oostingh, G.J., Pöschl, U., 2014. J. Proteome Res. 13, 1570–1577.

Ribeiro, H., Costa, C., Abreu, I., Esteves da Silva, J.C.G., 2017. Sci. Total Environ. 599–600, 291–297.

Ribeiro, H., Duque, L., Sousa, R., Cruz, A., Gomes, C., Esteves Da Silva, J., Abreu, I., 2014. Int. J. Environ. Health Res. 24, 515–527.

Roshchina, V. V., 2003. J. Fluoresc. 13, 403–420.

Roshchina, V. V., 2005. Izv. Akad. Nauk Ser. Biol. 32, 281–286.

Roshchina, V. V., Karnaukhov, V.N., 1999. Biol. Plant. 42, 273–278.

Roshchina, V. V., Mel'nikova, E. V., 2001. Russ. J. Plant Physiol. 48, 74–83.

Santarpia, J.L., Pan, Y.-L., Hill, S.C., Baker, N., Cottrell, B., McKee, L., Ratnesar-Shumate, S., Pinnick, R.G., 2012. Opt. Express 20, 29867.

Šauliene, I., Šukiene, L., Daunys, G., Valiulis, G., Vaitkevičius, L., Matavulj, P., Brdar, S., Panic, M., Sikoparija, B., Clot, B., Crouzy, B., Sofiev, M., 2019. Atmos. Meas. Tech. 12, 3435–3452.

Sauvageat, E., Zeder, Y., Auderset, K., Calpini, B., Clot, B., Crouzy, B., Konzelmann, T., Lieberherr, G., Tummon, F., Vasilatou, K., 2020. Atmos. Meas. Tech. 13, 1539–1550.

Savage, N.J., Krentz, C.E., Könemann, T., Han, T.T., Mainelis, G., Pöhlker, C., Alex Huffman, J., 2017. Atmos. Meas. Tech. 10, 4279–4302.

Schulte, F., Lingott, J., Panne, U., Kneipp, J., 2008. Anal. Chem. 80, 9551–9556.

Scott, R.J., 1994. Pollen exine – the sporopollenin enigma and the physics of pattern, in: Molecular and Cellular Aspects of Plant Reproduction. Cambridge University Press, pp. 49–82.

Sedghy, F., Varasteh, A.R., Sankian, M., Moghadam, M., 2018. Interaction between air pollutants and pollen grains: The role on the rising trend in allergy. Reports Biochem. Mol. Biol.

Sénéchal, H., Visez, N., Charpin, D., Shahali, Y., Peltre, G., Biolley, J.-P., Lhuissier, F., Couderc, R., Yamada, O., Malrat-Domenge, A., Pham-Thi, N., Poncet, P., Sutra, J.-P., 2015. Sci. World J. 2015, 1–29.

Solomon, W.R., 2002. J. Allergy Clin. Immunol. 109, 895–900.

Sousa, R., Duque, L., Duarte, A.J., Gomes, C.R., Ribeiro, H., Cruz, A., Da Silva, J.C.G.E., Abreu, I., 2012. Environ. Sci. Technol. 46, 2406–2412.

Speranza, A., Calzoni, G.L., Pacini, E., 1997. Sex. Plant Reprod. 10, 110–115.

Vega-Maray, A.M., Fernández-González, D., Valencia-Barrera, R., Suárez-Cervera, M., 2006. Ann. Allergy, Asthma Immunol. 97, 343–349.

Vesprini, J.L., Nepi, M., Cresti, L., Guarnieri, M., Pacini, E., 2002. Grana 41, 16–20.

Visez, N., Ivanovsky, A., Roose, A., Gosselin, S., Sénéchal, H., Poncet, P., Choël, M., 2020. Aerobiologia (Bologna). 36, 49–62.

Wang, J., Kliks, M.M., Jun, S., Jackson, M., Li, Q.X., 2010. J. Food Sci. 75, 208–214.

De Weger, L.A., Beerthuizen, T., Gast-Strookman, J.M., Van der Plas, D.T., Terreehorst, I.,

Hiemstra, P.S., Sont, J.K., 2011. Clin. Transl. Allergy 1, 1–11.

Zhao, F., Elkelish, A., Durner, J., Lindermayr, C., Winkler, J.B., Ruioff, F., Behrendt, H., Traidl-Hoffmann, C., Holzinger, A., Kofler, W., Braun, P., Von Toerne, C., Hauck, S.M., Ernst, D., Frank, U., 2016. Plant Cell Environ. 39, 147–164.

Zimmerman, B., Tafintseva, V., Baɬcioɨlu, M., Høegh Berdahl, M., Kohler, A., 2016. Anal. Chem. 88, 803–811.

Zimmermann, B., 2010. Appl. Spectrosc. 64, 1364–1373.

Zimmermann, B., 2018. Planta 247, 171–180.

Zimmermann, B., Bağcıoğlu, M., Sandt, C., Kohler, A., 2015a. Planta 242, 1237–1250.

Zimmermann, B., Bağcıoğlu, M., Tafinstseva, V., Kohler, A., Ohlson, M., Fjellheim, S., 2017. Ecol. Evol. 7, 10839–10849.

Zimmermann, B., Kohler, A., 2014. PLoS One 9.

Zimmermann, B., Tkalčec, Z., Mešić, A., Kohler, A., 2015b. PLoS One 10, 1–22.

Appendix A

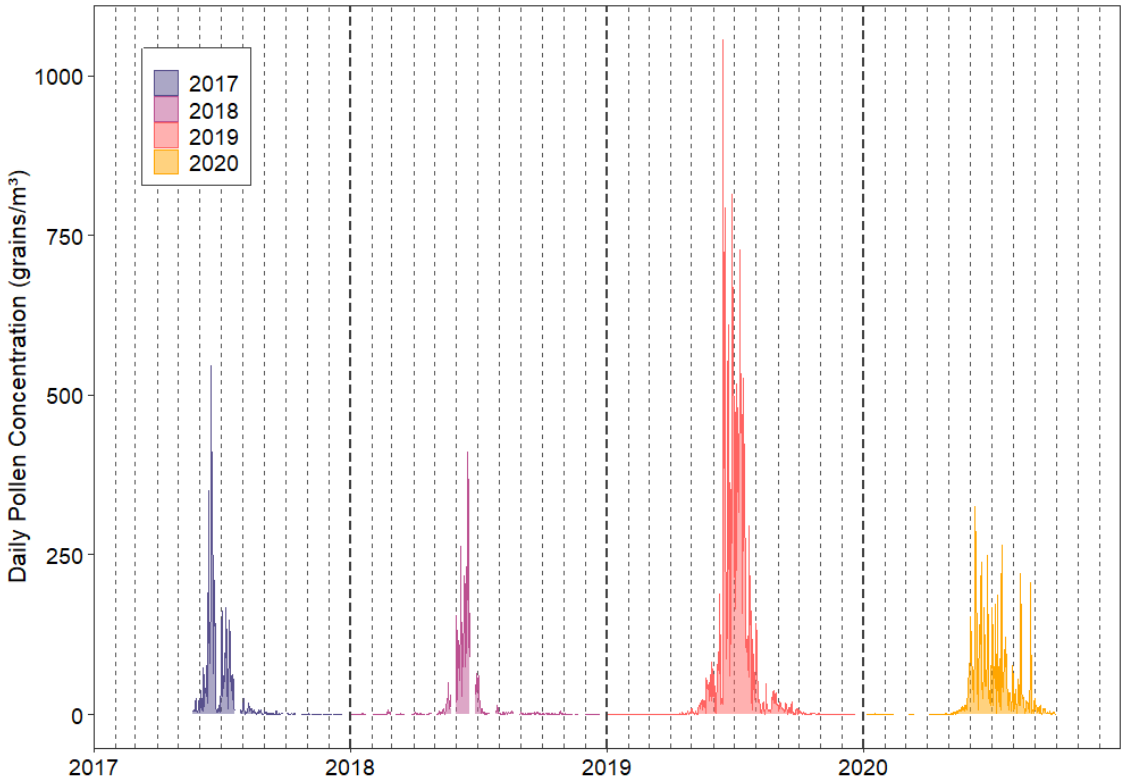

Figure A1: Time-series of Poaceae pollen concentrations from 2017 -2020 (Dublin)

Appendix B

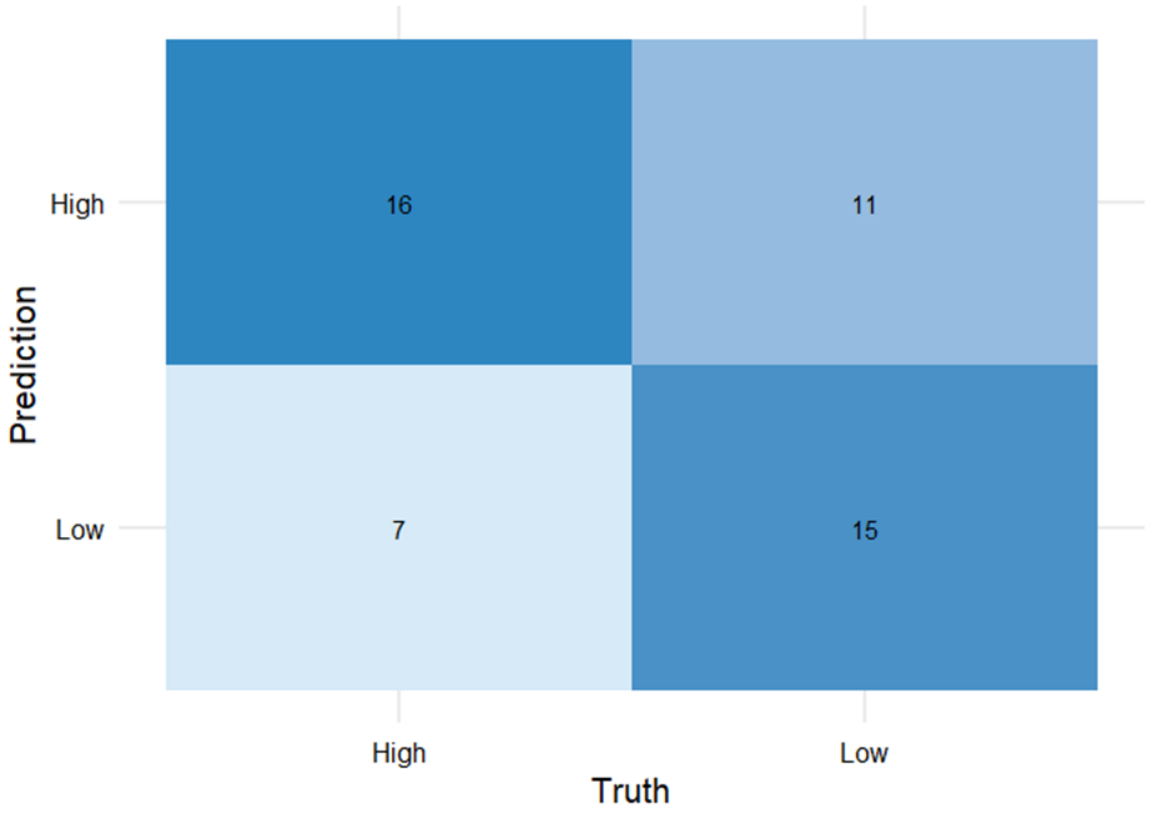

Figure B1: Confusion matrix of RF Poaceae model (30T)

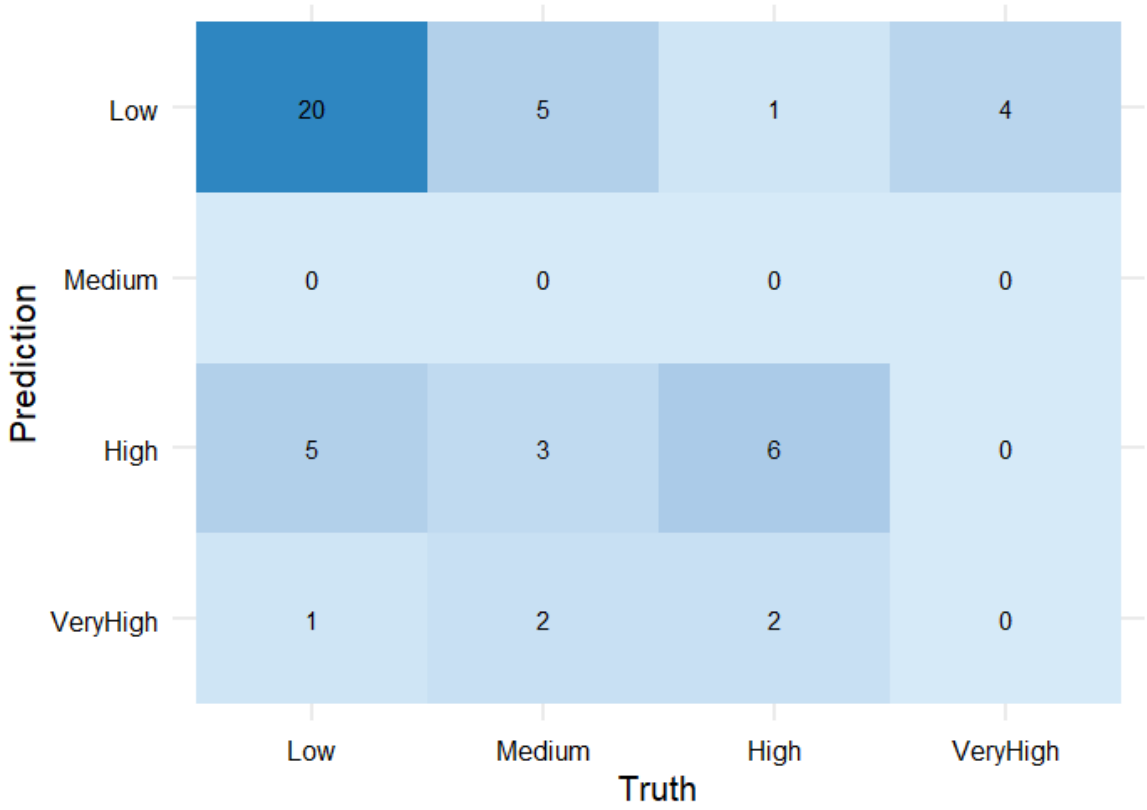

Figure B2: Confusion matrix of RF Poaceae model (UKT)

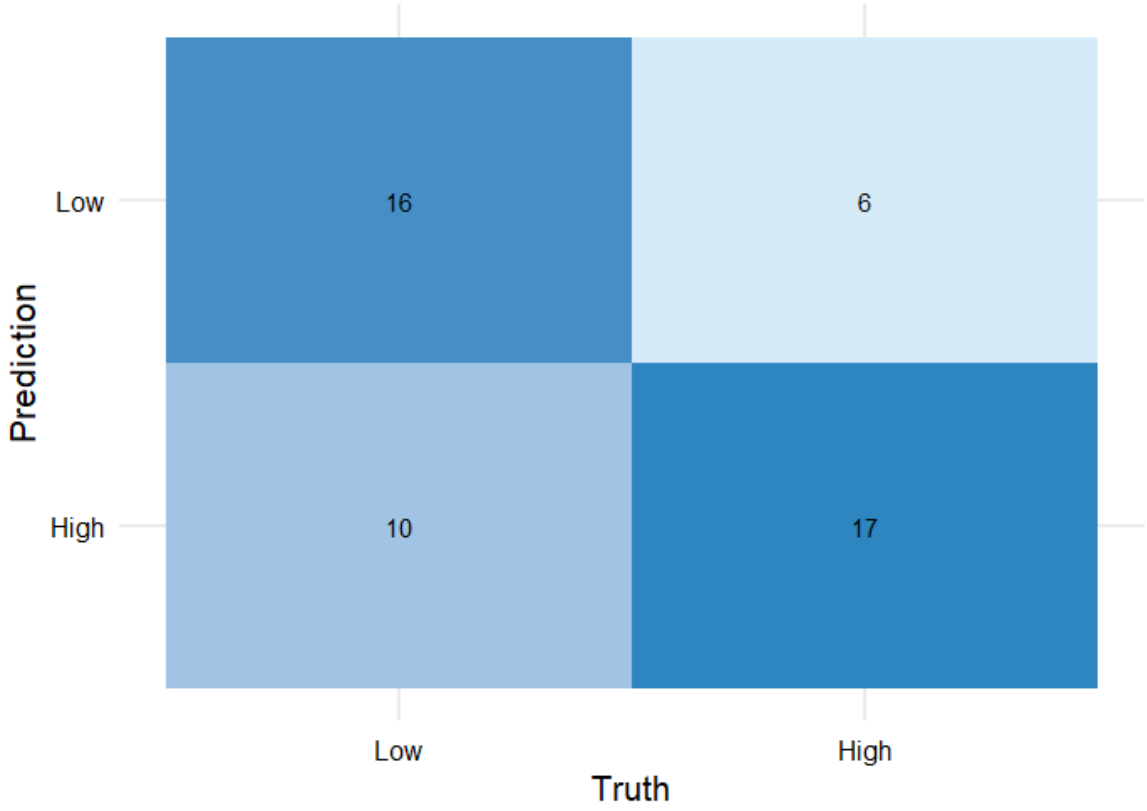

Figure B3: Confusion matrix of SVM-BOR Poaceae model (30T)

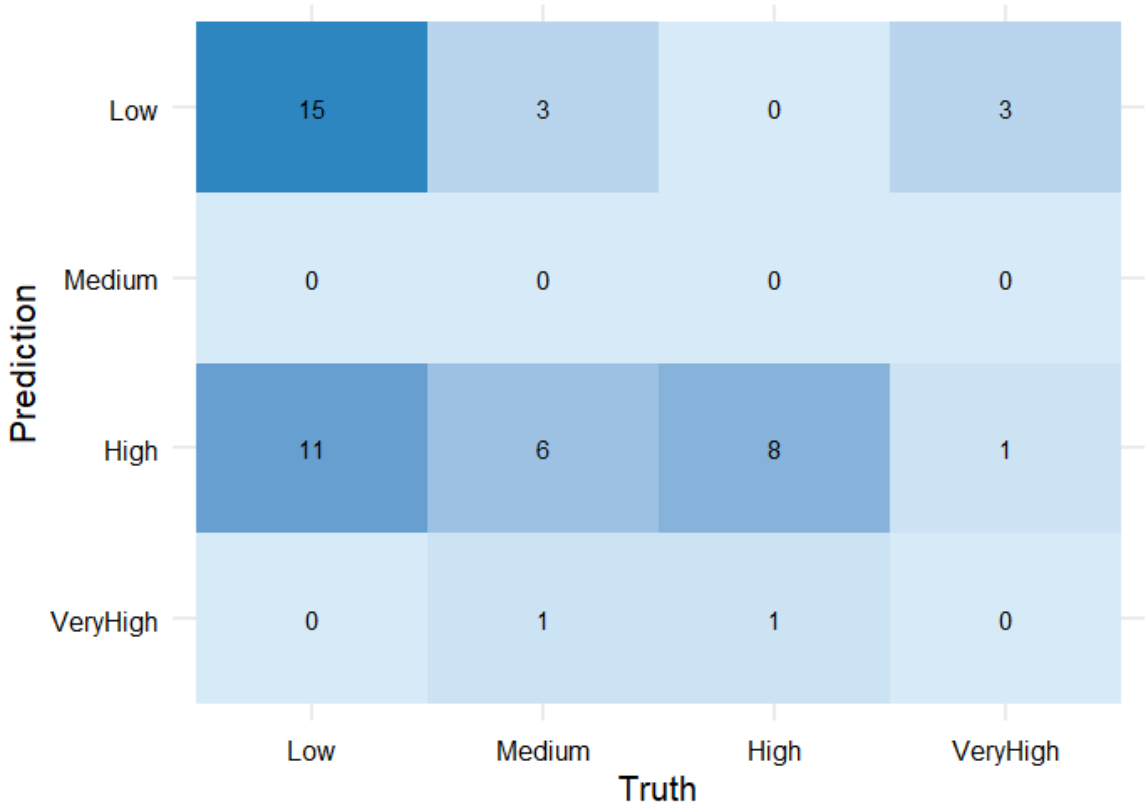

Figure B4: Confusion matrix of SVM Poaceae model (UKT)

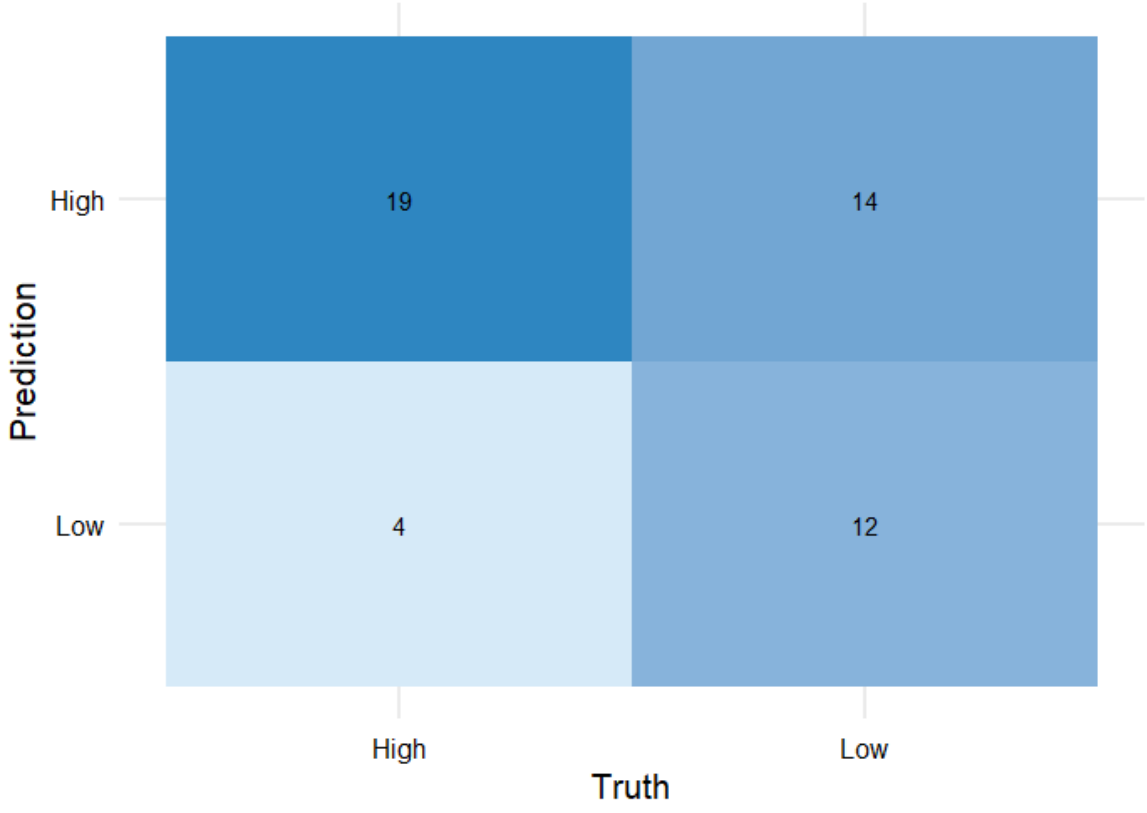

Figure B5: Confusion matrix of ANN Poaceae model (30T)

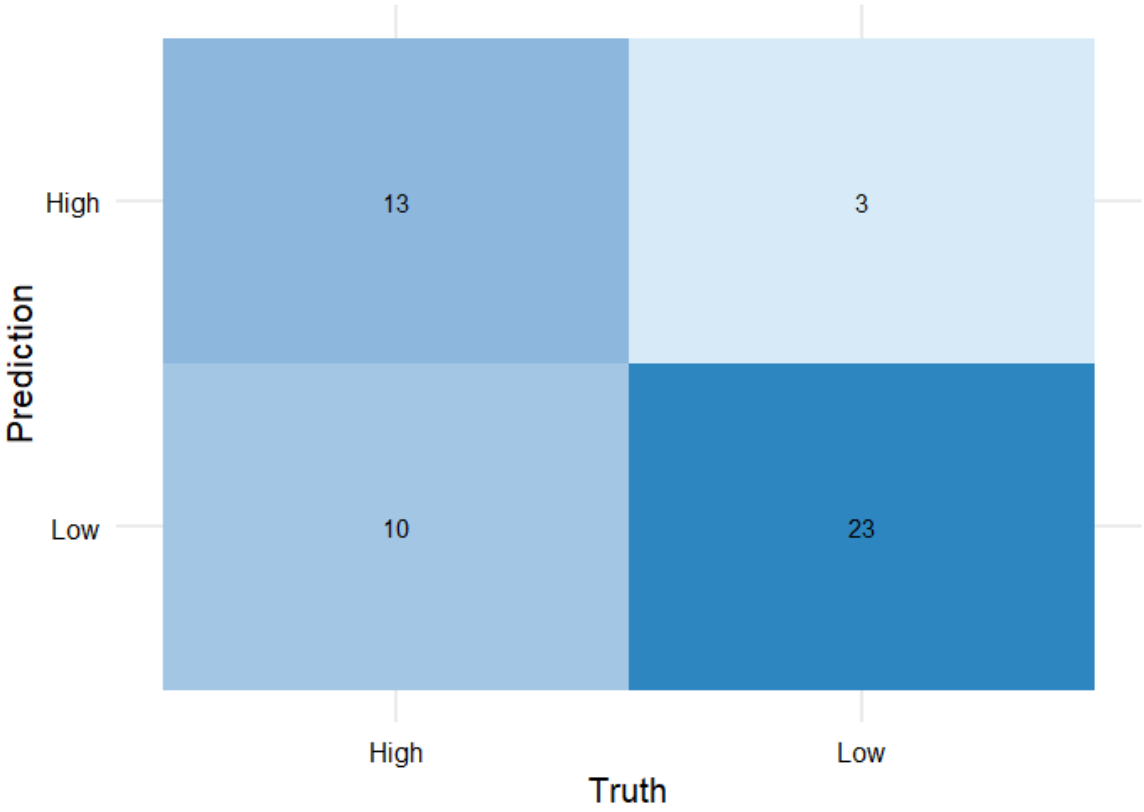

Figure B6: Confusion matrix of ANN-BOR Poaceae model (30T)

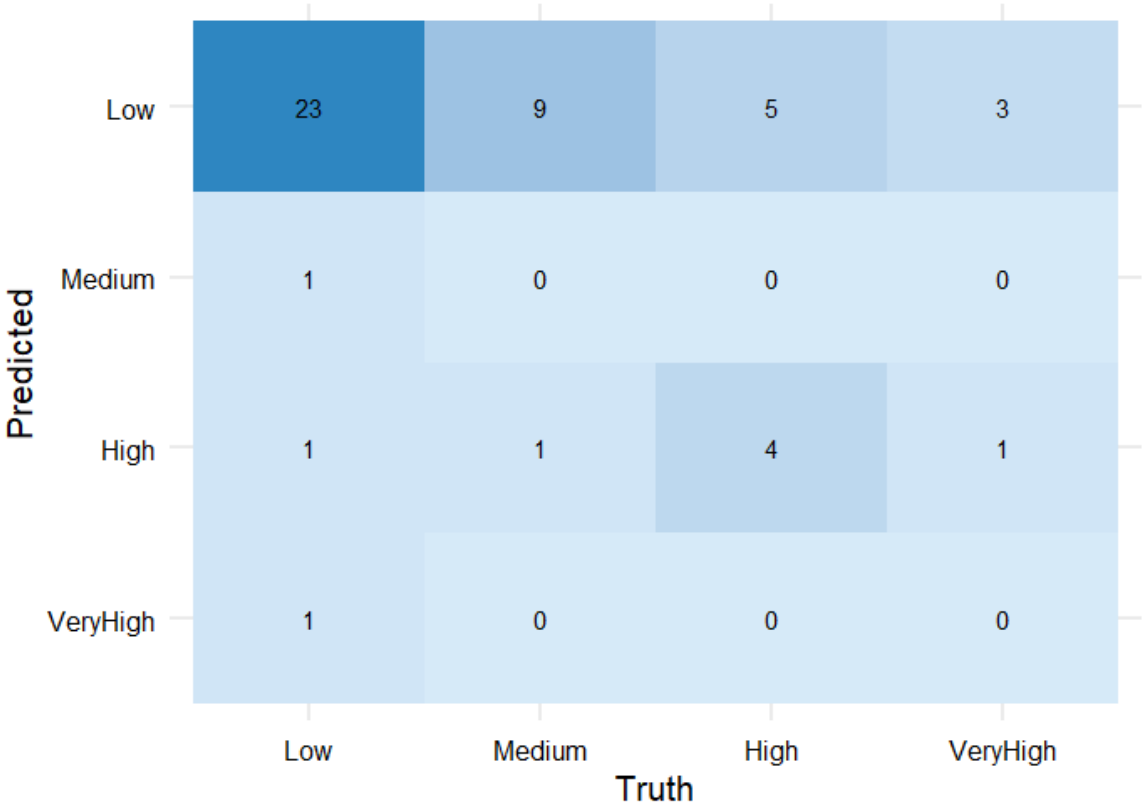

Figure B7: Confusion matrix of ANN Poaceae model (UKT)

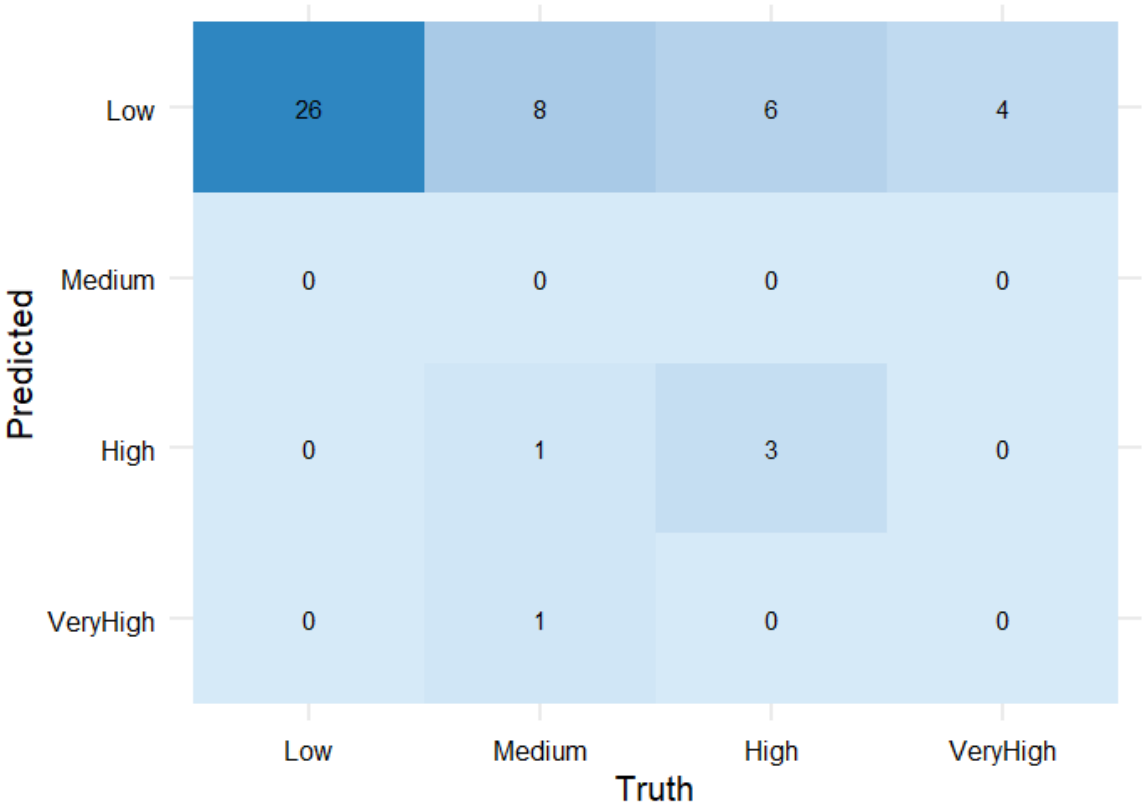

Figure B8: Confusion matrix of ANN-BOR Poaceae model (UKT)

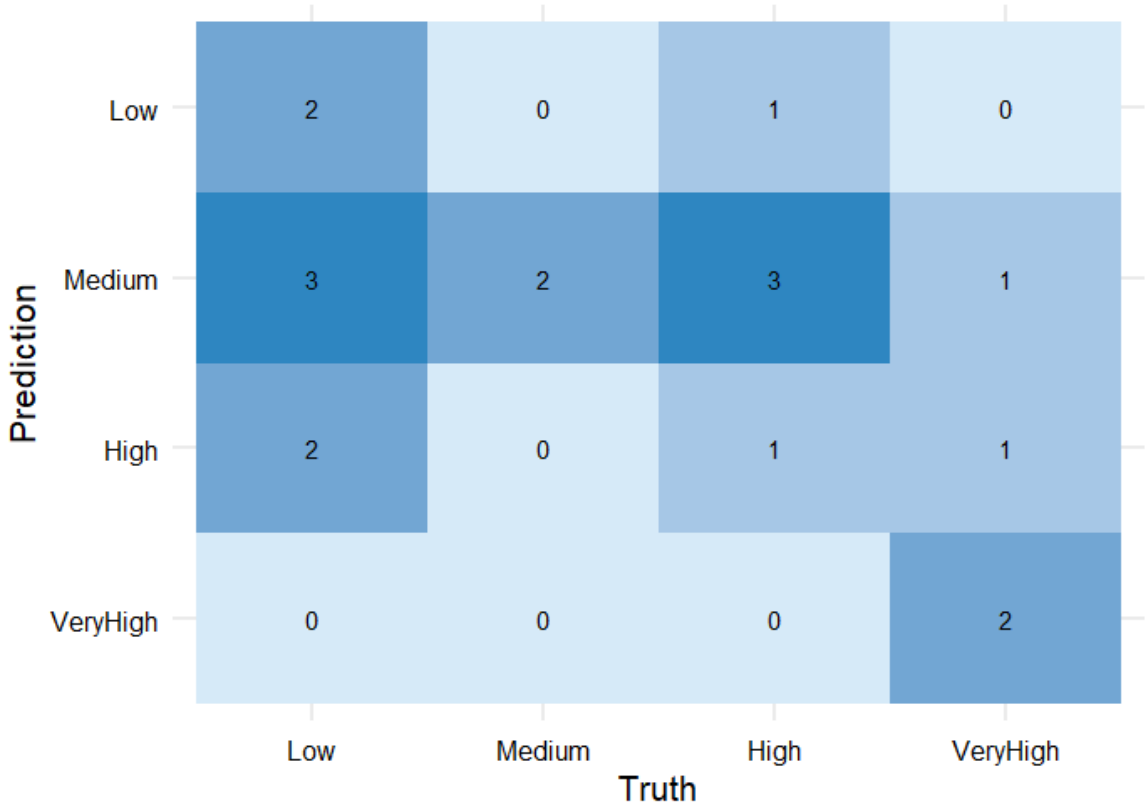

Figure B9: Confusion matrix of RF Betula model (UKT)

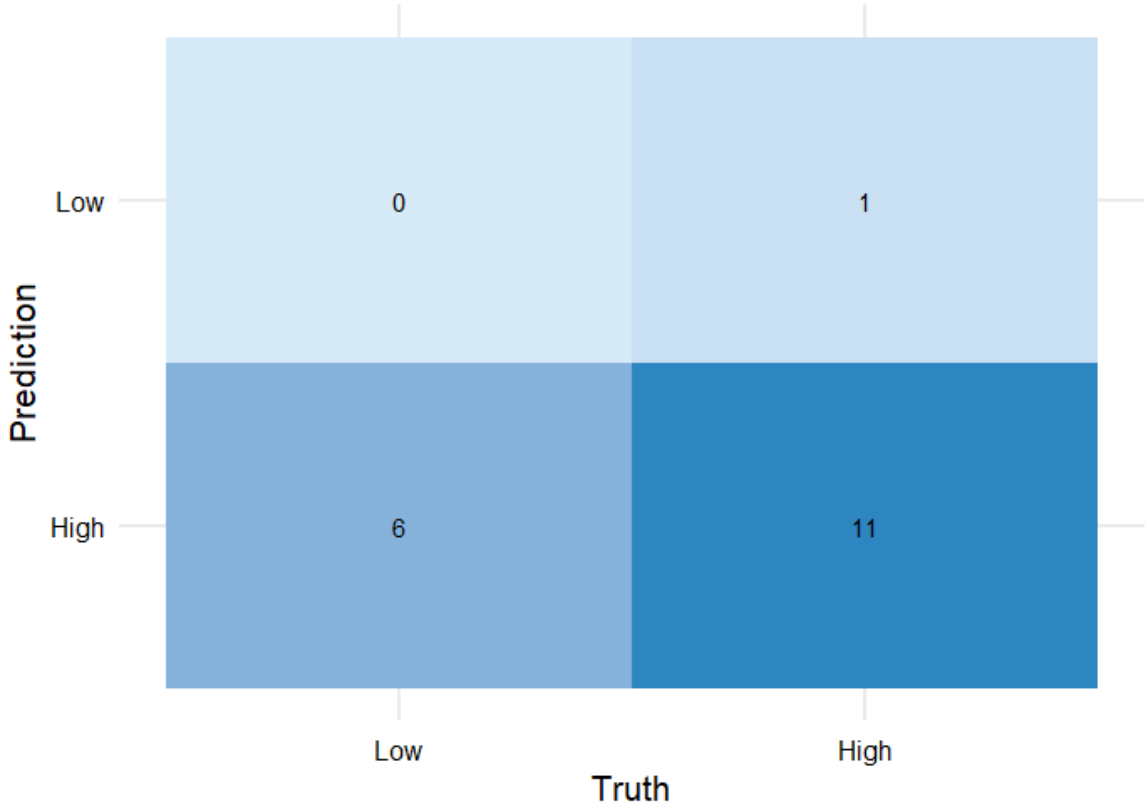

Figure B10: Confusion matrix of SVM Betula model (30T)

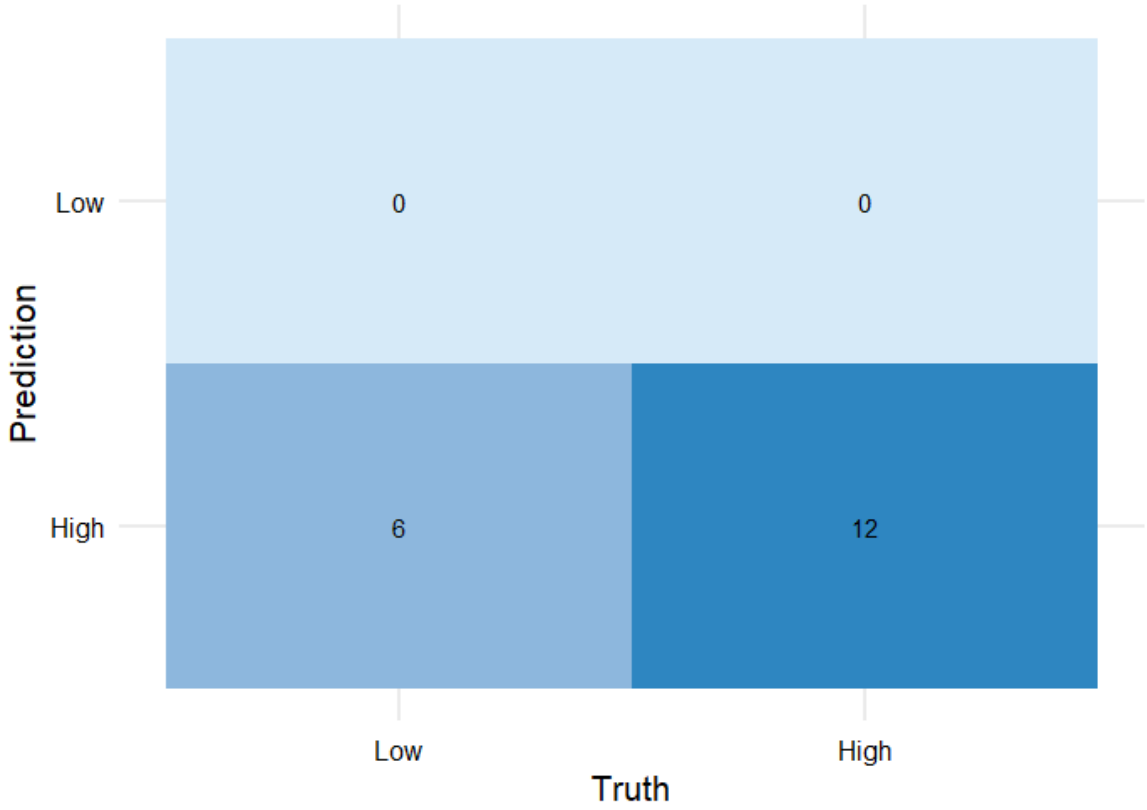

Figure B11: Confusion matrix of SVM-BOR Betula model (30T)

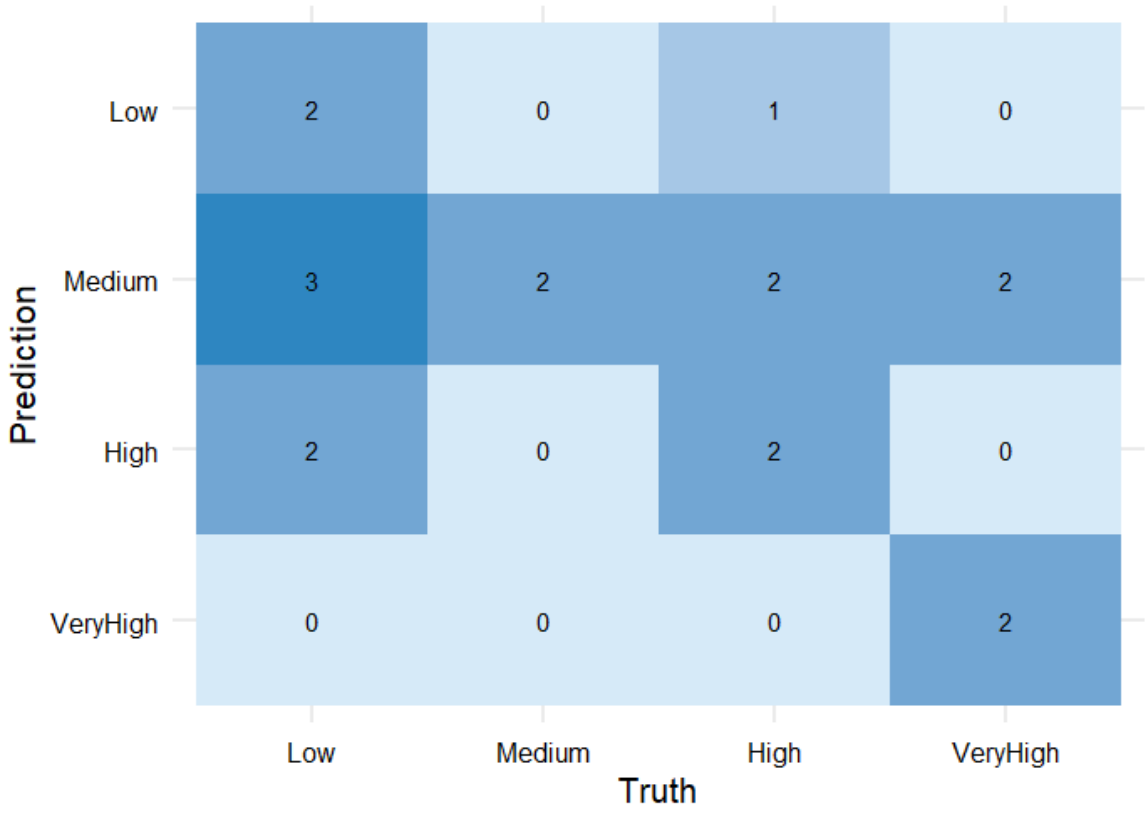

Figure B12: Confusion matrix of SVM Betula model (UKT)

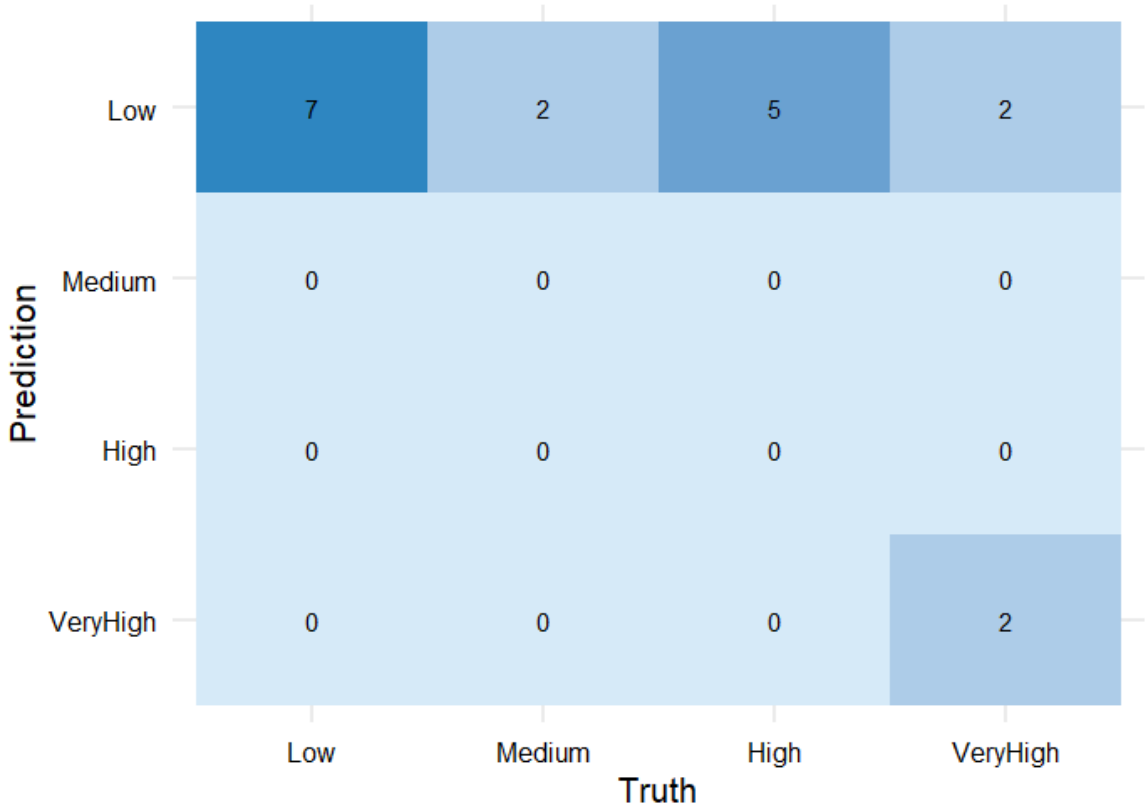

Figure B13: Confusion matrix of SVM-BOR Betula model (UKT)

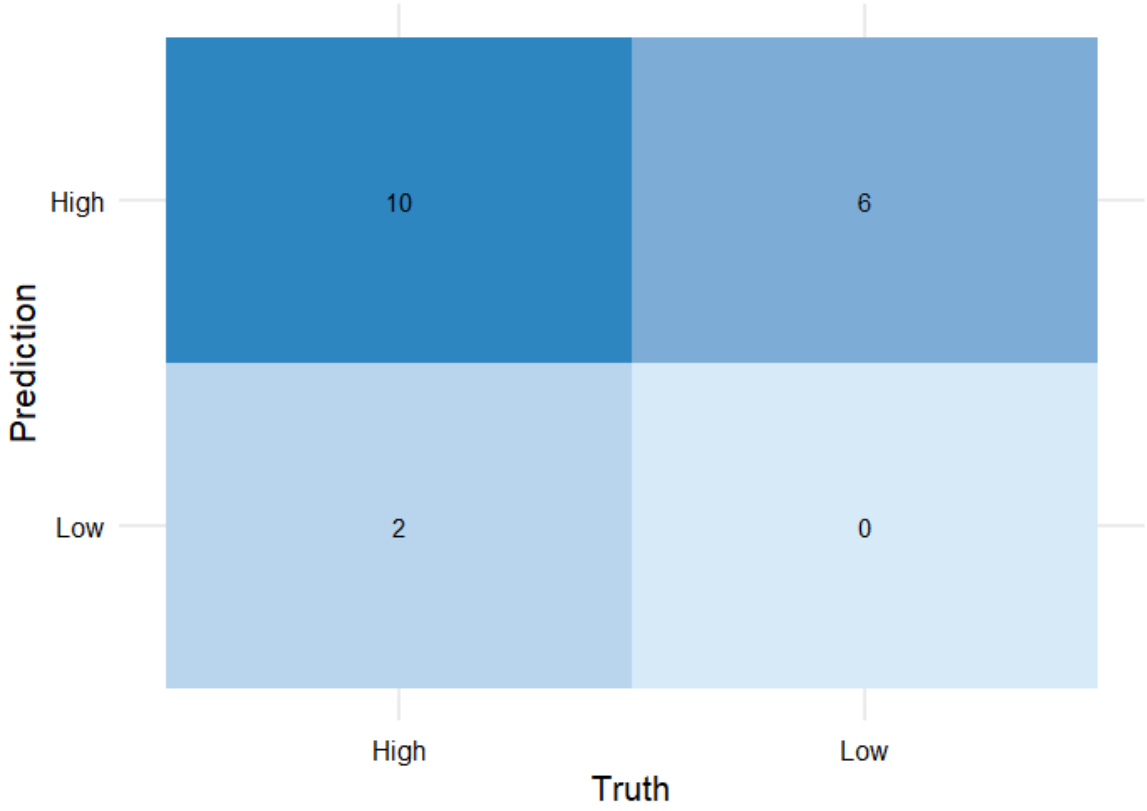

Figure B14: Confusion matrix of ANN Betula model (30T)

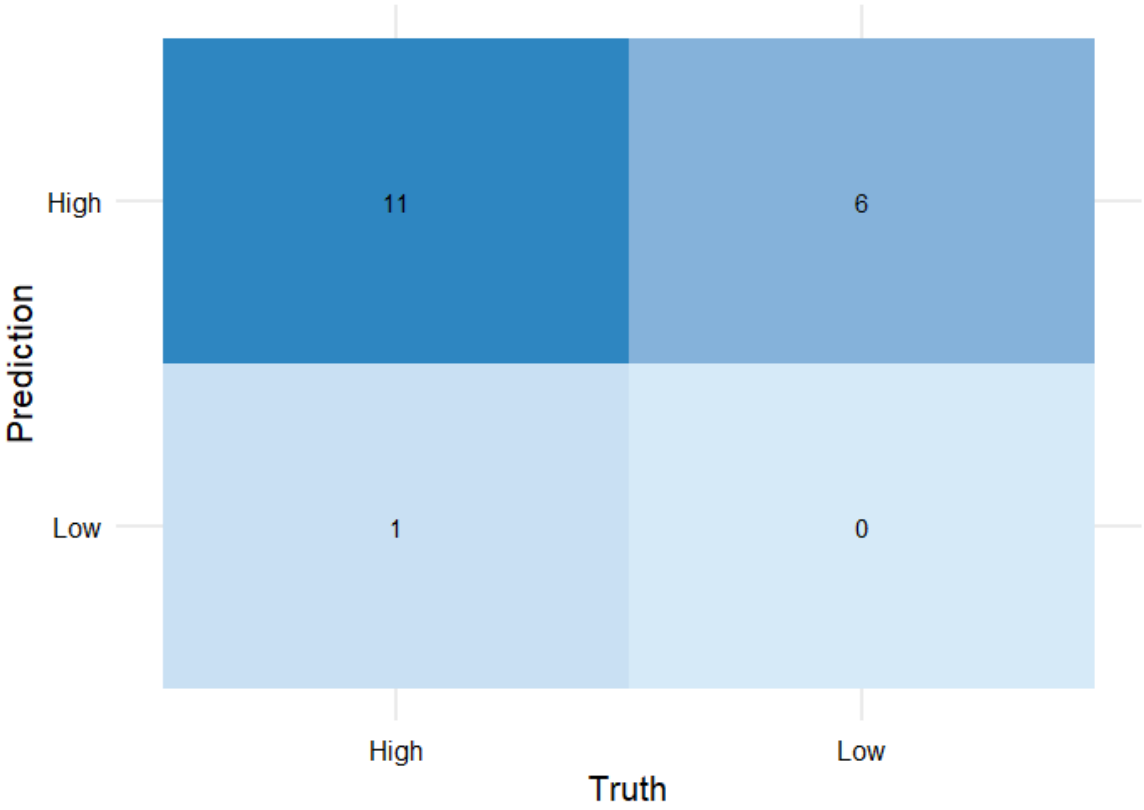

Figure B15: Confusion matrix of ANN-BOR Betula model (30T)

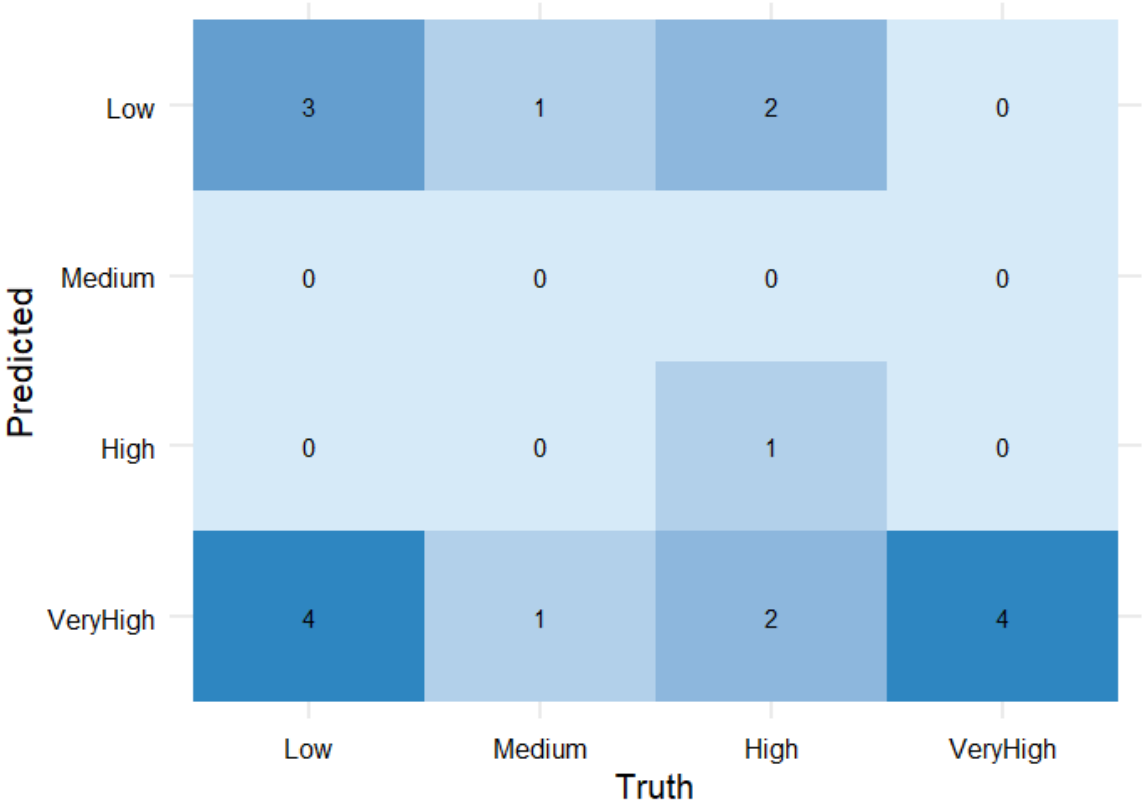

Figure B16: Confusion matrix of ANN Betula model (UKT)

Appendix C

Table C1: Spearman´s rank correlation coefficients between daily Dublin pollen data and meteorological parameters.

	Total	**Urticaceae**	**Poaceae**
Tmax	**0.32***	**0.32***	**0.40****
Tmed	0.16	0.13	0.16
Tmin	0.01	-0.04	-0.04
Rain	**-0.55***	-0.56	-0.47
Gmin	-0.19	-0.20	-0.12
Pres	-0.05	-0.01	-0.03
Wind_S	0.04	-0.03	0.15
Wind_D	-0.02	0.01	0.05
Day_L	0.25	0.24	0.29
G_rad	0.25	0.25	**0.33***
Soil	**0.33***	**0.32***	**0.35***
PE	0.26	0.22	**0.35***
Evap	0.25	0.21	**0.38***
RH	-0.49	-0.47	**-0.48***
PM2.5	**0.05****	**0.07****	-0.03
PM10	**0.25****	**0.21****	**0.25***
NO_X	-0.11	-0.06	-0.12
NO	-0.07	-0.02	-0.09
NO_2	-0.14	-0.10	-0.12
CO	0.09	0.12	-0.02
SO_2	0.09	0.12	-0.02

*significance at the 95% level, **significance at the 99% level

Appendix D

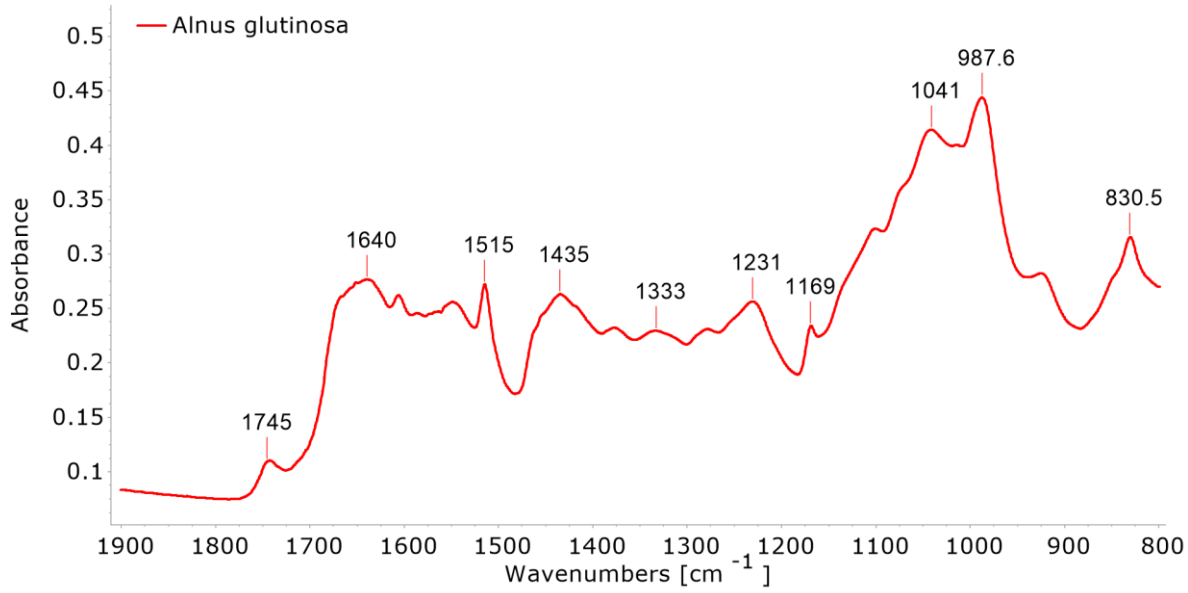

Figure D1: FTIR spectra obtained from the ATR analysis of Alnus glutinosa pollen

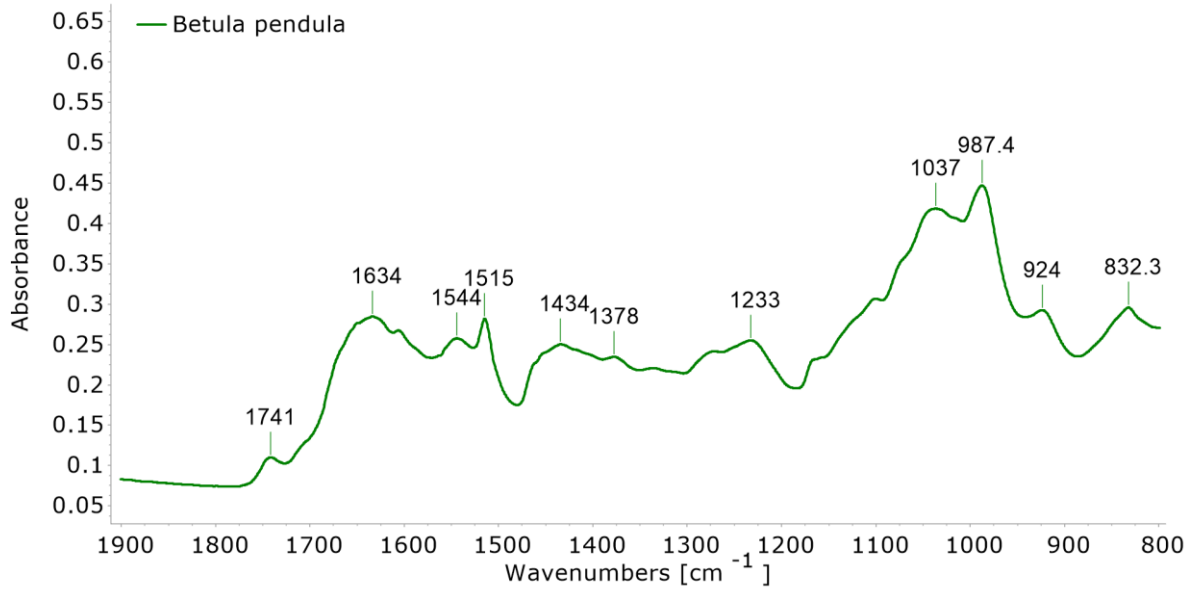

Figure D2: FTIR spectra obtained from the ATR analysis of Betula pendula pollen

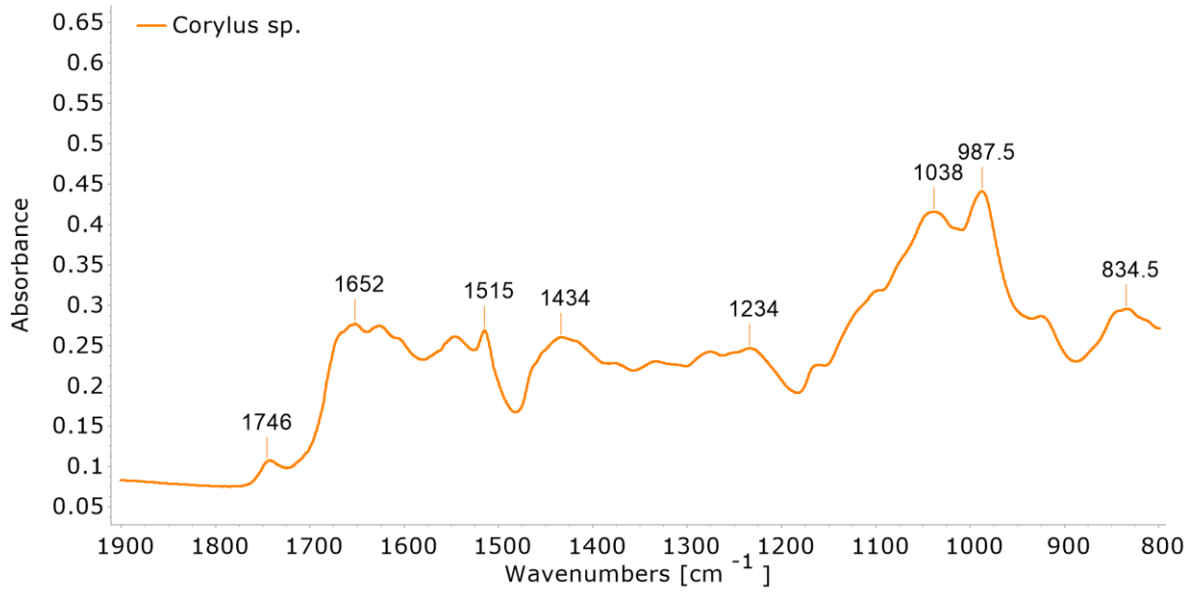

Figure D3: FTIR spectra obtained from the ATR analysis of Corylus pollen

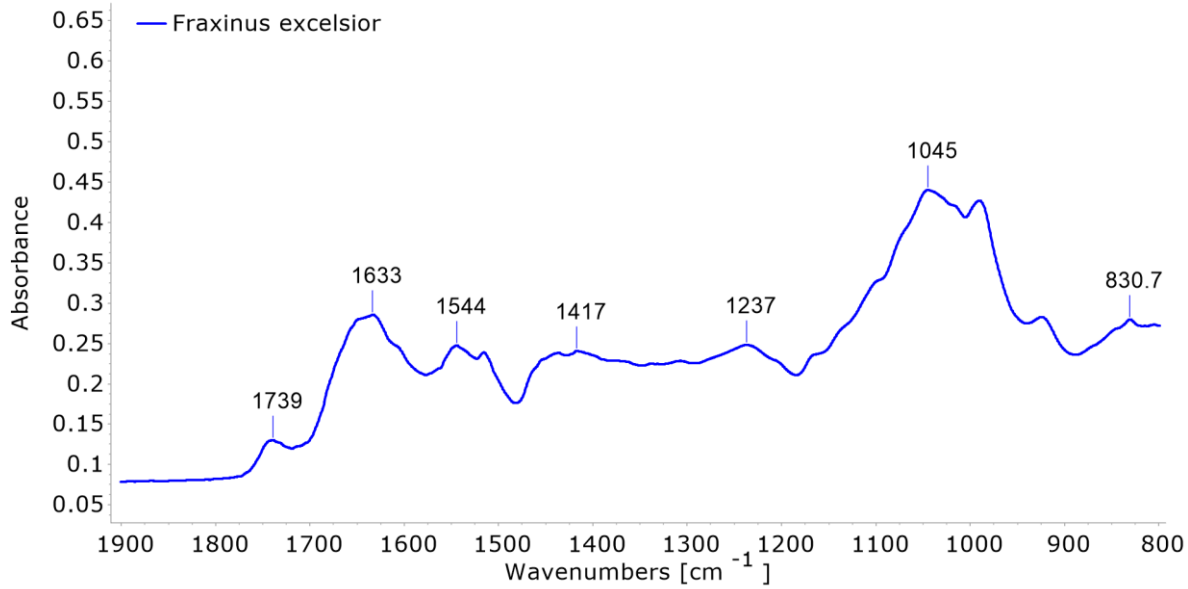

Figure D4: FTIR spectra obtained from the ATR analysis of Fraxinus excelsior pollen

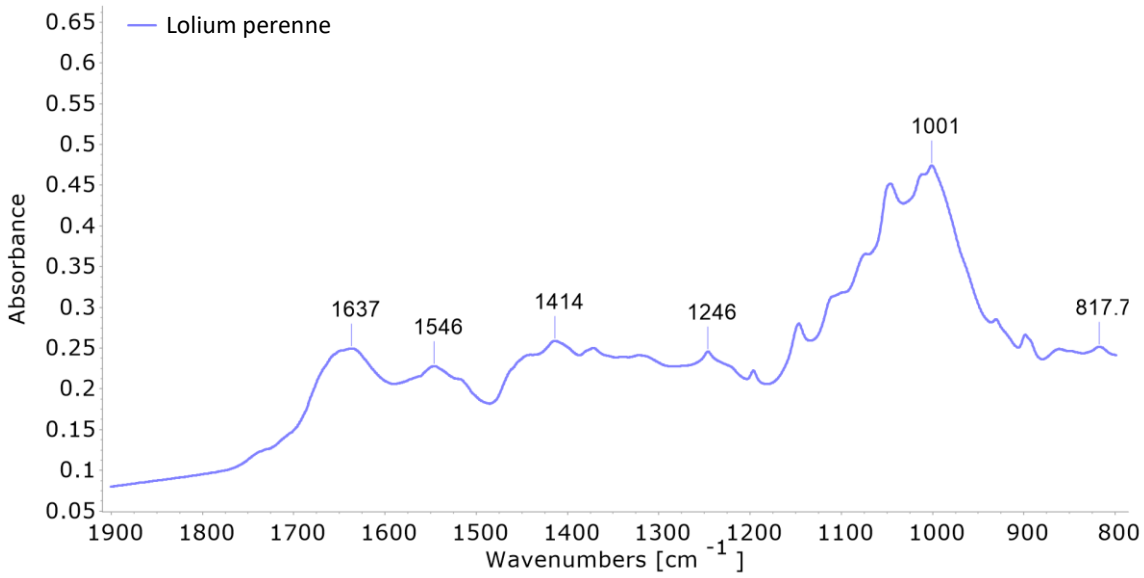

Figure D5: FTIR spectra obtained from the ATR analysis of Lolium perenne pollen

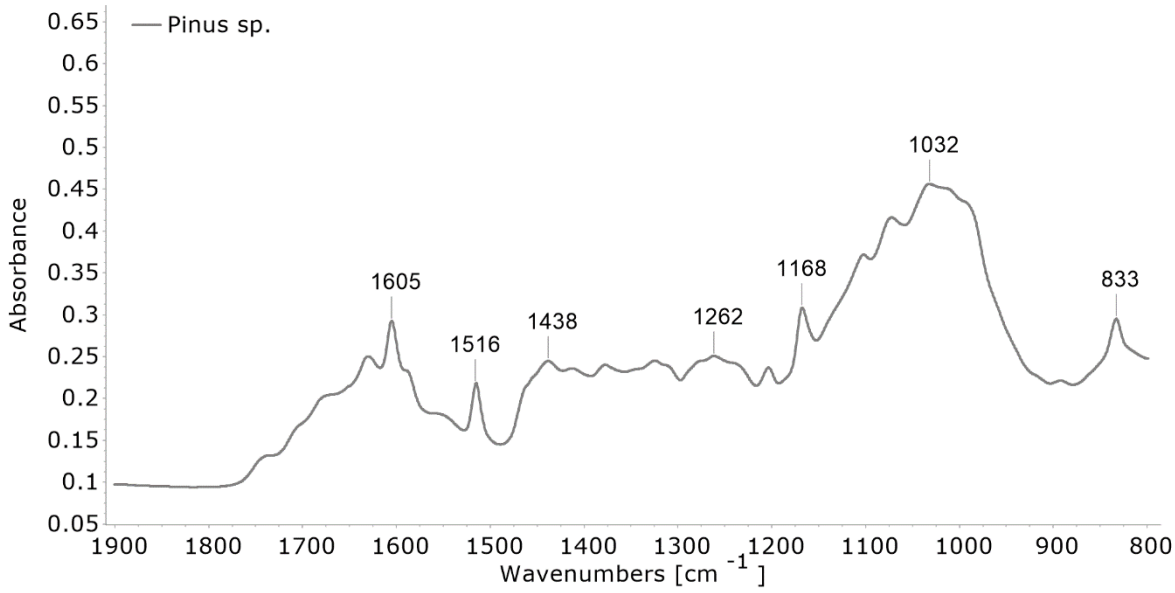

Figure D6: FTIR spectra obtained from the ATR analysis of Pinus pollen

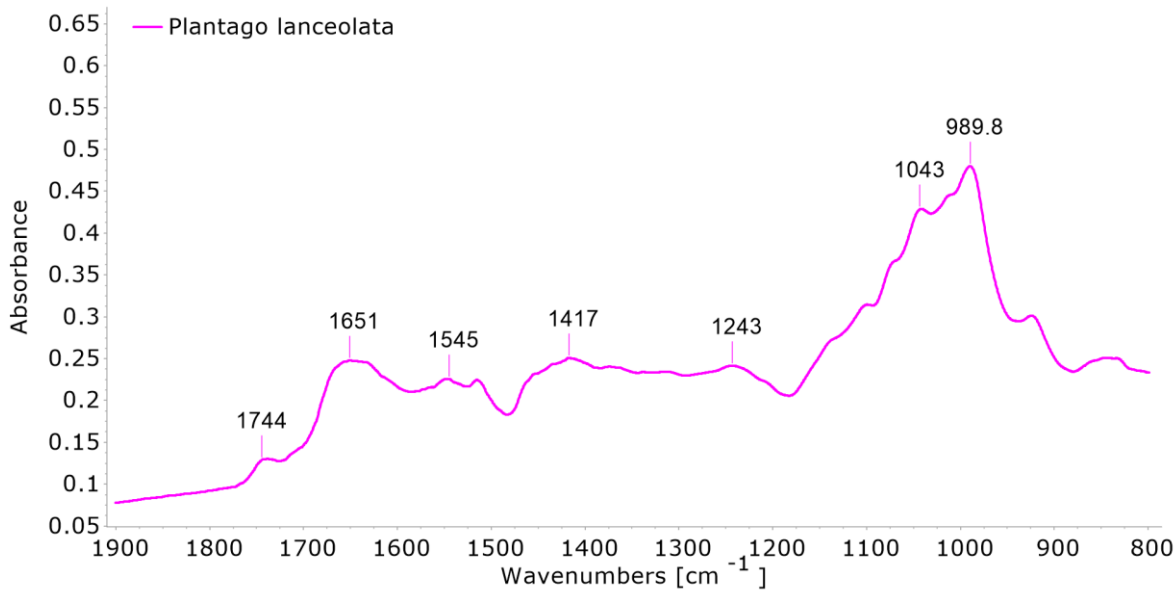

Figure D7: FTIR spectra obtained from the ATR analysis of Plantago lanceolata pollen

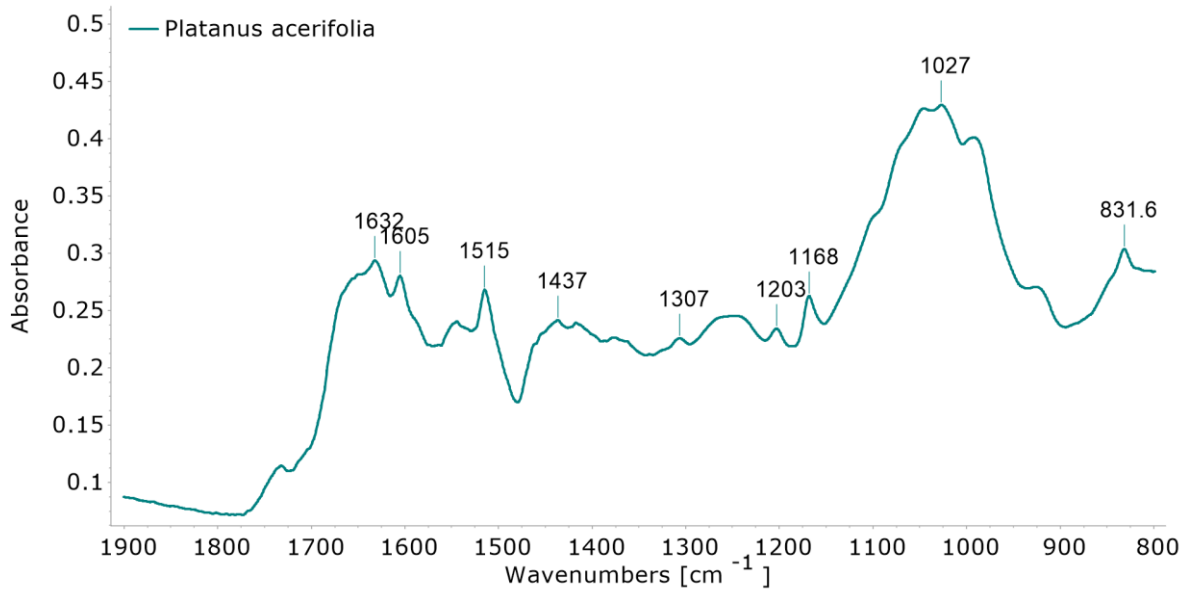

Figure D8: FTIR spectra obtained from the ATR analysis of Platanus acerifolia pollen

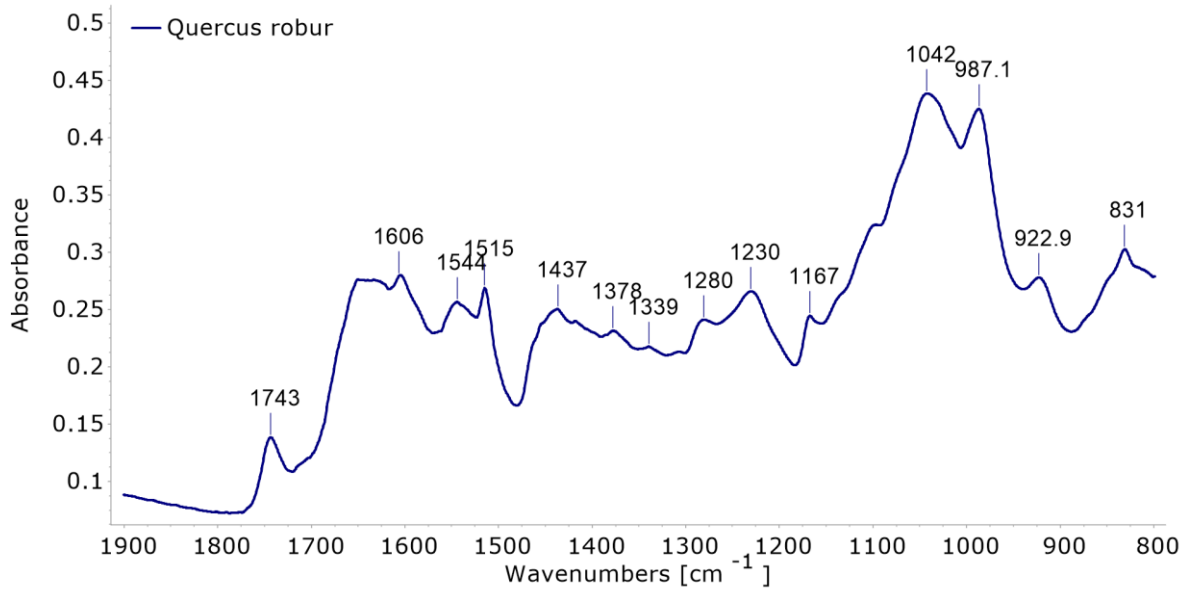

Figure D9: FTIR spectra obtained from the ATR analysis of Quercus robur pollen

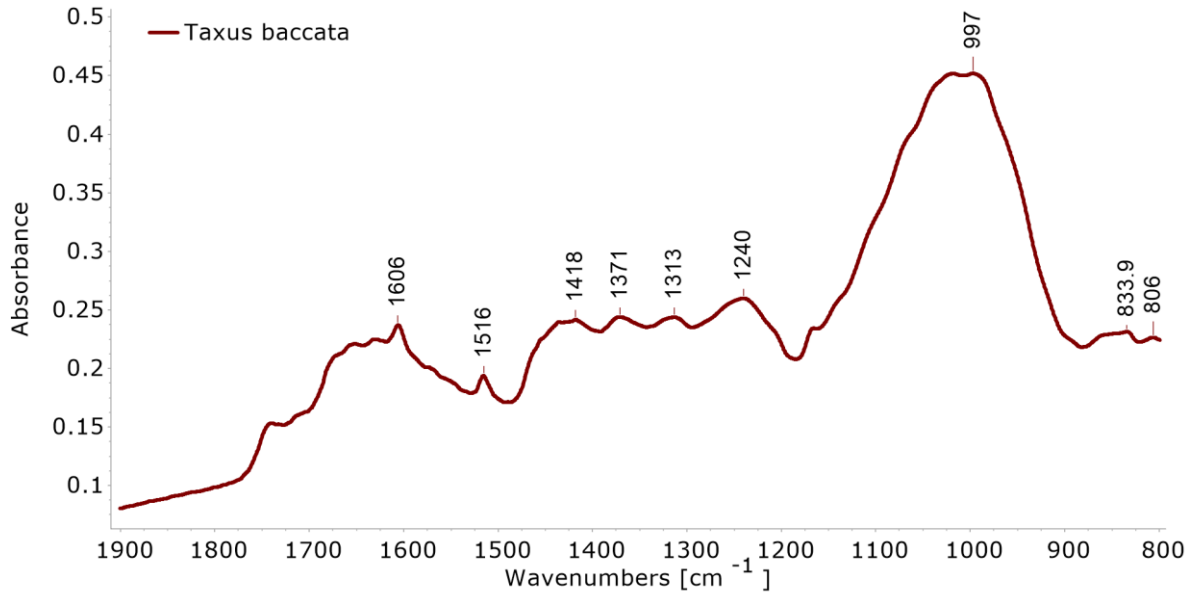

Figure D10: FTIR spectra obtained from the ATR analysis of Taxus baccata pollen

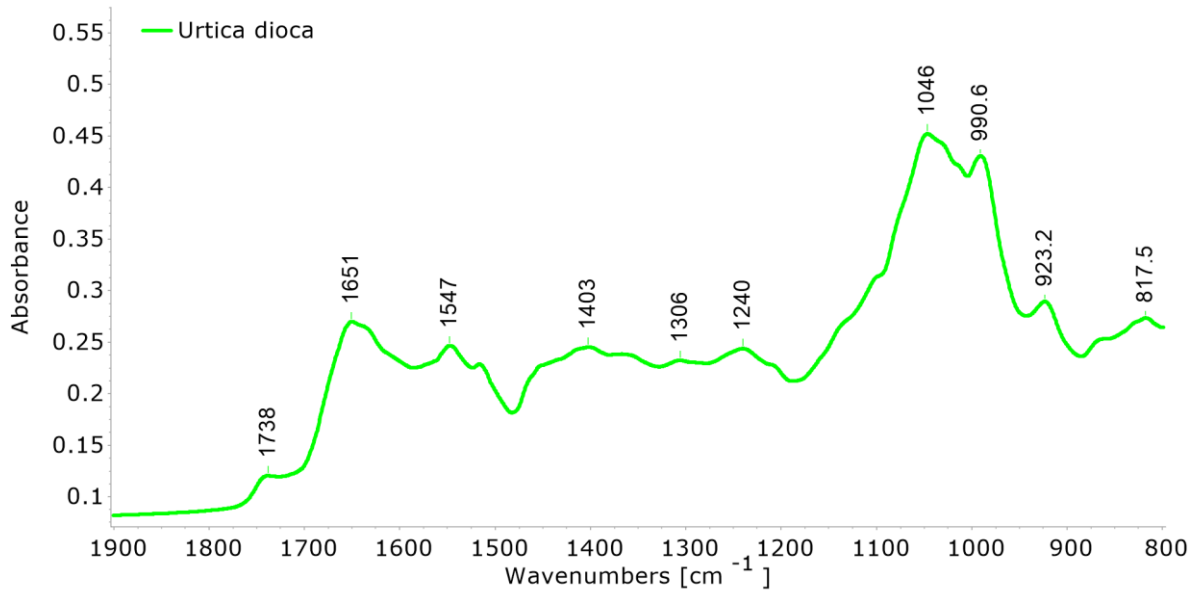

Figure D11: FTIR spectra obtained from the ATR analysis of Urtica dioica pollen

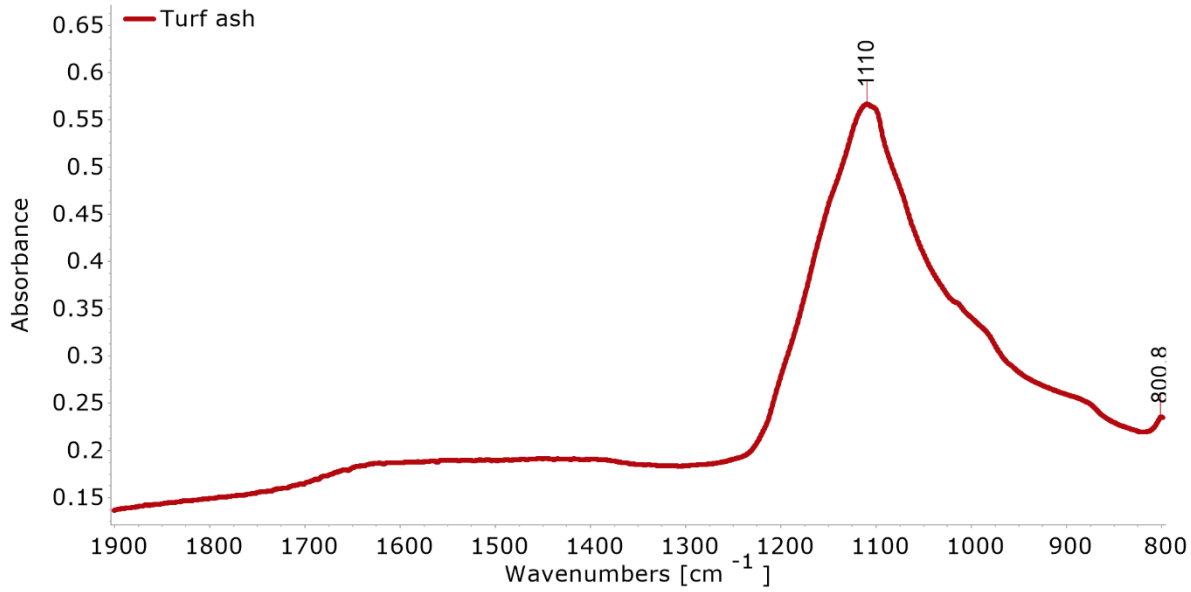

Figure D12: FTIR spectra obtained from the ATR analysis of turf ash

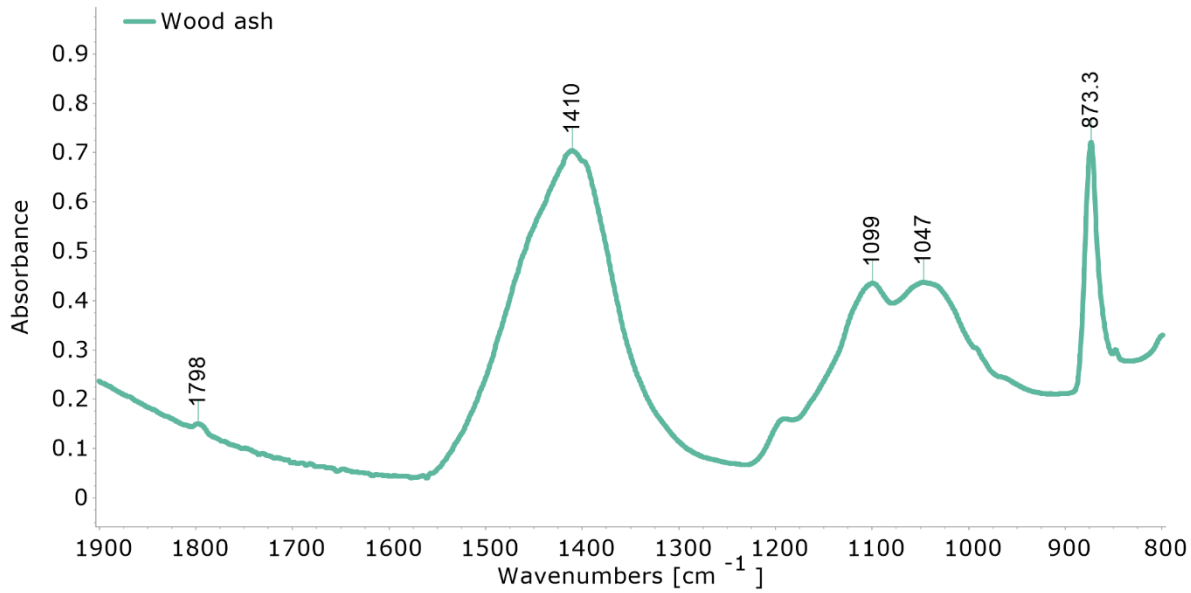

Figure D13: FTIR spectra obtained from the ATR analysis of wood ash

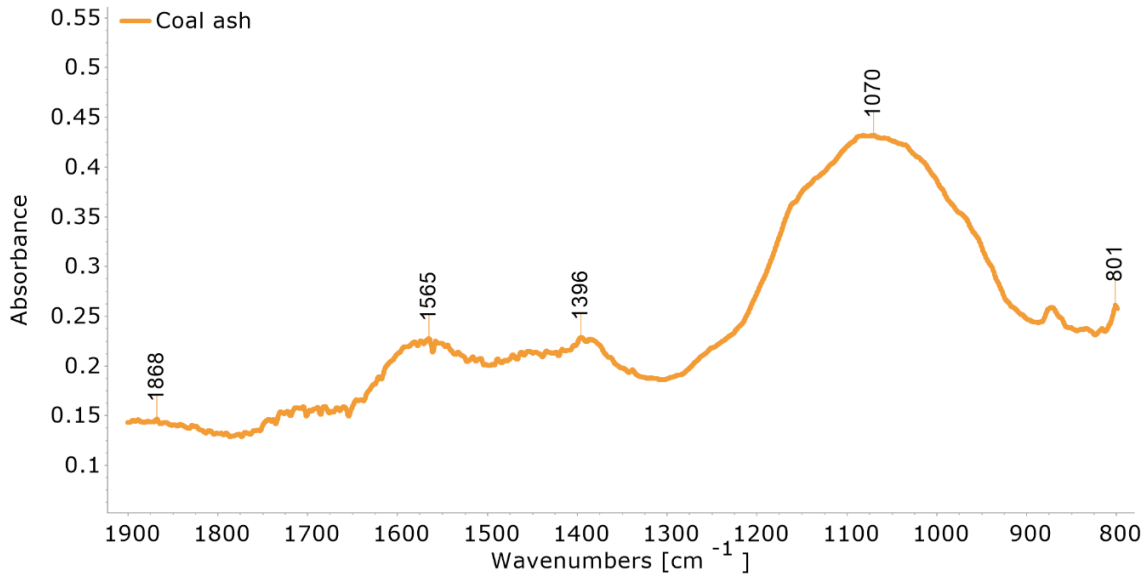

Figure D14: FTIR spectra obtained from the ATR analysis of coal ash

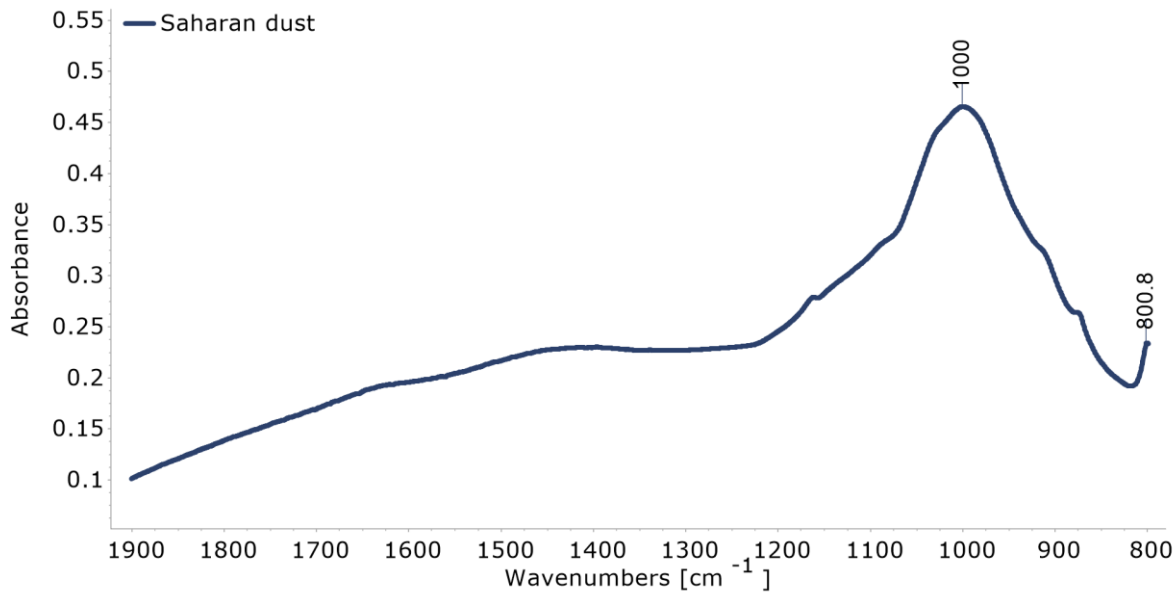

Figure D15: FTIR spectra obtained from the ATR analysis of Saharan dust